



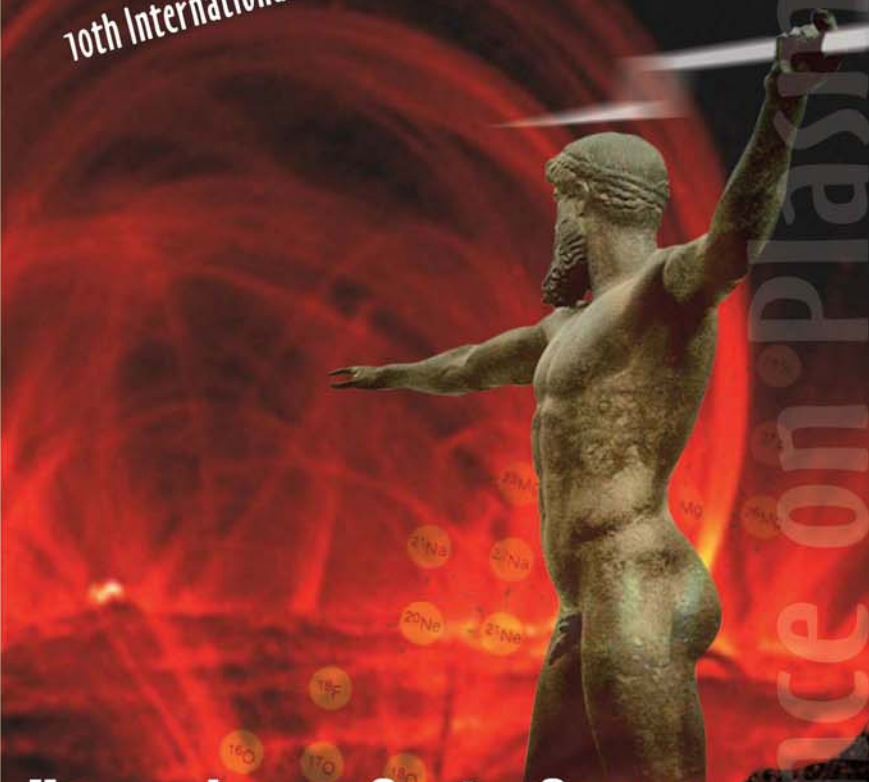
MAIN TOPICS:

- **Magnetic Confinement Fusion**
- **Beam Plasmas & Inertial Fusion**
- **Dusty & Low Temperature Plasmas**
- **Basic Plasmas & Space & Astrophysical Plasmas**

35th EUROPEAN PHYSICAL SOCIETY

Conference on Plasma Physics

10th International Workshop on Fast Ignition of Fusion Targets



**Hersonissos, Crete, Greece
9 - 13 June 2008**

PROGRAMME

Conference on Plasma Physics

35th EUROPEAN PHYSICAL SOCIETY

Conference on Plasma Physics 10th International Workshop on Fast Ignition of Fusion Targets

**Hersonissos, Crete, Greece
June 9-13, 2008**

PROGRAMME

Organized by:

- Association EURATOM – Hellenic Republic
- Institute of Electronic Structure and Laser (I.E.S.L.) – FO.R.T.H.

CONTENTS

	<i>Page</i>
Objectives of the Conference	3
Scope	3
Topics	3
EPS Programme Committee Members	4
The Local Organizing Committee	5
Conference date and location	5
Organisation	5
World Wide Web Site	5
Presentation ID	6
Oral Presentations	6
Poster Presentations	6
Paper abstracts	6
Proceedings	7
Awards	7
Education in Plasmas	8
ITER Session	8
Women in Physics	8
Satellite Meetings	9
Registration	9
Social Programme	10
Accompanying persons excursions	10
Lunches	10
Buses	10
Map of the Creta/Terra Maris Hotel	11
Plan of Conference Centre	12
PROGRAMME	13
List of Invited Talks	18
List of Contributed Orals	20
List of Posters	24
List of Post Deadline Presentations	69
Abstracts of Invited Talks	71
Author Index	155

Objectives of the Conference

One of the main objectives of the Conference is to facilitate the presentation and discussion of most recent developments in all areas of plasma physics and controlled fusion physics. The exchange of cross-disciplinary information among various plasma physics related fields is strongly encouraged. Plenary sessions covering the latest developments in plasma science are being held each day. Every day parallel invited talks related to the main topics of the Conference are held covering advanced technical aspects. Among the contributions submitted to the Conference, a number of papers are presented in parallel oral sessions, and the other contributed papers are presented as posters. A fraction of the Conference time during each day, after lunch, is exclusively devoted to poster sessions. During the Conference and afterwards the 10th International Workshop on Fast Ignition of Fusion Targets will take place.

Scope

This conference continues the series of **European Physical Society (EPS)** conferences on **Plasma Physics**, encompassing the fields of fusion research, magnetic confinement fusion, beam plasmas, laser-plasma interaction and inertial confinement fusion, dusty and low temperature plasmas, as well as space and astrophysical plasmas and basic plasmas.

TOPICS

- **Magnetic Confinement Fusion (MCF)**
 - Edge and plasma-wall interactions
 - Turbulence and transport
 - Equilibrium and MHD
 - Operational limits and plasma control
 - Diagnostics
 - Heating and fuelling
 - Concept development and engineering
- **Beam Plasmas & Inertial Fusion**
 - Inertial confinement and high gain
 - Hydrodynamics and instabilities
 - Ultra-intense laser interaction and fast ignition
 - Frontiers in hot dense matter research, pulsed power
 - Radiation hydrodynamics, laboratory astrophysics
 - Inertial fusion energy drivers and reactors
 - Laser and ion beam coupling with plasmas
 - Radiation sources - harmonics, X-ray lasers, etc.
 - Laser and plasma based accelerators
- **Dusty & Low Temperature Plasmas**
 - Theory and numerical simulations
 - Liquid and crystalline complex(dusty) plasmas

- Nucleation and growth
- Waves
- Diagnostics
- Plasma Processing and applications
- Dust in fusion
- **Basic Plasmas & Space & Astrophysical Plasmas**
 - Solar, space and astrophysical plasmas
 - Fundamental plasma physics.
 - Laboratory-based space and astrophysical plasmas

EPS PROGRAMME COMMITTEE MEMBERS

Carlos	Hidalgo	Spain	(Chair PC)
Jo	Lister	Switzerland	(Chair EPS PPD)
Paraskevas	Lalousis	Greece	(Chair LOC)
Vincent	Chan	USA	(APS)
Kazuo A.	Tanaka	Japan	(JSPF)

Magnetic Confinement Fusion

Xavier	Garbet	France
Howard	Wilson	United Kingdom
Paolo	Buratti	Italy
Ralph	Dux	Germany
Alberto	Loarte	EFDA/EU
Fernando	Meo	Denmark
Maria	Puiatti	Italy

Beam Plasmas and Inertial Fusion

Sylvie	Jacquemot	France
Martha	Fajardo	Portugal
Kate	Lancaster	United Kingdom
Manuel	Perlado	Spain
Francesco	Pegoraro	Italy

Dusty and Low Temperature Plasmas

Mark	Bowden	United Kingdom
Hubertus	Thomas	Germany
Francoise	Massines	France

Basic Plasmas and Space and Astrophysical Plasmas

Fabrice	Doveil	France
Michel	Tagger	France
Nigel	Woolsey	United Kingdom
Luis	Silva	Portugal

THE LOCAL ORGANISING COMMITTEE

Paraskevas Lalousis (chair)
Stavros Moustazis (Scientific Secretary)
Basil Duval (Switzerland)
Alkis Grecos
Kyriakos Hizanidis
Lucas Vlahos
Giannis Vomvoridis

Conference date and location

The Conference is being held on June 9-13 at the Creta Maris Conference Center, Hersonissos, Crete, Greece. The plenary invited talks are scheduled for early mornings from Monday to Friday, and also on Friday afternoon, in the Zeus theatre, in level 1 of the Conference Center. Parallel invited talks and contributed orals are held in four theatre rooms, Zeus, Minos, Danae, and Athina. The 10th International Workshop on Fast Ignition of Fusion Targets, will be held on June 12-13 at the Creta Maris Conference Centre, and will be continued on June 16-18 at the Apollo Room of Creta Maris Hotel.

Organisation

The organisation of the Conference is carried out by the Association EURATOM-Hellenic Republic and the Institute of Electronic Structure and Laser FORTH, Heraklion, Crete, Greece . The Secretary of EPS 2008 is :

Mrs. Ritsa Karali
FO.R.T.H. – I.E.S.L.
P.O. Box 1527,
71110 Heraklion, Crete,
GREECE
Tel: +30 2810 391300
Fax: +30 2810 391305
Email: eps2008@iesl.forth.gr

World Wide Web Site

Detailed and updated information on the 35th European Physical Society Conference on Plasma Physics is provided on the website: <http://eps2008.iesl.forth.gr>.

Presentation ID

The presentation ID (e.g. P1.001) reads as follows:

- First character indicates type of presentation
I – Invited talk *O – Oral contribution*
P – Poster contribution *D – post deadline paper*
- Second number indicates the day of presentation:
1 - Monday June 9, 2008 2 – Tuesday June 10, 2008
3 – Wednesday June 11, 2008 4 – Thursday June 12, 2008
5 – Friday June 13, 2008
- Third number (three digits) indicates the sequence number

Oral presentations

The allotted time for oral presentations is:

- Plenary invited oral: 40 minutes (including 5 minutes for discussion)
- Parallel invited oral: 30 minutes (including 5 minutes for discussion)
- Contributed oral: 20 minutes (including 5 minutes for discussion)

Speakers must keep strictly to the allotted time due to the large number of presentations. To avoid unnecessary delays between talks, all speakers are kindly requested to contact the Chairman five minutes before beginning of the session. Speakers are also requested to copy the file of their presentation at the conference slide Table on registration or at least one day before the oral presentation. Authors' laptop will not be allowed for presentation papers. Speakers with an oral presentation on Monday are requested to copy their presentation on Sunday afternoon. Speakers can also e-mail their file presentation to epstalks@iesl.forth.gr any time before the beginning of the Conference.

Poster presentations

All posters are to be presented on level 0 of the Creta Maris Conference Center. Authors of posters are reminded that they should put up their posters before the morning session commences and remove them at the end of the day, 18:00pm. The available poster area is 1.80 (height) x 0.95(width)m.

Paper abstracts

All abstracts are available on the Conference website: <http://eps2008.iesl.forth.gr>
Abstracts of the invited papers are included in this Programme.

Proceedings

All papers will be available on the website after the Conference. Invited papers will be published in a special issue of the Plasma Physics and Controlled Fusion Journal. Contributed orals and posters will be published on CD-ROM, and will be distributed after the Conference.

Awards

Hannes Alfvén prize of the European Physical Society for outstanding contributions to plasma physics

Each year, the European Physical Society awards this Prize to one or more persons who have made outstanding contributions to plasma physics in experimental, theoretical or technological areas. This year's Prize winner is Prof. Liu Chen from the University of California, Irvine, USA.

PhD Research Award

The Plasma Physics Division of the European Physical Society created the "European Physical Society Plasma Physics Division PhD Research Award" in 2005. This year (EPS2008) Prize winners are: Louise Willingale (UK), Ivo Classen (NL), and Bredan Dromey (IRL). The Prize winners will be presented on Monday morning.

EPS-PPD Innovation Prize

Research in Plasma Physics has multiple and rich outcomes with direct and/or indirect applications. These applications, which are sometimes inconspicuous and even unknown to the layman, can have significant impacts on daily human life as well as on economic activity. Surprisingly, some of the impacts seem far from the basic Plasma Physics research which gave birth to these key original ideas, but nonetheless represent exemplary innovative strategies. Today, applications of Plasma Physics flourish in vastly different domains, such as radioactive waste transmutation, medicine, isotope separation processes (with fundamental applications to cancer therapy), infection treatment, material processing, torch cutting and welding, flat TV screens, lighting systems, thrusters, as well as countless other medical, industrial and engineering applications. Within the general framework of the relationship between "Science and Society", there is a strong effort on communication between research and public domains in many countries.

The European Physical Society is keenly aware of these important applications. As a dual gesture of stimulation and recognition, a new annual prize has been created by the Plasma Physics Division of the European Physical Society. This prize targets research which has demonstrably led to robust innovative applications or important effects on society. Nominations in any fields are encouraged.

PPCF Poster Prize

The International Journal Plasma Physics and Controlled Fusion (PPCF) is proud to sponsor the PPCF Student Poster Prize at this Conference. Four €150 prizes (one for each of the Topics of the Conference) will be announced on Friday afternoon, during the Closing Session.

Itoh Project Prize in plasma Turbulence

This is the fourth time that Prof. Sanae-I Itoh, in agreement with the Conference organizers, has offered the Itoh Project Prize in Plasma Turbulence to students presenting a poster at the conference. The prize includes the chance to visit Kyushu University, Japan, for one week, including flights and living expenses.

Education in Plasmas

Theme: **European educational networks - what can it bring to plasma physics.** This session will be chaired by N. Lopes Cardozo, and held on Monday 9th from 18.15-19.00. Prof. Lopes Cardozo will give an introduction on the importance of education in attracting and training the next generation of plasma physics researchers, and on the opportunities for European cooperation to create an attractive education environment.

Speakers include Peter DeRegge (SCKSEN Mol, Belgium) on the European Nuclear Educational Network ENEN, Mark Westra (FOM Rijnhuizen, the Netherlands) on the European Fusion Education Network FUSENET, and Michael Geissler (QUB, Ireland) on the web-based Master course in Plasma Physics.

ITER Session

This session will be held on Tuesday 10 June, at 19:20-20:15, chaired by Jo Lister. Dr. Paul Thomas will present his views on “After the ITER Design Review”.

Women in Physics

On Thursday, June 12, 2008, the session “Women in Physics” will be held at 18:10-19:45 and chaired by S. Jacquemot.

Satellite meetings:

The following Workshops will take place after the Conference

10th International Workshop on Fast Ignition of Fusion Targets, 12-18 June 2008.

For the dates 12-13 June, 2008, it will be held in the Conference Center, and for 16-18 June in the Apollo Room of the Creta Maris Hotel .

EFTSOMP2008 - 11th Workshop on Electric Fields, Turbulence and Self-Organisation in Magnetized Plasmas

This Workshop will take place on 16-17 June, 2008, at the Hotel Albatros, Hersonissos.

Fuelling of Magnetic Confinement Machines, 16-17 June, 2008.

This Workshop will be held at the hotel Knossos Royal Village.

Registration

The registration desk opens at the Conference Centre on Sunday 8 June 2008 at 16:00 and closes at 20:00. On Monday morning, opening time is 08:15. Late registration fees are:

EPS Member	€ 530,00
Member of National Physical Society	€ 560,00
Non-EPS Member	€ 590,00
Student (on request by a supervisor)	€ 200,00
Accompanying person	€ 60,00

Access to the Conference centre will be restricted to participants wearing their badge. Registration fee for participants includes the welcome drink, the morning and afternoon refreshments, the Conference reception, the Conference services (Internet connection, etc.), a special Conference issue of Plasma Physics and Controlled Fusion containing the invited papers (if explicitly requested on the registration form), a Conference CD-ROM containing all contributed papers (distributed after the Conference).

Registration fee for accompanying persons includes the welcome drink, and the conference reception.

Registrations and hotel reservations are handled by:

Mrs. Maria Leventi

Ibis El Greco S.A. Conference Department

10 Meteoron St,

713 07 Heraklion-Crete,

GREECE

Tel.: + 30 2810 301711

Fax: + 30 2810 301689

E-mail: info@eps2008.gr

Social programme

Sunday June 8, 2008	19:30	Welcome drink	Romantic Bar, Creta Maris Hotel
Monday June 9, 2008	20:30	Conference Reception	Cochlias Restaurant, Creta Maris Hotel
Tuesday June 10, 2008	21:00	Choral Drama	Open-air theatre, Creta Maris Hotel
Wednesday June 11, 2008	14:00	Official excursion	Knossos Palace
Thursday June 12, 2008	20:15	Conference Dinner	Arolithos Village

Accompanying persons excursions

On Monday, before the excursions start, there will be greek coffee and sweets at 09:00 am for all accompanying persons. Meeting point is the Reception of Terra Maris Hotel.

Tour	Date
East Crete	09/06/2008
Spinalonga bbq	10/06/2008
Samaria Gorge	13/06/2008
Lassithi-Elounda & Spinalonga	12/06/2008
Festos-Gortys & Matala	12/06/2008
1-day Cruise to Santorini	11/06/2008
Rethymno-Arkadi & Chania	10/06/2008

Lunches

Creta Maris Restaurant, coupons which are available from the Secretariat desk.
Sandwich bar in the Terrace of the Conference Center.
List of Restaurants in the near by area is available in the Secretariat desk.

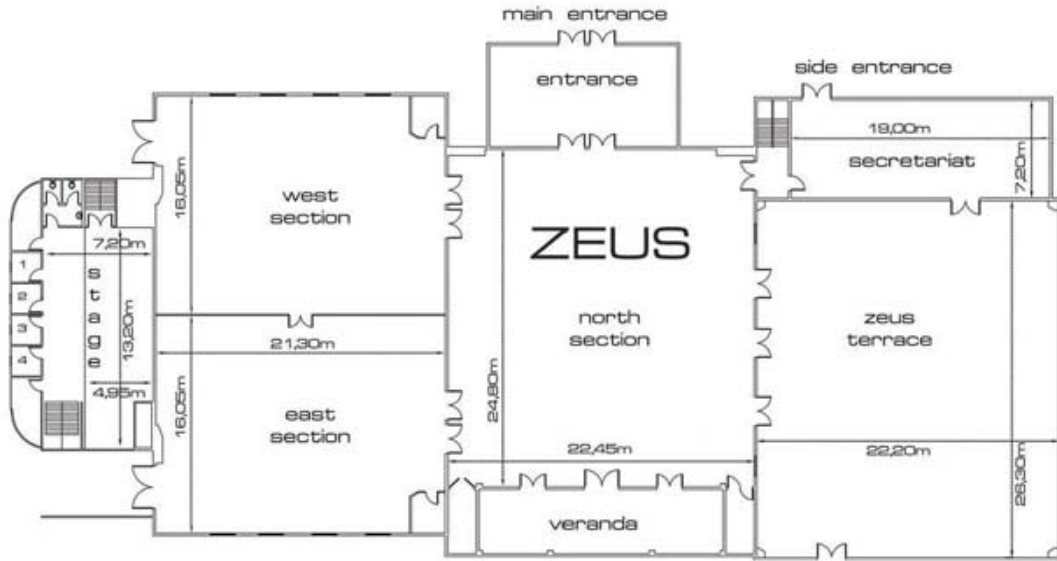
Buses

In the mornings there will be buses from the official Hotels to the Conference Center, and at the end of the day (18:00) there will be buses from the Conference Center to the Hotels. Also during the Conference days there will be a bus from the Conference Center to the Hotels and back to the Conference Center on the following times:

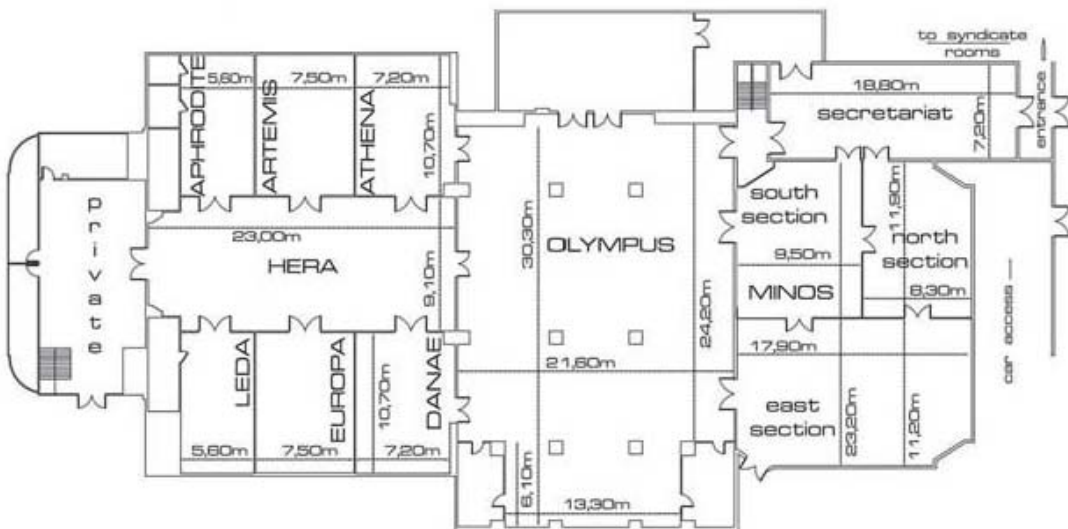
Monday –Tuesday-Thursday-Friday	10:30, 12:30, 14:30
Wednesday	10:30, 12:30

Plan of Conference Centre

Conference Centre Level 1 - Zeus Hall



Conference Centre Level 0 Olympus, Minos, Hera, Danae, Europa, Leda, Athena, Artemis & Aphrodite



PROGRAMME

Monday 9 June 2008				
	Room Zeus			
	Chair: J. Lister			
8:30-9:20	<i>Opening</i>			
9:20-10:00	Alfvén Prize: I1.001: L. Chen			
10:00-10:20	EPS PhD and Innovation in Plasma Science Prizes			
10:20-11:00	<i>Coffee Break</i>			
	Chair: A. Boozer			
11:00-11:40	I1.002: G. Tsakiris			
11:40-12:20	I1.003: A. Piel			
12:20-13:30	<i>Lunch Break</i>			
13:30-15:30	Poster Session			
15:30-16:00	Coffee break in Poster Session			
	Room Zeus Chair: M. Puiatti	Room Minos Chair : M. Fajardo	Room Athina Chair : F. Massines	Room Danae Chair: B. Lembege
16:00-16:30	I1.004 S. Günter	I1.008 T. Ceccotti	I1.012 C. Oehr	I1.016 D. Gericke
16:30-17:00	I1.005 S. Brezinsek	I1.009 D. Jaroszynski	I1.013 M. Kushner	I1.017 F. Paganucci
17:00-17:30	I1.006 A. Boozer	I1.010 F. Quéré	I1.014 L. Boufendi	Innovation in plasma science: Thesis I Thesis II
17:30-18:00	I1.007 S. Ide	I1.011 F. Albert	I1.015 D. Karabourniotis	
18:00	<i>Close</i>			
18:15	Education in plasmas (Chair: N. Lopes Cardozo)			
20:30	Reception			

Invited Plenary	40 min
Invited	30 min
Oral	20 min

Tuesday 10 June 2008				
	Room Zeus			
	Chair: P. Buratti			
8:30-09:10	I2.018: S. Pinches			
9:10-9:50	I2.019: T.C. Killian			
9:50-10:20	<i>Coffee Break</i>			
	Room Zeus Chair: R. Dux	Room Minos Chair: D. Batani	Room Athina Chair: H. Thomas	Room Danae Chair: R. Bingham
10:20-10:50	I2.020 B. Dudson	I2.024 P. Renaudin	I2.032 W. Goedheer	I2.034 D.F. Escande
10:50-11:20	I2.021 D. McDonald	I2.025 B. Rus	O2.007 A. Lipaev	I2.035 A. Schekochihin
11:20-11:50	I2.022 S. Sakakibara	I2.026 R. Singleton	O2.008 S. Khrapak	I2.036 R. Bamford
11:50:-12:20	I2.023 G. Falchetto	I2.027 L. Videau	O2.009 V. Tsytovich	I2.037 M. Marklund
12:20-13:30	<i>Lunch Break</i>			
13:30-15:30	Poster Session			
15:30-16:00	Coffee break in Poster Session			
	Room Zeus Chair: F. Meo	Room Minos Chair: X. Garbet	Room Athina Chair: S. Atzeni	Room Danae Chair: H.Kersten
16:00-16:20	O2.001 L.Bertalot	I2.028 P. Diamond	O2.010 G. Huser	I2.038 T. Gans
16:20-16:40	O2.002 Wolfrum	I2.029 F. Alladio	O2.011 R. Florido	I2.039 G. Kroesen
16:40-17:00	O2.003 A.C.C.Sips		O2.012 B. Yu Sharkov	
17:00-17:20	O2.004 S.H.Kim	I2.030 F. Casse	O2.013 C. Labaune	O2.016 B. James
17:20-17:40	O2.005 P.Gohil		O2.014 I.B. Földes	O2.017 J. Donoso
17:40-18:00	O2.006 V.Pericoli-Ridolfini	I2.031 D. Hughes	O2.015 R. Ramis	O2.018 A.B. Ustimenko
18:00	<i>Close</i>			
18:20-20:15	(chair J. Lister) ITER session			

Wednesday 11 June 2008				
	Room Zeus			
	Chair: H. Wilson			
8:30-9:10	I3.040: G. Conway			
9:10-9:50	I3.041: K.H. Spatschek			
9:50-10:20	<i>Coffee Break</i>			
	Room Zeus Chair: P. Monier-Garbet	Room Minos Chair: M. Perlado	Room Athena Chair: M. Bowden	Room Danae Chair: N. Woolsey
10:20-10:50	I3.042 O. Gruber	I3.047 T. Liseikina	I3.050 J.P. Borra	I3.053 K. Ronald
10:50-11:20	I3.043 O. Schmitz	I3.048 R. Fonseca	I3.051 U. Kortshagen/ R. Anthony	I3.054 Ch. Gregory
11:20-11:50	I3.044 M. Gryaznevich	I3.049 A. di Piazza	I3.052 P. Rocca	I3.055 F. Hansen
11:50-12:10	I3.045 M. Valisa	O3.019 M. Geissler	O3.022 A.E. Sorokin	O3.025 F. Delahaye
12:10-12:30		O3.020 H. Kuroda	O3.023 B. Layden	O3.026 A. Frank
12:30-12:50		I3.046 J. Garcia	O3.021 S. Kneip	O3.024 B.J. Lee
12:50-14:00	<i>Lunch Break</i>			
14:00	Excursion			
	Invited Plenary	40 min		
	Invited	30 min		
	Oral	20 min		

Thursday 12 June 2008				
	Room Zeus			
	Chair: K. Tanaka			
8:30-9:10	I4.056 : M. Borghesi			
9:10-9:50	I4.057 : J-P. Boeuf			
9:50-10:20	<i>Coffee Break</i>			
	Room Zeus Chair:W. Suttrop	Room Minos Workshop Chair: K.Lancaster	Room Athena Chair: J. Winter	Room Danae Chair: L. DaSilva
10:20-10:50	I4.058 J. Rice	I4.060 C. Stoeckl	I4.062 K. Bergmann	I4.064 G. Vastistas
10:50-11:20	I4.059 A. Murari	I4.061 N. Blanchot	I4.063 S. Ratynskaia	I4.065 S. Mueller
11:20-11:40	O4.028 M.Muraglia	D4.001 E. Storm (post-deadline)	O4.046 A.D. Gurchenko	O4.055 B. Rubinstein
11:40-12:00	O4.029 P.Piovesan	O4.038 H. Azechi	O4.047 A.G.Peeters	O4.056 M. Psimopoulos
12:00-12:20	O4.030 Ph.Lauber	O4.039 A. Henig	O4.048 M. Pedrosa	O4.057 S. Perri
12:20-13:30	<i>Lunch Break</i>			
13:30-15:30	Poster Session			
15:30-15:50	Coffee break in Poster Session			
	Room Zeus Chair: J. Ongena	Room Minos Worshop Chair: M. Key	Room Athena Chair: R. Wolf	Room Danae Chair: F. Doveil
16:00-16:20	O4.031 S.Zoletnik	O4.040 L. Willingale	O4.049 N.Vianello	I4.066 R. Trines
16:20-16:40	O4.032 S. de Graca	O4.041 I. Tsohantjis	O4.050 R.Guirlet	
16:40-17:00	O4.033 A.Huber	O4.042 L. Lancia	O4.051 Y.Kominis	I4.067 F. Peano
17:00-17:20	O4.034 G.P.Maddison	O4.043 J. Badziak	O4.052 Y.Xu	O4.058 M.V. Goldman
17:20-17:40	O4.035 M.Becoulet	O4.044 O.V. Polomarov	O4.053 R.E. Waltz	O4.059 A. Ram
17:40-18:00	O4.036 T.Kurki-Suonio	O4.045 T. Johzaki	O4.054 L. Garzotti	post deadline
18:00	<i>Close</i>			
18:10-19:45	Women in Physics (Chair: S. Jacquemot)			
20:15	Conference dinner			

Friday 13 June 2008				
	Room Zeus			
	Chair: P. Norreys			
8:30-9:10	I5.068 : M. Tabak			
9:10-9:50	I5.069: P. Pasko			
9:50-10:20	<i>Coffee Break</i>			
10:20	Room Zeus Chair: E.Rachlew	Room Minos Chair: K. Tanaka	Room Athena Chair: N. Cramer	Room Danae Chair: N. Vlahos
10:20-10:50	I5.070 J. Menard	O5.060 L. Hallo	I5.079 A. Ivlev	I5.081 V. T. Tikhonchuk
10:50-11:20	I5.071 F. Tabarés	O5.061 P. Koester	I5.080 V. Nosenko	I5.082 H. Takabe
11:20-11:50	I5.072 V. Udintsev	O5.062 P. Velarde	O5.063 H. Totsuji	O5.066 A.Y. Pankin
11:50-12:20	I5.073 Y. Andrew	I5.077 A. Robinson	O5.064 C. M. Ticos	O5.067 M.E.Dieckmann
		I5.078 J. Honrubia	O5.065 A. Fruchtman	O5.068 N. Leprovost
12:20-13:30	<i>Lunch Break</i>			
13:30-15:30	Poster Session			
15:30-16:00	Coffee break in Poster Session			
	Room Zeus			
	Chair: S. Jacquemot			
16:00-16:40	I5.074: F. Moreno-Insertis			
16:40-17:20	I5.075 : S. Krasheninnikov			
17:20-18:00	I5.076: A. Becoulet			
18:00-18:30	<i>Close</i>			

I. Pl.	40 min
I. par.	30 min
Or.	20 min
Workshop / BPIF	

LIST OF INVITED TALKS

I1.001	L. Chen	Alfven Waves: A Journey between Space and Fusion Plasmas
I1.002	G. Tsakiris	From relativistic laser-plasma interactions to intense attosecond pulses
I1.003	A. Piel	Complex plasmas: forces and dynamical behaviour
I1.004	S. Guenter	Three dimensional effects in tokamaks
I1.005	S. Brezinsek	Material erosion and migration studies in JET and implications for ITER
I1.006	A. Boozer	Stellarators and the path from ITER to DEMO
I1.007	S. Ide	JT-60U advanced tokamak research towards JT-60SA
I1.008	T. Ceccotti	First results on ions acceleration in an ultra-short, ultra high contrast 50 TW Laser Regime
I1.009	D. Jaroszynski	Radiation sources based on laser-plasma accelerators: current status and challenges
I1.010	F. Quere	Novel radiation sources using plasma mirrors
I1.011	F. Albert	Full characterization of a laser-produced keV X-ray betatron source and applications
I1.012	C. Oehr	Plasma deposition of ultrathin films for biomedical use
I1.013	M. Kushner	Modelling plasma modification on surfaces at low and high pressure. Achieving high control of reactants.
I1.014	L. Boufendi	Particle growth and detection in low temperature plasmas
I1.015	D. Karabourniotis	Diagnostics of dense dispersive plasmas from line reversal.
I1.016	D. Gericke	Temperature Equilibration in Dense Strongly Coupled Plasmas
I1.017	F. Paganucci	MHD instabilities in Magneto-Plasma-Dynamic Thrusters
I2.018	S. Pinches	The Physics of Fast Ion Driven Instabilities in Fusion Plasmas
I2.019	T. Killian	Watching Ions Dance Near Absolute Zero
I2.020	B. Dudson	Experiments and simulation of edge turbulence and filaments in MAST
I2.021	D. McDonald	JET confinement studies and their scaling to high β_N scenarios
I2.022	S. Sakakibara	Study of Reactor-Relevant High-Beta Regime in the Large Helical Device
I2.023	G. Falchetto	The European Turbulence Code Benchmarking Effort: Turbulence driven by Thermal Gradients in Magnetically Confined Plasmas
I2.024	P. Renaudin	Investigating atomic properties of warm dense matter produced by laser
I2.025	B. Rus	Warm Dense Matter Generation by soft X-ray laser heating of thin foils
I2.026	R. Singleton	An exact treatment of charged particle stopping in a plasma or The Coulomb logarithm revisited
I2.027	L. Videau	Overview of on-going LIL experiments
I2.028	P. Diamond	Anti-friction, Homogenization and Angular Momentum Transport in Tokamaks, Planets and the Solar Tachocline
I2.029	F. Alladio	Rotating twisted flux tubes buoyancy: comparison between the convective region of the Sun and the edge of a tokamak plasma
I2.030	F. Casse	Vertical angular momentum transport in astrophysical turbulent MHD accretion disks and the formation of large-scale collimated jets
I2.031	D. Hughes	Turbulent Transport and Coherence in MHD
I2.032	W. Goedheer	Simulation of dust voids in complex plasmas
I2.033	O. Petrov	Dusty plasmas under effect of external forces: basic phenomena and applications
I2.034	D. Escande	When can Fokker-Planck equation describe anomalous or chaotic particle transport?
I2.035	A. Schekochihin	Kinetic phase-space turbulence in space and laboratory Plasmas
I2.036	R. Bamford	Star Trek plasma shields: Measurements and Modelling of a diamagnetic cavity
I2.037	M. Marklund	Vacuum and plasma QED nonlinearities
I2.038	T. Gans	Phase resolved optical emission spectroscopy: Multi-frequency discharges and atmospheric pressure plasmas

I2.039	G. Kroesen	Electrical Breakdown: Experiments and Modeling
I3.040	G. Conway	Turbulence measurements in fusion plasmas
I3.041	K.H. Spatschek	Aspects of stochastic transport in laboratory and astrophysical plasmas
I3.042	O. Gruber	Compatibility of ITER scenarios with an all-W wall
I3.043	O. Schmitz	Three dimensional transport analysis for ELM control experiments in ITER similar shape plasmas at low collisionality in DIII-D
I3.044	M. Gryaznevich	Beta Limit in JET
I3.045	M. Valisa	Physics issues in the new high current regimes on RFX-mod.
I3.046	J. Garcia	Integrated modelling of ITER steady-state scenarios
I3.047	T. Liseykina	Radiation Pressure Acceleration by ultraintense laser pulses
I3.048	R. Fonseca	One-to-one direct modelling of experiments and astrophysical scenarios: pushing the envelope on kinetic plasma simulations
I3.049	A. Di Piazza	Quantum vacuum effects in strong laser beams
I3.050	J.P. Borra	Charging of aerosols and nucleation in atmospheric pressure electrical discharges
I3.051	U. Kortshagen	Plasma synthesis of silicon quantum dots for printed electronics and photovoltaics
I3.052	P. Roca	Low temperature plasma synthesis of silicon nanocrystals: the way for high deposition rate and efficient polymorphous and microcrystalline solar cells
I3.053	K. Ronald	Laboratory Investigations of Auroral Cyclotron Emission Processes
I3.054	C. Gregory	Astrophysical jet experiments
I3.055	F. Hansen	Experiments on interstellar cloud evolution following strong shock passage
I4.056	M. Borghesi	Laser driven proton acceleration: source optimization and perspectives for application
I4.057	J.-P. Boeuf	Hall Effect Thrusters for Satellite Propulsion
I4.058	J. Rice	Spontaneous rotation in alcator C-mod plasmas
I4.059	A. Murari	Innovative Diagnostics for ITER Physics addressed in JET
I4.060	C. Stoeckl	Fast ignition target design and experimental concept validation on OMEGA
I4.061	N. Blanchot	Overview of PETAL, the multi-Petawatt project on the LIL facility
I4.062	K. Bergmann	Present status of pinch plasmas for EUV and Soft X-ray Radiation
I4.063	S. Ratynskaia	In-situ dust detection in fusion devices
I4.064	G. Vattistas	The Dynamic Similarity Between Polygonal Satellite Vortices and Electron Columns in a Malberg-Penning Trap
I4.065	S. Mueller	Studies of blob formation, propagation and transport mechanisms in basic experimental plasmas (TORPEX and CSDX)
I4.066	R. Trines	The magnetopause is really a transport barrier like in tokamaks
I4.067	F. Peano	Expansion of nanoplasmas in ultraintense laser-matter interactions
I5.068	M. Tabak	Fast ignition: original concept and new developments
I5.069	V. Pasko	Lighting-related transient luminous events at high altitude in the Earth's atmosphere
I5.070	J. Menard	The response of tokamak plasmas to 3D magnetic field perturbations
I5.071	F. Tabares	Plasma performance and confinement in the TJ-II stellarator with lithium-coated walls
I5.072	V. Ushintsev	Global Plasma Oscillations in ITBs
I5.073	Y. Andrew	Access to H-mode on JET and implications for ITER
I5.074	F. Moreno-Inertis	Magnetized plasma eruptions in the solar atmosphere
I5.075	S. Krasheninnikov	Recent progress in understanding the behavior of dust in fusion devices
I5.076	A. Becoulet	Technology and science of steady state operation in magnetically confined plasmas
I5.077	A. Robinson	Magnetic collimation of fast electrons using structured targets
I5.078	J. Honrubia	Electron transport in imploded fast ignition targets
I5.079	A. Ivlev	New phenomena in liquid complex plasmas
I5.080	V. Nosenko	Monolayer complex plasma experiments

- I5.081 V. Tikhonchuk Laboratory Modeling of supersonic radiative jets propagation in plasmas and their scaling to astrophysical conditions
- I5.082 H. Takabe High-Mach Number Collisionless Shock and Photo-ionized Non-LTE Plasmas for Laboratory Astrophysics with Intense Lasers

LIST OF CONTRIBUTED ORALS

- O2.001 L. Bertalot, A. Costley, C. Walker, M. Sasao, A. Krasilnikov
The integrated way to high accuracy neutron measurements in ITER
- O2.002 E. Wolfrum, B. Langer, R. Fischer
Determination of the radial electric field from passive He II emission.
- O2.003 A.C.C. Sips, P. Lomas, O. Gruber, G.M.D. Hogeweij, J. Hobrik, L. Horton, F. Imbeaux, M. Mattei, F. Köchl, X. Litaudon, I. Nunes, V. Parail, A. Portone, G. Saibene, R. Sartori, G. Tardini
Current rise studies at ASDEX Upgrade and JET in preparation for ITER
- O2.004 S.H. Kim, J-F. Artaud, V. Basiuk, V. Dokouka, R.R. Khayrutdinov, J.B. Lister, V.E. Lukash
Full tokamak simulation of ITER Scenario 2 using the combined DINA-CH and CRONOS Simulator
- O2.005 P. Gohil, J.S. deGrassie, G.R. McKee, C.C. Petty, D.J. Schlossberg
H-mode Power Threshold for EC and NBI Heated Discharges in DIII-D and their Dependence on the Input Torque
- O2.006 V. Pericoli-Ridolfini, Yu. Baranov, M. Beurskens, M. Brix, P. Buratti, G. Calabrò, R. Castaldo, R. Cesario, C.D. Challis, R. DeAngelis, P.C. deVries, J. Ferron, E. Giovannozzi, C. Giroud, M. Gryaznevich, T.C. Hender, D. Howell, E. Joffrin, T. Luce, P. Lomas, J. Mailloux, D.C. McDonald, J. Menard, M. Murakami, F. Orsitto, F. Rimini, G. Saibene, S. Sharapov, P. Smeulders, I. Voitsekovitch, O. Zimmermann
High beta_N experiments at JET in ITER-like plasmas in support of the ITER steady state scenario
- O2.007 A.M. Lipaev, H.M. Thomas, G.E. Morfill, V.E. Fortov, A.V. Ivlev, V.I. Molotkov, T. Hagl, H. Rothermel, S.A. Khrapak, R.K. Suetterlin, M. Rubin-Zuzic, S.K. Krikalev, P.V. Vinogradov, A.I. Ivanov, V.I. Tokarev
Complex Plasma Laboratory PK-3 Plus on the International Space Station and First Experiments
- O2.008 Sergey Khrapak
Electric Potential Around a Small Object in Plasmas Effect of Plasma Absorption and Ion-Neutral Collisions
- O2.009 V.N. Tsyтович, G.E. Morfill
Attraction of dust clusters and formation of super-crystals
- O2.010 G. Huser, C. Courtois, M.-C. Monteil
Wall and laser spot motion in cylindrical hohlraums
- O2.011 R. Florido, J.M. Gil, P. Martel, M.A. Mendoza, E. Mínguez, R. Rodríguez, J.G. Rubiano, D. Suárez
Developments in the calculation of radiative properties of ICF plasmas at DENIM
- O2.012 B. Yu. Sharkov, N.N. Alexeev, D.G. Koshkarev, P.R. Zenkevich
Heavy ion accelerator-accumulator ITEP-TWAC for experiments on fusion and high energy density in matter physics.
- O2.013 C. Labaune, S. Depierreux, D. T. Michel, M. Grech, P. Nicolaï, C. Stenz, V. T. Tikhonchuk, S. Weber, C. Riconda, N. G. Borisenko, W. Nazarov, S. Hüller, D. Pesme, J. Limpouch, P. Loiseau, G. Riazuelo, M. Casanova, C. Meyer, P. Di-Nicola, R. Wrobel, E. Alozy, P. Romary, G. Thiell, G. Soullié, C. Reverdin, B. Villette
Smoothing of laser beam intensity fluctuations in low density foam plasmas with the LIL laser

- O2.014 I.B. Földes, S. Szatmári
Multiple-beam Fast Ignition with KrF Laser
- O2.015 R. Ramis
Three-dimensional simulations of cylindrical targets irradiated by heavy-ion beams
- O2.016 B.W. James, L. Couedel, A.A. Samarian, L. Boufendi
Discharge diagnostics during particle growth in a complex plasma
- O2.017 J. M. Donoso
Integral propagator solvers for plasma kinetic equations
- O2.018 O.A. Lavrichshev, V.E. Messerle, E.F. Osadchaya, A.B. Ustimenko
Plasma Gasification of Coal and Petrocoke
- O3.019 M. Geissler, S. Rykovanov, J. Schreiber, M. Zepf, J. Meyer-ter-Vehn, G. Tsakiris
Surface Harmonic Generation With High Power Laser Pulses
- O3.020 H. Kuroda, M. Suzuki, M. Baba, R. A. Ganeev, T. Ozaki
Highly Efficient and Brilliant High Harmonic Coherent Soft X-Ray Laser Source from Laser-Ablated Solid Target Plasma Towards a Water Window Region
- O3.021 S. Kneip, S.R. Nagel, C. Bellei, N. Bourgeois, A. E. Dangor, A. Gopal, R. Heathcote, S. P. D. Mangles, J. R. Marquès, A. Maksimchuk, P.M. Nilson, K. Ta Phuoc, S. Reed, M. Tzoufras, F.S. Tsung, L. Willingale, W. B. Mori, A. Rousse, K. Krushelnick, Z. Najmudin
Petawatt Laser Synchrotron Source
- O3.022 A.E. Sorokin
Selective ion capture instability for ion-particle interactions in weakly ionized gas
- O3.023 B. Layden, L. Couedel, A. Samarian, M. Mikikian, S.V. Vladimirov, L. Boufendi
Afterglow dynamics of a dust cloud
- O3.024 B.J. Lee, K.S. Oh, S.W. Choi, M.P. Hong, D.C. Kim, G.H. Kim, Y.C. Park, S.J. Yoo
Manufacturing Photovoltaic Cell with the Low Cost and High Efficiency Using Hyperthermal Neutral Beam
- O3.025 F. Delahaye
The ODALISC Project Accurate atomic data for complex radiation-hydrodynamics simulations
- O3.026 Anna Frank, Sergey Bugrov, Vladimir Markov
Experimental observations of the out-of-plane quadrupole magnetic fields resulting from Hall current generation in current sheets
- O3.027 L.P. Babich, A.N. Donsko, A.Y. Kudryavtsev, M.L. Kudryavtseva, I.M. Kutsyk
Simulation of ascending atmospheric discharge and its emissions in optical and gamma – ranges
- O4.028 M. Muraglia, O. Agullo, S. Benkadda, P. Beyer, X. Garbet
Nonlinear Dynamics of Magnetic Islands Imbedded in Edge Tokamak Plasma Microturbulence
- O4.029 P. Piovesan, M. Zuin, D. Bonfiglio, A. Canton, L. Carraro, R. Cavazzana, L. Marrelli, E. Martines, M. Spolaore, M. Valisa, N. Vianello, P. Zanca
Magnetic order improvement through high current and MHD feedback control in RFX-mod

- O4.030 Ph. Lauber, S. Guenter, M. Bruedgam, M. Garcia Munoz, S. da Graca, N. Hicks, V. Igochine, M. Maraschek
Fast Particle Driven Modes at ASDEX-Upgrade
- O4.031 S. Zoletnik, D. Dunai, A. R. Field, A. Kirk
ELM pre-cursor structures observed using Beam Emission Spectroscopy in MAST
- O4.032 S.daGraca, G.D.Conway, M.Maraschek, A.Silva, E.Wolfrum, R.Fisher, L.Cupido, F.Serra, M.E.Manso, ASDEX Upgrade Team
Studies of edge MHD modes in H-mode discharges in ASDEX Upgrade using reflectometry
- O4.033 A. Huber, R. A. Pitts, A. Loarte, V. Philipps, P. Andrew, S. Brezinsek, P. Coad, J.C. Fuchs, W. Fundamenski, S. Jachmich, A. Korotkov, G.F. Matthews, K. McCormick, Ph. Mertens, J. Rapp, G. Sergienko, M. Stamp
Plasma radiation during transient events in JET
- O4.034 G.P. Maddison, A.E. Hubbard, J.W. Hughes, I.M. Nunes, M.N.A. Beurskens, S.K. Erents, R. Pasqualotto, E. Giovannozzi, A. Alfier, M.A.H. Kempenaars, B. Alper, S.D. Pinches, J.A. Snipes, B. LaBombard
Dimensionless pedestal identity plasmas on JET and Alcator C-Mod
- O4.035 M. Becoulet, G. Huysmans, E. Nardon, M. Schaffer, A. Garofalo, A. Cole
Non-linear MHD Rotating Plasma Response to Resonant Magnetic Perturbations.
- O4.036 T. Kurki-Suonio, O. Asunta, V. Hynönen, T. Johnson, T. Koskela, J. Lönnroth, V. Parail, M. Roccella, G. Saibene, A. Salmi, S. Sipilä
Fast Particle Losses in ITER
- O4.038 H. Azechi, K. Mima, Y. Fujimoto, S. Fujioka, H. Homma, M. Isobe, A. Iwamoto, T. Jitsuno, T. Johzaki, R. Kodama, M. Koga, K. Kondo, J. Kawanaka, T. Mito, N. Miyanaga, O. Motojima, M. Murakami, H. Nagatomo, K. Nagai, M. Nakai, T. Nakamura, Y. Nakao, K. Nishihara, H. Nishimura, T. Norimatsu, T. Ozaki, H. Sakagami, K. Shigemori, H. Shiraga, A. Sunahara, T. Taguchi, K.A. Tanaka, K. Tsubakimoto
Update of FIREX Project
- O4.039 A. Henig, J. Schreiber, D. Kiefer, S. Karsch, Zs. Major, R. Hörlein, J. Osterhoff, M. Geissler, S. Rykovanov, J. Szerypo, S. Stanglmaier, F. Krausz, D. Habs
Enhanced ion acceleration from mass-limited targets irradiated by high-intensity laser pulses
- O4.040 L.Willingale, S.R.Nagel, A.G.R.Thomas, C.Bellei, R.J.Clark, A.E.Dangor, R.Heathcote, C.Joshi, M.C.Kaluza, C.Kamperides, S.Kneip, K.Krushenick, N.Lopes, S.P.D.Mangles, K.Marsh, W.Nazarov, P.M.Nilson, Z.Najmudin
Laser plasma interactions in the relativistic transparent regime
- O4.041 I. Tsohantjis, S. D. Moustazis, I. Ploumistakis
Pair creation from vacuum in the presence of ultra-intense laser beams
- O4.042 Livia Lancia, Jean-Raphaël Marquès, Julien Fuchs, Caterina Riconda, Ana Mancic, Patrizio Antici, Patrick Audebert, Stefan Weber, Vladimir T. Tikhonchuk, Stefan Hueller, Jean-Claude Adam, Anne Héron
Experimental investigation of short light pulse amplification using stimulated Brillouin backscattering
- O4.043 J. Badziak, S. Jablonski, P. Parys, M. Rosinski, J. Wolowski, A. Szydłowski, P. Antici, J. Fuchs, A. Mancic
Studies on proton beam generation for fast ignition-related applications
- O4.044 O. V. Polomarov, I. D. Kaganovich, G. Shvets
The Collective Energy Loss Of The Relativistic Electron Beam Propagating Through Background Plasma
- O4.045 T. Johzaki, Y. Sentoku, H. Sakagami, H. Nagatomo, K. Mima, Y. Nakao
Core Heating Properties in FIREX-I ~Influence of cone tip

- O4.046 A.D. Gurchenko, E.Z. Gusakov, A.B. Altukhov, A.Yu. Stepanov, S.I. Lashkul, D.V. Kouprienko, L.A. Esipov
Evolution of turbulence exponential wave number spectra during transition to improved confinement triggered by current ramp up at FT-2 tokamak
- O4.047 A.G. Peeters, C. Angioni, D. Strintzi
Toroidal momentum pinch velocity and turbulent equipartition
- O4.048 M.A. Pedrosa, C. Silva, C. Hidalgo, D. Carralero, B.A. Carreras, R.O. Orozco
Long-distance correlations of fluctuations and sheared flows during transitions to improved confinement regimes in the TJ-II stellarator
- O4.049 N. Vianello, M. Agostini, A. Alfier, A. Canton, R. Cavazzana, A. Fassina, R. Lorenzini, E. Martines, P. Scarin, G. Serianni, G. Spizzo, M. Spolaore, M. Zuin
Turbulence, transport and their relation with magnetic boundary in the RFX-mod device
- O4.050 R. Guirlet, T. Parisot, D. Villegas, C. Bourdelle, X. Garbet, F. Imbeaux, D. Pacella
Comparison of anomalous transport of light and heavy impurities in sawtooth-free Tore Supra plasmas
- O4.051 Y. Kominis, K. Hizanidis, A.K. Ram
Quasilinear Theory for Momentum and Spatial Diffusion due to Radio Frequency Waves in Non-Axisymmetric Toroidal Plasmas
- O4.052 Y. Xu, R. R. Weynants, M. Van Schoor, M. Vergote, S. Jachmich, M. W. Jakubowski, M. Mitri, D. Reiser, O. Schmitz, K. H. Finken, M. Lehnen, B. Unterberg, D. Reiter, U. Samm, the TEXTOR team
Impact of the Resonant Magnetic Perturbations RMP on Edge Turbulence and Turbulent Transport on TEXTOR
- O4.053 R.E. Waltz, G.M. Staebler
Gyrokinetic Theory and Simulation of Angular Momentum Transport
- O4.054 L.Garzotti, K.B.Axon, L.Baylor, J.Dowling, C.Gurl, F.Köchler, G.P.Maddison, H.Nehme, B.Pégourié, M.Price, R.Scannel, M.Valovic, M.Walsh.
Observation and analysis of pellet material grad B drift on MAST.
- O4.055 B. Rubinstein, J. Citrin, R. Doron, R. Arad, Y. Maron, A. Filler
Highly Resolved Spectroscopic Observations of Magnetic Field Penetration into an almost Collisionless Plasma
- O4.056 M. Psimopoulos, S. Tanriverdi, G. Kasotakis, M. Tatarakis
Cross field thermal transport in magnetized plasmas
- O4.057 S. Perri, E. Yordanova, V. Carbone, L. Sorriso-Valvo, M. André
Small-scale anisotropy in the heliosphere
- O4.058 M. V. Goldman, D. L. Newman
Weak Electron Phase Space Holes for Electron Distributions with a Tail
- O4.059 A.K. Ram, B. Dasgupta
Chaotic Magnetic Fields due to Asymmetric Current Configurations -- Modeling Cross-Field Particle Diffusion in Cosmic Rays
- O5.060 L. Hallo, V. Dréan, M. OLazabal-Loumé, X. Ribeyre, G. Schurtz
Hydrodynamic symmetry safety factor of HiPER's targets
- O5.061 P. Koester, K. Akli, A. Antonicci, D. Batani, S. Baton, R.G. Evans, E. Foerster, A. Giulietti, D. Giulietti, L.A. Gizzi, J.S. Green, T. Kaempfer, M. Koenig, L. Labate, K.L. Lancaster, T. Levato, A. Luebcke, A. Morace, P. Norreys, F. Perez, I. Uschmann, J. Waugh, N. Woolsey, F. Zamponi
Experimental investigation of fast electron transport through Kalpha imaging and spectroscopy in relativistic laser-solid interactions

- O5.062 P. Velarde, M. González, C.García, E.Oliva
Simulation of the shell-cone interaction in fast ignition targets
- O5.063 H. Totsuji
Critical Phenomena in Strongly Coupled Fine Particle Plasmas
- O5.064 C. M. Ticos, Zhehui Wang, G. A. Wurden
Plasma jet acceleration of a dust cloud to hypervelocities
- O5.065 A. Fruchtman
Plasma source as a thruster
- O5.066 A.Y. Pankin, Z. Mikic, S. Titov, J. Goodman, D.A. Uzdensky, D.D. Schnack
Magnetohydrodynamic Modeling of the Accretion Disk Corona
- O5.067 M.E.Dieckmann, P.K.Shukla, L.O.C.Drury
The formation of a relativistic planar plasma shock
- O5.068 N. Leprovost, E. Kim
Theory of turbulent transport and dynamos in astrophysical plasmas

LIST OF POSTERS

- P1.001 A.Y. Pankin, G. Bateman, C.S. Chang, F. Halpern, A.H. Kritz, S. Ku, D. McCune, G.Y. Park, T. Rafiq
Effects of Anomalous Transport on Kinetic H-mode Pedestal Evolution
- P1.002 Carrere M, Cartry G, Schiesko L, Layet JM,
Negative ion measurements H- and D- produced on a HOPG sample in a helicon reactor.
- P1.003 M.B. Kadomtsev, M.G. Levashova, V.S. Lisitsa
2D universal atomic kinetics for hydrogen-like systems in plasmas
- P1.004 J. Rosato, F.B. Rosmej, R. Stamm, M.B. Kadomtsev, M.G. Levashova, V.S. Lisitsa
Effects of transport and turbulence on lithium radiation in edge tokamak plasmas
- P1.005 J.W. Hughes, A.E. Hubbard, B. LaBombard, B. Lipschultz, K. Marr, R. McDermott, M.L. Reinke, J.L. Terry, S. Wolfe
H-mode optimization using magnetic topology variation in Alcator C-Mod
- P1.006 M. Kocan, J.P. Gunn, J.-Y. Pascal, G. Bonhomme, C. Fenzi, E. Gauthier, T. Gerbaud, O. Meyer, J.-L. Segui
Measurements of ion temperature in the SOL of Tore Supra
- P1.007 N. Ben Ayed, G. F. Counsell, B. Dudson, A. Kirk, R. G. L. Vann, H. R. Wilson, MAST team.
Edge turbulence studies of inter-ELM periods on MAST
- P1.008 O. Buzhinskij, E. Azizov, V. Otruschenko, V. Rodionova, N. Rodionov, S. Sotnikov, S.Tugarinov, A. Trapeznikov, I.Shipuk
Renewed First Wall Coating In The T-11M Tokamak Plasma Shot.

- P1.009 R. Kaita, H. Kugel, M.G. Bell, R. Bell, J. Boedo, C. Bush, D. Gates, T. Gray, J. Kallman, S.Kaye, B. LeBlanc, R. Majeski, R. Maingi, D. Mansfield, J. Menard, D.Mueller, M. Ono, S. Paul, R. Raman, A.L. Roquemore, P.W. Ross, S. Sabbagh, H. Schneider, C.H. Skinner, V. Soukhanovskii, T.Stevenson, J. Timberlake, J-W. Ahn, J.P. Allain, W.R. Wampler, L. Zakharov
Improvement in Plasma Performance with Lithium Coatings in NSTX
- P1.010 V.I.Golish, E.I.Karpenko, V.G.Lukiachshenko, V.E.Messerle, V.Zh.Ushanov, A.B.Ustimenko
Long Life Arc Plasmatron
- P1.011 A. Gupta, M. Tokar
A model for type I ELMs
- P1.012 A. Punjabi, H. Ali
Construction of the equilibrium generating function and an area-preserving map for the DIII-D shot 115467 at 3000 ms
- P1.013 A.S. Kukushkin, H.D. Pacher, V. Komarov, M. Merola, V. Kotov, D. Reiter, G.W. Pacher
Physics Analysis of Divertor Modifications in ITER
- P1.014 A.Vesel, A.Drenik, I.Poberaj, M.Balat – Pichelin, M.Passarelli, M.Mozetic
Oxidation of graphite with neutral oxygen atoms at elevated temperature
- P1.015 B. Bazylev, Y. Igitkhanov, G. Janeschitz
Simulation of Hot-Spot Formation at ITER Vessel Surface during Multiple Transient Events
- P1.016 A.B. Kukushkin, P.V. Minashin, V.S. Neverov
Similarity of Spatial Distributions of Net Electron Cyclotron Power Losses in Fusion Plasmas
- P1.017 A. Casati, C. Bourdelle, X. Garbet, F. Imbeaux, J. Candy, F. Clairet, G. Dif-Pradalier, G. Falchetto, T. Gerbaud, V. Grandgirard, P. Hennequin, R. Sabot, Y. Sarazin, L. Vermare, R. Waltz
Towards an improved first principle based transport model
- P1.018 A. Kendl, B.D. Scott
Gyrofluid Simulations of the Ideal Ballooning ELM Scenario
- P1.019 B.F. McMillan, S. Jolliet, T.M. Tran, L. Villard, A. Bottino, P. Angelino
Avalanche-like bursts in global gyrokinetic simulations
- P1.020 C. Morize, P. Hennequin, G. Ciraolo, Ph. Ghendrih, X. Garbet, Y. Sarazin, P. Tamain
Eulerian and Lagrangian statistical analysis of SOL turbulent transport
- P1.021 C. Silva, H. Figueiredo, I. Nedzelskij, H. Fernandes, P. Duarte, C. Hidalgo, M.A. Pedrosa, G. van Oost, A. Melnikov, C. Gutierrez-Tapia
Structure of the ISTTOK edge plasma fluctuations
- P1.022 E. Trier, P. Hennequin, L.-G. Eriksson, C. Fenzi, C. Bourdelle, G. Falchetto, X. Garbet, T. Aniel, F. Clairet, F. Imbeaux, R. Sabot
Direct measurement of the radial electric field in a tokamak with magnetic field ripple
- P1.023 Eun-jin Kim, J. Douglas, A. Thyagaraja, A.P. Newton
Transport barriers in magnetohydrodynamic turbulence
- P1.024 F. A. Marcus, I. L. Caldas, Z. O. Guimaraes-Filho
Transport Control Through Modified Electric Field

- P1.025 F. Castejón, D. López-Bruna, T. Estrada
Island healing and CERC formation in the TJ-II stellarator
- P1.026 F. Lepreti, V. Carbone, M. Spolaore, V. Antoni
Yaglom relation for electrostatic turbulence in the RFX reversed field pinch
- P1.027 G. Fuhr, S. Benkadda, P. Beyer, X. Garbet, I. Sandberg, H. Isliker
Self-organization of electromagnetic turbulence in plasma edge
- P1.028 G.Kamberov, L.Popova, P.Marinov, V.Hristov
Self-Organization of Plasma Transport
- P1.029 H. Isliker
Anomalous particle and heat transport modeled by the combined random walk in position and momentum space
- P1.030 H.M.Smith,E.Verwichte
Hot tail runaway electron generation in tokamak disruptions
- P1.031 I. Calvo, R. Sanchez,B.A. Carreras, B.Ph. Van Milligen
Fractional generalization of Fick's law. Derivation through Continuous-Time Random Walks
- P1.032 I. Pusztai, T. Fülöp, P. Helander
On the quasilinear transport fluxes driven by microinstabilities in tokamaks
- P1.033 J. Anderson, E. Kim
Non-perturbative models of intermittency in ITG drift wave turbulence with zonal flows
- P1.034 F. Meo, H. Bindslev, S. B. Korsholm, F. Leuterer, F. Leipold, P. K. Michelsen, S. K. Nielsen, M. Salewski, J. Stober, D. Wagner, P. Woskov, ASDEX Upgrade team
Commissioning and First Results of the Fast Ion Collective Thomson Scattering Diagnostic on ASDEX Upgrade
- P1.035 J.L.Velasco, F.Castejón, A.Tarancón
Non-diffusive effects in ion collisional transport in TJ-II
- P1.036 K. Hallatschek
Diamagnetic GAM Drive Mechanism
- P1.037 K. Rypdal, T. Zivkovic
Low-dimensional chaotic convection dynamics in the Helimak configuration
- P1.038 M.J.Pueschel, L.Laborde, F.Jenko
GENE simulations on the beta dependence of tokamak core turbulence
- P1.039 M.Onofri, F.Malara, L.Primavera, P.Veltri
Anisotropic turbulence in nonlinear magnetic reconnection
- P1.040 P. Morel, R. Klein, E. Gravier, N. Besse, P. Bertrand
Water bag modelling of a multi-species plasma
- P1.041 R. Klein, P.Morel, N.Besse, E.Gravier, P.Bertrand
ITG and collisional drift-waves in cylindrical geometry with a gyrowaterbag model
- P1.042 R. Sanchez, J.N. Leboeuf, D.E. Newman, V. Decyk, B.A. Carreras
Understanding non-diffusive transport in gyrokinetic simulations of electrostatic turbulence in tokamaks

- P1.043 S.Marsen, M.Endler, M.Otte, F.Wagner
Overview of Turbulence Studies in the WEGA Stellarator
- P1.044 T. Gerbaud, C. Bourdelle, L. Vermare, P. Hennequin, F. Imbeaux, T. Aniel, J. Candy, A. Casati, F. Clairet, G. Falchetto, C. Fenzi-Bonizec, S. Heuraux, R. Waltz
Collisionality scaling of confinement and turbulence in Tore Supra
- P1.045 V.P. Pastukhov, N.V. Chudin
Turbulence reduction and cross-field transport control by means of non-central plasma heating in tokamaks
- P1.046 A. Ajendouz, Th. Pierre, D. Saifaoui, K.Qotb A. Dezairi, A. Rouak ,M.El Moudden
Contribution to the experimental and theoretical study of instabilities in a toroidal confined plasma configuration
- P1.047 A.D. Beklemishev
Correlation of Parallel and Transverse Transport in Langmuir Turbulence
- P1.048 A. Eriksson, J. Weiland, Y. Liu, L. Garzotti
Resonance effects on turbulent particle pinches
- P1.049 A. Fukuyama, M. Miki
Dynamic Transport Simulation in Helical Plasmas
- P1.050 A.I. Smolyakov, S.I. Krashennnikov
Generation of meso-scale structures by drift-wave interactions
- P1.051 A. Biancalani, L. Chen, F. Pegoraro, F. Zonca
Continuum spectrum of shear Alfvén waves in the presence of a magnetic island
- P1.052 F.M. Poli, S.E. Sharapov
Study of the spectral characteristics and the nonlinear evolution of ELMs on JET using a wavelet analysis
- P1.053 I.V. Khalzov, V.I. Ilgisonis, A.I. Smolyakov
Coupling of Waves with Positive and Negative Energy as a Universal Mechanism for MHD Instabilities of Flowing Media
- P1.054 K. Toi, F. Watanabe, T. Tokuzawa, T. Ido, A. Shimizu, K. Ida, S. Ohdachi, S. Sakakibara, S. Yamamoto, H. Funaba, S. Inagaki, M. Isobe, S. Morita, K. Nagaoka, K. Narihara, Y. Narushima, M. Osakabe, K. Tanaka, K.Y. Watanabe
Nonlinear Interaction between Alfvén Eigenmode and Geodesic Acoustic Mode Excited by Energetic Ions in the Large Helical Device
- P1.055 M. Garcia-Muñoz, H.-U. Fahrbach, S. Günter, V. Igochine, M.-J. Mantsinen, M. Maraschek, P. Martin, S.-D. Pinches, P. Piovesan, K. Sassenberg, H. Zohm
Observation and modelling of fast ion losses due to high frequency MHD perturbations in the ASDEX Upgrade tokamak
- P1.056 M. Isobe, K. Toi, Y. Yoshimura, A. Shimizu, Y. Todo, K. Ida, C. Suzuki, T. Akiyama, T. Minami, K. Nagaoka, S. Nishimura, K. Matsuoka, S. Okamura
Energetic-particle modes driven by suprathermal electrons in second harmonic ECRH plasmas of the Compact Helical System
- P1.057 M.K. Lilley, S.E. Sharapov, H.M. Smith, R. Akers
Modelling of beam-driven high frequency compressional Alfvén eigenmodes in MAST

- P1.058 M.Lennholm, L.G.Eriksson, F.Turco, F.Bouquey, C.Darbos, R.Dumont, G.Giruzzi, R.Lambert, R.Magne, D.Molina, P.Moreau, F.Rimini, J.L. Segui, S.Song, E.Traisnel
Destabilisation Of Fast Ion Stabilised Sawteeth Using Electron Cyclotron Current Drive
- P1.059 S.A. Sabbagh, J.M. Bialek, R.E. Bell, J.W. Berkery, O.N.Katsuro-Hopkins, J.E. Menard, R.Betti, D.A.Gates, B.Hu, B.P. LeBlanc, J.Manickam, K.Tritz
Global MHD Mode Stabilization Research on NSTX
- P1.060 V.D. Pustovitov
Tokamak plasma response to asymmetric magnetic perturbations
- P1.061 V.I. Tereshin, P.Ya. Burchenko, S.P. Gubarev, G.G. Lesnyakov, A.V. Lozin, S.M. Maznichenko, V.E. Moiseenko, F.I. Ozhereliev, G.P. Opaleva, V.K. Pashnev, Yu.F. Sergeev, A.N. Shapoval, O.M. Shvets, V.S. Taran, S.A.Tsybenko, E.D. Volkov, M.I. Zolototrubova
First Results of Uragan-2M Torsatron
- P1.062 V. Igochine, O.Dumbrajs, H. Zohm
Sawtooth Crash as a Result of Quasiperiodic Transition to Chaos in ASDEX Upgrade
- P1.063 A.M.Popov
Excitation of Neoclassical Tearing Modes During Pellet Injection in the Presence of Error Field in ITER
- P1.064 W. Zwingmann
Three-dimensional magnetic field calculation for a localised current distribution in unbounded space
- P1.065 H. Thomsen, P.J. Carvalho, S. Gori, U.v. Toussaint, A. Weller, R. Coelho, H. Fernandes
Application of Neural Networks for Fast Tomographic Inversion on Wendelstein 7-X
- P1.066 D. Chandra, O. Agullo, S. Benkadda, X. Garbet, A. Sen
GAMs like dynamics due to nonlinear interaction of multiple NTMs in tokamaks
- P1.067 D.Testa, P.Blanchard, A.Fasoli, A.Klein, T.Panis, J.A.Snipes, JET-EFDA contributors
Measurement of the Damping Rate of High-n Toroidal Alfvén Eigenmodes in JET
- P1.068 N.V. Ivanov, A.N. Chudnovskiy, A.M. Kakurin, I.I. Orlovskiy
Analysis of T-10 Data on Magnetic Island Dynamics Using the TEAR Code
- P1.069 P. Buratti, C.D. Challis, M. Gryaznevich, T.C. Hender, E. Joffrin, T. Luce, P. Smeulders, JET-EFDA contributors
Radial analysis of beta-limiting modes in JET
- P1.070 A. Hojabri, F. Hajakbari, M. Ghoranneviss, M.K. Salem
Energy Limit of Runaway Electrons in the Iran Tokamak 1 IR-T1
- P1.071 M. Cecconello, L. Frassinetti, M. W. M. Khan, K. E. J. Olofsson, P. R. Brunzell
Resistive tearing modes dynamics with plasma control in a reversed field pinch
- P1.072 S. Yu. Medvedev, A.A. Ivanov, A.A. Martynov, Yu. Yu. Poshekhonov, R. Behn, Y.R. Martin, A. Pochelon, O. Sauter, L. Villard
Beta limits and Edge Stability for Negative Triangularity Plasma in TCV Tokamak
- P1.073 D. Keeling, R. Akers, C.D. Challis, G. Cunningham, H. Meyer
Tailoring the q-profile on MAST for scenario optimisation
- P1.074 J.A. Snipes, M. Greenwald, A. Hubbard, J. W. Hughes, B. LaBombard, J. E. Rice

Plasma Current Dependence of the H-mode Threshold Low Density Limit on Alcator C-Mod

- P1.075 J.K. Anderson, B.E. Chapman, F. Bonomo, K. Caspary, D. Craig, D.J. Den Hartog, F. Ebrahimi, D.A. Ennis, G. Fiksel, P. Franz, R.M. Magee, R. O'Connell, S.C. Prager, J.A. Reusch, J.S. Sarff, H.D. Stephens, M.D. Wyman
High Confinement, High beta Plasmas in the MST RFP
- P1.076 J. Miyazawa, R. Sakamoto, H. Yamada, M. Kobayashi, S. Masuzaki, T. Morisaki, N. Ohyaabu, A. Komori, O. Motojima, the LHD experimental group
Fusion triple product and the density limit of high-density internal diffusion barrier plasmas in LHD
- P1.077 M. Sempf, P. Merkel, E. Strumberger, S. Günter
Robust control of resistive wall modes using pseudospectra, with application to ITER
- P1.078 Q. Yu, S. Günter
Neoclassical tearing modes its locking by error fields and stabilization by RF current
- P1.079 S.A. Bozhenkov, M. Lehnen, K.H. Finken, M.W. Jakubowski, R. Jaspers, R.C. Wolf, S. Abdulaev, M. Kantor, G. van Wassenhove, D. Reiter
Runaway electrons after massive gas injections in TEXTOR importance of the gas mixing and of the resonant magnetic perturbations
- P1.080 S.V. Lebedev, L.G. Askinazi, F.V. Chernyshev, V.E. Golant, M.A. Irzak, V.A. Kornev, S.V. Krikunov, A.D. Melnik, D.V. Razumenko, V.V. Rozhdestvensky, A.A. Rushkevich, A.I. Smirnov, A.S. Tukachinsky, M.I. Vid'junas, N.A. Zhubr
Low Density LH Transition Triggered by Counter-NBI in the TUMAN-3M Tokamak
- P1.081 E. Westerhof, J.W. Oosterbeek, M. de Baar, M.A. van den Berg, W.A. Bongers, A. Bürger, M.F. Graswinckel, R. Heidinger, B.A. Hennen, J.A. Hoekzema, S.B. Korsholm, O.G. Kruijt, B. Lamers, F. Leipold, D.J. Thoen, B.C.E. Vaessen, P.M. Wortman, TEXTOR-Team
The TEXTOR line-of-sight ECE system for feedback controlled ECRH power deposition
- P1.082 E.Z. Gusakov, N.V. Kosolapova, S. Heuraux
Turbulence wave number spectra reconstruction using radial correlation reflectometry.
- P1.083 I.V. Moskalenko, N.A. Molodtsov, D.A. Shcheglov, D.A. Shuvaev
Laser-Induced Fluorescence Method for Measurements of Helium and Impurities in ITER Divertor Plasmas. *Advantages and Problems of LIF System.*
- P1.084 K. W. Hill, M. L. Bitter, S. Scott, A. Ince-Cushman, M. Reinke, J. E. Rice, P. Beiersdorfer, M-F Gu, S. G. Lee, Ch. Broennimann, E. F. Eikenberry
Ion-Temperature and Rotation-Velocity Profile Measurements from a Spatially Resolving X-Ray Crystal Spectrometer on the Alcator C-Mod Tokamak
- P1.085 M. Yoshikawa, Y. Miyata, T. Matsumoto, M. Noto, M. Mizuguchi, Y. Yoneda, S. Negishi, N. Imai, K. Kimura, Y. Shima, S. Goshu, M. Nakada, Y. Oono, A. Itakura, H. Hojo, T. Imai
Fluctuation measurements during the formation of potential confinement in GAMMA 10
- P1.086 P. Khorshid, M. Razavi, M. Molaii
Measurment of Plasma Displacements during resonance helical field application in IR-T1 Tokamak
- P1.087 V. Yavorskij, V. Goloborod'ko, L.-G. Eriksson, V. Kiptily, K. Schoepf, S.E. Sharapov
Results of predictive Fokker-Planck modeling of fusion alpha particles in ITER
- P1.088 Y. Podoba, I. Bondarenko, A. Chmyga, G. Deshko, S. Khrebtov, A. Komarov, A. Kozachok, L. Krupnik, A. Melnikov, M. Otte, S. Perfilov, M. Schubert, F. Wagner, A. Zhezhera

HIBP on WEGA Calibration and Measurements

- P1.089 T. Kudyakov, K.H. Finken, M. Jakubowski, M. Lehnen, Y. Xu, S. Bozhenkov, O. Willi
Measurements of the runaway electron spectrum in the TEXTOR tokamak
- P1.090 H.K. Park, C.W. Domier, I. Classen, A.J.H. Donné, R. Jaspers, G.J. Kramer, N.C. Luhmann, Jr., M. Kwon, E.J. Valeo, M.J. Van de Pol
2-D Microwave Imaging Projects on Tokamak Plasmas
- P1.091 F.S. Zaitsev, D.P. Kostomarov, E.P. Suchkov
Existence of substantially different solutions in an inverse problem of plasma equilibrium reconstruction
- P1.092 A.A. Lukianitsa, F.S. Zaitsev, S.V. Nosov
Processing of magnetic diagnostics data using Hidden Markov Models
- P1.093 F.S. Zaitsev, A. Gondhalekar, T.J. Johnson, V.G. Kiptily, A.A. Korotkov, S.E. Sharapov, JET EFDA contributors
Simulations to elucidate suprathreshold deuterium ion tail observed in He3 minority ICRF heated JET plasmas
- P1.094 D. Jimenez-Rey, B. Zurro, J. Guasp, M. Liniers, C. Fuentes, G. Garcia, L. Rodríguez-Barquero, A. Baciero, A. Fernández, A. Cappa, R. Jiménez-Gómez, M. García-Munoz
Fast Ion Losses Behaviour in the TJ-II stellarator
- P1.095 L. Barrera, E. de la Luna, F. Castejon, L. Figini, JET-EFDA contributors
Comparison of the inboard and outboard Type I ELM dynamics in JET
- P1.096 M. Schubert, A. Popov, S. Heuraux, E. Gusakov
Reconstruction of the turbulence density fluctuation profile from reflectometry phase fluctuation measurements revisited.
- P1.097 A.K. Ram, J. Decker
Relativistic Effects in Electron Cyclotron Resonance Heating and Current Drive
- P1.098 A.V. Anikeev, P.A. Bagryansky, A.S. Donin, A.A. Ivanov, A.V. Kireenko, K.Yu. Kirillov, M.S. Korzhavina, A.A. Lizunov, V.V. Maximov, S.V. Murakhtin, E.I. Pinzhenin, V.V. Prikhodko, V.Ya. Savkin, E.I. Soldatkina, A.L. Solomakhin
Steady-state confinement of hot ion plasma in the gas dynamic trap
- P1.099 J. Decker, A. K. Ram, Y. Peysson, S. Coda, L. Curchod, A. Pochelon
Electron Bernstein Waves Heating and Current Drive in Axisymmetric Toroidal Plasmas
- P1.100 JaeChun Seol
Nonlinear interactions between cold electrons and the microwaves at cyclotron resonances
- P1.101 P. T. Lang, B. Alper, D. Frigione, K. Gál, G. Kocsis, K. Lackner, T. Loarer, M. Maraschek, G. Saibene, T. Szepesi, R. Wenninger, H. Zohm, ASDEX Upgrade Team, JET-EFDA contributors
Pellet investigations related to ITER ELM pacing and particle fuelling
- P1.102 V. Vdovin
Electron Cyclotron Plasma Heating second harmonic modelling with full wave code in middle tokamaks and ITER
- P1.103 W. Kraus, M. Berger, H.-D. Falter, U. Fantz, P. Franzen, M. Fröschele, B. Heinemann, Ch. Martens, P. McNeely, R. Riedl, E. Speth, A. Stäbler
Development of RF driven H-/D- sources for ITER

- P1.104 G. Van Wassenhove, P. Dumortier, A. Lysoivan, A. Messiaen, M. Vervier, O. Schmitz, B. Unterberg, TEXTOR team
ICRF antenna coupling in different heating scenarios and impact of phasing during experiments on TEXTOR
- P1.105 S.Morita
Systematic study of impurity pellet injection with Z 6-42 for improvement of plasma performance in LHD
- P1.106 V. Petrzilka, M. Goniche, F. Clairet, G. Corrigan, P. Belo, J. Ongena
On SOL Variations as a Function of LH Power
- P1.107 J.M.García-Regaña,F.Castejón,A.Cappa,M.Tereshchenko
Linear Estimation of Electron Bernstein Current Drive in inhomogeneous plasmas
- P1.108 P.M. Ryan, R.E. Bell, L.A. Berry, P.T. Bonoli, R.W. Harvey, J.C. Hosea, E.F. Jaeger, B.P. LeBlanc, C.K. Phillips, G. Taylor, E.J. Valeo, J.B. Wilgen, J.R. Wilson, J.C. Wright, H. Yuh
Improved HHFW Heating And Current Drive At Long Wavelengths On NSTX
- P1.109 A.R. Polevoi, A.S. Kukushkin, W. Houlberg, S. Maruyama, K. Gal, P. Lang, B. Pegourie, H. Nehme, M. Sugihara, A. Loarte, D. Campbell, V.A.Chuyanov
Assessment of Pumping Requirements in ITER for Pellet Fuelling and ELM Pace Making
- P1.110 V.B. Minaev, B.B. Ayushin, A.G. Barsukov, F.V. Chernyshev, V.K. Gusev, G.S. Kurskiev, M.I. Mironov, A.A. Panasenkov, M.I. Patrov, Yu.V. Petrov, V.A. Rozhansky, N.V. Sakharov, I.Yu. Senichenkov, G.N. Tilinin, S.Yu. Tolstyakov, V.I. Varfolomeev, E.G. Zhilin
Progress in the Neutral Beam Heating Experiment on the Globus-M Spherical Tokamak
- P1.112 A.V.Burdakov, A.A.Ivanov, E.P.Kruglyakov
Axially symmetric magnetic mirror traps. Recent progress in plasma confinement and heating.
- P1.113 B. Coppi, F. Bombarda, P.Detragiache, A. Airoidi, G. Cenacchi
Novel Developments for Fusion Research and the Ignitor Approach
- P1.114 S.Ryzhkov
Modeling and engineering applications for wEAKLY turbulent plasma
- P1.115 L.P. Babich, A.M. Buyko, S.F. Garanin, A.V. Ivanovskiy, A.I. Kuzyayev, V.I. Mamyshev, V.N. Mokhov, E.S. Pavlovskiy, A.A. Petrukhin, V.Sh. Shaidulin, V.K. Chernyshev, V.B. Yakubov
Experimental research of implosion of plasma liners of the magnetocascade system for thermonuclear target heating
- P1.116 A.M. Buyko, B.E. Grinevich, S.F. Garanin, Yu.N. Gorbachev, A.V. Ivanovskiy, A.I. Kuzyayev, V.I. Mamyshev, V.N. Mokhov, A.A. Petrukhin, V.K. Chernyshev, V.B. Yakubov
Experiments with solid liners for further compression of heated plasma in MAGO system
- P1.117 A. Kasperczuk, T. Pisarczyk, M. Kalal, J. Ullschmied, E. Krousky, K. Masek, M. Pfeifer, K. Rohlena, J. Skala, P. Velarde, M. Gonzalez, C. Gonzalez, E. Oliva, P. Pisarczyk
Direct and indirect methods of the plasma jet generation
- P1.118 T. Pisarczyk, A. Kasperczuk, M. Kalal, J. Ullschmied, E. Krousky, K. Masek, M. Pfeifer, K. Rohlena, J. Skala, P. Pisarczyk
Characteristics of the plasma jet generated from a joint of materials with different atomic number
- P1.119 N. Naumova, C. Labaune, T Schlegel, V.T. Tikhonchuk, G. Mourou, I.V. Sokolov

Hole boring through overdense plasmas using multiple ultrahigh intensity laser pulses

- P1.120 V.S. Belyaev, A.P. Matafonov, V.I. Vinogradov
Relativistic Magneto-Active Laser Plasmas
- P1.121 Cheng Wang , Haiyang Lu, Guanglong Chen, Guoquan Ni, Jiansheng Liu, Ruxin Li, Zhizhan Xu
Nuclear Fusion in Deuterated Methane-Cluster Jets Irradiated by Intense Femtosecond Laser Pulses
- P1.122 G.C. Androulakis, M. Bakarezos E.L. Clark, J. Chatzakis, A. Gopal, S.M. Hassan, J. Kaliakatsos, S. Minardi, C. Petridis, M. Psimopoulos, A. Skoulakis, E. Tzianaki, N.A. Papadogiannis, M. Tatarakis
A new Centre for Plasma Physics and Lasers
- P1.123 I. Ploumistakis, I. Tsohantjis, S. D. Moustazis
New approaches on Laser Vacuum Breakdown for Pair Creation
- P1.124 V. Stancalie, V. Pais
Parametrisation of 2pns IP0 resonance structures in C4
- P1.125 V.I. Zaitsev, V.G. Novikov, I. Yu.Vichev, G.S. Volkov, A.D. Solomyannaya
Study of the x-ray spectrum of the heavy-ion z-pinch.
- P1.126 O. Renner, L. Juha, J. Krasa, E. Krousky, C. Granja, V. Linhart, A.A. Andrejev
Search for Low-Energy Nuclear Transitions in LPP
- P1.127 J. Wolowski, J. Badziak, A. Czarnecka, P. Parys, M. Rosinski, R. Turan, S. Yerci
The laser-produced plasma as a modern repetitive ion source for technological applications
- P1.128 R.M.G.M. Trines, R. Bingham, R.A. Cairns, L.O. Silva, P.A. Norreys
Numerical studies of Raman amplification of laser pulses in plasma
- P1.129 A.V. Glushkov, O. Yu. Khetselius
QED theory of radiation emission and absorption lines for atoms and ions of plasma in a strong electromagnetic field
- P1.130 L. O. Silva, B. Brandão, J. E. Santos, R. Bingham
Transverse modulational instability of intense white light in plasmas
- P1.131 B. Dromey, S.G. Rykovanov, D. Adams, R. Hörlein, Y. Nomura, P.S. Foster, S. Kar, K. Markey, D. Neely, M. Geissler, G.D. Tsakiris, M. Zepf
Bright coherent XUV harmonic emission from intense laser solid interactions
- P1.132 D. S. Whittaker, M. Fajardo, Ph. Zeitoun, G. Faivre, J. Gautier, A. S. Morlens, E. Oliva, S. Sebban, K. Cassou, D. Ros, P. Velarde, H. Merdji, J.P. Caumes, M. Kos, B. Rus, T. Mocek et al, A. L'huillier, O. Guillbaud
Reduced Extreme Ultra-Violet Pulse Durations Resulting from High-Harmonic Seeding of Suitably Tailored Plasma Gain Media.
- P1.133 Hui-Chun Wu, Jürgen Meyer-ter-Vehn
Phase-sensitive Terahertz Plasma Emission from Gas Targets Irradiated by Few-cycle Intense Laser Pulses
- P1.134 M. Zepf, B. Dromey, D. Adams, R. Hörlein, Y. Nomura, S. G. Rykovanov , D. C. Carroll, P.S Foster, M. Geissler, S. Kar, K. Markey, P. McKenna, D. Neely, G.D. Tsakiris
Near Diffraction Limited XUV Harmonics
- P1.135 S. Bastiani-Ceccotti, P. Renaudin, F. Dorchies, M. Harmand, E. Brambrink, M. Geissler, M. Koenig, O. Peyrusse,

- P. Audebert
Temporal and spectral behavior of sub-picosecond laser-created X-ray sources
- P1.136 Sepehri Javan N.
Free electron laser with relativistic electron bunches and a longitudinal electrostatic wiggler
- P1.137 B. Ersfeld, D.A. Jaroszynski
Thermal effects on Raman amplification in plasma
- P1.138 E. Abreu, M. Fajardo
Plasma density periodic modulation generated by a two-lasers interference pattern
- P1.139 E. Abreu, N. Timneanu, J. Hajdu
Proton acceleration in an x-ray Free Electron Laser
- P1.140 E. Brambrink, B. Brabrel, A. Benuzzi, T.Bohley, T. Endo, C. Gregory, T. Kimura, M. Rabec le Gloahec, H. G. Wei, M. Koenig
Short pulse laser driven hard x-ray sources for radiography of shocked matter
- P1.141 E. Oliva, P. Zeitoun, P. Velarde, K. Cassou, M. Fajardo, C. García-Fernández
Hydrodynamic and ray-tracing simulation of Seeded Soft X-Ray Laser amplifying stages.
- P1.142 I.F. Shaikhislamov, V.M. Antonov, E.L. Boyarintsev, V.G. Posukh, A.V. Melekhov, Yu.P. Zakharov, A.G. Ponomarenko
Charge-Exchange of Laser-Produced Ions on a Pulsed Gas Jet
- P1.143 M. Tamas, P. Vrba, M. Vrbova
Influence of wall material on soft X-ray radiation from discharge in nitrogen filled capillary
- P1.144 S. Cipiccia, A. Reitsma, D. Jaroszynski
X-ray production techniques using laser-plasma accelerators
- P1.145 S.G. Rykovanov, M. Geissler, Y. Nomura, R. Hoerlein, J. Schreiber, J. Meyer-ter-Vehn, G.D. Tsakiris
Properties of the harmonic emission from the interaction of intense laser pulses with overdense plasma
- P1.146 J. Meyer-ter-Vehn, H.-C. Wu
Dense Relativistic Electron Layers from Nanometer Foils surfing on Few-cycle multi-TW Laser Pulses
- P1.147 M. P. Anania, S. B. van der Geer, M. J. de Loos, A. J. W. Reitsma, D. A. Jaroszynski
Beam transport of ultra-short electron bunches
- P1.148 M. Tanimoto, K. Koyama, E. Miura, S. Kato, N. Saito, M. Adachi
The trapped particle sideband instability observed in laser-plasma accelerator experiments
- P1.149 N. Lemos, J. Berardo, R. Onofrei, N. Lopes, G. Figueira, F. Fiuza, L.O. Silva, J.G. Gallacher, R.C. Issac, D. A. Jaroszynski, J. M. Dias
Transverse dynamics of a plasma column created by field ionization
- P1.150 X. Yang, A. Lyachev, B. Ersfeld, E. Brunetti, G. Vieux, D.A. Jaroszynski
Amplification of short laser pulses based on Raman backscattering in plasma
- P1.151 L.P. Babich, I.M. Beketov, Î.M. Burenkov, V.K. Chernyshev, Yu.N. Dolin, P.V. Duday, V.I. Dudin, V.À. Ivanov, A.V. Ivanovsky, G.V. Karpov, V.P. Korchagin, A.I. Kraev, V.B. Kudel'kin, I.M. Markevtsev, O.D. Mikhailov, A.N. Moiseenko, I.V. Morozov, S.V. Pak, S.M. Polyushko, V.N. Romaev, A.N. Skobelev, V.A. Tokarev, V.Sh.

- Shaidullin, V.I. Shpagin., À.À. Volkov, G.I. Volkov, T.I. Volkova, À.À. Zabiralov
Experiments on prolong plasma confinement with the fusion chamber MAGO
- P1.152 M.V. Petrenko, I.V. Kuznetsova, Z.A. Stepanova, G.K. Tumakaev, S.V. Bobashev
Effective EUV radiation source based on laser-produced plasma in supersonic xenon jet and ways of its optimization.
- P1.153 A.Berbri, M.Tribeche
Weakly nonlinear ion acoustic double layers in a dusty plasma with non thermal electrons
- P1.154 R. Kompaneets, A.V. Ivlev, U. Konopka, V. Tsytovich, S.V. Vladimirov, G. Morfill
Screening of a charged dust particle in the rf plasma-wall transition layer
- P1.155 B.Klumov, S.V.Vladimirov, G.E.Morfill
Molecular dynamics simulations of a mesoscopic system of charged dust particles
- P1.156 B. P. Pandey, A. Samarian, S.V. Vladimirov
Dust motion in flowing magnetized plasma
- P1.157 D.J. Kedziora, S.V. Vladimirov, A.A. Samarian
Influence of the nature of charge fluctuations on dust cluster oscillation spectrum
- P1.158 A.M. Ignatov, S.A. Maiorov, P.P.J.M. Schram, S.A.Trigger
Modelling of Dust Particle Charging in the Upper Atmosphere
- P1.159 E.M.Apfelbaum
The reconstruction of the effective interaction potential in dusty plasma
- P1.160 L.G. D'yachkov, M.M. Vasiliev, S.N. Antipov, O.F. Petrov, V.E. Fortov
Rotation inversion of dust plasma structures in magnetic fields in a dc discharge
- P1.161 M.M. Vasiliev, L.G. D'yachkov, S.N. Antipov, O.F. Petrov, V.E. Fortov
Dusty Plasma under Magnetic Field Action in DC Glow Discharges
- P1.162 F. Fendrych, P. Repa, L. Peksa, J. PoltieroVa Vejpravova, A. Lancok, K. Seemann
UHV Hollow Cathode Plasma Jet System for Nanostructured Magnetic Films Deposition
- P1.163 B.P. Pandey, S.V. Vladimirov, A. Samarian
Nonlinear waves in collisional dusty plasma
- P1.164 A. Drenik, M. Mozeti, A. Vesel, D. Babi, M. Balat - Pichelin
Influence of a substrate holder on a neutral hydrogen atom density in a plasma reactor
- P1.165 E. Scime, Z.Harvey, S.Chakraborty-Thakur, A. Hansen, R. A. Hardin, W.S. Przybysz
Comparison of Gridded Energy Analyzer and Laser Induced Fluorescence Measurements of a Two-Component Ion Distribution
- P1.166 A.Andrei, C. Lungu, G. Oncioiu, C. Diaconu
Plasma processing for improvement of structural materials properties
- P1.167 C. Stancu, A. C. Galca, G. Dinescu
Removal of Carbon Residuals from Narrow Spaces by RF Discharges
- P1.168 A. Anghel, I. Mustata

MgF2-Co magneto-resistance granular thin films prepared by thermo-ionic vacuum arc technique

- P1.169 A. M. Lungu, C. P. Lungu, A. Anghel, C. Porosnicu, I. Mustata, C. M. Ticos
Plasma processing of nanostructured Ni/Al/Co Films
- P1.170 C. Bellecci, P. Gaudio, S. Martellucci, M. Richetta, D. Toscano, I. Vulkay
Gas jet characterization of a laser plasma system emitting in EUV
- P1.171 C. M. Ticos, C. P. Lungu, C. Surdu-Bob, I. Mustata, V. Zaroschi, A. Anghel, C. Porosnicu
Deposition of magnetic materials on dust particles levitated in vacuum arc plasmas
- P1.172 C. P. Lungu, C. C. Surdubob
Vacuum arc carbon-metal co-deposition for antifriction coatings
- P1.173 C. P. Lungu, A. M. Lungu
Comparison of the low friction graphite-metal coatings prepared by thermionic vacuum arc and plasma spray methods
- P1.174 D. Mascali, L. Celona, G. Ciavola, S. Gammino, F. Maimone, L. Allegra, N. Gambino, R. Miracoli
Microwave absorption in dense and overdense plasmas generated in a Plasma Reactor for Environmental Applications
- P1.175 C. Bellecci, P. Gaudio, I. Lupelli, A. Malizia, M. T. Porfiri, M. Richetta
Dust mobilization and transport measures in the STARDUST facility
- P1.176 F. Pegoraro, M. Faganello, F. Califano
Fast magnetic reconnection in collisionless plasmas with velocity shear
- P1.177 B. Coppi
Vertical Transport and Thermo-rotational Instability in Astrophysical Plasma Disks
- P1.178 S. A. Koryagin
Electron-ion collisions in low-temperature plasma embedded in quantizing magnetic field
- P1.179 Z. Osmanov
Efficiency of the curvature drift instability in AGN winds
- P1.180 A. Biancalani, F. Pegoraro
Cherenkov emission of electron cyclotron waves by a magnetized satellite orbiting the ionosphere
- P1.181 Konstantin V. Khishchenko
Equations of state for metals at high temperatures and pressures
- P1.182 M. Mehdipoor
Effects of positron density and temperature on ion acoustic solitary waves in magnetized electron-positron-ion plasmas
- P1.183 N. Sternberg, C. Sataline, V. Godyak
Influence of Ramsauer effect on bounded plasmas in magnetic fields
- P1.184 A. Fasoli, A. Diallo, I. Furno, D. Iraj, B. Labit, G. Plyushchev, P. Ricci, C. Theiler, S. Müller, M. Podestà, F. M. Poli
Fluctuations, turbulence and related transport in the TORPEX simple magnetized toroidal plasma

- P1.185 A.L. Khomkin, A.S. Shumikhin
Equation of state and conductivity of aluminum dense vapor plasma
- P1.186 A. Lejeune, L. Cherigier-Kovacic, F. Doveil
Study of hydrogen ion species in a multicusp ion source
- P1.187 A.V.Gavrikov, V.E.Fortov, O.F.Petrov, N.A.Vorona, M.N.Vasiliev
Investigation of electron beam charging of dust particles
- P1.188 B. Teaca, V. Remacle, C. Lalescu, C. Toniolo, B. Weysow
Test Particle Transport in Turbulent Electromagnetic Fields
- P1.190 M. E. Koepke, S. M. Finnegan, D. J. Knudsen, S. Vincena
Space-Plasma Campaign on stationary inertial Alfvén waves
- P1.191 A. Fredriksen, H.S. Byhring, C. Charles, L.N. Mishra, R. Boswell
Double layer beam formation in the Njord device and its dependence on magnetic field configuration.
- P1.192 A.G. Ponomarenko, V.M. Antonov, E.L. Boyarintsev, A.V. Melekhov, V.G. Posukh, I.F. Shaikhislamov, K.V. Vchivkov, Yu.P. Zakharov
Laboratory Simulation of Extreme Magnetosphere Compression under Impact of a Giant Coronal Mass Ejection
- P2.001 B. Kurzan, A. Scarabosio, M. Gemisic-Adamov
Large scale inter-ELM fluctuations in the pedestal and the density limit in ASDEX Upgrade
- P2.002 C. P. Lungu,
Plasma-wall erosion rate evaluation by markertile
- P2.003 E.M. Hollmann, J.A. Boedo, T.E. Evans, D.A. Humphreys, A. James, T.C. Jernigan, R.A. Moyer, P.B. Parks, D.L. Rudakov, E.J. Strait, M.A. van Zeeland, J.C. Wesley, W.P. West, W. Wu, J.H. Yu
Measurements of Injected Impurity Assimilation During Fast Shutdown Initiated by Multiple Gas Valves in DIII-D
- P2.004 E. M. Hollmann, P. S. Krstic, R. P. Doerner, D. Nishijima, A. Yu. Pigarov
Measurement and modelling of hydrogen molecule ro-vibrational accommodation on graphite
- P2.005 F. Bint-e-Munir, S. Kuhn, D.D. Tskhakaya sr.
Comprehensive study of a magnetised plasma-wall transition - MPWT
- P2.006 F. L. Waelbroeck
Formation of the velocity shear layer in the edge of a diverted tokamak
- P2.007 G.Pautasso, D.Coster, X.Bonnin
Modelling of massive gas injection with SOLPS
- P2.008 H. Ali, A. Punjabi
Robustness of Second Order Magnetic Barriers at Noble Irrationals in the ASDEX UG Tokamak
- P2.009 H.G. Frerichs, O. Schmitz, D. Harting, D. Reiter, B. Unterberg, Y. Feng, T.E. Evans, M.E. Fenstermacher, I. Joseph, R.A. Moyer
3D numerical analysis of magnetic topology and edge transport for TEXTOR-DED and DIII-D limiter configurations with resonant magnetic perturbations
- P2.010 H.W. Müller, A. Herrmann, B. Kurzan, R. Pugno, V. Rohde, M. Tsalias, M. Wischmeier, E. Wolfrum

From carbon to tungsten divertor plasmas in ASDEX Upgrade

- P2.011 J. Butikova, A. Sarakovskis, I. Tale
Laser-induced plasma spectroscopy of plasma facing materials
- P2.012 J.C. Fuchs, T. Eich, L. Giannone, A. Herrmann
Radiation Distribution in the Full Tungsten ASDEX Upgrade
- P2.013 J. Canik, R. Maingi, E.A. Unterberg, Y. Feng, D. Monticello, F. Sardei, M.C. Zarnstorff
Application of EMC3-EIRENE to NCSX
- P2.014 J. Cheng, L.W. Yan, W.Y. Hong, Adi Liu, J. Qian, K.J. Zhao, J.Q. Dong, H.L. Zhao
Turbulence Intermittency in the Scrape-off Layer of HL-2A Tokamak
- P2.015 J. P. Gunn, V. Fuchs
Quasineutral kinetic simulation of the scrape-off layer
- P2.016 A. Krämer-Flecken, S. Soldatov, D. Reiser, M. Jakubowski
Effect of Resonant Magnetic Perturbations on Zonal Flows and ambient Turbulence
- P2.017 A. Kuritsyn, A.F. Almagri, D.L. Brower, W.X. Ding, F. Ebrahimi, G. Fiksel, M. Miller, V.V. Mirnov, S.C. Prager, J.S. Sarff
Momentum Transport during Spontaneous Reconnection Events and Edge Biasing in the MST Reversed Field Pinch
- P2.018 A.R.Field, R.J.Akers, N.J.Conway, M-D.Hua, S.D.Pinches, M.Wisse
Momentum transport in MAST spherical tokamak plasmas
- P2.019 B. Nold, M. Ramisch, U. Stroth, H.W. Müller, V. Rohde
Comparison of Dimensionally Similar Turbulence in TJ-K and ASDEX Upgrade
- P2.020 B.P. Duval, A. Bortolon, A. Karpushov, A. Pochelon, O. Sauter, G. Turri
Effect of Sawteeth on the Spontaneous TCV Plasma Rotation
- P2.021 B.Ph. van Milligen, T. Kalhoff, M.A. Pedrosa, C. Hidalgo
Bicoherence and confinement transitions in TJ-II
- P2.022 C.-B. Kim
Response of MHD plasma to a parity-nonconserving driving noise
- P2.023 C. Crabtree, B. Coppi
Non-fluid Micro-Reconnecting Modes and Experimental Observations
- P2.024 C.F. Maggi, R.J. Groebner, A.W. Leonard, C.C. Petty, C. Konz, L.D. Horton, A.C.C. Sips
The role of the H-mode pedestal on global confinement in hybrid scenarios in DIII-D and ASDEX Upgrade
- P2.025 C. Ionita, R. Schrittwieser, C. Silva, P. Balan, H. Figueiredo, V. Naulin, J. Juul Rasmussen
Turbulence measurements with cold and emissive probes in ISTTOK
- P2.026 C. Mazzotta, M. Romanelli, O. Tudisco, L. Carraro, S. Cirant, L. Gabellieri, G. Granucci, M. Marinucci, M. Mattioli, S. Nowak, V. Pericoli, M.E. Puiatti, A. Romano, L. Lauro Taroni, FTU team
Particle Density behavior of electron heated plasmas in FTU
- P2.027 C. Riccardi, R. Barni, M. Arosio, M. Fontanesi

Plasma blob motion in the simple magnetised toroidal plasma of the Thorello device

- P2.028 D. Carralero, E. de la Cal, J.L. de Pablos, J.A. Alonso, M.A. Pedrosa, C. Hidalgo
Fast Imaging Experiments of Edge Transport in the TJ-II Stellarator
- P2.029 D.E. Newman, Debasmita Samaddar, R. Sanchez, B.A. Carreras
Impact of sheared flows on the fractional transport dynamics in a simple fluid drift-wave turbulence model
- P2.030 D. Lopez-Bruna, T. Estrada, F. Medina, E. de la Luna, E. Ascasibar, F. Castejon, V. I. Vargas
Effect of magnetic resonances in the effective electron heat transport of TJ-II ECH plasmas
- P2.031 D. Reiser
Zonal flow dynamics and GAM oscillations in tokamaks with Zonal flow dynamics and GAM oscillations in tokamaks with resonant magnetic field perturbations
- P2.032 D. Strintzi, A. G. Peeters, J. Weiland
The toroidal momentum diffusivity in a tokamak plasma a comparison of fluid and kinetic calculations
- P2.033 E. Anabitarte, O.F. Castellanos, M. Passas, J.M. Senties
First experimental results of statistical properties of turbulence plasma fluctuations in the SPLM upgrade
- P2.034 E. Belonohy, M. Hirsch, K. McCormick, G. Papp, G. Pokol, H. Thomsen, A. Werner, S. Zoletnik
Edge instabilities in the high density H-mode operation of W7-AS
- P2.035 E R Solano, K Rantamaki, T Tala
Plasma evolution towards critical equilibria and diamagnetism
- P2.036 Elina Asp, Jan Weiland, Stefano Alberti, Alessandro Bortolon, Basil Duval, Yves Martin, Laurie Porte, Olivier Sauter the TCV Team
Spontaneous rotation in TCV
- P2.037 F. Mehlmann, C. Ionita, H.W. Müller, P. Balan, A. Herrmann, A. Kendl, M. Maraschek, V. Naulin, A.H. Nielsen, J.J. Rasmussen, V. Rohde, R. Schrittwieser, ASDEX Upgrade Team
Radial transport in the L- and H-mode SOL of ASDEX Upgrade
- P2.038 G. Sonnino, Ph. Peeters, F. Zonca, G. Breyiannis
A Kinetic Model for the Collisional Diffusion Coefficients of Magnetically Confined Plasmas in the Low-collisional Regime
- P2.039 G. Sánchez Burillo, B. Ph. van Milligen, A. Thyagaraja
A study of radial tracer transport in a turbulent transport code
- P2.040 G. Van Oost, M. Gryasznevlch, H. Fernandes, C. Silva, A. Malaquias
Overview of results from the 3rd International Joint Experiment at Tokamak ISTTOK
- P2.041 H. Isliker, Th. Pisokas, L. Vlahos
An MHD compatible model for Self-Organized Criticality in toroidally confined plasma
- P2.042 H. Nordman, R. Singh, T. Fülöp, L.-G. Eriksson, R. Dumont, P. Strand, M. Tokar, J. Weiland
Anomalous Impurity Transport in Tokamaks in the Presence of RF Fields
- P2.043 I. Calvo, L. Garcia, B. A. Carreras, R. Sanchez, B. Ph. van Milligen
Pseudochaotic poloidal transport in toroidal geometry. Pressure-gradient-driven turbulence and plasma flow topology

- P2.044 I.E. Sarris, B. Cassart, D. Carati, N.S. Vlachos
Development of a numerical method for the modelling of nonlinear fusion plasma instabilities in Tokamaks
- P2.045 I.Sandberg,G.Fuhr,H.Isliker,K.Hizanidis,S.Benkadda,P.Beyer,X.Garbet
Intermittency in Resistive Ballooning Electromagnetic Turbulence
- P2.046 I.Yu. Senichenkov, V.A. Rozhansky, A.V. Bogomolov, V.K. Gusev, N.V. Sakharov, Yu.V. Petrov, V.B. Minaev, S.Yu Tolstyakov, M.I. Patrov, F.V. Chernyshev, B.B. Ayushin, G.S Kurskiev, the Globus-M team
Simulation of L and H regimes for spherical tokamak Globus-M with ASTRA transport code
- P2.047 J.M.Delgado
Diamagnetic effects in a simple transition model
- P2.048 J.M. Dewhurst, B. Hnat, N.Ohno, R.O. Dendy, S. Masuzaki, T. Morisaki, A. Komori, B.D. Dudson, G.F. Counsell, A. Kirk
Statistical properties of edge plasma turbulence in the Mega-Amp Spherical Tokamak and the Large Helical Device stellarator
- P2.049 J.M. Reynolds, D. Lopez-Bruna, J. Guasp, J.L. Velasco, A. Tarancon
Simulating drift kinetic electron-ion equation with collisions in complex geometry
- P2.051 A.Sengupta, A.Werner, M.Otte, J.Geiger
Fast recovery of vacuum configuration of WEGA stellarator with error field effects
- P2.052 P. Maget, G.T.A. Huysmans, H. Lütjens, Ph. Moreau, J.-L. Ségui
Evaluation of Two-Fluid effects on Double-Tearing Mode stability
- P2.053 K.Ichiguchi, B.A.Carreras
Numerical Analysis of Non-Resonant Pressure Driven Mode in Heliotron Plasma
- P2.054 F. Bonomo, D. Terranova, A. Alfier, M. Gobbin, R. Lorenzini, L. Marrelli, R. Pasqualotto
QSH in high current RFX-mod plasmas thermal and topological features
- P2.055 H. M. Smith, E. Verwichte, L. Appel, M. K. Lilley, S. D. Pinches, S. E. Sharapov
Two-dimensional compressional Alfvén eigenmode structure
- P2.056 L. Frassinetti, P. Brunzell, M. Cecconello, J. R. Drake, M. W. M. Khan, S. Menmuir, K.E.J. Olofsson
Active feedback control of QSH in EXTRAP-T2R
- P2.057 D. Apostolaki, G.N. Throumoulopoulos, H. Tasso
A contribution to the equilibrium and stability of axisymmetric plasmas with field aligned flow
- P2.058 S. P. Hirshman, R. A. Sanchez, V. E. Lynch, E. A. D'Azevedo
SIESTA A Scalable Iterative Equilibrium Solver for Toroidal Applications
- P2.059 D.P. Brennan, S.E. Kruger, R.J. La Haye
Flow Shear Effects on Resistive MHD Instabilities in Tokamaks
- P2.060 R. Takahashi, D.P. Brennan, C.C. Kim
Kinetic Effects of Energetic Particles on Resistive MHD Stability
- P2.061 F. Watanabe, K. Toi, S. Ohdachi, S. Sakakibara, S. Morita, K. Narihara, I. Yamada, Y. Narushima, T. Morisaki, C. Suzuki, K. Tanaka, T. Tokuzawa, K.Y. Watanabe
Ballooning Structure of Edge MHD Mode Observed in the Large Helical Device Plasmas with Externally

Applied Magnetic Perturbations

- P2.062 J. Geiger
Investigation of Wendelstein 7-X Configurations with Increased Toroidal Mirror
- P2.063 A.A. Martynov, S. Yu. Medvedev, L. Villard
Tokamaks with Reversed Current Density Stability of Equilibria with Axisymmetric Islands
- P2.064 M. Hölzl, S. Günter, Q. Yu
Heat Diffusion across Magnetic Islands and Ergodic Layers in Realistic Tokamak Geometry
- P2.065 G.T.A. Huysmans, R. Abgrall, R. Huart, B. Nkonga, S. Pamela, P. Ramet
Non-linear MHD code development for ELM simulations
- P2.066 V. Igochine, T. Bolzonella, M. Baruzzo, G. Marchiori, A. Soppelsa, D. Yadikin, H. Zohm
Externally Induced Rotation of the Resistive Wall Modes in RFX-MOD
- P2.067 F. Villone, T. Bolzonella, Y. Q. Liu, G. Marchiori, R. Paccagnella, G. Rubinacci, A. Soppelsa
RWM modelling in RFX-mod including 3D conducting structures
- P2.068 L. Urso, H. Zohm, A. Isayama, Y. Kamada
Fitting of the Modified Rutherford Equation a comparison between ASDEX Upgrade and JT-60U results
- P2.069 A.A. Ivanov, A.A. Martynov, S. Yu. Medvedev, D.A. Kislov, B.V. Kuteev, V.D. Pustovitov, A.M. Popov
Threshold Effects for Pellet-Plasma Interaction in Tokamak - MHD Modeling
- P2.070 G. Kocsis, A. Aranyi, V. Igochine, S. Kalvin, L. Lackner, P.T. Lang, M. Maraschek, V. Mertens, T. Szepesi
Investigation of pellet-driven plasma perturbations for ELM trigger studies
- P2.071 C. Konz, P.B. Snyder, N. Aiba, L.D. Horton, C.F. Maggi, S. Guenter, P.J. Mc Carthy, ASDEX Upgrade Team, DIII-D Team
Cross-Machine and Cross-Code Comparisons in Linear MHD Stability Analysis for Tokamaks
- P2.072 T. Voslion, O. Agullo, P. Beyer, S. Benkadda, X. Garbet
Nonlinear Interaction of Magnetic Islands In Presence of Shear Flow
- P2.073 T.C. Luce, E.J. Doyle, J.C. DeBoo, G.L. Jackson, T.A. Casper, J.R. Ferron, P.A. Politzer, M.R. Wade, R.J. Groebner, C.T. Holcomb, D.A. Humphreys, A.W. Hyatt, M. Murakami, T.W. Petrie, C.C. Petty, W.P. West
Simulation of ITER Operational and Startup Scenarios in the DIII-D Tokamak
- P2.074 V.E. Lukash, A.A. Kavin, R.R. Khayrutdinov, Y.V. Gribov, A.B. Mineev
Study of early phase of current ramp-up in ITER with DINA code
- P2.075 Y. Nakamura, H. Fujieda, N. Takei, S. Miyamoto, Y. Kusama, R. Yoshino
A Simulation Modelling of Inductive/Non-inductive Current Ramp-up at Slow Rate for Low l_i , High Vertical Stability
- P2.076 B. Wu, C.Y. Lin, Y.D. Pan
Discharge simulation of EAST first plasma
- P2.077 V. M. Leonov, V.E. Zhogolev
Possibility of scenarios with the ignition for ITER
- P2.078 T. Fulop, G. Pokol, H. Smith, P. Helander, M. Lisak

Magnetic field threshold for runaway generation in tokamak disruptions

- P2.079 T.A. Casper, J.R. Ferron, D.A. Humphreys, G.L. Jackson, J.A. Leuer, L.L. LoDestro, T.C. Luce, W.H. Meyer, L.D. Pearlstien, A.S. Welander
ITER Scenario Performance Simulations Assessing Control and Vertical Stability
- P2.080 F. Villone, R. Albanese, G. Ambrosino, Y.Q. Liu, A. Pironti, A. Portone, G. Rubinacci
RWM control in ITER including a realistic 3D geometry
- P2.081 D. Stutman, G. Caravelli, M. Finkenthal, G. Wright, D. Whyte, R. Kaita
Free-standing Diffractive Optical Elements as Light Extractors for Burning Plasma Experiments
- P2.082 N.Yamaguchi, S.Morita, M.B.Chowdhuri, M.Goto, H.Y.Zhou
Space-resolving flat-field EUV spectrograph for Large Helical Device
- P2.083 T.Pütterich, C.F.Maggi, L.D.Horton, R.Dux, B.Langer, E.Wolfrum
Fast CXRS-measurements in the Edge Transport Barrier of ASDEX Upgrade
- P2.084 S.G. Lee, J.G. Bak, U.W. Nam, M.K. Moon, J.K. Cheon
Calibration of advanced X-ray imaging crystal spectrometer for KSTAR tokamak
- P2.085 Y. Feng, J. Kisslinger, F. Sardei, D. Reiter
EMC3/EIRENE Transport Modelling of the Island Divertor in W7-X
- P2.086 F. Leipold, H. Bindslev, V. Furtula, S.B. Korsholm, F. Meo, P.K. Michelsen, M. Salewski
Fast Ion CTS Diagnostic for ITER - State of Design
- P2.087 S.I. Lashkul, A.B. Altukhov, A.O. Bogdanenko, E.O. Vekshina, V.V. Dyachenko, L.A. Esipov, S.V. Shatalin
Visualization of the Plasma Processes at Additional Lower Hybrid Heating on the FT-2 Tokamak
- P2.088 M.Wisse, N.J.Conway, J.F.G. McCone, D. Muir
Measurements of plasma rotation in the MAST tokamak
- P2.089 E. Gusakov, S. Heuraux, A. Popov
Nonlinear regime of Bragg backscattering leading to probing wave trapping and time delay jumps in fast frequency sweep reflectometry
- P2.090 B. Zurro, A. Baciero, V. Tribaldos, D. Jiménez-Rey
An Investigation on the Mechanisms for Differential Poloidal Rotation of Proton and Impurities in the TJ-II Stellarator
- P2.092 M. Sato, A. Isayama
Radiation temperature of ECE in bi-Maxwellian tokamak plasma
- P2.093 V.V. Bulanin, L.G. Askinazi, S.V. Lebedev, V.A. Kornev, A.V.Petrov, A.S. Tukachinsky, M.I. Vildjunas, A.Yu. Yashin
The two-frequency Doppler reflectometer application for plasma sheared rotation study in the TUMAN 3M tokamak
- P2.094 A. Baciero, B. Zurro, D. Jiménez-Rey, R.J. Peláez
Measurement of carbon ion emissions from TJ-II stellarator plasmas and their relation with plasma properties
- P2.095 Y. Shibata, M. Okamoto, N. Ohno, M. Goto, K.Y. Watanabe
Evaluation of Electron Temperature Dependence of Current Decay Time in the Large Helical Device

- P2.096 J. Preinhaelter, V. Fuchs, J. Urban, J. Zajac, S. Nanobashvili
Plans for electron Bernstein waves emission detection in COMPASS-D
- P2.097 F.V. Chernyshev, B.B. Ayushin, V.V. Dyachenko, V.K. Gusev, S.A. Khitrov, S.V. Krikunov, G.S. Kurskiev, V.B. Minaev, M.I. Mironov, Yu.V. Petrov, N.V. Sakharov, O.N. Shcherbinin, S.Yu.Tolstyakov
Fast Particle Confinement Studies in Globus-M Spherical Tokamak
- P2.098 V. Fuchs, O. Bilyková, R. Pánek, M. Stránský, J. Stöckel, J. Urban, F. Žáček, J. Decker, Y. Peysson, I. Voitsekhovitch, M.Valovic
Heating and current drive modeling for the IPP Prague COMPASS tokamak
- P2.099 E. J. Valeo, C. K. Phillips, J. R. Wilson, P. T. Bonoli, J. C. Wright, R. Bilato, M. Brambilla
Full-wave simulations of lower hybrid wave propagation in toroidal plasma with nonthermal electron distributions
- P2.100 R.J. Dumont, L.-G. Eriksson
Self-consistent modelling of FWCD in tokamak plasmas
- P2.101 A. Frattolillo, F. Bombarda, S. Migliori, L.R. Baylor, S.K. Combs, J.B.O. Caughman, C. Foust, B. Coppi, G. Roveta
Development of the High Speed Pellet Injector for Ignitor
- P2.102 D. Wunderlich, R. Gutser, U. Fantz, M. Berger, S. Christ-Koch, P. Franzen, M. Fröschle, B. Heinemann, W. Kraus, C. Martens, P. McNeely, R. Riedl, E. Speth
Modeling of Negative Ion RF Sources for ITER NBI - Current Status and Recent Achievements
- P2.103 V.A. Kornev, L.G. Askinazi, F.V. Chernyshev, V.E. Golant, S.V. Krikunov, S.V. Lebedev, A.D. Melnik, D.V. Razumenko, V.V. Rozhdestvensky, A.S. Tukachinsky, M.I. Vildjunas, N.A. Zhubr
Analysis of density dependence of neutron rate in NBI experiments on TUMAN-3M
- P2.104 A.V. Voronin, V.K.Gusev, G.S. Kurskiev, B.B. Ayushin, M.M.Kochergin, E.E.Mukhin, V.B.Minaev, Yu.V.Petrov, N.V.Sakharov, S.Yu.Tolstyakov
Two stage plasma gun as the fuelling tool of the Globus-M tokamak
- P2.105 B. Van Compernelle, R. Maggiora, G. Vecchi, D. Milanesio, R. Koch
Implementation of sheath effects into TOPICA
- P2.106 R. Cesario, G. Calabrò, A. Cardinali, C. Castaldo, M. Marinucci, V. Pericoli-Ridolfini
Lower hybrid current drive at high densities of ITER
- P2.107 R. Ikeda, K. Toi, M. Takeuchi, C. Suzuki, T. Shoji, T. Akiyama, M. Isobe, S. Nishimura, S. Okamura, K. Matsuoka
Production and heating of over-dense plasmas by mode-converted electron Bernstein waves at very low toroidal field in the Compact Helical System
- P2.108 S.Yu. Tolstyakov, S.E. Aleksandrov, B.B. Aushin, V.K. Gusev, M.M. Kochergin, N.A. Khromov, G.S. Kurskiev, V.B. Minaev, A.B. Mineev, E.E. Mukhin, M.I. Patrov, Yu.V. Petrov, A.V. Voronin, V.V. Semenov, N.V. Sakharov, V.I. Varfolomeev, V.A. Rozhansky, I.Yu. Senichenkov
Kinetic measurements of plasma electron component dynamics in the Globus-M tokamak during plasma gun injection experiment
- P2.109 V.A. Soukhanovskii, J.-W. Ahn, M.G. Bell, R.E. Bell, J. Boedo, D.A. Gates, R. Kaita, H.W. Kugel, B.P. LeBlanc, D.P. Lundberg, R. Maingi, J.E. Menard, R. Raman, A.L. Roquemore, D.P. Stotler, NSTX
H-mode fueling optimization with supersonic deuterium jet in the National Spherical Torus Experiment NSTX

- P2.110 M.C. Kaufman, J.A. Goetz, J.K. Anderson, A.F. Almagri, D.R. Burke, W.A. Cox, C.B. Forest, J.G. Kulpin, P.D. Nonn, S.P. Oliva, S.C. Prager
Lower Hybrid and Electron Bernstein Wave Experiments in MST
- P2.111 S.Kalvin, G.Kocsis, G.Verés, D. Wagner
Quasi two-dimensional simulation of the hydrogenic pellet ablation and plasmoid expansion
- P2.112 F. Imbeaux, J.B. Lister, G.T.A. Huysmans, L. Appel, W. Zwingmann, M. Airaj, V. Basiuk, D. Coster, B. Guillerminet, D. Kalupin, C. Konz, G. Manduchi, G. Pereverzev, Y. Peysson, L.G. Eriksson, M. Romanelli, P. Strand
Data structure for the European Integrated Modelling Task Force
- P2.113 A. Kus, D. Pretty, E. Ascasibar, C.D. Beidler, B. D. Blackwell, R. Brakel, R. Burhenn, F.Castejon, A. Dinklage, T. Estrada, Y. Feng, A. Fujisawa, H. Funaba, J. Geiger, J.H. Harris, C. Hidalgo, K. Ida, M. Kobayashi, R. König, G. Kühner, D. Lopez Bruna, H. Maaßberg, K.McCarthy, D. Mikkelsen, T. Minami, T. Mizuuchi, S. Murakami, N. Nakajima, S. Okamura, R. Preuss, S. Sakakibara, F. Sano, F. Sardei, T. Shimozuma, U. Stroth, Y. Suzuki, Y. Takeiri, J. Talmadge, V. Tribaldos, H. Thomsen, Yu. A. Turkin, J. Vega, K.Y. Watanabe, A. Weller, A. Werner, R. Wolf, H. Yamada, M. Yokoyama
Status of the International Stellarator/Heliotron Profile Database
- P2.114 V.E.Moiseenko, K.Noack, O.Agren
Stellarator-Mirror Based Driven Fusion-Fission Reactor
- P2.115 H. Ferrari, R. Farengo
Current Drive and Heating in a D-3He FRC Fusion Reactor
- P2.116 D.Grasso,R.J.Hastie,P.Helander
Effect of a runaway electron current on tearing modes
- P2.117 C. Meyer, O. Bonville, A. Boscheron, P. Canal, A. Casner, J. F. Charrier, G. Huser, C. Lepage, O. Henry, L. Marmande, E. Mazataud, D. Raffestin, J. L. Rullier
Overview of ALISE laser facility at CEA
- P2.118 J.Fuchs, L. Lancia, J.-R. Marquès, L. Romagnani, M. Grech, T. Grismayer, S. Weber, P. Antici, N. Bourgeois, T. Lin, M. Nakatsutsumi, R. Kodama, P. Audebert
Experimental demonstration of ion viscosity and non-local heat transport effects in high-power laser propagation in underdense plasmas
- P2.120 A. Velyhan, B. Bienkowska, M. Chernyshova, I. M. Ivanova-Stanik, L. Juha, Z. Kalinowska, M. Králík, J. Krása, J. Kravárik, P. Kubeš, H. Schmidt, M. Scholz
Influence of emission time on energy distribution of neutrons produced by plasma focus
- P2.121 S. E. Jiang, S.W. Li
Investigation of scaling laws for radiation temperature with Al shock wave velocity
- P2.122 B. Canaud, D. Elbaz, R. Piron, F. Philippe
Shock propagation in wetted foams in the context of Inertial Confinement Fusion
- P2.123 V. Bychkov, M. Modestov, M. Marklund, L.E. Eriksson
The darrieus-landau instability in laser ablation
- P2.124 V. Drean, M.Olazabal-Loume, X. Ribeyre, J. Sanz, V. Tikhonchuk
Numerical simulations and stability study of double ablation front structures, using radiation transport effects in direct-drive ICF

- P2.125 J.J. Martinell, R.M. Fajardo
A model for ion acceleration in a z-pinch during an m 0 instability
- P2.126 J. Sanz, R. Betti, M. Olazabal-Loume, J. Feugeas, X. Ribeyre, V. Drean
Analytical theory of radiative ablation fronts for direct drive ICF targets
- P2.127 C. K. Li, F. H. Séguin, J. R. Rygg, J. Frenje, M. Manuel, R. D. Petrasso, R. Betti, J. Delettrez, J. P. Knauer, F. Marshall, D. D. Meyerhofer, D. Shvarts, V. A. Smalyuk, C. Stoeckl, W. Theobald, O. L. Landen, R. P. J. Town, C. A. Back, J. D. Kilkenny
Monoenergetic Proton Radiography of Fields, Areal Density and Implosion Dynamics in Direct-Drive Inertial Confinement Fusion
- P2.128 M. Rabec le Gloahec, A.M. Sautivet
Overview of the LULI2000 laser and experimental facility
- P2.129 N.C. Woolsey, J. Howe, D.M. Chambers, C. Courtois, E. Foerster, C.D. Gregory, I.M. Hall, O. Renner, I. Uschmann
Parametric instabilities measurement via X-ray spectroscopy
- P2.130 A.A. Golubev, M.M. Basko, K.L. Gubskii, A.A. Drozdovskii, D.D. Iosseliani, A.V. Kantsyrev, M.A. Karpov, A.P. Kuznetsov, Yu.B. Novozhilov, O.V. Pronin, S.M. Savin, P.V. Satorov, D.A. Sobur, B.Yu. Sharkov, V.V. Yanenko
Plasma lens for high energy density in matter produced by heavy ion beam.
- P2.131 B.T. Egorychev, A.V. Ivanovsky, G.I. Volkov, I.V. Morozov, A.I. Kraev, A.A. Petrukhin
Experimental study of a possibility of quasi-spherical compression of thermonuclear target using a model
- P2.132 J. Meyer-ter-Vehn, A. Tronnier, Y. Cang
Physical Collision Frequency for Metals and Warm Dense Matter
- P2.133 C. Garcia-Fernandez, M. González, P. Velarde
Study of the influence of numerical techniques of radiation in laser-matter interaction problems
- P2.134 G.I. Dolgachev, D.D. Maslennikov, A.A. Shvedov, A.G. Ushakov, A.S. Fedotkin, I.A. Khodeev
Plasma opening switches in the inertial confinement fusion programs
- P2.135 J.M. Perlado, M.J. Caturla, A. Abanades, C. Arevalo, D. Diaz, L. Gámez, B. Gamez, Y. Herreras, A. Lafuente, J. Marian, E. Martínez, F. Mota, C. Ortiz, E. del Rio, F. Sordo, M. Velarde, M. Victoria, T. Villar
Damage, Fluidynamics and Tritium handling in IFE reactors
- P2.136 O.M. Burenkov, A.V. Ivanovsky, V.P. Korchagin, I.V. Morozov, V.K. Chernyshev, S.V. Pak, G.I. Volkov, Yu.N. Dolin, V.I. Dudin, P.V. Duday, V.V. Avdoshin, A.A. Zabiralov, V.A. Ivanov, V.B. Kudelkin, O.D. Mikhailov, A.N. Skobelev, A.I. Krayev, A.M. Glybin, S.M. Polyushko, A.T. Shakhalkin
Experimental Study Of "Mago" Chamber With Cylindrical Compression Compartment
- P2.137 Yu. Kalinin, S. Anan'ev, Yu. Bakshaev, A. Bartov, P. Blinov, A. Chernenko, S. Danko, E. Kazakov, A. Kingsep, V. Korolev, V. Mizhiritsky, S. Pikuz, V. Romanova, T. Shelkovenko, V. Smirnov, S. Tkachenko, A. Zelenin
Pulsed plasma dynamics in different kinds of imploding loads of megaampere range.
- P2.138 Didier Benisti, David J. Strozzi, Laurent Gremillet
Nonlinear kinetic modelling of Stimulated Raman Scattering
- P2.139 I. D. Kaganovich, A. B. Sefkow, E.A. Startsev, R.C. Davidson
Transport Of Intense Beam Pulses Through Background Plasma

- P2.140 M.Grech,G.Riazuelo,D.Pesme,S.Weber,V.T.Tikhonchuk
A new figure of merit for the control of laser beam propagation in inertial confinement fusion plasmas
- P2.141 B.Brandao, R.Bingham, L.O.Silva
Stimulated Brillouin scattering driven by white light
- P2.142 D. Margarone, D. Mascali, L. Torrisci, R. Miracoli, N. Gambino, S.G ammino
Langmuir Probe Diagnostics of Plasma Produced by Laser Ablation
- P2.143 J. Limpouch, O. Renner, O. Klimo, D. Klir, V. Kmetik, E. Krousky, R. Liska, K. Masek, W. Nazarov, M. Sinor
Line X-Ray Emission from Laser Irradiated Low-Density Foams Doped by Chlorine
- P2.144 L. Torrisci, A. Borrielli, F. Caridi, D. Margarone, S. Gammino
Optical Spectroscopy in Laser-generated Plasma at a pulse intensity of 10 10 W/cm²
- P2.145 V.I.Turtikov, A.A.Golubey, A.D.Fertman, V.E.Fortov, V.S.Demidov, E.V.Demidova, S.V.Dudin, M.M.Katz, S.B.Kolerov, S.A.Kolesnikov, V.A.Korolev, V.B.Mintzev, G.N.Smirnov, B.Yu.Sharkov, A.V.Utkin
Application of ITEP TWAC Accelerator Beams for Diagnostics Of Fast Process
- P2.146 V.V. Vatulin
Investigation of intense ion beams interaction with matter and dynamic processes in irradiated targets
- P2.148 S. M. Hassan, E. O. Baronova, E. L. Clark, G. C. Androulakis, C. Petridis, A. Gopal, S. Minardi, J. Chatzakis, V. V. Vikhrev, E. Tzianaki, P. Lee, M. Bakarezos, N.A. Papadogiannis, M. Tatarakis
Spectroscopic Investigation of Radiation from a Low Current X-Pinch
- P2.149 V.I. Annenkov, A.V. Bessarab, V.V. Vatulin, S.G. Garanin, N.V. Zhidkov, V.M. Izgorodin, G.A. Kirillov, V.P. Kovalenko, V.A. Krotov, P.G. Kuznetsov, A.V. Kunin, S.P. Martynenko, V.M. Murugov, S.I. Petrov, A.V. Pinegin, A.V. Senik, N.A. Suslov, G.V. Tachaev
Investigation of x-ray radiation interaction with matter on “Iskra-5” laser
- P2.150 J.Berardo, N. Lemos, C. Clayton, J. M. Dias
Refractometry diagnostic for plasma columns produced by intense laser pulses
- P2.151 C. Mezel, A. Bourgeade, L. Hallo, O. Saut
Electron generation in femtosecond laser heated dielectrics
- P2.152 A. Grinenko, D.O. Gericke, J. Vorberger
Simulations for Dynamic Compression of Hydrogen with Intense Heavy Ion Beams
- P2.153 O. Morice, M. Casanova
Nanosecond Raman scattering computation in large plasmas
- P2.154 V.V.Vikhrev, G.C.Androulakis, E.O.Baronova, S.M.Hassan, E.L.Clark, A.Gopal, S.Minardi, C.Petridis, J.Chatzakis, A.Skoulakis, E.Tzianaki, M.Bakarezos, N.A.Papadogiannis, M.Tatarakis
MHD Simulation for X-pinch plasma dynamics
- P2.155 E. Havlickova, P. Bartos, R. Hrach, V. Hrachova
Computational study of sheath structure in electronegative gases at various pressures
- P2.156 I. Litovko
Computer modeling of sharp electron beam generation by plasma electron gun
- P2.157 J.D.E. Stokes, A.A. Samarian, S.V. Vladimirov

Two-stage transition in dust particle alignment in a plasma sheath

- P2.158 M. Bacharis, D. Selemir, M. Coppins, J. E. Allen
Radio frequency effects on the charging of dust grains
- P2.159 M. Rubin-Zuzic, H. M. Thomas, S. K. Zhdanov, G. E. Morfill
Circulation' dynamo in complex plasma
- P2.160 N.F.Cramer
Nonlinear dust-lattice waves - a modified Toda lattice
- P2.161 N.G. Gusein-zade, I.A. Lubashevsky, S.A. Maiorov
Dust chain with asymmetrical interaction
- P2.162 P. Huber, G. E. Mor, A. V. Ivlev, B. A. Klumov, H. M. Thomas, V. E. Fortov, A. M. Lipaev, V. I. Molotkov, O. F. Petrov
Observation of 3 dimensional structures of electrorheological plasmas
- P2.163 E. Benova, T. Bogdanov
Wave propagation characteristics of coaxial discharge sustained by traveling electromagnetic wave
- P2.164 H. Kersten, I. Teliban, V. Schneider, T. Trottenberg, H. Neumann, M. Tartz, F. Scholze
Diagnostics of ECR-MW Broad Beam Ion Sources
- P2.165 M. Haass, T. Ockenga, J. Blazec, R. Basner, M. Wolter, H. Kersten
Micro-Particles as Electrostatic Probes for Plasma Sheath Diagnostics
- P2.166 M. Cercek, T. Gyergyek
Potential Structures Formed in Two - Temperature Plasma With Two Positive Ion Species
- P2.167 E.R. Ionita, M.D. Ionita, C. Stancu, M. Teodorescu, G. Dinescu
Operation Domains of a Small Size Atmospheric Pressure Cold Plasma Source and its Application to Polymer Surface Modification
- P2.169 F. Massines, Et.Es-sebbar, N. Gherardi, N. Naudé, D. Tsyganov, P. Ségur, S. Pancheshnyi
Comparison of Townsend dielectric barrier discharge in N_2 , N_2-O_2 and N_2-N_2O behaviour
- P2.170 I.E. Garkusha, V.V. Chebotarev, A. Hassanein, M.S. Ladygina, A.K. Marchenko, Yu.V. Petrov, D.G. Solyakov, V.I. Tereshin, S.A. Trubchaninov
EUV Radiation of Xenon Plasma Streams Generated by Magnetoplasma Compressor
- P2.171 I. Litovko, V. Gushenets
Computer Simulation for Optimization of Ion Sources
- P2.172 I. Litovko, A. Goncharov
Plasma-dynamical Model Of Magnetron Type Cylindrical Gas Discharge
- P2.173 A. Sadovski
Electromagnetic waves generated by the ion distribution function with velocity space holes
- P2.174 A. Stockem, M. E. Dieckmann, R. Schlickeiser
Suppression of the filamentation instability by a flow-aligned magnetic field
- P2.175 A.V.Glushkov, O.Yu.Khetselius, E.P.Gurnitskaya, S.V.Malinovskaya

QED approach to the photon-plasmon transitions and diagnostics of the space plasma turbulence

- P2.176 F. Ceccherini, A. Biancalani, F. Pegoraro
Active Magnetic Experiment a magnetic bubble in the ionospheric stream
- P2.177 C. Ionita, R. Stenzel, R. Schrittwieser
Plasma Fireballs
- P2.178 C. Montagna, F. Pegoraro
Role of temperature and density in stationary solutions of the Vlasov-Maxwell system
- P2.179 E. Tassi, D. Grasso, F. Pegoraro
Nonlinear dynamics of magnetic reconnection in collisionless plasmas
- P2.180 G.N. Throumoulopoulos, H. Tasso
A sufficient condition for the linear stability of magnetohydrodynamic equilibria with field aligned incompressible flows
- P2.181 Gyergyek T., Cercek M.
A one-dimensional kinetic model of the current-voltage characteristics of an electron emitting electrode immersed in a two-electron temperature plasma
- P2.182 I. Furno, A. Fasoli, B. Labit, M. Podestà, P. Ricci, C. Theiler
Investigation of the existence of an improved confinement regime in simple magnetized toroidal plasmas
- P2.183 Juan Miguel Gil de la Fe
Determination of level populations and radiative properties of optically thin and tick carbon plasmas
- P2.184 L. Galeotti, F. Califano, A. Mangeney, F. Pegoraro
Limits of a plasma mean field theory, a numerical experiment
- P2.185 Y. Kominis, K. Hizanidis, A.K. Ram
Nonlinear Theory of Cyclotron Resonant Wave-Particle Interactions Analytical results beyond the Quasilinear Approximation
- P2.186 B.J. Kellett, V. Graffagnino, R. Bingham, T.W.B. Muxlow, A.G. Gunn, D.C. Speirs, S.L. McConville, K.M. Gillespie, K. Ronald, A.D.R. Phelps, A.W. Cross, C.W. Robertson, C.G. Whyte, I. Vorgul, R.A. Cairns
Plasma Physics of Pulsar Emission
- P2.187 J.N. Waugh, E. Brambrink, C.D. Gregory, R. Kodama, M. Koenig, B. Loupiau, Y. Kuramitsu, Y. Sakawa, H. Takabe, L.A. Wilson, N.C. Woolsey
A jet production experiment using a short pulse laser
- P2.188 N.P. Kyrie, A.G. Frank, V.S. Markov, G.S. Voronov
Plasma heating and generation of plasma jets in current sheets formed in 3D magnetic configurations
- P2.189 S. Oldenbuerger, N. Lemoine, F. Brochard, G. Bonhomme, A. Lazurenko, S. Mazouffre
Investigation of high-frequency plasma oscillations in Hall thrusters
- P4.001 J. R. Myra, M. V. Umansky
Linear Analysis Tools for Edge and SOL Plasmas
- P4.002 M. Gemisic Adamov, B. Kurzan, H. Murmann, W. Suttrop
ELM synchronized Thomson scattering measurements on ASDEX Upgrade

- P4.003 M. Groth, M. Wischmeier, N.H. Brooks, D.P. Coster, J. Harhausen, A. Kallenbach, C.J. Lasnier, A.W. Leonard, H.W. Muller, T.H. Osborne, G.D. Porter, J.G. Watkins
Comparison and SOL Modeling of Ohmic Plasmas in ASDEX Upgrade and DIII-D
- P4.004 M.L. Apicella, G. Apruzzese, G. Mazzitelli, A.G. Alekseyev, V.B. Lazarev, S.V. Mirnov
Lithiation of the FTU tokamak with a critical level of lithium injection
- P4.005 M.N.A. Beurskens, A. Alfier, W. Fundamenski, E. Giovannozzi, M. Kempenaars, G. Maddison, R. Pasqualotto, R. A. Pitts, S. Saarelma, J.W. Weber
Pedestal dynamics in ELMy H-mode plasmas in JET
- P4.006 M. Shoucri
Numerical Simulation for the Formation of a Charge Separation and an Electric Field at a Plasma Edge
- P4.007 P. Devoy, P.K. Browning, C.G. Gimblett
Amplitude bifurcation in the peeling-relaxation ELM model
- P4.009 R.C. Wieggers, H.J. de Blank, V. Kotov, P. Boerner, D. Reiter, W. J. Goedheer
B2-Eirene study of the effects of heating in a linear plasma device
- P4.010 R. Fischer, E. Wolfrum, W. Suttrop, A. Kallenbach
Integrated density profile analysis in ASDEX Upgrade H-modes
- P4.011 R. Pugno, R. Dux, A. Kallenbach, M. Mayer, R. Neu, V. Rohde, T. Puetterich, C. Maggi, ASDEX Upgrade Team
Evolution of carbon content in ASDEX Upgrade during the transition to a full W machine
- P4.012 S.A. Barengolts, G.A. Mesyats, M.M. Tsventoukh
The Initial Stage of the Unipolar Arc Hot Spot Formation Due to the Microexplosion at the Surface
- P4.013 S. Jachmich, M. Van Schoor, R.R. Weynants, Y. Xu, M. Jakubowski, M. Lehnen, M. Mitri, O. Schmitz
Experimental study of toroidal and poloidal rotation induced by edge ergodization and electrode biasing in TEXTOR
- P4.014 S. Pestchanyi, I. Landman
Simplified model for carbon plasma production by ELMs in ITER
- P4.015 S. Suwanna, T. Onjun, P. Leekhapphan, D. Sukboon, P. Thanasutives, R. Picha, N. Poolyarat, O. Onjun
The Development of Pedestal Temperature Model with Self-consistent Calculation of Safety Factor and Magnetic Shear
- P4.016 J.W. Coenen, M. Clever, K.H. Finken, H. Frerichs, M. Jakubowski, A. Krämer-Flecken, M. Lehnen, M. Mitri, U. Samm, B. Schweer, O. Schmitz, B. Unterberg, TEXTOR-team
Spectroscopic Measurements of the radial electric field under conditions of improved particle confinement with the Dynamic Ergodic Divertor in TEXTOR
- P4.017 K. Allmaier, S.V. Kasilov, W. Kernbichler, G.O. Leitold
Delta f Monte Carlo computations of neoclassical transport in stellarators with reduced variance
- P4.018 K. Crombe, Y. Andrew, T.M. Biewer, P. de Vries, C. Giroud, N.C. Hawkes, A. Meigs, T. Tala
Radial electric field profiles in JET advanced tokamak scenarios with toroidal field ripple
- P4.019 L. Carraro, D. Terranova, F. Auriemma, F. Bonomo, A. Canton, A. Fassina, P. Innocente, R. Lorenzini, R. Pasqualotto, M.E. Puiatti

Particle transport in different magnetic field topological configurations in the RFX-mod experiment

- P4.020 L. Garcia, J.A. Mier, R. Sanchez, B.A. Carreras, I. Calvo, D.E. Newman
Nondiffusive transport in plasma turbulence
- P4.021 L. Vermare, G. Leclert, S. Heuraux, P. Hennequin
2D numerical simulations of wave propagation on turbulent plasma to help experimental k-spectrum determination
- P4.022 M.-D.Hua, P.C. DeVries, D.C. McDonald, C.Giroud, M.Janvier, M.F.Johnson, T.Tala, K.D.Zastrow
Scaling of rotation and momentum confinement in JET plasmas
- P4.023 M. Aizawa
Improved Magnetic Field Properties in Low Aspect Ratio L 1 Helical Systems
- P4.024 M. Ansar Mahmood, J. Weiland, M. Persson, T. Rafiq
Study of collisionless TE and ITG modes in an ITER-like equilibrium
- P4.025 M.C. Varischetti, M. Lontano, E. Lazzaro
Energy and momentum transport induced by unstable ITG modes
- P4.026 M.C. Varischetti, M. Lontano, L. Valdetaro, E. Lazzaro
Global stability analysis of ITG modes with shear velocity
- P4.027 M. Landreman, B. Coppi
Confinement Regimes Transition, Angular Momentum Ejection by Toroidal Edge Modes and Relation to Current Experiments
- P4.028 M. Ramisch, A. Köhn, N. Mahdizadeh, U.Stroth
Poloidal asymmetry of turbulent fluctuations in the torsatron TJ-K
- P4.029 M. Reshko, N. F. Loureiro, C. M. Roach, H. R. Wilson
On Theory and Simulations of the Effects of Equilibrium ExB Flow Shear on Drift Waves and Anomalous Transport in Tokamaks
- P4.030 N.Poolyarat,T.Onjun,J.Prompting,R.Picha,S.Suwanna,O.Onjun
The Study of Transport in Small Tokamak Experiments Using Integrated Predictive Modeling Code
- P4.031 O.A. Shyshkin, B. Weyssow
Monte Carlo collision operator for the test particle tracing in fusion non Maxwellian plasma
- P4.032 O. Tudisco
Studies of electron temperature characteristic length in FTU
- P4.033 P. Angelino, X. Garbet, L. Villard, A. Bottino, S. Jolliet, Ph. Ghendrih,V. Grandgirard, B. F. McMillan, Y. Sarazin, G. Dif-Pradalier, T. M. Tran
Effects of plasma current and elongation on drift wave-zonal flow turbulence
- P4.034 P. J. Catto, F. Parra, G. Kagan, A. N. Simakov
Gyrokinetic Limitations and Improvements
- P4.035 P. Molchanov, V. Rozhansky, S. Voskoboynikov, S. Tallents, G. Counsell, A. Kirk
Comparison of measured and simulated parallel flows at the edge plasma of MAST

- P4.036 P.Strand,J.Kinsey,H.Nordman,J.Weiland
Drift-wave particle transport - TGLF and EDWM comparisons
- P4.037 R.J. McKay, K.G. McClements, A. Thyagaraja, L. Fletcher
Test-particle simulations of collisional impurity transport in rotating spherical tokamak plasmas
- P4.038 R.Klein, P.Morel, N.Besse, E.Gravier, P.Bertrand
Instabilities in toroidal geometry a Water Bag approach
- P4.039 R. Neu, R. Dux, A. Kallenbach, B. Kurzan, C.F. Maggi, R. Pugno, T. Pütterich, F. Rytter, G. Tardini, ASDEX Upgrade Team
Influence of the 4He Concentration on H-Mode Confinement and Transport in ASDEX Upgrade
- P4.040 R.Picha
The Dependence of ITER Performance on Pedestal Temperature, Density, Heating Power, and Impurity Content
- P4.041 S.C. Assas, L.-G. Eriksson, G.D. Conway, C.F. Maggi, M. Maraschek, J.-M. Noterdaeme, V.I.V Bobkov
Toroidal rotation in ICRF only heated ASDEX Upgrade plasmas
- P4.042 S.Futatani, S.Benkadda, D.del-Castillo-Negrete, Y.Nakamura, K.Kondo
Multiscale Analysis of Impurity Transport in Edge Tokamak Plasmas
- P4.043 S.I. Lashkul, S.V. Shatalin, P.V. Vajnov, E.O. Vekshina, A.Yu. Popov, L.A. Esipov
Analyze of the plasma periphery fluctuation parameters measured by multipin Langmuir probes near LCFS on the FT-2 tokamak
- P4.044 S. Inagaki, T. Maruta, T. Yamada, Y. Nagashima, N. Kasuya, S. Shinohara, K. Terasaka, K. Kamataki, M. Yagi, Y. Kawai, A. Fujisawa, K. Itoh, S.-I. Itoh
Two-Dimensional Spatial Structure of Plasma Turbulence in LMD-U
- P4.045 S.J. Janhunen, J.A. Heikkinen, T.P. Kiviniemi, S. Leerink, M. Nora, F. Ogando
Transport dynamics of the Cyclone Base case on ELMFIRE
- P4.046 S. Jaeger, T. Pierre, C. Rebont, N. Claire, A. Escarguel, A. Ajendouz, K. Quothb
Current transport and turbulence in a cylindrical plasma magnetically confined
- P4.047 S. Leerink, O. Dumbrajs, J.A. Heikkinen, S.J. Janhunen, T.P.Kiviniemi, M.Nora, F.Ogando
A full f analysis of turbulent transport in the FT-2 Tokamak configuration
- P4.048 S.Moradi, D.Kalupin, H.Nordman, R.Singh, M.Tokar, B. Weysow
Modeling of confinement improvement and impurity transport in high power JET H-mode discharges with neon seeding
- P4.049 S.Oldenbürger,F.Brochard,N.Lemoine,G.Bonhomme
Investigation of cross-field transport in a linear magnetized plasma
- P4.050 T.Estrada,L.Guimaraes,T.Happel,E.Blanco,L.Cupido,M.E.Manso
Velocity shear layer formation and turbulence correlation characteristics measured by reflectometry in TJ-II
- P4.051 H.R. Wilson, D.A. Applegate, J.W. Connor, M. James
The Interaction between Tearing Modes and Transport
- P4.052 A.D.Beklemishev, M.S.Chaschin
Shear-Flow Modification of Interchange

- P4.053 A.J. Cerfon, J.P. Freidberg
The Vanishing MHD Compressibility Stabilization in Closed Line Systems
- P4.054 S.L. Newton, S.E. Sharapov, F. Zonca
On Kinetic Theory and Hall MHD Description of the q equal to 1 Inertial Layer in Fishbone Modes
- P4.055 M. Okabayashi, M.S. Chance, M.S. Chu, A.M. Garofalo, Y. In, G.L. Jackson, R.J. La Haye, M.J. Lanctot, Y.Q. Liu, T.C. Luce, G.A. Navratil, H. Reimerdes, E.J. Strait, H. Takahashi, A.S. Welander
Control of Transiently-Excited Resistive Wall Modes Under Rotationally Stabilized Regime in DIII-D Advanced Tokamak Plasmas
- P4.056 M.J. Lanctot, I.N. Bogatu, M.S. Chu, A.M. Garofalo, Y. In, G.L. Jackson, R.J. La Haye, Y.Q. Liu, G.A. Navratil, M. Okabayashi, H. Reimerdes, W.M. Solomon, E.J. Strait
Mode Structure of the Plasma Response to Error Fields
- P4.057 M.M. Tsventoukh
Equilibrium and Stability of the Plasma Confined by Double-Dipole Device
- P4.058 L.E. Zakharov, E.D. Fredrickson, E.M. Granstedt, S.I. Krashennnikov, H. Takahashi
Wall touching kink modes in disruptions and at the plasma edge in tokamaks
- P4.059 Pablo Martin, Enrique Castro, Julio Puerta
Triangularity and Ellipticity effects on low-vorticity non-linear collisional diffusion in tokamaks
- P4.060 Y.R. Martin, J.B. Lister
Current quench time in TCV disruptions
- P4.061 W.A. Cooper, J.P. Graves, S.P. Hirshman, P. Merkel
Three-Dimensional Free-Boundary Anisotropic Pressure Equilibria
- P4.062 A. Macor, P. Buratti, J. Decker, D. Elbeze, X. Garbet, M. Goniche, P. Maget, C. Nguyen, R. Sabot, J.L. Segui, F. Zonca
Fast particle triggered modes experimental investigation of Electron Fishbones on TORE SUPRA
- P4.063 P. Rodrigues, J. P. S. Bizarro
Noniterative equilibria reconstruction without up-down symmetry
- P4.064 R.G.L. Vann, L. Appel, P.J. Denner, M.P. Gryaznevich, M.K. Lilley, R. Martin, S.D. Pinches, S.E. Sharapov
Modelling observations of mode polarisation from MAST
- P4.065 J. P. S. Bizarro, P. Rodrigues
Grad-Shafranov equilibria with negative core toroidal current vs. experimental data
- P4.066 M.J. Windridge, T.C. Hender, G. Cunningham, J.B. Lister, V. Lukash, R. Khayrutdinov, V. Dokuka
MAST Plasma Response Investigations using DINA-CH
- P4.067 R. Ikezoe, T. Onchi, K. Murata, K. Oki, H. Shimazu, T. Yamashita, A. Sanpei, H. Himura, S. Masamune
Effects of lowering aspect ratio on magnetic fluctuations in RFP
- P4.068 A. Sanpei, S. Masamune, R. Ikezoe, T. Onchi, K. Murata, K. Oki, H. Shimazu, T. Yamashita, H. Himura
Neoclassical Equilibrium in a Low-Aspect Ratio RFP Machine RELAX
- P4.069 C.V. Atanasiu, A. Moraru, L.E. Zakharov
The investigation of resistive wall modes in a diverted tokamak configuration

- P4.070 M.K. Zedda, M. Camplani, B.Cannas, A.Fanni, P.Sonato, E.R. Solano
Dynamic behaviour of type I and type III Edge localized modes in the JET tokamak
- P4.071 S.E.Sharapov, F.M.Poli
Magnetic turbulence associated with confinement changes in JET plasmas
- P4.072 O.P. Fesenyuk, Ya.I. Kolesnichenko, A. Weller, A. Werner, Yu.V. Yakovenko
Generation of kinetic Alfvén waves by Non-conventional Global Alfvén Eigenmodes
- P4.073 F. Bombarda, B. Coppi, E. Paulicelli, G. Pizzicaroli, G. Ramogida, R. Rubinacci, F. Villone
Plasma Position Control Strategies for Ignitor
- P4.074 M.E. Puiatti, M. Agostini, A. Canton, S. Cappello, P. Innocente, R. Lorenzini, R.Paccagnella, P. Scarin, G. Spizzo, D. Terranova, M.Valisa
High density limit in Reversed Field Pinches
- P4.075 W. Suttrop, A. Herrmann, M. Rott, T. Vierle, U. Seidel, B. Streibl, D. Yadikin, O. Neubauer, B. Unterberg, E. Gaio, V. Toigo, P. Brunsell
Design of in-vessel saddle coils for MHD control in ASDEX Upgrade
- P4.076 D. Mueller, R. Raman, T.R. Jarboe, B.A. Nelson, M.G.Bell
Coxial Helicity Injection plasma start-up coupled to inductively driven sustainment on the National Spherical Torus Experiment
- P4.077 T. Fehér, K. Gál, H. Smith, T. Fülöp, P. Helander
Simulation of runaway electron generation during plasma shutdown by doped pellet injection
- P4.078 M. Mattei, R. Albanese, A. Portone, G.Saibene, A.A.Sips
ITER Plasma scenarios scaled from ASDEX-U and JET experimental data and their impact on ITER operational space
- P4.079 G.W. Pacher, H.D. Pacher, A.S. Kukushkin, G. Janeschitz
Iter Operating Windows with Varying Plasma-Facing Materials and Divertor Constraints
- P4.080 J. Havlicek, J. Horacek
Modelling of COMPASS tokamak PF coils magnetic fields
- P4.081 Tsv. K. Popov, P. Ivanova, E. Benova, F. M. Dias, J. Stöckel, R. Dejarnac
On the Interpretation of the Electron Part of the Langmuir Probe Characteristics in Tokamak Edge Plasma
- P4.082 N. K. Hicks, W. Suttrop, J. Stober, S. Cirant, M. Maraschek, K. Behler, L. Giannone, G. Raupp, M. Reich, A.C.C. Sips, W. Treutterer
Measurement of NTMs, Modulated ECRH Deposition, and Current Ramp-Up MHD Activity Using the Upgraded 1 MHz ECE Radiometer on ASDEX Upgrade
- P4.083 M.A. Van Zeeland, M.S. Chu, T.C. Luce, C.C. Petty, J.H. Yu
Spectrally Filtered Fast Imaging of Internal MHD Activity in the DIII-D Tokamak
- P4.084 G. Bonheure, J. Mlynar, L. Bertalot, A. Murari, S. Popovichev, EFDA-JET contributors
A novel method for tritium transport studies and its validation at JET
- P4.085 M.A. Makowski, M. Brix, N. Hawkes
Semi-Empirical Calibration Technique for the MSE Diagnostic on the JET and DIII-D Tokamaks

- P4.086 V.A.Pisarev,E.Z.Gusakov,D.M.Grésillon
Investigation of turbulence in magnetized toroidal plasma by correlative enhanced scattering diagnostics
- P4.087 U.W. Nam, S.G.Lee, J.G.Bak, M.K.Moon, J.K.Cheon
Data acquisition system of a four segmented position sensitive detector for an advanced X-ray imaging crystal spectrometer
- P4.088 Hoon Kyun Na
H_alpha monitor and multi-chord visible spectroscopy for KSTAR diagnostics
- P4.089 M. K. Moon, J. K. Cheon, S. S. Desai, U. W. Nam, S. G. Lee, J. G. Bak
Multi-segmented position-sensitive detector for X-ray imaging crystal spectrometer
- P4.090 K.-S. Chung, H.-J. Woo, M.J. Lee
Effect of Recombination, Charge-Exchange and Ionization on the Deduction of Mach Numbers in flowing Magnetized Plasmas
- P4.091 K.-S. Chung, H.-J. Woo, T. Lho, M.J. Lee
Transient SOL during the start-up of tokamak in divertor plasma simulator DiPS
- P4.092 O. Marchuk, G. Bertschinger, W. Biel, E. Delabie, M.G. vonHellermann, R. Jaspers, D. Reiter
A review of atomic data needs for active charge-exchange spectroscopy on ITER
- P4.093 I. Mihaila, C. Costin, M.L. Solomon, G. Popa, C. Ionita, R. Starz, R. Schrittwieser, J. Rapp, N.J. Lopes-Cardozo, H.J van der Meiden, G.J. van Rooij
Probe investigations of the Pilot-PSI plasma
- P4.094 T.M. Biewer, Y. Andrew, K. Crombe, N.C. Hawkes, D.L. Hillis, C. Strege, K.-D. Zastrow, JET EFDA contributors
Expanded Capability of the Edge Charge-Exchange Recombination Spectroscopy System on JET
- P4.095 D.E.Kravtsov , V.F. Andreev, A.V. Sushkov
Electron temperature measurements by the duplex multiwire proportional X-ray detector on T-10 tokamak
- P4.096 J.G. Bak, S.G. Lee, E.M. Ka
Performance test of vessel current monitors for KSTAR
- P4.097 R.I. Pinsker, T.E. Evans, F.W. Baity, P.M. Ryan, J.C. Hosea
Experiments on Minimizing ELM-induced Fast Wave Antenna Breakdown in DIII-D
- P4.098 L.R. Baylor, T.C. Jernigan, S.K. Combs, P.B. Parks, T.E. Evans, M.E. Fenstermacher, R.A. Moyer, J.H. Yu
ELMs Triggered from Deuterium Pellets Injected into DIII-D and Extrapolation to ITER
- P4.099 D.Frigione, L.Garzotti, G.Kamelander, F.Köchler, H.Nehme, B.Pégourié
Pellet Drift Modelling – Validation and ITER Predictions
- P4.100 M .Irie, M.Kubo-Irie, FBX team
LCDC The Local Cold and Dense Compress formed by the Injected Pellets and the MHD Instability in Reactor Level Tokamaks
- P4.101 T.Seki, T.Mutoh, R.Kumazawa, K.Saito, H.Kasahara, S.Kubo, T.Shimozuma, Y.Yoshimura, H.Igami, H.Takahashi, Y.Nakamura, N.Ashikawa, S.Masuzaki, F.Shimpo, G.Nomura, C.Takahashi, M.Yokota, Y.P.Zhao, J.G.Kwak, A.Komori, O.Motojima, LHD Experimental Group
ICRF mode-conversion heating and its application to long pulse discharge in LHD

- P4.102 B. J. Ding, L. Z. Zhang, Y. L. Qin, J. F. Shan, F. K. Liu, M. Wang, L. G. Meng, D. X. Wang, J. Q. Feng, Y. X. Jie, Y. W. Sun, B. Shen, X. M. Wang, J. H. Ling, X. Gao, X. D. Zhang, G. L. Luo, Y. P. Zhao, B. N. Wan, J. G. Li
Coupling LHW Power to Plasma by Gas Puffing in HT-7
- P4.103 V.V. Postupaev, A.V. Arzhannikov, V.T. Astrelin, V.I. Batkin, A.V. Burdakov, V.S. Burmasov, I.A. Ivanov, M.V. Ivantsivsky, K.N. Kuklin, K.I. Mekler, S.V. Polosatkin, S.S. Popov, A.F. Rovenskikh, A.A. Shoshin, N.V. Sorokina, S.L. Sinitsky, Yu.S. Sulyaev, Yu.A. Trunev, L.N. Vyacheslavov, Ed.R. Zubairov
First experiments on neutral injection in multimirror trap GOL-3
- P4.104 G.Kamelander, D.Frigione, L.Garzotti, F.Köchler, H.Nehme, B.Pégourié
Modelling of the Pellet Rocket Acceleration Effect
- P4.105 K. A. Avramides, O. Dumbrajs, S. Kern, I. Gr. Pagonakis, J. L. Vomvoridis
Mode selection for a 170 GHz, 1 MW Gyrotron
- P4.106 I. Miroshnikov, I. A. Sharov, V. Yu. Sergeev, N. Tamura, B. V. Kuteev, O. A. Bakhareva, D. M. Ivanova, D. Kalinina, V. M. Timokhin, K. Sato, S. Sudo
Study of Pellet Clouds in LHD via 2-D Spectroscopy Imaging
- P4.107 F. Louche, P. Dumortier, A. Messiaen, P. Tamain
Recent Progress in 3D Electromagnetic Modeling of the ITER ICRH Antenna
- P4.108 A.I. Meshcheryakov, A.E. Morozov, A.A. Golikov
Peculiarities of Propagation and Damping of Fast Magnetosonic Waves in Hydrogen Plasma in the L2-M Stellarator
- P4.109 E. Yatsuka, D. Sakata, K. Kinjo, S. Tanaka, J. Morikawa, Y. Ogawa
Excitation and Propagating of Electron Bernstein Waves in the Internal Coil Device Mini-RT
- P4.110 A. Köhn, B. Birkenmeier, H. Höhnle, E. Holzhauer, W. Kasperek, M. Ramisch, U. Stroth
Microwave heating and toroidal currents in the torsatron TJ-K
- P4.111 R.R. Parker, J.R. Wilson, P.T. Bonoli, R.W. Harvey, A.E. Hubbard, A. Ince-Cushman, J.-S. Ko, O. Meneghini, M. Porkolab, J.E. Rice, A.E. Schmidt, S.D. Scott, S. Shiraiwa, G.M. Wallace, J.C. Wright
Current Profile Control Using LHCD in Alcator C-Mod
- P4.112 M.X.Chen, C.Y.Liu, B.Wu
The Economic Analysis of the Compact Fusion-Fission Hybrid Reactor
- P4.113 V. Bailescu, G. Burcea, N. Balan, G. Dinuta, G. Serban, C.P.Lungu, A.M.Lungu, M.Rubel, P.Coad, L.Pedrick, R. Handley
Inconel tiles coated with beryllium by thermal evaporation
- P4.114 J.C. Wright, P.T. Bonoli, E. Valeo, C.K. Phillips, M. Brambilla, R. Bilato
The importance of the effects of diffraction and focusing on current deposition of lower hybrid waves
- P4.115 L.-G. Eriksson, T. Hellsten, K. Holmström, T. Johnson, J. Brzozowski, F. Nave, J. Ongena, K.-D. Zastrow
Simulation of Fast Ion Contribution to Toroidal Rotation in ICRF Heated JET Plasmas
- P4.116 I. Loupasakis, S.D. Moustazis, P. Lalousis
MHD computations for plasma trapping in open magnetic field devices for high neutron flux production
- P4.117 A. Sid, M. Bekhouche, A. Ghezal, M. Smadi, D. Bahloul, D. Debbache

Weibel instability in a bi-maxwellian laser fusion plasma

- P4.118 G. Schurtz, X. Ribeyre, J. Breil
Bipolar shock ignition studies in the HiPER context
- P4.119 K. A. Flippo, E. d'Humières, S. A. Gaillard, M. Schollmeier, J. Rassuchine, D. C. Gautier, Y. Sentoku, R. P. Johnson, J. Kline, F. Nürnberg, K. Harres, T. Shimada, M. Roth, T. E. Cowan, B. M. Hegelich, J. C. Fernández
Efficient Proton Beam Generation from Novel Flat-Top Cone Targets Relevant for Fast Ignition Fusion
- P4.120 K. Mima, H. Nagatomo, T. Johzaki, H. Sakagami, T. Nakamura
Advanced target design for FIRX-I with the integrated code F13
- P4.121 S. G. Bochkarev, V. Yu. Bychenkov, K. I. Popov, W. Rozmus, R. D. Sydora
Charged particle acceleration in vacuum by ultra-strong laser pulses
- P4.122 A. Blažević, A. Frank, M. Günther, K. Harres, T. Heßling, D.H.H. Hoffmann, R. Knobloch-Maas, F. Nürnberg, M. Roth, A. Pelka, G. Schaumann, A. Schökel, M. Schollmeier, D. Schuhmacher, J. Schüttrumpf, H.G. Bohlen, W. von Oertzen
Energy loss and charge states of Argon ions penetrating hot and dense C plasma
- P4.123 A. Czarnecka, J. Krasa, L. Laska, P. Parys, M. Rosinski, L. Ryc, J. Wolowski
Particular currents of ion species emitted from Fe 2 Si plasma produced by a Nd YAG laser
- P4.124 M. Sherlock, S. Rose
Interaction of Deuterium Beams with Dense Tritium Targets
- P4.126 A. Schiavi
Interpretation of laser-produced ion beam diagnostics using the PTRACE code
- P4.127 M. Roth, M. Schollmeier, S. Becker, M. Geissel, K.A. Flippo, A. Blazevic, F. Grüner, K. Harres, F. Nuernberg, P. Rambo, J. Schreiber, J. Schüttrumpf, J. Schwarz, B. Atherton, M. Hegelich, D. Habs
Beam Control and Transport of Laser-Accelerated Protons
- P4.128 A.A.Andreev, J.Limpouch, K.Yu.Platonov
Laser acceleration of light ions in shaped mass-limited multi-species targets
- P4.129 A.Flacco, F.Sylla, N.Venkatakrishnan, M.Veltcheva, T.Desai, D.Batani, V.Malka
Ion acceleration with ultra-high contrast laser pulses
- P4.130 B. M. Hegelich, L. Yin, B. Albright, W. Daughton, K. A. Flippo, C. Gautier, A. Henig, R. Johnson, D. Kiefer, S. Letzring, R. Shah, J. Schreiber, T. Shimada, J. C. Fernandez, D. Habs
Relativistic Particle Acceleration with Ultrahigh Power Lasers Towards Applications in Fusion and Medicine
- P4.131 E. L. Clark, E. T. Gumbrell, C. R. D. Brown, L. Thornton, A. Moore, M. T. Girling, D. Lavender, D. J. Hoarty
Electric Field Collimation of Intense Laser Accelerated Proton Beams
- P4.132 J. Faure, C. Rechatin, R. Fitour, K. Ta Phuoc, A. Benismail, J. Lim, V. Malka
Injection of electrons in plasma waves by non collinear colliding laser pulses
- P4.133 J. Krasa, A. Velyhan, K. Jungwirth, E. Krousky, L. Laska, K. Rohlena, M. Pfeifer, J. Ullschmied
Generation of MeV carbon and fluorine ions by sub-nanosecond laser pulses
- P4.134 K. Cassou, F. Wojda, G. Genoud, M. Burza, A. Persson, C.-G. Wahlström, N.E. Andreev, B. Cros
Plasma wave excitation in the wake of a short intense laser pulse guided in hydrogen-filled capillary tube

- P4.135 K. I. Popov, V. Yu. Bychenkov, W. Rozmus, V. F. Kovalev, R. D. Sydora
Mono-energetic ions from collisionless expansion of spherical multi-species clusters
- P4.136 K. Schmid, L. Veisz, S. Benavides, F. Tavella, R. Tautz, D. Herrmann, A. Marcinkevicius, B. Hidding, M. Geissler, U. Schramm, J. Meyer-ter-Vehn, D. Habs, F. Krausz
Monoenergetic Electron Acceleration Driven by a sub-10 fs OPCPA System
- P4.137 M.C. Kaluza, J. Polz, O.J äckel, S. Pfotenhauer, B. Beleites, F. Ronneberger
Optical probing of the rear-surface ion acceleration sheath
- P4.138 O. Klimo, J. Psikal, J. Limpouch, V.T. Tikhonchuk
Ultrathin foil irradiated by circularly polarized laser pulse as an efficient sources of quasi-monoenergetic ions
- P4.139 P. Mora, Z. Chen, T. Grismayer, J.-C. Adam, A. Héron
Electron kinetic effects in the plasma expansion into a vacuum and ion acceleration
- P4.140 Parviz Zobdeh, R. Sedighi-Bonabi, H. Afarideh, R. Rezaei-Nasirabad
Density Transition Effect on Electron Trapping and Field Propagation in LWFA
- P4.141 R. Nuter, L. Gremillet, P. Combis, M. Drouin, E. Lefebvre, A. Flacco, V. Malka
Electron heating and proton acceleration in ultraintense laser beam interacting with a pre-irradiated target.
- P4.142 S. A. Gaillard, K. A. Flippo, M. Schollmeier, F. Nürnberg, J. S. Cowan, D. C. Gautier, K. Harres, M. Roth, B. M. Hegelich, J. C. Fernandez, W. P. Leemans, T. E. Cowan
Calibration of Radiochromic Film Gafchromic MD-55, HD-810 and HS for proton energies of ~ 5 to 20 MeV
- P4.143 S. Karsch, J. Osterhoff, A. Popp, Zs. Major, R. Hörlein, T.P. Rowlands-Rees, S. Rykovanov, M. Geissler, M. Fuchs, B. Marx, R. Weingartner, F. Grüner, U. Schramm, D. Habs, J. Vieira, R.A. Fonseca, L.O. Silva, F. Krausz, S.M. Hooker
Steering of stable laser-accelerated electron beams by controlling the laser parameters
- P4.144 S.P.D. Mangles, A.G.R. Thomas, C. Bellei, A.E. Dangor, C. Kamperidis, S. Kneip, S.R. Nagel, L. Willingale, Z. Najmudin,
Self-guided wakefield experiments driven by petawatt class ultra-short laser pulses
- P4.145 Sargis Ter-Avetisyan, Matthias Schnürer, Robert Polster, Peter V. Nickles, Wolfgang Sandner
Novel use of a quadrupole magnet lens system for collimation and monochromatisation of laser accelerated proton bursts
- P4.146 Zs. Major, J. Osterhoff, A. Popp, T.P. Rowlands-Rees, R. Hörlein, B. Marx, M. Fuchs, R. Weingartner, F. Grüner, K. Schmid, L. Veisz, U. Schramm, D. Habs, F. Krausz, S.M. Hooker, S. Karsch
Generation of stable laser-accelerated electrons from a gas-filled capillary
- P4.147 F. Peano, J. Vieira, R. Mulas, G. Coppa, L. O. Silva
All-optical trapping and acceleration of heavy particles
- P4.148 J.L. Martins, F. Peano, R.A. Fonseca, L.O. Silva
PIC modeling of the radiation processes in the laser-wakefield self-injection process
- P4.149 J. Psikal, V.T. Tikhonchuk, J. Limpouch
Ion acceleration by relativistically intense laser pulses with a large incidence angle
- P4.150 J. Vieira, F. Fiúza, R.A. Fonseca, L.O. Silva
Non-linear longitudinal laser dynamics in the laser wake field accelerator

- P4.151 M.R.Islam, B.Ersfeld, A.Reitsma, D.A.Jaroszynski
Electron trapping in moving void of laser-plasma interaction
- P4.152 M.Shoucri
Numerical Simulation of Wake-Field Acceleration using Two Counter-Propagating Laser Pulses
- P4.153 R.A. Bendoyro, C. Russo, N.C. Lopes, C.E. Clayton, F. Fang
Plasma waveguides for electron accelerators using discharges in a structured gas cell
- P4.154 S. Cavallaro, D. Margarone, L.Torrise
Charge and energy discrimination of ions in CR39 track detectors by diameter-depth correlations
- P4.155 S. F. Martins, R. A. Fonseca, W. Lu, W. B. Mori, L. O. Silva
Full-PIC 3D simulations of LWFA in boosted frames for long propagation distances
- P4.156 P.R.Levashov, V.S.Filinov, M.Bonitz, G.Schubert, A.V.Filinov, H.Fehske, V.E.Fortov
Tomographic Representation of Quantum Mechanics for Calculation of Electrical Conductivity of Dense Plasma
- P4.157 N. Mizuno, K. Sekine, Y. Nejoh
Study of discharge oscillations in Hall thrusters
- P4.158 O.S.Vaulina, X.G.Adamovich, O.F.Petrov, V.E.Fortov
Transport processes in dusty plasma of RF-discharge
- P4.159 R.I. Golyatina, S.A. Maiorov
Modeling of plasmas structure near electrode layer with magnetic field
- P4.160 S.A. Maiorov, A.A. Shcherbakov
Coulomb microfield distribution in an ion cluster
- P4.161 S. Celestin, N. Liu, A. Bourdon, V. P. Pasko
Study of the Efficient Photoionization Model 3-Group SP3 for the Modeling of Streamer Propagation
- P4.162 P. Kevrekidis, V. Koukouloyannis, D. Frantzeskakis, I. Kourakis
Discrete breathers, multibreathers and vortices in hexagonal dust crystals
- P4.163 S.A. Maiorov, A.A. Shcherbakov
Void formation modeling in two-component dust structure
- P4.164 W. F. El-Taibany, I. Kourakis, M. Wadati
Modulational instability of low frequency electrostatic waves in multi-dust-component complex plasmas
- P4.165 I. Kourakis, V. Koukouloyannis, B. Farokhi, P. K. Shukla
Nonlinear excitations in Debye crystals a survey of theoretical results
- P4.166 S.A. Kamneva, L.N. Khimchenko, V.P. Budaev, B.V. Kuteev
Surface morphology, X-ray crystal analysis and electron emission properties of fractal films from tokamak T-10
- P4.167 J. Puerta, E. Castro, P. Martin, A. Moller
Extended Treatment for the Drift Instability Growth rates in Non-ideal Inhomogeneous Dusty Plasmas
- P4.168 M. Wolter, M. Stahl, C. Terasa, H. Kersten
Spatially Resolved Measurement of the Energy Influx in an RF Plasma

- P4.169 O.S.Stoican
Study of the plasma rf absorption using a noise generator
- P4.170 L. Torrisi, G. Mondio, D. Margarone, T. Serafino
Laser and Electron Beams physical analyses applied to the comparison between two Silver Tetradrachm Greek Coins
- P4.171 M. K. Ko, E. Y. Yun, R. M. Mansur, Y. S. Mok, H. J. Lee
Reduction of Toluene Vapour by a Hybrid Technology of Plasma and Catalyst
- P4.172 Ph. G.Rutberg, G.V. Nakonechny, S.A. Kushev, A.V. Pavlov, S.D. Popov, A.V.Surov
Plasma torch optical and spectral diagnostic of arc plasma generators of alternating current
- P4.173 R. Foest, J. Schäfer, A. Quade, A. Ohl, K.-D.Weltmann
Miniaturized Atmospheric Pressure Plasma Jet APPJ for Deposition of SiO_x films with different Silicon-organic Compounds – A comparative Study
- P4.174 Sun-TaekLim, Jung-HyunCho, Sung-RyulHuh, Gon-HoKim
Improvement of Field Emission Properties of Plasma Ion Irradiated Multi-Walled Carbon Nanotubes
- P4.175 T. Lho, M. Jung, S.J. Yoo, D.C. Kim, B.J. Lee, M.H. Cho
Effects of Neutralizer Geometries on the Hyper-Thermal Neutral Beam Generation
- P4.176 V. Lisovskiy, N. Kharchenko, V. Yegorenkov
Radial structure of the longitudinal combined RF/DC discharges
- P4.177 I.F. Shaikhislamov
MHD Instability of the near Earth Magnetotail
- P4.178 J. Vranjes, S. Poedts
Coupling of drift and ion cyclotron modes in solar atmosphere
- P4.179 K.M. Gillespie, D.C. Speirs, K. Ronald, A.D.R. Phelps, S.L. McConville, A.W. Cross, R. Bingham, I. Vorgul, R.A. Cairns, B.J. Kellett
3D PiC code simulations of a scaled laboratory experiment investigating AKR
- P4.180 L. Gargaté, R. A. Fonseca, R. Bingham, L. O. Silva
Surfatron acceleration and solar energetic particle production in coronal shocks
- P4.181 L.P. Babich, E.I. Bochkov, I.M. Kutsyk
Source of runaway electrons in thundercloud field stimulated by cosmic ray showers
- P4.182 M.E. Dieckmann, G. Rowlands, P.K. Shukla
The plasma filamentation instability in one dimension
- P4.183 M.Taguchi
Basic Equations for RF-Current Drive Theory in Turbulent Plasma
- P4.184 O.Agren, V.E.Moiseenko, A, Hagnestal
Jeans Theorem and the Number of Independent Constants of Motion
- P4.185 R.A. Cairns, I.Vorgul, R. Bingham, B.J.Kellett, K.Ronald, D.C. Speirs, S.L.McConville, K.M. Gillespie, A.D.R. Phelps
Properties of cyclotron maser emission in inhomogeneous plasma

- P4.186 S.I. Tkachenko, V.M. Romanova, T.A. Shelkovenko, A.E. Ter-Oganesyan, A.R. Mingaleev, S.A. Pikuz
Inhomogeneity of plasma parameters upon electrical wire explosion
- P4.187 T. Sunn Pedersen, J. Berkery, A. H. Boozer, R. G. Lefrancois, Q. R. Marksteiner, M. S. Hahn, P. W. Brenner, B. Durand de Gevigney
Pure electron plasmas in the CNT stellarator
- P4.188 V.I. Arkhipenko, Z. Gusakov, L.V. Simonchik, F. Truhachev
Anomalous reflection control by the pump frequency modulation
- P4.189 S. Tsikata, N. Lemoine, V.A. Pisarev, D.M. Grésillon
A collective scattering device for observation of a Hall thruster plasma
- P4.190 M. Tagger, H. Méheut, P. Varnière, J. Rodriguez
MHD models of Quasi-Periodic Oscillations in accretion disks
- P4.191 R. Marchand, J.-J. Berthelier
Kinetic modelling of particle distribution measurements in DEMETER
- P4.192 P. V. Bakharev, A. V. Kudrin, T. M. Zaboronkova
Whistler eigenmodes of magnetic flux tubes in a magnetoplasma
- P5.001 T. Koskela, O. Asunta, V. Hynönen, T. Johnson, T. Kurki-Suonio, J. Lönnroth, V. Parail, M. Roccella, G. Saibene, A. Salmi, S. Sipilä
Alpha particle orbits in a locally perturbed ITER 3D magnetic field
- P5.002 T. Lunt, O. Waldmann, G. Fussmann
Laser induced fluorescence measurements in an argon plasma in front of a tungsten target under oblique incidence
- P5.003 T. Morisaki, H. Tsuchiya, H. Zushi, T. Ryokai, R. Bhattacharyay, S. Masuzaki, H. Yamada, A. Komori, O. Motojima
Two Dimensional Measurements of Edge Density Fluctuations in LHD heliotron and CPD spherical tokamak
- P5.004 V.B. Lazarev, Ya.V. Gorbunov, S.V. Mirnov
Investigation of lithium distribution in the SOL of T-11M tokamak with lithium limiter
- P5.005 V. Bobkov, F. Braun, J.-M. Noterdaeme
Calculations of Near-Fields of ICRF Antenna for ASDEX Upgrade
- P5.006 V.I. Dudin, I.V. Morozov, V.P. Korchagin
Gas Discharge Chamber of "Plasma Focus" Type with Ceramic Inserts on Electrodes
- P5.007 B. Rasul, F. Zappa, N. Endstrasser, A. Kendl, J.D. Skalny, Z. Herman, P. Scheier, T.D. Märk
Ion-surface collisions relevant for fusion devices CD2, CD3 and CD4 on beryllium and tungsten films
- P5.008 F. Schwander, G. Chiavassa, G. Ciraolo, X. Garbet, Ph. Ghendrih, V. Grandgirard, Y. Sarazin, E. Serre
Symmetry and evolution of radiative patterns in simulations of the tokamak edge plasma
- P5.009 M. F. Heyn, I. B. Ivanov, S. V. Kasilov, W. Kernbichler, M. Mulec
Quasi-linear modeling of the interaction of resonant magnetic field perturbations with a tokamak plasma
- P5.011 Y. Igitkhanov, I. Landman, B. Bazylev, G. Janeschitz
Attenuation of Plasma Flow in Detached Divertor

- P5.012 T.K.Soboleva, I.F.Potapenko, S.I.Krasheninnikov
Time dependent solutions of collisional electron kinetic equation
- P5.013 T. Hoppel, T. Estrada, L. Cupido, C. Hidalgo, E. Blanco
Radial propagation of poloidal plasma velocity changes in the stellarator TJ-II measured by reflectometry
- P5.014 T. Hellsten, T. Johnson
Neoclassical Electric Field in Presence of Large Gradients and Particle Losses
- P5.015 T.P. Kiviniemi, J.A. Heikkinen, S.J.J. Anhunen, S. Leerink, M. Nora, F. Ogando
Gyrokinetic full-f particle simulation of edge heat transport
- P5.016 T.S. Hahm, P.H. Diamond, O.D. Gurcan, W.X. Wang, G. Rewoldt, C.J. McDevitt
Roles of Curvature Driven Momentum Pinch and Residual Stress in Intrinsic Rotation
- P5.017 T. Tokuzawa, N. Tamura, R. Sakamoto, K. Tanaka, S. Inagaki, K. Kawahata, I. Yamada
Particle Transport Characteristics around Expanding Static Magnetic Island in the Large Helical Device
- P5.018 V.I. Vargas, D. López-Bruna, J. García, A. Fernández, A. Cappa, J. Herranz, F. Castejón
ECH power dependence of electron heat diffusion in ECH plasmas of the TJ-II stellarator
- P5.019 V.P. Budaev
The log-Poisson model of edge plasma turbulence in fusion devices
- P5.020 V. Rozhansky, E. Kaveeva, M. Tendler
Interpretation of the observed radial electric field inversion in TUMAN-3M tokamak during MHD-activity
- P5.021 V.V. Nemov, S.V. Kasilov, W. Kernbichler, G.O. Leitold
Poloidal drift of trapped particle orbits in real-space coordinates
- P5.022 W.M. Solomon, K.H. Burrell, A.M. Garofalo, S.M. Kaye, R.E. Bell, R.V. Budny, J.S. deGrassie, B.P. LeBlanc, F.M. Levinton, J.E. Menard, C.C. Petty, G.L. Jackson, H. Reimerdes, S.A. Sabbagh, E.J. Strait, H. Yuh
Comparison of Momentum Transport Between DIII-D and NSTX
- P5.023 W. X. Wang, T. S. Hahm, M. Adams, S. Ethier, S. M. Kaye, W. W. Lee, G. Rewoldt, W. M. Tang
Relationship between Toroidal Momentum and Heat Transport in Tokamaks
- P5.024 Y. Li, J. Li, X.D. Zhang, T. Zhang, S.Y. Lin
Small scale turbulence experiment in HT-7 tokamak
- P5.025 Yong-Su Na, L. Terzolo, J.Y. Kim
Time-dependent Simulations of the Hybrid Operation Mode Including the Neoclassical Tearing Mode Activity in KSTAR and Its Projection to DEMO
- P5.026 Z. Cui, Y. Zhou, W. Li, B. Feng, P. Sun, Y. Liu, Y. Huang, W. Hong, Q. Yang, X. Ding, X. Duan
Observation of Impurity Accumulation during Density Peaking in HL-2A Plasma
- P5.027 D. Kalupin, J. F. Artaud, D. Coster, S. Glowacz, S. Moradi, G. Pereverzev, R. Stankiewicz, M. Tokar, V. Basiuk, G. Huysmans, F. Imbeaux, Y. Peysson, L.-G. Eriksson, M. Romanelli, P. Strand
Construction of the European Transport Solver under the European Integrated Tokamak Modelling Task Force
- P5.028 Z. Lin, A. Bierwage, S. Briguglio, L. Chen, M. S. Chu, W. Heidbrink, Y. Nishimura, D. Spong, G. Vlad, R. E. Waltz, W. L. Zhang, F. Zonca
Gyrokinetic Simulation of Energetic Particle Turbulence and Transport

- P5.029 A. Salmi, V. Parail, T. Johnson, C. S. Chang, S. Ku, G. Park, JET EFDA contributors
Numerical study of neoclassical particle losses with static 2D electric fields
- P5.030 B Scott
Fully Nonlinear Electromagnetic Gyrokinetic Computations
- P5.031 B Scott
Rotation in the Presence of Turbulence in Large Tokamaks
- P5.032 G.V. Pereverzev
Properties of numeric schemes for stiff transport models
- P5.033 G. Breyiannis, D. Valougeorgis
Lattice kinetic Schemes in Fusion Plasmas
- P5.034 G.M.D.Hogeweyj, F.Imbeaux, F.Köchl, X.Litaudon, V. Parail, A.C.C. Sips, for the EU Integrated Tokamak Modelling Task Force
Simulation of the current ramp-up phase of ITER discharges
- P5.035 M. Gobbin, F. Sattin, S.C. Guo, L.Marrelli, S. Cappello
Numerical studies of particle transport in RFX-mod low chaos regimes
- P5.036 M. Nora, J.A. Heikkinen, S.J. Janhunen, T.P Kiviniemi, S. Leerink, F. Ogando
Derivation of gyrokinetic equations for full-f particle simulation with polarization drift
- P5.037 R.V. Shurygin, A.A. Mavrin, A.V. Melnikov
Computation of radial electric field in the turbulent edge plasma of the T-10 tokamak
- P5.038 S. V. Neudatchin
New interpretation of slow heat pulse propagation during ITB formation in Tokamaks
- P5.039 T.T. Ribeiro, B. Scott
Drift wave vs. interchange turbulence geometrical effects on the ballooning threshold
- P5.040 J. Vranjes, S. Poedts
Drift and acoustic modes in radially and axially inhomogeneous plasma
- P5.041 M. Jucker, V.P. Pavlenko
Large Scale Magnetic Field Generation via Modulation Instability in Electron Drift Turbulence
- P5.042 P. Martin, E. Castro
Triangularity and Ellipticity Effects on Ware Pinch
- P5.043 F. Schwander, K.G. McClements, A. Thyagaraja
Rotation driven by fast ions in tokamaks
- P5.044 J. Manickam
Predictive Stability Analysis
- P5.045 F. Sartori, P. Lomas, F. Piccolo, M.K. Zedda
Synchronous ELM Pacing at JET using the Vertical Stabilisation Controller
- P5.046 S.Nowak, E.Lazzaro, C.Marchetto
NTM avoidance through control of island rotation by external torque exploring the role of the polarisation

current

- P5.047 G. Marchiori, L. Marrelli, P. Piovesan, A. Soppelsa, F. Villone
Comparison between an experimentally estimated and a finite element model of RFX-mod MHD active control system
- P5.048 A. Ishida, L.C. Steinhauer, Y.K.M. Peng
Formalism for multi-fluid magnetohydrodynamics equilibrium with strong flows and application to CT and ST
- P5.049 P. L. Garcia-Martinez, R. Farengo
Flux Core Spheromak Formation from an Unstable Screw Pinch
- P5.050 M.C. Zarnstorff, N. Pomphrey, G. Fu
Edge Pedestal Stability in NCSX
- P5.051 D. Yu. Eremin
Unstable Drift-Kinetic Alfvén Modes in the Lowest Part of the Alfvénic Spectrum of Optimized Stellarators
- P5.052 N Ben Ayed, K. G. McClements, A. Thyagaraja
Alfvén eigenmodes in magnetic X-point configurations with strong longitudinal fields
- P5.053 S. Wiesen, V. Parail, G. Corrigan, W. Fundamenski, J. Lonnroth
Progress on integrated modelling of type-I ELMs at JET with COCONUT
- P5.054 A. Perona, L.-G. Eriksson, D. Grasso
Generation of suprathermal electrons during magnetic reconnection
- P5.055 C. Di Troia, S. Briguglio, G. Calabrò, A. Cardinali, F. Crisanti, G. Fogaccia, M. Marinucci, G. Vlad, F. Zonca
Investigation of fast ion behaviors in burning plasmas via Ion Cyclotron Resonance Heating
- P5.056 F. Zonca, L. Chen
Self-consistent energetic particle nonlinear dynamics due to shear Alfvén wave excitations
- P5.057 I.S. Landman, G. Janeschitz
Calculation of Poloidal Magnetic Field in Tokamak Code TOKES
- P5.058 N. Pomphrey, A. Boozer, A. Brooks, M. Zarnstorff
Analysis Methods for Trim Coils in NCSX
- P5.059 S. Nishimura, S. Benkadda, M. Yagi, S.-I. Itoh, K. Itoh
Rotation of Magnetic Islands with Micro-Scale Fluctuations
- P5.060 E. D. Fredrickson, N. A. Crocker, D. Darrow, N. N. Gorelenkov, W. W. Heidbrink, S. Kubota, F. M. Levinton, D. Liu, S. S. Medley, M. Podesta, H. Yuh, R. E. Bell
Toroidal Alfvén Eigenmode Avalanches in NSTX
- P5.061 J. Vranjes, H. Saleem, S. Poedts
Magnetic field generation at ion acoustic time scale
- P5.062 J. P. Graves, I. Chapman, S. Coda, L.-G. Eriksson, T. Johnson
Sawtooth control mechanism using counter current propagating ICRH in JET
- P5.063 H.R. Koslowski, Y. Liang, E. Delabie, TEXTOR-team
Investigation of resonant and non-resonant plasma momentum braking using the Dynamic Ergodic Divertor on

TEXTOR

- P5.064 J. Scheffel, A. Mirza
Pressure driven resistive modes in the advanced RFP
- P5.065 L. Marrelli, P. Zanca, R. Paccagnella, P. Piovesan, G. Marchiori, L. Novello, A. Soppelsa
Advances in MHD mode control in RFX-mod
- P5.067 D.Kh.Morozov, A.A.Pshenov, A.B.Mineev
Improvement of start-up in tokamaks by modulation of ECR source.
- P5.068 J.F. Artaud, V.Basiuk, G. Giruzzi, X. Litaudon
Simulation of present-day Tokamak Discharges Mimicking a Fully non-Inductive Burning Plasma
- P5.069 O. Asunta, T. Kurki-Suonio, T. Tala, S. Sipilä, R. Salomaa
Fusion Alpha Performance in Advanced Scenario Plasmas
- P5.070 M. Salewski, H. Bindslev, V. Furtula, S.B. Korsholm, F. Leipold, F. Meo, P.K. Michelsen, S.K. Nielsen
Comparison of CTS Signals due to Auxiliary Heating in ITER
- P5.071 S.E. Grebenshchikov, I.Yu. Vafin, A.I. Meshcheryakov
Procedure for Reconstructing the Electron Energy Distribution Function from the Soft X-Ray Spectrum
- P5.072 P. Acedo, P. Pedreira, A.R. Criado, H. Lamela, M. Sánchez, J. Sánchez
Systematic Study of the Sources of Error in the High Spatial Resolution Two-Color Laser Interferometer for the TJ-II Stellarator
- P5.073 G. Serianni, N. Pomaro, R. Pasqualotto, M. Spolaore, M. Valisa
The diagnostic system for the characterisation of ITER Neutral Beam Injectors
- P5.074 G.Grossetti, C.Sozzi, E.De La Luna, D.Farina, J.Fessey, L.Figini, S.Garavaglia, S.Nowak, P.Platania, A.Simonetto, M.Zerbini
Bayesian approach to data validation of the oblique ECE diagnostic at JET
- P5.075 V.V. Plyusnin, L. Jakubowski, J. Zebrowski, H. Fernandes, C.Silva, P. Duarte, K. Malinowski, M. Rabinski, M.J. Sadowski
Detection of Runaway Electrons Using Cherenkov-type Detectors in the ISTTOK Tokamak.
- P5.076 G. Petravich, D. Dunai, G. Anda, J. Sárközi, S. Zoletnik, B. Schweer
First measurements with the re-installed accelerated Lithium beam diagnostics on TEXTOR
- P5.077 S.K. Nielsen, H.Bindslev, S.B. Korsholm, F. Leipold, F. Meo, J.W. Oosterbeek, M. Salewski, M. Vervier, G. Van Wassenhove, E. Westerhof, P. Woskov
Anisotropic fast-ion velocity distributions measured by collective Thomson scattering in the TEXTOR tokamak
- P5.078 R. C. Wolf, R. König, W. Biel, J. Cantarini, M. Endler, H.-J. Hartfuß, D. Hildebrandt, M. Hirsch, G. Kocsis, P. Kornejew, M. Laux, M. Otte, E. Pasch, A. Pospieszczyk, S. Recsei, W. Schneider, B. Schweer, J. Svensson, V. Szabó, H. Thomsen, A. Weller, A. Werner, M.Y. Ye, S. Zoletnik
Diagnostic Challenges for the Optimized Stellarator Wendelstein 7-X
- P5.079 G. Por, D. Bódizs, Sz. Czifrus, G. Kocsis, K. Nagy, J. Pálfalvi, T. Pázmándi, A. Szappanos, S. Zoletnik
Radiation damage in Video Diagnostic Device for Wendelstein 7-X
- P5.080 P.V.Savrukhin, E.V.Popova, D.V.Sarichev

- Measurements of the small-scale plasma perturbations during sawtooth crash and disruption instability in the T-10 tokamak plasma*
- P5.081 W. Schneider, M. Turnyanskiy, F.V. Chernyshev, M. Kick, T. Richert
Neutral Particle Diagnostics at MAST with a Compact Energy Analyser and Comparison with Charge Exchange Recombination Spectroscopy
- P5.082 M. Kubo-Irie, M.Irie, FBX team
Phase Imaging Passive Holography on LCDC the Local Cold and Dense Compress in Tokamaks
- P5.083 A. Klein, D.Testa , J. Snipes, A. Fasoli, JET-EFDA Contributors
Toroidal mode number analysis of degenerate Alfvén Eigenmodes in the active MHD spectroscopy on JET
- P5.084 M. R. Turnyanskiy, A. J. Akers, G. Cunningham
Off axis NBCD experiments on MAST
- P5.085 S.J. Wukitch, M. Porkolab, Y. Lin, P.T. Bonoli, J.C. Wright, the Alcator C-Mod Team
Recent ICRF Results in Alcator C-Mod
- P5.086 G.J.Lei, G. W. Zhong, J.Y. Cao, J.Rao,B.Li,S. F. Jiang, D. L.Lu, G.Q.Zou, J.F. Yang, H.Liu,X.M. Zhang, X.Y.Wang, J.X.Yang, G.Q.Zhang, L.M.Yu,T. Jiang, L.Li, K.Feng, Z.H.Kang, M.W.Wang, W.M.Xuan,L.Y.Yao,L.Y.Cheng, Z.Cao
Neutral Beam Injection System and Preliminary Experiment on HL-2A
- P5.087 T.Oikawa, D.J.Campbell, M.Henderson
Heating and Current Drive Issues towards ITER Operations
- P5.088 A. Mendes, L. Colas, A. Argouarch, S. Brémond, F. Clairet, C. Desgranges, A. Ekedahl, J.P. Gunn, G. Lombard, D. Milanese, L. Millon, P. Mollard, D. Volpe, K. Vulliez
Interaction of ITER-like ICRF antenna with Tore Supra plasmas insight from modelling.
- P5.089 C. Tsironis, T. Samaras, L. Vlahos
FDTD algorithm for the propagation of EC waves in hot anisotropic plasma
- P5.090 A. Aïssi, F. André, F. Doveil
New model of a travelling-wave tube
- P5.091 B.H.Park, S.S.Kim, S.W.Yoon, J.Y.Kim
Development of a Full Wave ICRF Code for KSTAR Plasma
- P5.092 A.N.Saveliev
Propagation and absorption of EM microwave beams in toroidal plasmas
- P5.093 I. Chatziantonaki, L. Vlahos, C. Tsironis
Propagation and absorption of EC waves in the presence of magnetic islands
- P5.094 R. Bilato, M. Brambilla
FELHS code for lower-hybrid launcher coupling and near fields
- P5.095 R.Bilato,E.Poli,F.Volpe,R.Paccagnella,M.Brambilla
ECCD Feasibility Study for RFX
- P5.096 Yu.M. Aliev, M. Kraemer
Mode conversion of non-axisymmetric modes in strongly non-uniform helicon-sustained plasma

- P5.097 T. Bolzonella, L. Marrelli, A. Alfieri, L. Carraro, P. Innocente, R. Pasqualotto, D. Terranova
Insights on ohmic input power evaluation in the RFX-mod Reversed Field Pinch
- P5.098 V.V. Postupaev, A.V. Arzhannikov, V.T. Astrelin, V.V. Belykh, A.V. Burdakov, V.S. Burmasov, I.A. Ivanov, M.V. Ivantsivsky, M.V. Kolosov, A.S. Krygina, K.N. Kuklin, K.I. Mekler, S.V. Polosatkin, S.S. Popov, A.F. Rovenskikh, A.A. Shoshin, N.V.S. Orokina, S.L. Sinitzky, Yu.S. Sulyaev, Yu.A. Trunev, L.N. Vyacheslavov, Ed.R. Zubairov
Dynamics of electron distribution function in multiple mirror trap GOL-3
- P5.099 R. Nazikian, M.E. Austin, H.L. Berk, R.V. Budny, G.Y. Fu, W.W. Heidbrink, G.J. Kramer, M.A. Makowski, G.R.M. McKee, N.N. Gorelenkov, W.M. Solomon, E.J. Strait, M.A. VanZeeland, A.E. White, R.B. White
N 0 Instability Driven by Counter-Injected Neutral Beam Ions in DIII-D
- P5.100 E.M. Edlund, M. Porkolab, L. Lin, N. Tsujii, S.J. Wukitch, G.J. Kramer
Reversed Shear Alfvén Eigenmodes in Alcator C-Mod During ICRF Minority Heating and Relationship to Sawtooth Crash Phenomena
- P5.101 X.Q. Ji, Q.W. Yang, W. Deng, J. Zhou, B.B. Feng, B.S. Yuan, W.M. Xie, Y. Liu
Tearing mode suppression by ECRH in the HL-2A tokamak
- P5.102 L.J. Perkins, K.N. Lafortune, A.R. Miles, R. Betti
Shock Ignition - A New Approach to High Gain/Yield Targets for the National Ignition Facility and Inertial Fusion Energy
- P5.103 S. Kar, K. Markey, D.C. Carroll, A.P.L. Robinson, R. Jafer, P. McKenna, P. Norreys, D. Neely, M. Zepf,
Guided transport of hot electron beam inside a solid density plasma
- P5.104 I.V. Timofeev, A.V. Terekhov, K.V. Lotov
Computer simulation of relativistic electron beam relaxation in plasma
- P5.105 A. Bret, L. Gremillet, D. Bénisti, E. Lefebvre
Exact relativistic kinetic theory of an electron beam-plasma system hierarchy of the competing modes in the system parameter space
- P5.106 S. Atzeni, A. Schiavi, J.R. Davies
Stopping and scattering of relativistic electrons in high density plasmas for fast ignition studies
- P5.107 A. G. Mordovanakis, J. Easter, M. G. Haines, B. Hou, P. E. Masson-Laborde, G. Mourou, J. Nees, W. Rozmus, K. Krushelnick
Scaling of Hot Electron Temperature in the Relativistic Regime using a High Repetition Rate Laser
- P5.108 C. Bellei, S. Nagel, S. Kar, A. Henig, S. Kneip, C. Palmer, A. Saevert, L. Willingale, D. Carroll, B. Dromey, J. Green, K. Markey, P. Simpson, R. J. Clark, D. Neely, A. E. Dangor, S. P. D. Mangles, P. McKenna, P. A. Norreys, J. Schreiber, M. Zepf, M. Kaluza, K. Krushelnick, Z. Najmudin
Polarization Properties of Transition Radiation and Observation of Recirculating Currents from High-Intensity Laser Solid Interactions
- P5.109 J.J. Santos, D. Batani, P. McKenna, C. Rousseaux, S.D. Baton, F. Dorchie, A. Dubrouil, C. Fourment, S. Hulin, P. Carpeggiani, M. Veltcheva, M. Quinn, E. Brambrink, M. Koenig, F. Perez, M. Rabec Le Gloahec
Fast electron propagation in high density plasmas created by shock wave compression relevant to fast ignition
- P5.110 J. Pasley
Simulations of the motion of cone material and its effects upon ignition and burn

- P5.111 K.A. Tanaka, H. Habara, R. Kodama, K. Kondo, T. Tanimoto, T. Yabu-uchi, K. Mima, T. Notimasu, K. Nagatomo, K. Nagai, A. Lei
Increase of hot electron production and its behavior under strong static potential
- P5.112 L. Gremillet, D. Bénisti, M. Drouin, E. Lefebvre, F. Perez, S. D. Baton
Coupling of relativistic laser pulses with cone-guided targets
- P5.113 L. Romagnani, P.A. Wilson, K. Quinn, B. Ramakrishna, M. Borghesi, P. Antici, L. Lancia, J. Fuchs, M. Amin, C.A. Pipahl, T. Toncian, O. Willi, M. Tampo, R. Kodama, R.J. Clarke, M. Notley
Relativistic electron dynamics in high intensity laser matter interactions
- P5.114 M. G. Haines, F.N. Beg, M. Wei, R.B. Stephens
On the scaling of the hot electron temperature and laser absorption in fast ignition
- P5.116 S.R. Nagel, C. Bellei, R.J. Clarke, R. Heathcote, A. Henig, M. Kaluza, S. Kar, S. Kneip, S.P.D. Mangles, K. Markey, C. Palmer, A. Sävert, J. Schreiber, P. Simpson, L. Willingale, M. Zepf, A.E. Dangor, Z. Najmudin
Electron acceleration from solid targets
- P5.117 Y. Sentoku, T. Johzaki, B. Chrisman, A. Kemp
Numerical Modeling of Ultra-fast Heated Au Target by Intense Laser
- P5.118 A.G.R. Thomas, R.G. Evans, S.J. Rose
Particle-in-cell modelling of electron transport under Fast Ignition relevant conditions
- P5.119 D. Batani, A. Aliverdiev, R. Dezulian, T. Vinci, A. Benuzzi-Mounaix, M. Koenig, V. Malka
Hydrodynamics of Laser-Produced Plasmas Experiment and MULTI hydrocode Simulations
- P5.120 F. Fiuza, J.R. Davies, R.A. Fonseca, L.O. Silva
Heat flux in solid targets irradiated by fast ignition laser beams
- P5.121 H. Sakagami, T. Johzaki, H. Nagatomo, T. Nakamura, K. Mima
Generation Control for Fast Electron Beam in Fast Ignition
- P5.122 L.F. Ibañez, J. Sanz
Surface Current layer induced by Relativistic Electrons
- P5.123 R. Redaelli, D. Batani, A. Morace, P. Carpeggiani, M. H. Xu, F. Liu, Y. Zhang, Z. Zhang, X. X. Lin, F. Liu, S. J. Wang, P. F. Zhu, L. M. Meng, Z. H. Wang, Y. T. Li, Z. M. Sheng, Z. Y. Wei, J. Zhang
Transport of Intense Laser-Produced Electron Beams in Matter
- P5.124 Y. T. Li, X. H. Yuan, M. H. Xu, Z. Y. Zheng, M. Chen, W. M. Wang, Q. Z. Yu, S. J. Wang, Z. H. Wang, Z. Y. Wei, Z. M. Sheng, J. Zhang
Fast Electron Transport in High-Intensity Laser-Plasma Interactions
- P5.125 J.J. Honrubia, M. Temporal, J. Badziak, S. Jablonsky
Fast ignition of imploded fusion targets by ion beams
- P5.126 H. Nishimura, D. Batani, Y. Inubushi, Y. Okano, S. Fujioka, T. Kai, T. Kawamura, A. Morace, R. Redaelli, C. Fourment, J. Santos, G. Malka, A. Boscheron, A. Casner, M. Koenig, T. Nakamura, T. Johzaki, H. Nagatomo, K. Mima
X-ray polarization spectroscopy to study energy transport in ultra-high intensity laser produced plasmas
- P5.127 P. Mulser, D. Bauer, H. Ruhl
Anharmonic resonance absorption of high power laser beams

- P5.128 M.Charboneau-Lefort, M.Shoucri, B.Afeyan
Numerical Simulation for an Intense Laser Wave Incident on an Overdense Plasma
- P5.129 M.Mašek, K.Rohlina
Numerical simulation of wave-particle interaction in laser plasmas
- P5.130 C. Rechatin, J. Faure, A. Lifschitz, X. Davoine, E. Lefebvre, V. Malka
Quasimonoenergetic electron beams produced by colliding cross-polarized laser pulses
- P5.131 V.N.Tsyтовich
Nonlinear equilibrium states of self-organized dust structures
- P5.132 W.J. Miloch, S.V. Vladimirov, H.L. Pécseli, J. Trulsen
Wake formation behind elongated insulating dust grains in drifting plasmas numerical simulations
- P5.133 Y. Saitou, A. Tsushima
Two-Dimensional PIC Simulations on Face-to-face Double Probe
- P5.134 A.B. Kukushkin, N.L. Marusov, P.V. Minashin, V.S. Neverov
Self-Assembling of Filaments and Closing the Electric Circuit in a Random Ensemble of a Strongly Magnetized Dust
- P5.135 A.Bustos, F.Castejón, L.A. Fernández, V. Martín-Mayor, A.Tarancón, J.L.Velasco
Kinetic Simulations of ion Heating and Collisional Transport in a 3D Tokamak.
- P5.135 L. Couëdel, A. Samarian, M. Mikikian, L. Boufendi
Dust Particles in Discharge Afterglow
- P5.136 T. Antonova, B. M. Annaratone, H.M.Thomas, G.E. Morfill
Dust particle manipulation in plasma discharge
- P5.137 X.G.Adamovich, O.S.Vaulina, Yu.V.Khrustalev, Yu.Yu.Nekhaevsky, O.F.Petrov, V.E.Fortov
Phase transitions in dusty plasma systems of RF-disharge
- P5.138 Y.Peng,R.Hugon,F.Brochard,D.Lacroix,J.Bougdira
Carbon dusts formation and transport in a radiofrequency discharge
- P5.139 M. Schwabe, S.K. Zhdanov, M. Rubin-Zuzic, H.M. Thomas, A.V. Ivlev,G.E. Morfill, V.I. Molotkov, A.M. Lipaev, V.E. Fortov
Dust Waves in Complex Plasmas under Microgravity Conditions
- P5.140 V. V. Yaroshenko, H. M. Thomas , G. E. Morfill
Dust acoustic waves in a complex plasma layer
- P5.141 H. Terças, J. T. Mendonça
Quantum Tonks-Dattner resonances in cold plasmas
- P5.142 P. Pokorný, M. Novotný, J. Bulir, J. Lancok, M. Misina, J. Musil
Study of processes in a pulsed magnetron Ar/O₂ plasma by mass and optical emission spectroscopy
- P5.143 R. A. Hardin, E. E. Scime
A 300 GHz Collective Scattering Diagnostic for Low Temperature Plasmas
- P5.144 S.S. Ciobanu, C. Negutu, M. Stafe, V. Pais, V. Stancalie, N.N. Puscas

Spectroscopic studies and kinetic calculations of laser induced aluminum plasma in air

- P5.145 V.V. Peskov, V.A. Kurnaev, N.V. Isaev, E.G. Shustin
Plasma interaction with non-conducting surface in beam plasma discharge at low magnetic field
- P5.146 W. Gao, H.L. Liao, C. Coddet
Synthesis and characterization of apatite-type lanthanum silicate electrolyte powders
- P5.147 W. Oohara, O. Fukumasa
Surface production of hydrogen negative ions using catalyst
- P5.148 A.S. Askarova, E.I. Karpenko, V.E. Messerle, A.B. Ustimenko
Plasma Enhancement of Coal Dust Combustion
- P5.149 D. Sydorenko, I.D. Kaganovich, Y. Raitses, A. Smolyakov
Electron Kinetic Effects And Beam-Related Instabilities In Hall Thrusters
- P5.150 L. Hallo, D. Hébert, A. Bourgade, C. Mézel, A. Bourgade
Femtosecond laser obtained cavities in dielectrics Femtosecond laser obtained cavities in dielectrics fluid and elastoplastic behaviour
- P5.151 N. Dubuit, J.C. Adam, A. Héron, J.P. Boeuf, J. Perez-Luna, L. Garrigues, G.J.M. Hagelaar
Kinetic simulations of turbulence and anomalous transport in Hall-effect thrusters
- P5.152 J.D. Martin, M. Bacharis, M. Coppins, G.F. Counsell, J.E. Allen
Dust in Tokamaks a comparison of different ion drag models
- P5.153 L.P. Babich, A.N. Donskoi, R.I. Il'kaev, I.M. Kutsyk
The fundamental characteristics of relativistic runaway electron avalanche in air
- P5.154 P. Rebusco, B. Coppi
Spiral Modes in Astrophysical Plasma Disks and Quasi Periodic Oscillations of Radiation Emission
- P5.155 R. Bingham, B.J. Kellett
Turbulent Plasma Heating as a Mechanism to Explain the Extended X-ray Emission from the Orion Nebula
- P5.156 R. Kissmann, J. Kleimann, H. Fichtner, R. Grauer
High-res simulations of interstellar MHD turbulence -- Spatial structure and statistics
- P5.157 S. Bahamida
Linear and nonlinear dust-acoustic waves in inhomogeneous non-thermal dusty plasma
- P5.158 Y. Nagashima, S.-I. Itoh, S. Shinohara, M. Fukao, A. Fujisawa, K. Terasaka, T. Nishijima, M. Kawaguchi, Y. Kawai, N. Kasuya, G.R. Tynan, P.H. Diamond, M. Yagi, S. Inagaki, T. Yamada, K. Kamataki, T. Maruta, K. Itoh
Coexistence of the drift wave spectrum and low-frequency zonal flow potential in cylindrical laboratory plasmas
- P2.147 J.G. Rubiano, R. Rodriguez, J.M. Gil, R. Florido, P. Martel, M. Mendoza, D. Suarez, E. Minguez
Opacity calculations of low Z plasmas for ICF
- P5.160 F. Bencheriet, M. Djebli, W. M. Moslem
Dust-ion-acoustic soliton in magnetized dusty plasma with nonthermal electrons
- P5.161 K. Annou
A Spherical Kadomtsev-Petviashvili Equation for Solitary

- P5.162 V.E. Fortov, A.V. Gavrikov, D.N. Goranskaya, A.S. Ivanov, O.F. Petrov, R.A. Timirkhanov
Experimental investigation of the viscoplastic flow in dusty plasma crystal
- P5.163 Nasser Sepehri Javan
Simulation of Raman Backscattering Instability in the Interaction of Two Short and Intense Laser Pulses in Cold Plasma
- P5.164 Nasser Sepehri Javan
Investigation of dispersion and group velocity of electromagnetically induced transparency for two noncollinear lasers in plasma
- P5.165 J.M. Donoso, L. Conde
Propagation modes of the ionization instability in a dusty plasma under electron beam injection
- P5.166 V.E. Fortov
Pressure and Charge Coupling of Strongly Nonideal Plasmas
- P5.167 Z. Ehsan, N. L. Tsintsadze, H.A. Shah, G. Murtaza
Decay of Lower Hybrid wave in two lower hybrid waves and cusp soliton in dusty plasmas
- P5.168 N. Elkina, K.W. Lee, J. Buechner
Multi-fluid simulation of interaction between reconnection jet and solar coronal plasma
- P5.169 C. Rebont, N. Claire, Th. Pierre, F. Doveil
Ion velocity in a coherent instability of a linear magnetized plasma
- P5.170 S. Perri, G. Zimbardo
Superdiffusive transport of energetic particles through the heliosphere
- P5.171 A.V. Gavrikov, V.E. Fortov, O.F. Petrov, V.N. Babichev, A.V. Filippov, A.F. Pal', A.N. Starostin
Investigation of photoemissive dusty plasma

LIST OF POST DEADLINE ABSTRACTS

- D1.001 S.N. Antipov, E.I. Asinovskii, A.V. Kirillin, S.A. Maiorov, V.V. Markovets, O.F. Petrov, V.E. Fortov
Dusty Plasma structures at temperatures of 4.2-300 K
- D1.002 A. Canton, S. Dal Bello, R. Cavazzana, P. Innocente, P. Sonato
Density control in RFX-mod Reversed Field Pinch device
- D1.003 L. Lauro-Taroni, G. Corrigan, A. Foster, M.O' Mullane, J. Strachan, H.P. Summers, A. Whiteford³, S. Wiesen
Assessment of the superstate description of heavy impurities for JET and ITER
- D2.001 GAO Yaoming, LI Yunsheng
Simulation for X-ray spectroscopic diagnostics of implosion capsule in IC
- D2.002 Ángel De Andrea González
Initial value problem of the ablative Rayleigh–Taylor Instability: the disappearance of the cut-off wave number
- D2.003 J.B. Chen, S.E. Jiang, Zhurong. Cao, W. Yong. Miao, W.M. Zhou, M. Chen and Zh.J. Liu
Fuel area density diagnostic by secondary protons for ICF

- D2.004 Li Jinghong
Two dimensional Simulation of Radiative Transfer for SG Laser Facility
- D2.005 G. J. Lei, G. W. Zhong, J.Y. Cao, J.Rao,B.Li,S. F. Jiang, D. L.Lu, G.Q.Zou, J.F. Yang, H.Liu,X.M. Zhang, X.Y.Wang, J.X.Yang, G.Q.Zhang, L.M.Yu,T. Jiang, L.Li, K.Feng, Z.H.Kang, M.W.Wang, W.M. Xuan,L.Y.Yao, L.Y.Cheng, Z.Cao
Neutral Beam Injection System and Preliminary Experiment on HL-2A
- D2.006 Pakzad Hamid Reza
Effect of dust charge variation on energy of soliton and linear dispersion in dusty plasma with variable dust charge and two temperature ions
- D4.001 Storm Erik
Indirectly Driven Fast Ignition Fusion Energy: A Path Forward (ORAL PRESENTATION)
- D4.002 Pakzad Hamid Reza
Dust acoustic solitary and shock waves in coupled dusty plasmas with variable dust charge and isononthermal ions
- D4.003 B. Weyssow , C. Toniolo and Q. Vanhaelen
On determining the smoothing length in the Smoothed Particle Hydrodynamics (SPH) description of fluids
- D4.004 X.L. Zou, S.D. Song, W.W. Xiaoa, G. Giruzzi, J.L. Ségui, F. Bouquey, C. Darbos, M. Lennholm, R. Magne, E. Traisnel
Investigation of the Heat Pinch by Low Frequency ECRH Modulation Experiments in Tore Supra
- D5.001 P. Amendt, D. Clark, D. Ho, J.Latkowski, J. Lindl, E. Storm, M. Tabak and R.P.J. Town
Inertial Fusion Energy with Fast Ignition: Progress in Integrated Hohlräum Designs
- D5.002 Bell A.
The inhibition of charged particle transport by a new streaming instability
- D5.003 W.W. Xiao, X.L. Zoua, X.T. Ding, L.H. Yao, B.B. Feng, X.M. Song, Y. Zhou, H.J. Sun, Y.D. Gao, L.W. Yan, Q.W. Yang, Yi Liu, J.Q. Dong, X.R. Duan, Yong Liu, C.H. Pan, and HL-2A team
Observation of a Natural Particle Transport Barrier in HL-2A Tokamak
- D5.004 Huang Xiuguang, Fu Sizu, Shu Hua, Ye Junjian, Wu Jiang, He Juhua, Gu Yuan
Recent experimental researches on laser driving shocks at Shenguang- II facility
- D5.005 A.G.Oreshko
Possibility ball lightning application for nuclear fusion
- D5.006 J. Robiche, J. Fuchs, A. Mancic, P. Antici and P. Audebert
Hydrodynamic of metal target isochorically heated by protons in the warm dense regime

ABSTRACTS OF INVITED TALKS

Alfvén Waves: A Journey between Space and Fusion Plasmas[†]

Liu Chen^{1,2}

Alfvén waves discovered by Hannes Alfvén are fundamental electromagnetic oscillations in magnetized plasmas existing in the nature and laboratories. Alfvén waves play important roles in the heating, stability, and transport of plasmas. The anisotropic nearly-incompressible shear Alfvén wave is particularly interesting; since, in realistic non-uniform plasmas, its wave spectra consist of both the regular discrete and the singular continuous components. In this Alfvén Lecture, I will discuss these spectral properties and examine their significant linear and nonlinear physics implications. These discussions will be based on perspectives from my own research in both space and laboratory fusion plasmas; and will demonstrate the positive feedbacks and cross-fertilization between these two important sub-disciplines of plasma physics research. Some open issues of nonlinear Alfvén wave physics in burning fusion as well as magnetospheric space plasmas will also be explored.

[†] Research supported by U.S. DOE, NSF grants, and Guangbiao Foundation of Zhejiang University.

¹ Department of Physics and Astronomy, University of California, Irvine, USA.

² Institute for Fusion Theory and Simulation, Zhejiang University, Hangzhou, China.

**From relativistic laser-plasma interactions
to intense attosecond pulses**

G. D. Tsakiris

*Max-Planck-Institut für Quantenoptik,
Hans-Kopfermann-Str. 1, 85748 Garching, Germany*

The dawn of lasers capable of delivering Terawatt to Petawatt power output set off the exploration of a host of processes in the realm of relativistic laser-plasma interaction. At intensities beyond 10^{18} W/cm² where the electrons mean quiver energy becomes comparable to their rest mass energy, a plethora of new phenomena emerge: X- and γ -rays are copiously generated, the laser light undergoes relativistic self-focusing, electrons and protons are accelerated to breakthrough energies, neutron and positrons are produced, and the laser frequency is up-shifted to harmonic radiation reaching the keV photon energy. The last process of harmonic generation accompanying the interaction of high intensity laser pulses with solid targets gives rise to an intriguing prospect: the production of intense single attosecond pulses. The advent of such pulses will open up the way to real-time observation of a wide range of fast evolving phenomena in atomic, molecular and plasma physics.

Complex plasmas: Forces and dynamical behaviour

Alexander Piel

Christian-Albrechts-University, Kiel, Germany

The field of complex (dusty) plasmas, which experienced a tremendous growth after the discovery of “plasma crystals” [1], in 1994, has now become an integral part of plasma physics. This talk addresses some basic physical mechanisms that illuminate typical features of complex plasmas and discusses recent developments.

The first part of the talk is devoted to the confinement and structure of two-dimensional and 2.5-dimensional plasma crystals in the sheath of radio-frequency discharges. It is shown how the super-sonic ion flow affects the interparticle forces and the structure of the plasma crystal. Recently, three-dimensional plasma crystals could be formed [2], which possess an unusual crystal structure of nested shells. The principle of the shell structure and the differences from “Coulomb crystals” in systems of laser-cooled ions are outlined. The imaging methods have evolved from video-microscopy to stereoscopic imaging and holography.

In a second part, the ion wind force on dust particles is discussed, which leads to the formation of particle-free regions (“voids”) of the dust cloud, that are found in many experiments under micro-gravity. Experiments with tracer particles reveal the position where the ion-drag force balances the Coulomb force from the ambipolar electric field. The same technique was used to visualize the sheath around a Langmuir probe. In magnetized plasmas, ion drag leads to torus-shaped dust clouds that are set into poloidal rotation by the ion wind.

The third part addresses 2D dust-lattice waves and 3D dust-density waves. Waves are indispensable tools for the diagnostics of dusty plasmas. On the other hand, complex plasmas can serve as model systems to study phonons in solid and liquid phases of strongly coupled matter.

References

- [1] J.H. Chu and Lin I, Phys. Rev. Lett. **72**, 4009 (1994); Y. Hayashi and K. Tachibana, Jap. J. Appl. Phys. **33**, 4208 (1994); H. Thomas *et al*, Phys. Rev. Lett. **73**, 652 (1994)
- [2] O. Arp *et al*, Phys. Rev. Lett. **93**, 165004 (2004); Phys. Plasmas **12**, 122102 (2005)

THREE DIMENSIONAL EFFECTS IN TOKAMAKS

S. Günter, K. Lackner, Ph. Lauber, P. Merkel, E. Strumberger and the ASDEX Upgrade team

*Max-Planck Institut für Plasmaphysik,
85748 Garching, Germany, EURATOM Association*

We give an overview of 3-d effects in tokamaks, stressing synergies with stellarator research, in particular in the development and use of computational tools. We restrict to situations, where perturbations grow slowly ($\gamma \ll R/V_{\text{alf}}$), so that the plasma passes through a sequence of 3-d ideal-MHD equilibrium states, with the time-dependence determined by the resistive decay of plasma or wall currents (excluding thereby Alfvén-type modes). The actuality of the topics is given by the recent ITER and DEMO discussions, emphasising the active control of neoclassical tearing (NTM) and resistive wall modes (RWM) as well as edge profiles (through resonant perturbations). The slow rate of change of all these states raises the possibility of external feedback.

Localized current deficits at resonant surfaces in standard-q profile discharges can be induced by conductivity (pellet injection or radiation enhancement) or bootstrap current reduction (NTMs), and can result in ideal-MHD stable helical equilibrium states (sometimes termed snakes) with closed flux surfaces and evidently good energy and particle confinement. These perturbations lead to losses of fast particles, generally not associated with resonances in velocity space, but similar to those in non-optimized stellarators. They can now be well diagnosed with fast particle analyzers having high-resolution in time and velocity space.

Even ideal-MHD unstable low-n modes can be reduced to slowly developing equilibrium states by the presence of sufficiently close resistive walls. Realistic wall structures thereby lead to a coupling of different toroidal modes, effectively suggesting the use of stellarator codes for their analysis. Plasma rotation has a strong effect on the predicted growth rate, but the magnitude of the rotation and the critical field amplitude for mode locking depend strongly on rotation damping by 3-d magnetic field perturbations. Even for a given rotation speed the dispersion relation of the mode depends on kinetic effects, and we describe also recent efforts to apply truly kinetic stability codes (developed originally for fast particle driven instabilities) to the analysis of resistive wall modes.

Material erosion and migration studies in JET and its implications for ITER

S. Brezinsek and JET EFDA contributors*

JET-EFDA, Culham Science Centre, OX14 3DB, Abingdon, UK

Institut für Energieforschung-4, Forschungszentrum Jülich GmbH, EURATOM Association,

Trilateral Euregio Cluster, D-52425 Jülich, Germany

Material erosion, long and short range migration, re-deposition, and tritium retention are among the most outstanding problems for future fusion devices aiming to operate in a steady state mode. This is one of the main research topics presently in JET which operates with full carbon walls and Be evaporation, with the particular aim to prepare for future comparison after the installation of the new ITER like wall at JET. A number of important and new insights have been obtained with the help of improved diagnostics and dedicated pulse sequences. Spatial distribution and layer characteristics have been identified with dedicated slow plasma sweeps and spatially resolved hydrocarbon spectroscopy and Quartz microbalance deposition detectors which have been placed around the JET divertor. The main results can be summarised as following:

- (i) carbon is mainly released from first wall and deposited in the inner divertor. The magnetic configuration is the main factor which determines the deposition pattern at first, e.g. the private flux region turns from net deposition to erosion when the configuration changes from vertical to horizontal target operation.
- (ii) the deposited carbon undergoes further transport inside the divertor by a stepwise process induced by new magnetic configurations which lead to enhanced re-erosion of freshly deposited layers. This erosion is much stronger than for bulk graphite substrate.
- (iii) this effect is partly attributed to the disintegration of deposited layers by plasma impact far below normal carbon sublimation sets in. Spectroscopy shows that this is accompanied by an enhanced release of carbon clusters.
- (iv) a strongly nonlinear increase of the local carbon release and migration inside the divertor with ELM size has been found such that a few large type I ELMs lead to a stronger migration than many small ELMs.

These observations can explain the large carbon deposition and tritium retention on remote areas (louvers) in the JET DTE1 experiment. They show also that the dynamics of carbon transport is a specific carbon property since it is coupled with the deposition and fast disintegration of carbon layers. Such effects are not expected for metallic layers such as Be. This view is also supported by the fact that the Be content in layers on plasma facing areas in the inner divertor reach values typically of 20% while the Be is strongly de-enriched in C-layers in remote areas by factors between 10-100.

* See the Appendix of M.L. Watkins et al., Fusion Energy 2006 (Proc. 21st Int. Conf. Chengdu, 2006) IAEA (2006)

Stellarators and the path from ITER to DEMO

Allen H. Boozer

Columbia University, New York, NY 10027, USA

A low risk extrapolation from ITER to a demonstration of fusion power, DEMO requires information from a broader fusion program on materials and physics issues. Five of the physics issues have been addressed by non-axisymmetric shaping: (1) robustness of the plasma equilibrium, (2) insensitivity to details of profiles, (3) limits on the plasma density, (4) mitigation of magnetic field errors, and (5) the control of large pulses of energy to divertors through ELM's. Operational limits in tokamaks are often set by disruptions, which cannot be tolerated in DEMO and are an extreme example of non-robustness. Profile sensitivity comes in part through the bootstrap current, which is far more important in DEMO than in ITER. The profile sensitivity in tokamak experiments is also implicated in the sustainable pressure being significantly lower than the maximum achievable pressure. The Greenwald density limit of tokamaks would force DEMO to operate where the pressure of alphas makes energetic particle instabilities problematic and the divertors difficult. The only known experimental solution to these three issues is the non-axisymmetric shaping of stellarators. In addition, magnetic field errors due to displacements of coil currents cannot be eliminated, but the deleterious effects can be greatly reduced by controlled non-axisymmetric shaping. Using related techniques, an asymmetric perturbation can be chosen to modify the H-mode pedestal for ELM control while having minimal effects on the central plasma. Non-axisymmetric shaping can be expected on DEMO. The question is the type and the level: (1) a low level for error field and ELM control; (2) a moderate level for robustness against disruptions, reduced profile sensitivity, and elimination of current drive, or (3) a high level to make DEMO as insensitive to plasma profiles as possible. The NCSX stellarator will study quasi-axisymmetric shaping, which means non-axisymmetric shaping consistent with the P_φ invariance of axisymmetry. This shaping can be applied to a tokamak at any level from low to moderately strong. The non-axisymmetric shaping used on the W7-X stellarator allows even more complete plasma control through minimization of $j_{||}/B$. The broader fusion program will determine the degree to which non-axisymmetric shaping can be used to minimize the risks of DEMO—both the physics benefits and the feasibility of the engineering. Supported by the U.S. Department of Energy grant ER54333.

JT-60U advanced tokamak research towards JT-60SA

S. Ide¹, the JT-60 team¹

¹Japan Atomic Energy Agency, 801-1 Mukouyama, Naka, Ibaraki, 311-0193 JAPAN

Towards realization of a steady-state tokamak reactor, establishing operational scenario with a plasma of high normalized beta (β_N) and high bootstrap current fraction (f_{BS}) is a key issue. Such a plasma is known as an advanced tokamak (AT) plasma. Development of AT plasmas has been intensively pursued in JT-60U [1]. In the AT development, increasing the key parameters (β_N, f_{BS} , etc.) and extending the sustaining duration are both important equally. In recent JT-60U experiments, $\beta_N \sim 4.2$ and $f_{BS} \sim 100\%$ have been achieved separately in short time scale (\sim energy confinement time) and sustainment of $\beta_N = 2.3$ for 23 s and $f_{BS} = 70\%$ for 8 s in long time scale (several to several tens of current diffusion time) have been demonstrated. These achievements have been supported and stimulated progress in understanding of physics issues: effect of plasma rotation on resistive wall mode and energy confinement, effect of localized current drive on neo-classical tearing mode, off-axis current drive by NBI and so forth. Based on the physics understanding, integrated active control on local/global current profile, rotation profile, plasma pressure, either separately or combined, has been developed. These research and development are, as mentioned before, towards DEMO and ultimately a reactor. Moreover, in nearer term, they will contribute to ITER, especially development of the advanced scenarios in ITER. Now a project on modification of JT-60U into a super-conducting machine (JT-60SA [2,3]) is in progress. These JT-60U results will contribute not only to development towards ITER and DEMO, but also to establishing physics operation in JT-60SA. In this presentation, recent progress in AT development in JT-60U will be discussed with emphasis on their impact for JT-60SA.

References

- [1] H. Takenaga and the JT-60 team, Nuclear Fusion 47, S563 (2007)
- [2] M. Kikuchi et.al., proc. of 21st IAEA Fusion Energy Conference (2006)
IAEA-CN-149/FT/2-5
- [3] T. Fujita et.al., Nuclear Fusion 47, 1512 (2007)

FIRST RESULTS ON IONS ACCELERATION IN AN ULTRA-SHORT, ULTRA HIGH CONTRAST 50 TW LASER REGIME

T. Ceccotti, A. Lévy, F. Réau, P. D'Oliveira, P. Monot and Ph. Martin

*Service des Photons, Atomes et Molécules, Commissariat à l'Energie Atomique,
DSM/IRAMIS, CEN Saclay, 91191 Gif sur Yvette, France*

Recent progresses on laser beam contrast ratio improvement devices [1] have allowed obtaining contrast values as high as 10^{10} . First experiments using ultra high contrast (UHC) pulses for proton acceleration [2] have demonstrated the expected important increase in maximum proton energies reducing the target thickness and, as a consequence, the benefits of UHC pulses in enhancing proton energy scaling laws. Even more, it has been possible to highlight the symmetrical behaviour of ions bunches production from both sides of the target and the role of beam polarization [3]. The recent upgrade of the laser chain at Saclay from 10 TW to 100 TW gives us access to an interaction domain for ion acceleration never explored so far, characterized by ultra short pulse duration (< 25 fs), very high intensity ($>10^{19}$ W/cm²) and UHC (close to 10^{12}). Measurements of ions bunches properties in this laser intensity range will allow building scaling laws and predicting parameters for future applications. Finally, due to the outstanding high contrast shot-to-shot repeatability, all collected data are of main importance for numerical codes validation.

The first results on ions and protons acceleration obtained using the 100 TW Saclay laser will be presented and the perspectives they open will be discussed.

References

- [1] A.Lévy et al., Opt. Lett. **32**, 310 (2007); A. Julien et al., Opt. Lett., **30**, 920 (2004).
- [2] D.Neely et al., Appl. Phys. Lett. **89**, 021502 (2006); P.Antici et al., Phys. Plasmas **14**, 030701 (2007)
- [3] T.Ceccotti et al., PRL **99**, 185002 (2007)

RADIATION SOURCES BASED ON LASER-PLASMA ACCELERATORS: CURRENT STATUS AND CHALLENGES

D.A. Jaroszynski¹

¹*University of Strathclyde, Glasgow, United Kingdom*

Radiation sources are ubiquitous tools for studying the structure and dynamics of matter. Current light sources can produce both brilliant and picosecond duration x-ray pulses which are useful for time resolved studies. There is a drive to reduce their pulse durations to a few femtoseconds or less, and increase their brilliance to enable single-shot measurements for unravelling structural or chemical changes on unprecedented time scales. Synchrotron source provide high average power and tuneable x-ray radiation, whereas the next generation x-ray free-electron lasers (FELs), which are currently being developed, will provide intense coherent radiation with several tens of femtosecond pulse durations. However, these sources are some of the largest instruments that exist. Their huge size and cost is a result of the microwave accelerator technology on which they are based. The acceleration gradients are restricted to gradients of 10–100 MV/m. The recent development of table-top multi-terawatt femtosecond lasers has provided the opportunity to significantly miniaturise accelerator technology by harnessing plasma waves as a medium for generating electrostatic fields with gradients approaching 1 TV/m. Recent pioneering developments in laser-driven plasma wakefield accelerators has resulted in controllable high quality electron bunches [1,2] that are providing a realistic prospect of realising a table-top synchrotron source and possibly an X-ray FEL. This could transform the way science is done by making available compact femtosecond infrared, UV and X-ray sources to University sized establishments. We will present the significant challenges facing the realisation of a compact plasma based source and review the first major advance where synchrotron radiation from an undulator driven by wakefield accelerator was demonstrated [3]. Recent progress towards an FEL based on a plasma wakefield accelerator and results from the ALPHA-X project [4] will be presented.

References

- [1] S. P. D. Mangles, et al., *Nature*, **431**, 535 (2004)
- [2] W. P. Leemans et al., *Nature Physics* **2**, 696 (2006)
- [3] H.-P. Schlenvoigt, et al., *Nature Physics*, doi:10.1038/nphys811 (2007)
- [4] D. A. Jaroszynski, et al., *Phil. Trans. R. Soc. A* **364**, 689 (2006).

Novel radiation sources using plasma mirrors

Fabien Quéré¹, Cédric Thauray¹, Hervé George¹, Jean-Paul Geindre², Pascal Monot¹, Philippe Martin¹

¹*Service des Photons, Atomes et Molécules, Commissariat à l’Energie Atomique,
DSM/IRAMIS, CEN Saclay, 91191 Gif-sur-Yvette, France*

²*Laboratoire pour l’Utilisation des Lasers Intenses, CNRS, Ecole Polytechnique, 91128
Palaiseau, France*

e-mail: fabien.quere@cea.fr

When an intense ultrashort laser pulse hits an optically-polished solid target, it generates a dense plasma that acts as a mirror, known as a plasma mirror (PM). PMs can be used as ultrafast optical switches to improve the temporal contrast of ultrashort laser pulses [1]. At high enough intensities, high-order harmonics of the incident frequency, associated in the time-domain to attosecond pulses, can also be generated upon reflection on this mirror. Because there is in principle no limit on the laser intensity that can be applied to such a medium, this is a promising path to generate coherent beams of attosecond pulses with higher photon and pulse energies than those obtained by High-order Harmonic Generation (HHG) in gases. HHG from plasma mirrors is also likely to become a unique tool to investigate many key features of high-intensity laser-plasma interactions.

Using Particle-in-Cell simulations, we identify two very distinct harmonic generation mechanisms on PMs: Coherent Wake Emission (CWE) [2] and the Relativistic Oscillating Mirror [1]. Exploiting ultrashort pulses with a high temporal contrast, we demonstrate that harmonics generated by these two mechanisms can be clearly discriminated experimentally [1], through different features, such as their spectral width, spectral range, and intensity dependence. Due to the coherent character of the generation, the properties of the harmonics - e.g. their divergence- can be controlled through the phase of the driving laser field [3]. Finally, we demonstrate the mutual coherence of several harmonic beams generated by three spatially-separated focal spots of different intensities, and use the resulting interference pattern to measure the dependence of the CWE harmonic phase on laser intensity [4].

[1] C. Thauray *et al*, *Nature Physics* **3**, 424 – 429 (2007)

[2] F. Quéré *et al*, *Phys. Rev. Lett.* **96**, 125004 (2006)

[3] F. Quéré *et al*, accepted for publication in *Phys. Rev. Lett.* (2008)

[4] C. Thauray *et al*, submitted (2008)

11.011, Monday 9 June 2008

Full characterisation of a laser-produced keV X-ray Betatron source and applications

F. Albert, K. Ta Phuoc, R. Shah, S. Corde, R. Fitour and A. Rousse

Laboratoire d'Optique Appliquée, ENSTA, CNRS UMR 7639, Ecole Polytechnique, Chemin de la Hunière,
91767, Palaiseau, France

A. Pukhov

Institute für Theoretische Physik I, Heinrich-Heine-Universität, 40225, Düsseldorf, Germany

The advance of ultrafast laser technology, with chirped pulse amplification (CPA) laser systems, has allowed the production of X-ray sources in the femtosecond regime.

In previous work [1] a novel laser based hard (a few keV) X-ray source, the Betatron source, that combines the key features of synchrotron radiation, collimation and polychromaticity, with, in addition, a femtosecond pulse duration, has been observed. Relativistic (>100 MeV) electrons are accelerated and oscillate in the electrostatic fields generated in the wake of an ultraintense (30 fs, 50 TW) laser pulse to produce a synchrotron-like X-ray beam.

Following this result, which has provided a novel approach for laser based X-ray generation, the main parameters of the Betatron source have been investigated using three independent methods relying on spectral and spatial properties of the source.

First we will show new studies on the spectral correlation between electrons and X-rays that is analysed by use of a numerical code to calculate expected photon spectra from the experimentally measured electron spectra. High resolution X-ray spectrometers have been used to characterize the X-ray spectra within 0.8-3 keV and to show that the Betatron oscillations lie within $1 \mu\text{m}$ [2].

Then, we observed Fresnel edge diffraction of the X-ray beam. The observed diffraction at center energy 4 keV agrees with Gaussian incoherent source profile of full width half maximum (FWHM) $<5 \mu\text{m}$, meaning that the amplitude of the Betatron oscillations is less than $2.5 \mu\text{m}$ [3].

Finally, by measuring the far field spatial profile of the radiation, we have been able to characterize the electron's trajectories inside the plasma accelerator structure with a resolution better than $0.5 \mu\text{m}$ [4].

We will as well demonstrate the potential of the Betatron X-ray source for applications. It has been used as a probe to perform a time-resolved X-ray diffraction experiment [5]. The ultrafast nature of the source has been shown by measuring an ultrafast phase transition (non thermal melting in InSb).

References

- 1- A. Rousse, K. Ta Phuoc, R. Shah, A. Pukhov, E. Lefebvre, V. Malka, S. Kiselev, F. Burgy, J.P. Rousseau, D. Umstadter, and D. Hulin, *Phys. Rev. Lett.*, **93**, 13 135005 (2004); K. Ta Phuoc, F. Burgy, J.P. Rousseau, V. Malka, A. Rousse, R. Shah, D. Umstadter, A. Pukhov, S. Kiselev, *Phys Plasmas*, **12**, 023101 (2005).
- 2- F. Albert, R. Shah, K. Ta Phuoc, R. Fitour, F. Burgy, J.P. Rousseau, A. Tafzi, D. Douillet, T. Lefrou and A. Rousse, submitted to *Phys. Rev. E* (2007).
- 3- R. Shah, F. Albert, K. Ta Phuoc, O. Shevchenko, D. Boschetto, A. Pukhov, S. Kiselev, F. Burgy, J.P. Rousseau and A. Rousse, *Phys. Rev. E* **74** 045401(R) (2006).
- 4- K. Ta Phuoc, S. Corde, R. Shah, F. Albert, R. Fitour, J.P. Rousseau, F. Burgy, B. Mercier and A. Rousse, *Phys. Rev. Lett.*, **97**, 225002 (2006).
- 5- K. Ta Phuoc, R. Fitour, A. Tafzi, T. Garl, N. Artemiev, R. Shah, F. Albert, D. Boschetto, A. Rousse, D-E. Kim, A. Pukhov, V. Seredov, I. Kostyukov, *Phys. Plasmas*, **14** 080701 (2007)

Plasmadeposition of ultrathin films for biomedical use

C. Oehr, J. Barz, B. Elkin, Michael Haupt, M. Mueller, U. Vohrer

Fraunhofer Institute for Interfacial Engineering and Biotechnology

Nobelstrasse 12, in 70569 Stuttgart

Email: oehr@igb.fraunhofer.de

Abstract

Plasma Polymerization is used since more than 40 years to develop thin films for different kinds of applications. At least since the sixties of the last century these films are used in the fields of medicine and pharmacy.

Due to the fact that polymers are applied to design low-weight devices and to realize different geometries very easily, the films are mainly deposited onto polymeric substrates. It is a characteristic property of plasma polymerized films that they show strong adhesion to polymer substrates due to creation of radical sites at the interface when deposition starts. Thus thin layers with good adhesion, a defined amount of chemical functionalities and stability to sterilization processes are generated. This fits to the needs for medical application.

In principle plasma processing offers different approaches for the deposition of thin films with a variable amount of functionalities available for reaction with bio-molecules. Advantages and disadvantages of the different deposition strategies will be discussed.

The interaction of biological systems with materials can be divided in three subsystems. First, the interaction with bio-molecules. Here the binding of molecules with specific activities on one hand and the minimizing of unspecific protein adsorption on the other hand can be influenced by thin plasma polymers deposited on medical devices. Second, the interaction between bacteria and surfaces can be modulated via deposition of thin films with bacteriostatic or bacteriocidal properties on devices. Third, the interaction of surfaces with mammalian cells can also be influenced to enhance the cell growth and cell proliferation for the development of test kits or implants. In this contribution examples for these three categories will be shortly reviewed.

Beside the preparation of the mentioned films also the analytical tools necessary for film development and control of its properties are stressed in the final chapter of this contribution. A correlation between physico-chemical properties of the applied plasma polymerized films and the biological requirements will be tried.

References

1. C. Oehr, Plasma Processes and Polymers Wiley-VCH 2005 p 23-37, p 39-49, p309-317
2. V. Sciaratta et al, Plasma Process. Polym. 2006,3, 532-539
3. J. Barz et al, Plasma Process. Polym. 2006,3, 540-552
4. M. Haupt, J. Barz, C. Oehr Plasma Process. Polym. 2008,5, 33-43

II.013, Monday 9 June 2008

MODELING PLASMA MODIFICATION OF SURFACES AT LOW AND HIGH PRESSURE: ACHIEVING HIGH CONTROL OF REACTANTS*

M. J. Kushner

Iowa State University, Ames, Iowa, 50011 USA mjk@iastate.edu

The plasma modification of surface layers has made significant progress, particularly at low pressure where the control of uniformity over large areas and real-time-control strategies are more easily achieved. Ultimately, the quality of the materials produced depends on the ability to deliver the desired reactants and activation energy to those surfaces with a high degree of control. As feature sizes diminish and requirements for selectivity increase, the ability to control the energy and identity of reactants to the surface becomes more important. As plasma modification of surfaces at atmospheric pressure are applied to higher value materials, similar strategies must be developed to achieve uniformity over larger areas. Real-time-control strategies may also be required. In this talk, we will discuss the use of plasma models to develop strategies, both intrinsic to the plasma and externally through real-time-control, to specify reactant fluxes to the substrate to achieve mono-layer resolution of surface modification. The modelling platforms used in these investigations will first be described followed by examples, from low and high pressure plasma modification of surfaces, of how control of reactants to the surface can be achieved.

One such example is the etching of extremely high aspect ratio contacts (HARC) in low pressure plasmas. HARCs having aspect ratios of tens to as much as a hundred, with contact openings of only 50-60 nm, are particularly challenging to uniformly etch with high selectivity. The opening to the feature is so small that the incident charged and neutral fluxes are stochastic in nature. This leads to occasional non-uniform charging inside the feature, producing lateral electric fields and eventually “twisting” (that is, turning of straight features). Advanced equipment concepts that tailor high energy electron fluxes with a narrow angular spread enables those fluxes to penetrate into the feature and neutralize the errant positive charge. HARCs also are challenged by micro-trenching which requires extremely high selectivity to address. Achieving this high selectivity may ultimately require atomic-layer, self-limiting processes. Results will be discussed from plasma modelling of these processes which has provided strategies for optimizing the shape of features.

* Work supported by Semiconductor Research Corporation, Micron Technologies, Applied Materials and TEL, Inc.

Particle growth and detection in low temperature plasmas

L. Boufendi, C. Dupuis, G. Wattieaux, Y. Tessier and M. Mikikian,

*Groupe de Recherches sur l'Energétique des Milieux Ionisés, Université d'Orléans, 45067
Orléans Cedex2, France*

Dust particle nucleation and growth has been widely studied these last fifteen years in different chemistries and experimental conditions. This phenomenon is correlated with various electrical changes at electrodes, including self-bias voltage and amplitudes of the various harmonics of current and voltage[1]. Some of these changes, such as the appearance of more resistive plasma impedance, are correctly attributed to loss of electrons in the bulk plasma to form negative molecular ions (e.g. SiH_3^-) and more precisely charged nanoparticles. These changes were studied and correlated to the different phases on the dust particle formation. It is well known now that, in silane argon gas mixture discharges, in the first step of this particle formation we have formation of nanometer sized crystallites. These small entities accumulate and when their number density reaches a critical value, about 10^{11} to 10^{12} cm^{-3} , they start to aggregate to form bigger particles. The different phases are well defined and determined thanks to the time evolution of the different electrical parameter changes.

The purpose of this contribution is to compare different chemistries to highlight similarities and/or differences in order to establish possible universal dust particle growth mechanisms. The chemistries we studied concern SiH_4 -Ar, CH_4 , CH_4 - N_2 and $Sn(CH_3)_4$ [2]. We also refer to works performed in other laboratories in different discharge configurations[3].

[1] L. Boufendi, J. Gaudin, S. Huet, G. Viera and M. Dudemaine, Appl. Phys. Lett. **79**, 4301 (2001).

[2] M. Jubault, J. Pulpytel, H. Cachet, L. Boufendi, F. Arefi-Khonsari, Plasma Process. Polym, 4, S330-S335 (2007)

[3] D. Samsonov and J. Goree, J. Vac. Sci. Technol. A17, 2835 (1999).

Diagnostics of dense dispersive plasmas by line reversal

D. Karaboumiotis

Department of Physics, Institute of Plasma Physics, University of Crete, Heraklion, Greece

Plasma spectroscopy by optically thick lines is yet an open problem due to a lack in the knowledge of fundamental mechanisms of the line formation. For instance, the intensity in the central part of self-reversed lines emitted from the high-pressure plasmas of high-intensity discharge (HID) lamps is much higher than that calculated by solving the conventional radiative transfer equation [1]. On the other hand, absorption measurements have proved that the optical depth at the central part of the line is one to two orders of magnitude less than that calculated according to the conventional theory of radiation transport [1, 2]. These striking differences between experimental and theoretical results in dense, strongly absorbing plasmas might be explained by the possibility of non-radiative transfer of excitation in the neighborhood of the transition frequency by resonant collisions leading to a rapid increase of the intensity in the vicinity of the line center followed by a rapid increase of the corresponding optical depth [3]. This phenomenon depends on the dispersion of the radiation in the dense plasma-medium and it arises when the mean free path of the photons with respect to absorption is comparable to the wavelength of the radiation. A diagnostic method was proposed [1, 4] for temperature determination from line reversal based on an approximation for the source function [5]. This method relates the radiance at the reversal maxima of the spectral line to the maximum temperature along the line of sight through the so-called inhomogeneity parameter which strongly depends on the central line minimum. In this work we show that the presence of dispersion effects does not affect the determination of the inhomogeneity parameter and therefore the applicability of the diagnostic method. The temperatures in a high-intensity discharge (HID) lamp are therefore determined from self-reversed lines and the changes in the minimum intensity and the optical depth caused by the dispersion-related effects are determined by comparing the experimental results with those obtained by numerical simulation of the studied dense discharges.

[1] D. Karabourniotis, *J. Phys.D : Appl. Phys.* 40 (2007) 6608

[2] E. Drakakis, A. Palladas, D. Karabourniotis, *J. Phys. D : Appl. Phys.* 25 (1992) 1733

[3] A.Yu. Sechin *et al*, *J. Quant. Spectrosc. Radiat. Transfer* 58 (1997) 887

[4] D. Karabourniotis, *J. Phys.D : Appl. Phys.* 16 (1983) 1267

[5] D. Karabourniotis, E. Drakakis, J.J.A.M. van der Mullen, *J. Quant. Spectrosc. Radiat. Transfer* 108 (2007) 319

Temperature Equilibration in Dense, Strongly Coupled Plasmas

Dirk O. Gericke

*Centre for Fusion, Space and Astrophysics, Department of Physics, University of Warwick,
Coventry CV4 7AL, United Kingdom*

The equilibration of multi-temperature plasmas is a fundamental problem in plasma physics since such systems are often created after laser or particle beam interactions with matter. In dilute, weakly coupled plasmas, where binary collisions dominate the energy transfer, this process is well understood whereas in dense and strongly coupled plasmas, more complicated processes have to be considered: first of all the surrounding medium modifies the electron-ion collisions [1]; moreover, the collisions seemed to be suppressed by collective modes in the system [2]. Energy transfer through such modes is therefore an important relaxation process and the fact if low energy ion modes occur or not strongly influences the relation times [3]. Furthermore, the potential energy due to correlations must be included in the description of the equilibration process [5, 4].

This contribution will focus on the influence of coupled collective modes: firstly, their influence on the electron-ion energy transfer is discussed for weakly coupled plasmas where the modes can be described by the well-known Lenard-Balescu equation. Explicite expressions when coupled mode effects are expected can be derived. Strong coupling effects included by static local field corrections shift these modes and, accordingly, reduce the energy transfer rates. The description of the full relaxation process must include potential energy contributions on the same level [5]. These correlation energies have the overall effect of an energy sink that slows down the ion heating during temperature equilibration in laser heated plasmas.

References

- [1] D.O. Gericke, M.S. Murillo, and M. Schlanges, *Phys. Rev. E* **65**, 036418 (2002).
- [2] D.O. Gericke, *J. Phys. (Conference Section)* **11**, 111 (2005).
- [3] J. Vorberger and D.O. Gericke, in preparation for *Phys. Rev. E*.
- [4] D.O. Gericke, G.K. Grubert, Th. Bornath, and M. Schlanges, *J. Phys. A* **39**, 4727 (2006).
- [5] D.O. Gericke, Th. Bornath, and M. Schlanges, *J. Phys. A* **39**, 4739 (2006).

MHD Instabilities in Magneto-Plasma-Dynamic Thrusters

F. Paganucci^{§*}, M. Agostini[‡], M. Andrenucci^{§*}, V. Antoni[‡], F. Bonomo, R. Cavazzana[‡], P. Franz[‡], L. Marrelli[‡], P. Martin[‡], E. Martines[‡], P. Rossetti^{*}, P. Scarin[‡], G. Serianni[‡], M. Signori^{*‡},
G. Spizzo[‡] and M. Zuin[‡]

[§]*Department of Aerospace Engineering, University of Pisa, Italy.*

^{*}*Centrosazio- ALTA S.p.A., Via A. Gherardesca 5, 56014 Pisa, Italy*

[‡]*Consorzio RFX, Euratom-ENEA Association, corso Stati Uniti 4, 35127 Padova, Italy*

Magneto-plasma-dynamic (MPD) thrusters represent a high power electric propulsion option for primary space missions. They act as electromagnetic plasma accelerators, with a possible range of operations spanning from orbit-raising to interplanetary missions of large spacecrafts. One of the major problems facing MPD thruster operation is the onset of a critical regime, which is found when the power is increased beyond a threshold value, mainly depending on thruster geometry, type and mass flow rate of propellant, applied magnetic field intensity. In this regime, large fluctuations in the electrode voltage signals and damage to the anode are observed along with efficiency degradation. Since 2000, Centrosazio-Alta and Consorzio RFX have been carried out several experimental campaigns aimed at investigating the electrostatic and magnetic properties of plasma fluctuations, by means of electromagnetic and optic probes and ultraviolet tomography. The experimental results have evidenced a strong relation between the onset phenomena and the growth of a large-scale magnetohydrodynamic (MHD) instability, with the features of a helical kink mode. Its growth is well described by the Kruskal-Shafranov stability criterion, which gives results in very good agreement with a semi-empirical stability criterion for MPD thrusters, proposed by other authors. On the basis of the experimental observations, some active as well as passive instability suppression methods have been proposed and partially tested, with encouraging results. The paper gives a synthesis of the main results of the activity carried out so far and indications for the next investigations.

12.018, Tuesday 10 June 2008

The Physics of Fast Ion Driven Instabilities in Fusion Plasmas

S.D. Pinches and JET EFDA Contributors*

EURATOM/UKAEA Fusion Association, Culham Science Centre, Oxon, OX14 3DB, UK

As the fusion community moves towards the realisation of devices containing burning plasmas, i.e. devices in which the intrinsic heating from energetic particles (by-products of fusion reactions) is dominant, it is timely to examine the recent progress made to understand the range of energetic particle driven modes observed and their consequences in terms of fast ion redistribution and loss.

JET's large size and high current capabilities furnish it with excellent fast ion confinement properties which together with its extensive range of dedicated fast ion diagnostics (scintillator probe, Faraday cup array, gamma-ray spectrometer, gamma-ray tomography, neutral particle analyser) and extensive range of sensitive fluctuation measurements (magnetics, far infra-red interferometry, O and X-mode microwave reflectometry, soft X-rays, electron cyclotron emissions) make it an ideal testing ground for investigating the instabilities driven by fast ions with energies in the MeV range.

Dedicated experiments examining fast ion losses and redistribution have been conducted, drawing together the extensive range of diagnostic information to reveal the modes responsible, together with quantitative measurements of their consequences in terms of fast ion redistribution and loss. Experiments in which minority ions are accelerated to MeV energies have been used to study the redistribution of fast ions due to various instabilities including large core modes ($n = 1$ fishbones and sawtooth) which have been observed to redistribute fast ions across the $q = 1$ surface. In other experiments, fishbones have been observed to trigger neoclassical tearing modes, indicating that sawtooth control alone may be insufficient to avoid these confinement degrading modes.

Core-localised modes are often difficult to detect using magnetic pick-up coils and so the use of X-mode reflectometry techniques to detect and localise these modes has been pioneered. Experiments examining fast ion losses due to tornado modes (core-localised toroidal Alfvén eigenmodes) have been conducted using far infra-red interferometry measurements to detect these Alfvénic perturbations. In general, the radial gradient of the fast ions provides the drive for modes, however recently Alfvénic modes that propagate both co and counter to the plasma current have been observed following sawteeth, indicating the possibility that such modes can be driven by fast ion anisotropy. The application of these core fluctuation diagnostics have made MHD spectroscopy an even more powerful tool in assisting scenario development.

Even modes which are expected to be unstable in burning plasmas but which are stable in JET are not beyond scrutiny. The new active excitation system installed on JET is capable of driving the modes predicted to be most unstable in ITER and measuring their properties. This provides a measurement of the proximity to instability and valuable data against which theoretical understanding can be validated.

As a result of these advances, both our linear and nonlinear understanding of the phenomena expected to arise in burning plasmas have been enhanced and we can move towards the realisation of fusion devices with an increased level of confidence.

This work was funded jointly by the UK EPSRC and by the European Communities under the contract of Association between EURATOM and UKAEA. The views and opinions expressed herein do not necessarily reflect those of the European Commission.

* See Appendix of M.L. Watkins *et al.*, Fusion Energy 2006 (Proc. 21st Int. Conf. Chengdu, 2006) IAEA, (2006)

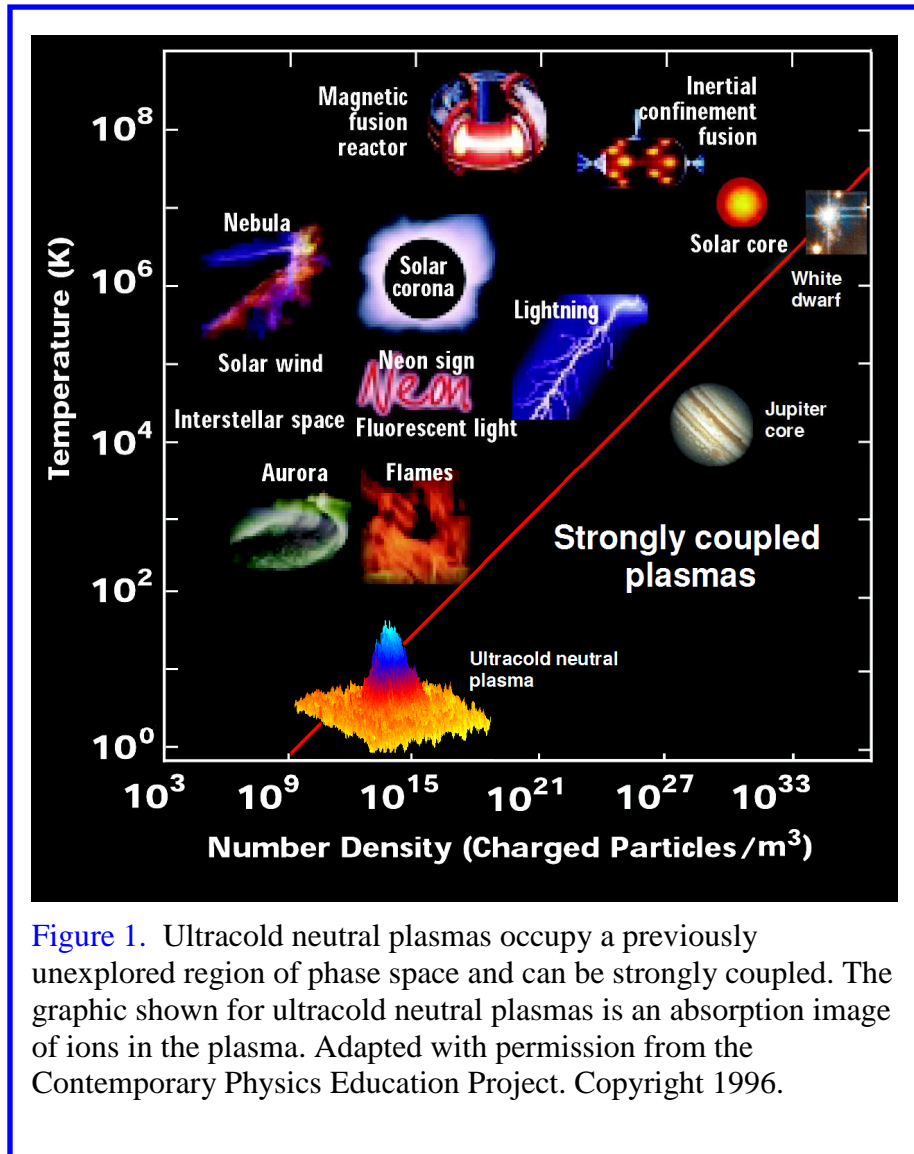
Watching Ions Dance Near Absolute Zero

Thomas C. Killian

Department of Physics & Astronomy, Rice University; Houston, TX 77005

Ultracold neutral plasmas, formed by photoionizing laser-cooled atoms near the ionization threshold, stretch the boundaries of traditional neutral plasma physics. The electron temperature in these plasmas is from 1-1000K and the ion temperature is around 1 K. The density can be as high as 10^{10} cm^{-3} . They provide a playground for studying strongly coupled plasmas, in which the Coulomb interaction energy exceeds the thermal energy. Strong coupling is of interest in many areas of physics, and in ultracold plasmas it leads to spatial correlations and surprising equilibration dynamics. The expansion of ultracold plasmas into the surrounding vacuum can also probe the physics of plasmas produced with short-pulse laser irradiation of solid, liquid, foil, and cluster targets.

This work is supported by the U.S. National Science Foundation and David and Lucille Packard Foundation.



Experiments and simulation of edge turbulence and filaments in MAST

B.Dudson¹, N.Ben Ayed^{1,2}, S.Tallents², A.Kirk², H.Wilson¹, B.Hnat³, R.Dendy², S.Saarelma², G.Counsell², B.Lloyd²

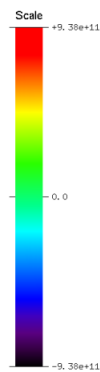
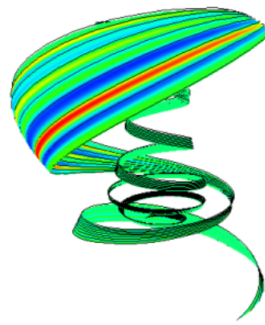
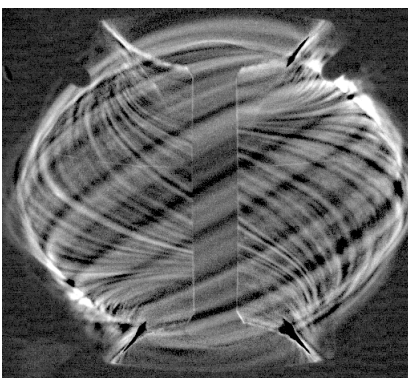
¹ Department of Physics, University of York, YO10 5DD. Contact bd512@york.ac.uk

² EURATOM/UKAEA Fusion Association, Culham Science Centre, Oxfordshire OX14 3DB

³ Department of Physics, Warwick University, Coventry CV4 7AL

Experimental and simulation results on filament structures observed in MAST from L-mode and H-mode plasmas will be presented. Understanding these structures is important both due to their influence on transport in the pedestal, and also due to their effect on cross-field transport in the SOL and hence power loading on plasma-facing components.

Fast camera and reciprocating Langmuir probe data have been used to determine the mode-number, toroidal and radial velocities of the filaments observed. A comparison of the data from L-mode, inter-ELM and during ELMs shows that while ELM filaments



move coherently, those observed in L-mode and inter-ELM regimes move toroidally and radially independent of each other. In both L-mode and inter-ELM regimes, the number of filaments is found to increase with plasma density. L-mode simulations using the 3D, 2-fluid BOUT code produce similar widths and radial velocities to the observations. Detailed examination of simulation

Fast imaging (left) and BOUT simulations (right) of MAST L-mode plasmas

results indicate the presence of a mixing layer within 2cm of the separatrix, across which the character of the turbulence changes.

Statistical analysis of L-mode edge fluctuations associated with edge filamentary structures is presented, examining correlation functions, scaling of moments and PDFs. These results confirm a dual temporal scaling with a time $t \sim 40\text{-}60\mu\text{s}$ separating the two regimes. Combining these results with the image analysis indicates that the dual temporal scaling is due to the properties of the individual filaments.

Progress in understanding ELM events using linear and non-linear codes is reviewed, including results concerning the effect of x-point geometry, edge rotation and poloidal beta on ELM stability. First results from a new modular code (developed from BOUT in collaboration with LLNL) for non-linear ELM simulations will be presented. This code is capable of simulating a wide variety of plasma fluid models and magnetic geometries. One objective is to study and compare plasma eruptions in a range of different situations, such as ELMs and solar flares.

This work was supported in part by the Engineering and Physical Sciences Research Council and by Euratom. The content of the publication is the sole responsibility of the authors and it does not necessarily represent the views of the Commission of the European Union or their services.

JET confinement studies and their scaling to high β_N , ITER scenarios

D C McDonald¹, C D Challis¹, J C DeBoo², P de Vries¹, J Hobirk⁵, E Joffrin³, L Laborde¹,
T C Luce², J Mailloux¹, V Pericoli-Ridolfini⁴, F Ryter⁵ and JET EFDA contributors*

JET-EFDA, Culham Science Centre, Abingdon OX14 3DB, UK

¹ *EURATOM-UKAEA Fusion Association, Culham Science Centre, Abingdon OX14 3DB, UK,*

² *General Atomics, P O Box 85608, San Diego, California 92186-5608, USA,*

³ *Association Euratom-CEA, CEA Cadarache, F-13108, St Paul lez Durance, France,*

⁴ *Associazione Euratom-ENEA sulla Fusione, C R Frascati, C P 65, 00044-Frascati, Italy,*

⁵ *Max Planck-Institute fur Plasmaphysik, EURATOM Association, D-85748 Garching, Germany.*

Operating at high β_N (plasma pressure normalised to the Troyon limit), the ITER Hybrid and Steady State scenarios aim to use increased bootstrap current to enable burn times $\sim 1000s$. To achieve this, and optimise fusion performance, these scenarios must have good energy confinement. ELMy H-mode plasma studies, with β_N primarily in the range $1 < \beta_N < 2$, have been described by scalings, such as IPB98(y,2), which are used for extrapolation to ITER. However, dedicated ELMy H-mode β_N studies in JET and DIII-D did not find the negative dependence of confinement on β_N in IPB98(y,2). Focusing on recent JET results, this paper describes the extension of confinement scaling to higher $\beta_N \sim 2-4$ and to different scenarios. In the Hybrid scenario, JET has attained $\beta_{MHD} = 3.6$. Despite a different initial phase, plasma parameters evolve rapidly towards those of equivalent ELMy H-modes with confinement normalised to IPB98(y,2), $H_{98(y,2)} \sim 1$. Dedicated scans in this scenario have found decreasing confinement with increasing β_N . This is strongest in the pedestal - consistent with gyro-fluid transport modeling which predicts β_N independent core confinement. Study of a wider database suggests that the different scaling is related to operating at higher triangularity. In contrast, DIII-D and ASDEX Upgrade Hybrid scenarios have confinement that is not well described by IPB98(y,2). This implies that either the machines are in different confinement modes or that the Hybrid scenario has a different size scaling to IPB98(y,2). Both cases will be discussed. Candidate Steady State scenario plasmas with and without ITBs on JET have attained $\beta_{MHD} = 3$. Pedestal confinement losses associated with gas fuelled small ELMs are compensated by core confinement improvements from ITBs giving $H_{98(y,2)} \sim 1$. Without ITBs, $H_{98(y,2)} \sim 1$ plasmas are observed with increased confinement associated with low values of minimum safety factor. Confinement in all of the scenarios will be compared and conclusions for high β_N , ITER operation discussed.

* see appendix of M Watkins et al, Fusion Energy 2006 (Proc 21st Int Conf Chengdu, 2006) IAEA

Study of Reactor-Relevant High-Beta Regime in the Large Helical Device

S. Sakakibara, K.Y. Watanabe, S. Ohdachi, Y. Suzuki, H. Funaba, Y. Narushima, K. Toi,
I. Yamada, K. Tanaka, T. Tokuzawa, R.Sakamoto, K. Ida,
H. Yamada, A. Komori, O.Motojima,
and LHD Experimental Group

National Institute for Fusion Science, Toki 509-5292, Japan

The volume averaged beta value of 5 %, which is relevant to that required in a fusion energy reactor, has been achieved in the Large Helical Device (LHD). The obtained high beta plasmas are free from disruptive phenomena. The extended high beta regime serves to expand the understanding of physics concerning the beta-limit as well as to demonstrate the potential capability of a helical fusion reactor. The magnetic configuration was optimized in terms of MHD equilibrium, stability and transport properties [1]. Net-current free heliotron plasmas are free from current-driven instabilities unlike in tokamaks, therefore the characterization of pressure-driven instabilities and their control in the high beta regime are critical issues for stable steady state operation. The dominant low- m MHD modes move from the core region to the periphery when the beta increases, and the modes excited at the outermost resonance near the plasma edge are enhanced in the beta range over 4 %. A clear dependence of the amplitude of the mode on the magnetic Reynolds number has been found, which is close to that of the linear growth rate of the resistive interchange mode [1]. The increase in equilibrium currents with the increment of the beta value leads to the disorder of the peripheral magnetic field structure, which possibly limits the confinement region. This effect on the confinement property should be clarified experimentally. The comparison between the measured temperature profile and the magnetic field structure calculated by the 3D MHD code HINT has been done in order to investigate the effect of the change of the magnetic topology on the confinement. The temperature gradient in the periphery with a disordered magnetic field structure seems to be lower than that in the core region with nested magnetic surfaces. Although the clear beta limits due to stability and equilibrium have not been observed in the present beta range of experiments, it has been found out that the global confinement gradually deteriorates with the increment of the beta value. This is mainly due to the increment of the heat transport in the periphery, and the causal relation with enhanced resistive-g mode turbulence is discussed [2].

[1] S.Sakakibara et al., *Fusion Science and Technology* **50** (2006) 177.

[2] K.Y. Watanabe et al., *Nuclear Fusion* **45** (2005) 1247.

The European turbulence code benchmarking effort:

Turbulence driven by thermal gradients in magnetically confined plasmas

G.L. Falchetto¹, B.D. Scott², P. Angelino¹, A. Bottino², T. Dannert³, V. Grandgirard¹,
S. Janhunen⁴, F. Jenko², S. Jolliet³, A. Kendl⁵, V. Naulin⁶, A.H. Nielsen⁶, M. Ottaviani¹,
M.J. Pueschel², D. Reiser⁷, T. Ribeiro² and M. Romanelli⁸

¹*Institut de recherche sur la fusion par confinement magnétique, Association Euratom-CEA, CE-Cadarache, F-13108 Saint-Paul-Lez-Durance, France;* ²*Max-Planck-Institut für Plasmaphysik, IPP-Euratom Association, D-85748 Garching, Germany;* ³*Centre de Recherches en Physique des Plasmas, Association Euratom-Confédération Suisse, EPFL, CH-1015 Lausanne, Switzerland;* ⁴*Helsinki University of Technology, FIN-02015 TKK, Finland;* ⁵*Institute for Theoretical Physics, University of Innsbruck, Association Euratom-OAW, A-6020 Innsbruck, Austria;* ⁶*Risø National Laboratory, DTU, DK-4000 Roskilde, Denmark;* ⁷*Institut für Plasmaphysik, Forschungszentrum Jülich GmbH, Euratom Association, D-52425 Jülich, Germany;* ⁸*Euratom-UKAEA Fusion Association, Culham Science Centre, Abingdon, UK*

Computation of turbulence and transport in magnetised plasmas continues to make rapid advances. Global electromagnetic gyrofluid simulations are now possible, and global electromagnetic gyrokinetic simulations are beginning. Local "fluxtube" cases have been available for several years. Nevertheless, since the last major effort ten years ago there has been only sporadic work to benchmark the various approaches generally and individual implementations ("codes") particularly. We report the establishment of such an effort within the EFDA Task Force on Integrated Tokamak Modelling. Standard cases for both core and edge turbulence are included. Not only time trace information of anomalous fluxes are included, but the mode structure (spectra, radial envelopes, zonal flow amplitude, etc) are also compared. Results so far include good agreement between gyrofluid and gyrokinetic codes for core ion temperature gradient (ITG) driven turbulence but for trapped electron cases (driven mostly by the density gradient) the gyrokinetic models are needed as fluid ones predict stability. However, there is still an important disagreement on the core ITG zonal flow saturation level, even between gyrokinetic codes. More diagnostics on the global core cases will be reported and the main physical reasons for disagreement outlined. Edge results agree very well on collisionality scaling and acceptably well on beta scaling below the MHD boundary for cold-ion cases. They also agree well on the elements of mode structure. A sufficient number of warm ion edge turbulence codes for benchmarking is still lacking.

The support infrastructure for the benchmarking effort is also to be briefly described. This is a novel element allowing the continuously renewed effort required to assure quality control of ITER simulation in the longer term.

Investigating atomic properties of warm dense matter produced by laser

P. Renaudin¹, S. Bastiani-Ceccotti², L. Lecherbourg²⁻³, J. Fuchs², P. Antici², J.-P. Geindre², L. Lancia², A. Mancic², J. Robiche², R. Shepherd⁴, C. Blancard¹, P. Combis¹, P. Cossé¹, G. Faussurier¹, P. Audebert²

1 Département de Physique Théorique et Appliquée, CEA/DAM Ile de France, Bruyères-le-Châtel, 91297 Arpajon Cedex, France

2 Laboratoire pour l'Utilisation des Lasers Intenses, École Polytechnique, CNRS, CEA, UPMC, 91128 Palaiseau cedex, France

3 Université du Québec, INRS énergie et matériaux, Varennes, Québec, Canada

4 Lawrence Livermore National Laboratory, University of California, Livermore CA 94550, USA

Warm dense matter (WDM) is at the center of the density-temperature plane and, for some material, it is a barrier between different regions. Therefore a large number of technologic and scientific applications cross the WDM or need WDM properties. Recently, generation of WDM with minimized gradients has been obtained by irradiating solids with intense laser or ion beams. Short-pulse X-ray sources of a few ps duration emitting in the sub-5-keV range have been generated by irradiating high-Z materials with a sub-ps laser pulse. This offers the possibility to use point-projection time-resolved absorption spectroscopy for the study of spectral opacities of dense plasmas.

I will present results of recent X-UV pump-probe experiments performed in France with the 100 TW LULI facility. The experimental setup uses two ultra-fast laser beams to produce the plasma and the X-ray probe. The first ultra-short laser pulse was used to create a thin, high-density plasma slab fairly uniform in temperature or a short MeV ions bunch that allows an energy deposition in the bulk of a second target. Each shot allows to measure transmission spectra in the WDM regime.

The laser produced plasma is weakly ionised and density effects are not negligible. The continuum lowering modifies the ionization balance and pressure ionization tends to delocalize atomic orbitals. The temperature of the ions beam produced plasma is lower than the Fermi temperature. As the density remains high, the increasing temperature induces a change of the free electron degeneracy and a thermal smoothing of K-edge.

Warm dense matter generation by soft x-ray laser heating of thin foils

*B.Rus, T.Mocek, M.Kozlová, J.Polan, P.Homer, M.Stupka
Institute of Physics v.v.i./ PALS Centre, Prague 8, Czech Republic*

*M.Fajardo
Centro de Física dos Plasmas, Instituto Superior Técnico, Lisbon, Portugal*

*R.W.Lee, M.E.Foord, H.Chung, S.J.Moon
Lawrence Livermore National Laboratory, Livermore, USA*

We present results of experimental and numerical studies of generation of cold, near solid density, plasmas by volumetric heating of thin foils by focused soft x-ray laser (21.2 nm, i.e., 58.5 eV) pulses. Time-integrated and time-dependent transmission of the soft x-ray radiation through aluminium and polyimide was experimentally investigated for intensities of up to 10^{12} Wcm⁻². A simple diagnostics based on VIS camera was employed to assess temperature (<20 eV) of the heated matter. As the critical electron density for the 21.2-nm radiation is 2.4×10^{24} cm⁻³, the incident x-ray laser always encounters undercritical matter or plasma and heats the entire volume of the irradiated foil; the heating is near-isochoric in the beginning of the x-ray laser pulse. The initial absorption of the soft x-ray radiation is dominated by bound-free transitions (photoionization). The experimental data show significant difference in transmission of the 21.2-nm radiation through heated aluminium and polyimide. In Al, the transmission of heated matter essentially corresponds to that of the solid-state, however in polyimide the absorption increases significantly for intensities $>5 \times 10^{11}$ Wcm⁻². This increase is seen to occur transiently during the rising edge of the heating pulse, and was identified as due to bound-bound transitions in Li-like C resonant with the soft x-ray laser. The experimental data were simulated by radiation hydrodynamic code Lasnex, using a hybrid equation of state model interfaced with a model solving non-LTE rate equations in a hydrogenic approximation. Results of the simulations were found to be in good agreement with the experimental data, providing benchmarked insight into the absorption mechanisms of intense soft x-ray radiation in matter heated from cold solid through the warm dense matter regime to plasma states.

**An exact treatment of charged particle stopping in a plasma
or
The Coulomb logarithm revisited**

Robert L. Singleton Jr.¹

¹ *Los Alamos National Laboratory, Los Alamos, New Mexico 87545, USA*

The charged particle stopping power in a highly ionized and weakly coupled plasma has recently been calculated exactly to logarithmic accuracy by Brown, Preston, and Singleton (BPS) [1]. A very powerful regularization method from quantum field theory, called dimensional continuation, was employed in a novel way by BPS to calculate the Coulomb logarithm exactly, without appealing to *ad hoc* long- and short-distance cutoffs. The exact transition between the classical and quantum regimes was also included in the calculation. Since the technique of dimensional continuation might be unfamiliar to many plasma physicists, and since the same methodology can also be used for other energy transport phenomena, such as electron-ion temperature equilibration in a plasma [1, 3], I will spend the first part of the lecture reviewing the main ideas behind the calculation. I will then talk about the implications for ignition in Inertial Confinement Fusion (ICF). The BPS stopping power gives longer ranges and delivers less energy to the plasma ions than typical models in the literature, thereby making ignition harder to achieve. This could have implications for the Laser Mégajoule (LMJ) facility in France and the National Ignition Facility (NIF) in the United States.

References

- [1] L.S. Brown, D.L. Preston, and R.L. Singleton Jr., *Charged Particle Motion in a Highly Ionized Plasma*, Phys. Rep. **410** (2005) 237, arXiv: physics/0501084; For a detailed pedagogical exposition see also Ref. [2].
- [2] R.L. Singleton Jr., *BPS Explained I: Temperature Relaxation in a Plasma*, arXiv: 0706.2680; *BPS Explained II: Calculating the Equilibration Rate in the Extreme Quantum Limit*, arXiv: 0712.0639.
- [3] L.S. Brown and R.L. Singleton Jr, *Temperature Equilibration Rate with Fermi-Dirac Statistics*, Physical Review E **76** (2007) 066404, arXiv:0707.2370.

OVERVIEW OF ON-GOING LIL EXPERIMENTS

L. Videau¹, E. Alozy¹, I. Bailly¹, N. Borisenko⁴, J.Y. Boutin¹, J. Breil², S. Brygoo¹, M. Casanova¹, A. Casner¹, C. Chenais-Popovics³, C. Courtois¹, S. Darbon¹, S. Depierreux¹, P. Di-Nicola¹, F. Durut¹, A. Duval¹, J.L. Feugeas², C. Fourment², S. Gary¹, J.C. Gauthier², M. Grech¹, O. Henry¹, A. Hervé¹, S. Hulin², G. Huser¹, J.P. Jadaud¹, F. Jequier¹, Ch. Labaune³, J. Limpouch⁵, P. Loiseau¹, O. Lutz¹, P.H. Maire², M. Mangeant¹, C. Meyer¹, D.T. Michel¹, J.L. Miquel¹, M.C. Monteil¹, M. Naudy¹, W. Nazarov⁶, P. Nicolai², O. Peyrusse², F. Philippe¹, D. Raffestin¹, C. Reverdin¹, Ph. Romary¹, R. Rosch¹, C. Rousseaux¹, G. Soullié¹, S. Schmitt¹, G. Schurtz², Ch. Stenz², V. Tassin¹, C. Thessieux¹, G. Thiell¹, M. Theobald¹, V. Tikhonchuk², J.L. Ulmer¹, B. Villette¹, R. Wrobel¹

¹Commissariat à l'Energie Atomique, DIF-CESTA-VA, 91297 Arpaçon Cedex, France

²Université Bordeaux I; Centre Lasers Intenses et Applications, 33405 Talence, France

³Laboratoire pour l'Utilisation des Lasers Intenses, 91128 Palaiseau, France

⁴Lebedev Physical Institute, 53 Leninskyi Prospect, Moscow, 119991 Russia

⁵FNSPE, Czech Technical University in Prague, 115 19 Prague 1, Czech Republic

⁶University of St Andrews, Fife KY16 9ST, Scotland, UK

The Ligne d'Intégration Laser (LIL) has been completed in 2002 and was first dedicated to laser physics experiments as a prototype for the future Laser MegaJoule. It delivers up to 15kJ at 3ω on target. We will present the experimental setup at the LIL facility and some plasma experiments carried out during 2005-2008. We have installed X-ray and visible-UV diagnostics allowing full characterization of the laser-plasma interaction (LPI) including the transmitted, scattered and backscattered 3ω beams. During the first LPI campaign of 2007 with gas-filled Au-hohlraums, we have obtained high quality signals for both Raman and Brillouin measurements. Another LPI campaign in collaboration with the Institute of Laser Plasma was devoted to the study of plasma smoothing in foam targets. Measurement of the transmitted beam after propagation through the foam demonstrated the effectiveness of laser plasma smoothing. Supersonic propagation of the ionization wave has been evidenced using time-resolved side-on X-ray imaging. Two CELIA campaigns devoted to the study of the nonlocal electron-energy transport, used x-ray diagnostics : hard x-ray time-resolved Bragg spectrometer allowed a discrimination between different modellings of the heat flow. Finally, we will present the last installed standard diagnostic devoted to EOS experiments, which is composed of a pyrometer, a VISAR and a shock breakout measurement.

Anti-friction, Homogenization and Angular Momentum Transport in Tokamaks, Planets and the Solar Tachocline

P.H. Diamond

*Center for Astrophysics and Space Sciences and Dept. of Physics
University of California, San Diego, La Jolla, CA 92093-0424 USA*

This lecture will address the ubiquitous phenomenon of 'up-gradient' momentum transport (i.e. anti-friction) which is known to occur in tokamak plasmas - i.e. inward convective momentum 'pinch' and stress, planetary atmospheres - i.e. sharpening of high latitude zonal flows by Rossby wave breaking, and the solar tachocline - i.e. a thin, stably stratified layer at the base of the convection zone formed by spin-down driven meridional cells and turbulent momentum transport. These seemingly unrelated phenomena each have the common elements of low 'effective Rossby number', quasi-geostrophic dynamics, and a governing homogenization or relaxation principle. Like the Taylor Relaxation Hypothesis in low- β MHD, homogenization principles provide conceptually simple guiding frameworks which facilitate understanding the complex dynamics of turbulent relaxation, evolution and transport. This lecture emphasizes the physics of homogenization principles and their application to tokamak and tachocline phenomena.

In the case of tokamak plasmas, the homogenization of toroidal angular momentum by a compressible turbulent flow (n.b. inhomogeneous $B_0(r)$ implies $\underline{V}_{E \times B}$ compressible!) enables the formulation of a turbulent equipartition (TEP) theory for angular momentum (L_ϕ) transport. This is equivalent to a homogenization theory for L_ϕ/B^α , ($\alpha \sim 2$), which naturally leads to a toroidicity-induced inward pinch of toroidal angular momentum. Zonal flow formation, which is a common element of tokamak, planetary atmosphere and tachocline dynamics, is encapsulated by the principle of PV (potential vorticity) homogenization. Of particular relevance to tokamak phenomenology is the fact that PV homogenization encompasses the relative branching of total PV flux between guiding center flux (i.e. particle or thermal transport) and polarization charge flux (i.e. vorticity transport or, equivalently, Reynolds stresses), such as occurs in transport barrier formation. PV homogenization theory can be used to predict a critical fluctuation intensity gradient for the dominance of the polarization charge flux channel (i.e. transition threshold for transport barrier formation).

The tachocline is a more challenging application, on account of its dynamically active toroidal field. We note, though, that the details of PV and momentum transport are central to *both* tachocline formation scenarios (Spiegel-Zahn; Gough-McIntyre) and may also ultimately hold the key to deciding between these two competing approaches. Here, PV homogenization theory can be used to understand relevant but subtle questions, such as how strong an ambient magnetic field must be in order to convert 2D fluid turbulent dynamics (i.e. inverse energy cascade) to 2D MHD dynamics (i.e. forward energy cascade). Similarly, we show how stronger magnetic fields inhibit PV mixing and thus the formation of a zonal jet 'staircase' in the tachocline. This simple insight into PV transport processes in the unusual tachocline environment has profound complications for tachocline formation, and suggests that the fossil field scenario of Gough and McIntyre is the more viable one, since it limits tachocline penetration by fossil field magnetic stresses, rather than by turbulent viscosity.

Rotating twisted flux tubes buoyancy: comparison between the convective region of the Sun and the edge of a tokamak plasma

F. Alladio, A. Mancuso, P. Micozzi

Associazione Euratom-ENEA sulla Fusione, CP 65 Frascati (Roma), Italy

The filament state of magnetic field is the usual way for plasmas to avoid magnetic inhibition of convective overturning. However it requires Dynamo conversion of kinetic into magnetic energy and is therefore often associated with a plasma velocity shear layer.

In the Sun, isolated current carrying magnetic filaments (twisted flux tubes) are produced by the Solar Dynamo from a continuous strong toroidal field, sitting just below the radiative-convective transition, on the Sun rotation shear layer (Tachocline, $R_{\text{Tach}} \sim 2 \cdot R_{\odot} / 3$ in terms of the solar radius, R_{\odot}). The twisted flux tubes, because of their internally suppressed convective transport, experience a net heating due to non-zero divergence of radiative heat flux at the radiative-convective transition; the mechanical equilibrium (magnetic curvature force vs. rotation) is altered and the filaments become buoyant: the emergence of the rotating magnetic filaments through the solar convection zone is influenced by viscosity, which adds external kink to the their internal twist. Some rotating filaments, after winding dragged by viscosity, in the more rapidly rotating convective zone, fall back into the Tachocline adding up to the continuous toroidal field; some emerge from the photosphere kinked and twisted, reconnect and produce flares.

In the mode of high magnetic confinement (H-mode), when a magnetic separatrix bounds the axisymmetric tokamak discharge and a sheared plasma rotation is present, magnetic filaments with concentrated internal currents (nonergodic twisted flux tubes, ELMs) are produced at integer values of the MHD safety factor ($q=4,5,6$) near the velocity shear layer (pressure Pedestal, at $\rho_{\text{Ped}} \geq 0.94 \cdot a_{\text{Sep}}$ in terms of the minor radius of the plasma boundary, a_{Sep}): again a Dynamo conversion of kinetic into magnetic energy is required in order to filament the current density at the Pedestal. The current carrying filaments break the unperturbed axisymmetric tokamak equilibrium, producing ergodicity in the edge plasma that surrounds them. The faster loss of energy from the ergodic plasma makes the nonergodic rotating magnetic filaments outboards buoyant: therefore they convect outboards from the Pedestal, without any further reconnections with the ergodic background plasma.

The buoyancy and motion model for the tokamak case will be compared with the buoyancy and motion model for the Sun.

Vertical angular momentum transport in astrophysical turbulent MHD accretion disks and the formation of large-scale collimated jets

Fabien Casse

Laboratoire AstroParticule & Cosmologie - Université Paris Diderot, France

Accretion is a quite common phenomenon that occurs in many types of systems across the Universe. Under the action of a central object (star, black hole, etc.), the plasma surrounding this object is prone to a rotating motion counteracting the gravity. The resulting disk (called “Keplerian” disk) exhibits an angular momentum distribution such that the plasma angular velocity is $\Omega \propto R^{-3/2}$, where R is the distance to the central object. Simultaneously to the presence of such disk, large-scale twin jets are often observed in these systems. These jets, flowing perpendicularly to the disk, are made of plasma and contain magnetic fields acting to maintain their excellent collimation. Accretion thus requires an anomalous transport of angular momentum coming from plasma turbulence. This turbulence is likely provoked by MHD instabilities occurring in the disk, and the ubiquitous connection observed between accretion and ejection indicates that this turbulence is also at the origin of the jets.

In this talk I will first present observational data that shed light on the mechanisms at work within a magnetized accretion disk launching large-scale magnetized jets. In particular I will show how important is the presence of the magnetic field in the jet in order to explain the marvelous collimation of these cylindrical flows occurring over distances larger than thousands of light-years. MHD models also show that these jets are an important contribution to the removal of the disk angular momentum. However, as I will discuss in this talk, usual MHD simulations showing the role of the magneto-rotational instability (MRI) as the source of the disk turbulence are not yet able to provide near-stationary solutions of fully accreting disks associated with the formation of jets. I will present a family of models where the turbulence is parameterized by the use of turbulent transport coefficients for viscosity and magnetic diffusivity such that these coefficients can be written as $\nu = \alpha C_s H$ where C_s is the local disk sound speed, H is the disk scale height and α a dimensionless parameter. In these models, it is possible to obtain near-stationary solutions where accretion is allowed thanks to a vertical angular momentum transfer from the disk into the jet. The angular momentum carried away by the jet is then used locally to speed-up mass and the twisting of the jet magnetic field due to the disk differential rotation provides a self-collimating mechanism for the jet just as in tokamaks. I will finish my talk by discussing the missing parts of accretion-ejection theory and the remaining issues regarding the description of disk turbulence.

Turbulent Transport and Coherence in MHD

David W. Hughes

Department of Applied Mathematics, University of Leeds, Leeds LS2 9JT, UK

A topic of fundamental importance in magnetohydrodynamic turbulence is mean induction. In plasma devices such as the RFP this may arise from interactions between small-scale fluid velocity and small-scale magnetic field in the presence of a strong imposed magnetic field. In an astrophysical context the interest is in the means of generating a magnetic field that has a significant component on scales large compared with those of the velocity field. For example, the Sun has a coherent global scale field that is generated, at least in part, by much smaller scale motions.

The concept of mean induction has traditionally been studied within the framework of mean field electrodynamics, a one-point closure model for MHD turbulence. A formal averaging of the magnetic induction equation leads to the new term (in comparison with the unaveraged equation) $\mathcal{E} = \langle \mathbf{u} \times \mathbf{b} \rangle$ — the mean electromotive force arising from correlations between small-scale fluid velocity and small-scale magnetic field. The system is then closed by linking \mathcal{E} to the mean (large-scale) magnetic field \mathbf{B}_0 in a formal expansion

$$\mathcal{E}_i = \alpha_{ij} B_{0j} + \beta_{ijk} \frac{\partial B_{0j}}{\partial x_k} + \dots$$

I shall discuss some of the problems involved in determining and interpreting the leading term in this expression — the so-called α -effect of mean field electrodynamics. Parity considerations show that the symmetric part of the α_{ij} tensor (the part responsible for field regeneration) can be non-zero only in turbulence lacking reflectional symmetry — a feature typically characterised by non-zero helicity. At small values of the magnetic Reynolds number Rm the relation between the α -effect and the helicity of the flow can be made explicit. The more interesting question though concerns the nature of α_{ij} at *high* values of Rm , the astrophysically relevant case.

I shall discuss two recent series of numerical experiments that explore the nature of the α -effect in turbulent flows. The first explores rotating turbulent convection, and highlights the difficulties in obtaining a significant α -effect even in flows possessing considerable helicity. The problem turns out to be not one of *local* induction, but of very weak *average* induction. The second series, motivated by the results from the investigations into convection, considers more idealised, but more controllable flows, in which the influence of spatial correlation on the α -effect can be carefully examined. The issues explored are I believe extremely general ones pertaining to the nature of averaging in highly turbulent flows.

Simulation of dust voids in complex plasmas

W.J. Goedheer and V. Land

*FOM-Institute for Plasma Physics 'Rijnhuizen', Association EURATOM-FOM,
Trilateral Euregio Cluster, P.O. Box 1207, 3430 BE Nieuwegein, The Netherlands*

A well-known phenomenon in dusty radio-frequency (RF) discharges under micro-gravity conditions is the generation of a void, a dust free region in the discharge centre. This void is generated by the drag of the positive ions that are pulled out of the discharge by the ambipolar electric field. In the last decade, the theoretical insight into the interaction of the ions with a negatively charged dust particle has reached a level that enables realistic simulations of these complex plasmas. We have used a hydrodynamic model for dusty radio-frequency discharges in argon to study the interaction between the dust and the plasma background. This model is based on expressions for the ion drag force and the dust charge that contain the effects of large-angle scattering, the ion flow speed and ion-neutral collisions [1]. With this model, we studied the plasma inside the void and obtained insight into the way it is sustained by heat generated in the surrounding dust cloud [2].

When this mechanism is suppressed by lowering the RF power, the plasma density inside the void decreases, even below the level where the void collapses, as was recently shown in experiments [3]. Results of simulations of this collapse will be presented. At reduced power levels the collapsed central cloud behaves as an electronegative plasma with corresponding low time-averaged electric fields. In this case the potential well that contains the dust becomes very shallow and the internal pressure of the leads to large and relatively homogeneous Yukawa balls, containing more than 100.000 particles. The generation of a Yukawa ball and the evolution of a void at higher power levels can also be studied from the other side, that is, along a scheme where we start at a low power, inject dust, and increase the power. No hysteresis was observed in this transition.

The creation of large homogeneous Yukawa balls along this scheme possibly opens a route to studies of, for instance, wave propagation and phase transitions in a three dimensional dust structure.

[1] V. Land and W.J. Goedheer, *New J. Phys.* 8 (2006) 8.

[2] V. Land, W. J. Goedheer, *Proc. 34th EPS Conf. on Plasma Phys.*, ECA vol. 31F, O4-010.

[3] A.M. Lipaev et al., *Phys. Rev. Lett.* 98 (2007) 265006.

Dusty Plasmas under Effect of External Forces: Basic Phenomena and Applications

Oleg F.Petrov, Vladimir E.Fortov and Olga S.Vaulina

Joint Institute for High Temperatures, Russian Academy of Sciences, Moscow, Russia

The dusty plasma is a partly ionized gas with negatively or positively charged ($\sim 10^3$ - $10^5 e$) dust particles of micron size (~ 1 - $10 \mu\text{m}$) that may form quasi-stationary plasma-dust structures similar to a liquid or a solid. In view of this, dusty plasma may be experimentally investigated on a kinetic level with high temporal and spatial resolution. As a result, dusty plasmas are good experimental models for studying the properties of non-ideal systems and for proofing existing empirical models and numerical results.

Investigations were directed on the study of dusty plasma structures and dynamics on kinetic level under action of different external forces (visible and uv radiation, magnetic and thermal fields, electron beam) in glow rf and dc discharges.

Results of experimental study of the dusty plasma kinematic viscosity and the diffusion are presented. A uniform flow of dusty plasma liquid was experimentally realized under laser beam action, and the results of analysis of the obtained data made it possible to estimate the viscosity coefficient of dusty plasma liquid.

The results are given of an experimental investigation of heat transport processes in fluid dusty structures in rf discharge plasmas under different conditions: for discharge in argon, and for discharge in air under an action of electron beam. The analysis of steady-state and unsteady-state heat transfer is used to obtain the coefficients of thermal conductivity and thermal diffusivity.

Experimental investigations of structures of monodisperse dust particles in dc low-pressure glow discharge at temperatures of liquid nitrogen ($\sim 77 \text{ K}$) and liquid helium ($\sim 4.2 \text{ K}$) are presented. Structural and dynamic characteristics of the cryogenic dust structures were measured.

The influence of high magnetic field on dusty plasma structures is now of great interest in the field of dusty plasma physics. In the present work the rotation of the dusty clouds and anomalous dust acceleration near the discharge tube wall in strong magnetic field was observed. This work was supported by the Russian Foundation for Basic Research (Grants No.06-02-17532, No. 06-08-01584 and No. 07-02-13600).

When can the Fokker-Planck equation describe anomalous or chaotic particle transport ?

D.F. Escande¹ and F. Sattin²

¹ CNRS-Université de Provence, Marseille, France

² Consorzio RFX, Associazione Euratom-ENEA sulla Fusione, Padova, Italy

The Fokker-Planck Equation (FPE) is a basic model for the description of transport processes in several scientific fields. It has been used a lot in plasma physics to model chaotic and/or collisional kinetic effects. Furthermore, FPE backs up the diffusion-convection picture of anomalous transport in magnetized thermonuclear fusion plasmas. Though very popular, the drift-diffusive picture underlying FPE breaks down in some cases. This was shown for electron dynamics due to Langmuir waves [1], for the transport of tracer particles suddenly released in pressure-gradient-driven turbulence [2], and for pollutant transport in fluid dynamics. These facts triggered a series of studies where the Brownian paradigm was abandoned, and transport was described in terms of Lévy jumps, and of fractional diffusion models [3]. This sets the issue: when is FPE relevant for anomalous or chaotic transport, when is it not? This work [4] shows that, for particle transport ruled by chaotic Hamiltonian dynamics, FPE can be justified for generic particle transport provided that there is enough randomness in the Hamiltonian describing the dynamics. Then, except for 1 degree-of-freedom, the two transport coefficients of FPE (diffusion coefficient and dynamic friction) are largely independent. Depending on the kind and amount of averaging performed on it, the same dynamical system may be found diffusive or dominated by its Lévy flights. FPE may work even whenever the dynamics of individual particles exhibit strong trapping motion. Diffusion is justified by locality of trapping in phase-space, or by locality in velocity of particle resonance with fluctuating fields, then leading to a quasilinear estimate. If the system involves a particle source that is narrower than the mean random step of the true dynamics, FPE fails, while the density displays spatial features that are not related to the transport coefficients. If the width of the density distribution is of the order of the system size, there are indications that, even whenever Lévy flights rule the dynamics, FPE becomes a good description. Indeed Lévy flights bring efficiently into the system the information that the matter is lost outside of it.

[1] D. Bénisti and D.F. Escande, Phys. Rev. Lett. 80, 4871 (1998)

[2] D. del-Castillo-Negrete, B.A. Carreras, and V.E. Lynch, Phys. Plasmas 11, 3854 (2004)

[3] D. del-Castillo-Negrete, Phys. Plasmas 13, 082308 (2006)

[4] D.F. Escande et F. Sattin, Phys. Rev. Lett. 99, 185005 (2007).

I2.035, Tuesday 10 June 2008

Kinetic phase-space turbulence in space and laboratory plasmas

Alexander Schekochihin

Plasma Physics, 735 Blackett Laboratory, Imperial College, London SW7 2AZ , U.K.

I will first discuss how the gyrokinetic theory, originally developed for fusion applications, is applicable to astrophysical and space plasma turbulence problems. I will then explain how the familiar "fluid" turbulence ideas such as the energy cascade are generalized for a kinetic turbulence in a weakly collisional plasma. I will introduce the concept of a cascade of generalised energy in a 5D phase space and explain how small-scale structure develops both in the real and velocity space ("the entropy cascade") and how this process is fundamental in the conversion of electromagnetic fluctuation energy into heat. Astrophysical applications are the dissipation range of the solar wind and the heating of minority ion species. I will discuss how theory and measurements of turbulence in space can help us understand the fundamental features of plasma turbulence, also applicable to the microturbulence in fusion devices.

Reference.

A. A. Schekochihin, S. C. Cowley, W. Dorland, G. W. Hammett, G. G. Howes, E. Quataert, T. Tatsuno, *Astrophysical Journal Supplement*, submitted (2007) [eprint [arXiv:0704.0044](https://arxiv.org/abs/0704.0044)]

Star Trek plasma shields: Measurements and modelling of a diamagnetic cavity

R. Bamford¹, K. J. Gibson², A. T. Thornton², J. Bradford¹, R Bingham^{1,6},
L. Gargate^{1,3}, L..O. Silva³, R.A. Fonseca³, M. Hapgood¹, C. Norberg⁴,
T. Todd⁵, R. Stamper¹

¹*Space Plasmas, Rutherford Appleton Laboratory, Chilton, Didcot, OX11 0QX, U.K.*

²*Department of Physics, University of York, Heslington, York, YO10 5DD, U.K.*

³*Centro de Física dos Plasmas, Inst Superior Técnico, 1049-001 Lisboa, PORTUGAL*

⁴*Umea University, Box 812, 981 28 Kiruna, SWEDEN.*

⁵*EFDA-JET, Culham Science Centre, Abingdon, Oxfordshire, OX14 3DB, U.K.*

⁶*Physics Department, University of Strathclyde, Glasgow G4 0NG.*

Solar energetic ions are a known hazard to both spacecraft electronics and to astronauts health. Of primary concern is the exposure to keV--MeV protons on manned space flights to the Moon and Mars that extend over long periods of time. Attempts to protect the spacecraft include active shields that are reminiscent of Star Trek "deflector" shields. Here we describe a new experiment to test the shielding concept of a dipole-like magnetic field and plasma, surrounding the spacecraft forming a "mini magnetosphere". Initial laboratory experiments have been conducted to determine the effectiveness of a magnetized plasma barrier to be able to expel an impacting, low beta, supersonic flowing energetic plasma representing the Solar Wind. Optical and Langmuir probe data of the plasma density, the plasma flow velocity, and the intensity of the dipole field clearly show the creation of a narrow transport barrier region and diamagnetic cavity virtually devoid of energetic plasma particles. This demonstrates the potential viability of being able to create a small "hole" in a Solar Wind plasma, of the order of the ion Larmor orbit width, in which an inhabited spacecraft could reside in relative safety. The experimental results have been quantitatively compared to a 3D particle-in-cell 'hybrid' code simulation that uses kinetic ions and fluid electrons, showing good qualitative agreement and excellent quantitative agreement. Together the results demonstrate the pivotal role of particle kinetics in determining generic plasma transport barriers.

Vacuum and plasma QED nonlinearities

M. Marklund

Department of Physics, Umeå University, SE-901 87 Umeå, Sweden

Classically, the vacuum constitutes a trivial nothingness. However, this notion dramatically changed with the marriage of quantum mechanics and special relativity. The natural theory for photon interactions with matter, quantum electrodynamics (QED), indeed shows that the vacuum has certain nontrivial properties [1]. Currently, laser intensities are developing rapidly [2], and systems such as ELI [3] and HiPER [4] is expected to take this development to a new level. Moreover, techniques such as harmonic focusing [5] and plasma induced ultra-short pulse generation [6, 7] could be able, using front-ends such as ELI or HiPER, to produce pulse intensities above the Schwinger limit $\sim 10^{29}$ W/cm² [8]. In fact, even current technology allows for laser induced pair creation, albeit in combination with accelerator generated electron beams [9]. Previous experiments on the quantum vacuum has used atomic nuclei or accelerator based *high-energy* techniques as a means for testing quantum field theory, and in particular QED. The future development of laser sources will in this sense give completely new tools for testing QED in the *high-intensity* regime. In light of this, new laser-based tests of quantum vacuum phenomena is described. Moreover, many environments in which such high fields are present also contain plasmas. Thus, the alteration of mode propagation and nonlinear dynamics due to quantum vacuum/plasma interactions, such as nonlinear photon splitting (i.e., frequency down-conversion) will be reviewed.

References

- [1] M. Marklund and P. K. Shukla, Rev. Mod. Phys. **78**, 591 (2006).
- [2] G. A. Mourou, T. Tajima, and S. V. Bulanov, Rev. Mod. Phys. **78**, 309 (2006).
- [3] See the ELI website <http://www.extreme-light-infrastructure.eu/> .
- [4] See the HiPER website <http://www.hiper-laser.org/> .
- [5] S. Gordienko et al., Phys. Rev. Lett. **94**, 103903 (2005).
- [6] N. M. Naumova et al., Phys. Rev. Lett. **92**, 063902 (2004).
- [7] B. Dromey et al., Nature Phys. **2**, 456 (2006).
- [8] J. Schwinger, Phys. Rev. **82**, 664 (1951).
- [9] D. L. Burke et al., Phys. Rev. Lett. **79**, 1626 (1997).

**Phase resolved optical emission spectroscopy:
Multi-frequency discharges and atmospheric pressure plasmas**

Timo Gans

Centre for Plasma Physics, Queen's University Belfast, Northern Ireland, UK

E-mail: t.gans@qub.ac.uk

Despite its technological significance, important aspects of power coupling and ionisation mechanisms in radio-frequency (rf) discharges are not yet fully understood. Of particular interest are multi-frequency discharges and recently developed homogenous non-equilibrium rf discharges at ambient pressure. Insight into the complex plasma dynamics requires close combination of advanced diagnostics and specifically adapted simulations. Phase resolved optical emission spectroscopy (PROES) in combination with numerical computer simulations reveal details of the dynamics on a nanosecond time scale within the rf cycle.

Multi-frequency discharges provide additional process control for technological applications. The electron dynamics exhibits a complex spatio-temporal structure. Excitation and ionisation, and, therefore, plasma sustainment is dominated through directed energetic electrons created through the dynamics of the plasma boundary sheath. Non-linear frequency coupling is observed in plasma boundary sheaths governed by two frequencies simultaneously. The nature of these coupling effects strongly depends on the ratio of the applied voltages. Under technologically relevant conditions (low frequency voltage \gg high frequency voltage) interesting phenomena depending on the phase relation of the voltages are observed.

Recently developed rf discharges at ambient pressure bear enormous potential for future technological applications providing high reaction rates without the need of expensive vacuum systems. Fundamental discharge mechanisms are, however, only rudimentarily understood. The atmospheric pressure plasma jet (APPJ) is a homogeneous non-equilibrium discharge. A specially designed rf μ -APPJ provides excellent optical diagnostic access to the discharge volume and the interface to the effluent region. This allows investigations of the discharge dynamics and energy transport mechanisms from the discharge to the effluent. PROES measurements in the discharge volume show a complex combination of different excitation and ionisation mechanisms controlled by the dynamics of the plasma boundary sheaths. Interesting interaction phenomena between the two plasma boundary sheaths are observed.

Funding: EPSRC, DFG, SFI

Electrical Breakdown: Experiments and Modeling

Erik Wagenaars, Wouter Brok, Mark Bowden, Jan van Dijk, Joost van der Mullen, and Gerrit Kroesen

Eindhoven University of Technology, Netherlands

Plasma breakdown is a highly transient process that involves particles drifting in electric fields, charge multiplication in electron avalanches and moving ionization fronts. The driving force for these processes is the electric field in the discharge volume. The temporal evolution of the electrical field strength and other parameters have been studied by in-situ diagnostics as well as numerical modeling.

A pulsed discharge between parabolic, metal electrodes in a low pressure argon environment has been studied by light emission imaging with an ICCD camera. This diagnostic provided time- and space-resolved information on the characteristic features of the breakdown process. Different phases in the breakdown process were identified. Firstly, the build-up of a light emission region in the discharge gap in front of the anode, followed by a light front crossing the electrode gap from anode to cathode and finally, a stable discharge, which gradually covers the cathode surface. The experimental results also showed that before the main breakdown process started, a weak flash of light could be observed around the anode. This stratified pre-breakdown light emission occurred during the rise of the applied voltage, but before the breakdown voltage was reached. The origin of this feature was found to be electron avalanches seeded by volume charges left over from previous discharges in combination with the specific discharge geometry used in our experiments.

Additionally, a new diagnostic was developed to measure electric field distributions during the breakdown phase of a discharge. With this diagnostic, electric field strengths were determined by measuring Stark effects in xenon atoms using laser-induced fluorescence-dip spectroscopy. Stark shifts of up to 4.8 cm^{-1} (160 pm) were observed for *ns* and *nd* Rydberg states, with principal quantum numbers ranging from 12 to 18. This corresponds to electric fields between 250 and 4000 V/cm, which were measured with an accuracy of about 50 to 150 V/cm.

For the first time, quantitative, direct measurements of the evolution of electric field during breakdown were obtained. Electric fields between 0 and 1600 V/cm were measured with a resolution of 200–400 V/cm, depending on the magnitude of the electric field. These experiments showed that the ionization front, already observed in the ICCD imaging experiments, is sustained by a spatially narrow, rapidly moving region of strong electric field. Additionally, this ionization front did not completely modify the potential distribution in the discharge gap; the discharge continued developing towards a steady-state after the ionization front crossed the gap.

The discharge was also modeled numerically using a fluid code and a hybrid fluid-particle code. The prebreakdown flash is modeled with the hybrid model. It is caused by the charges that remained in the volume from previous pulses. The model results correctly reproduce the striations in the electron energy and density, which are found to occur due to the specific electric field configuration of the electrodes in the discharge chamber. The crossing of the light front is described with the fluid model. Ionization avalanches that start at the cathode due to secondary electrons cause a space charge that is largest near the anode and starts to affect the electric field there first. This extends the anode potential toward the cathode and is observed as a moving front. The results of both models agree qualitatively with the experimental observations.

Turbulence measurements in fusion plasmas

G.D.Conway

*Max-Planck Institut für Plasmaphysik, Euratom-Association IPP, Garching,
D-85748, Germany*

Turbulence measurements in magnetically confined toroidal plasmas have a long history, and indeed relevance due to the role of turbulence induced anomalous transport on particle, energy, impurity and momentum confinement. Turbulence - the microscopic random fluctuations in particle density, temperature, potential and magnetic field - is generally driven by gradients or sheared flows. The correlation between the turbulence properties and global confinement, via enhanced diffusion, convection and direct conduction, is now well documented. Theory, together with recent measurements, also indicate that non-linear interactions within the turbulence generate large scale “zonal” flows and geodesic oscillations, which can feed back onto the turbulence and equilibrium profiles creating a complex interdependence. An introduction to turbulence basics will be given, together with an overview of the current status of plasma turbulence measurements in tokamak/stellarator fusion devices highlighting recent developments and outstanding problems. Emphasis will be given to measurement techniques, such as new microwave based diagnostics for density and electric field fluctuations in the closed flux surface confinement region.

Aspects of stochastic transport in laboratory and astrophysical plasmas

Karl H. Spatschek*

Institut für Theoretische Physik, Heinrich-Heine-Universität Düsseldorf
D-40225 Düsseldorf, Germany

Anomalous transport belongs to the key problems in plasma research and nuclear fusion applications. During the last decades, considerable progress was reported in understanding basic features. Since in general analytical evaluations based on turbulence models are very difficult, numerical simulations become more and more important. Fusion-orientated plasma physics leads to a rich data base with many hints for fundamental transport scaling. Anomalous charged particle transport is also a long-standing problem in astrophysical issues. A variety of observational evidences, such as low-energy cosmic ray penetration into the heliosphere, the transport of galactic cosmic rays in and out of the interstellar magnetic field, the Fermi acceleration mechanism, exist which await full theoretical understanding.

A possible approach to the problem of anomalous plasma transport is to consider the (passive) motion of (test) particles under the influence of given perturbations. Such a treatment is quite common in fluid turbulence where passive motion of scalars, vectors, particles, etc has been investigated extensively. In fusion-orientated plasma physics, there exists an additional, qualitatively important reason to investigate particle motion in given stochastic fields. Perturbations in the magnetic field structure are more or less unavoidable because of errors in the coil arrangements of the devices. In addition, and recently that aspect became very important, additional coils are being installed in tokamaks to control the particle and heat loads on the walls via magnetic stochastization of the edge. The strength of the magnetic field fluctuations may be quite small, e.g. less than one-tenth of a percent of the zeroth-order confining field, for a strong influence on transport. It turns out that perpendicular fluctuations in the magnetic field are effective channels of parallel diffusivity in perpendicular direction.

The proposed talk reviews the present state of art of stochastic transport theory in fluctuating electric and magnetic fields. It dwells on recent developments such as, e.g., non-diffusive motion along tangles, Lagrangian closures, trapping and percolation limit, relativistic particle drifts, generation of radial electric fields, non-Gaussian magnetic field statistics, pitch angle scattering, and control of stochasticity.

*in collaboration with S. Abdullaev, M. Neuer, A. Wingen

Compatibility of ITER Scenarios with an all-W Wall

O. Gruber for the ASDEX Upgrade Team

MPI für Plasmaphysik, EURATOM Association IPP, D-85748 Garching, Germany

The wall material mix of the present ITER design tries to optimize the use of the armour materials beryllium, carbon and tungsten at appropriate positions. This concept will be tested in the ITER like wall project at JET. But a future reactor cannot rely on low-Z plasma facing components due to the high erosion and - in case of carbon - tritium co-deposition and neutron damage. The tungsten programme at ASDEX Upgrade emphasizes the plasma wall interaction, its implications for the plasma operation and the compatibility of ITER relevant scenarios in an all-metal divertor tokamak, including the characterization of the transition from a carbon to a W machine and the behaviour of different heating methods. Main elements are the extension of the working space of radiatively cooled integrated scenarios (using impurity seeding) and advanced operation modes as the improved H-mode (hybrid scenario) and H-modes with internal transport barriers. Starting with the 2007 campaign all PFCs including the bottom divertor targets are equipped with W coated graphite tiles.

Restarts were successfully performed without boronizations strengthening the credibility of possible operation with a W wall. The ITER baseline H-mode scenario was established over a wide density range with plasma currents up to 1 MA, $H_{98P} \sim 1$, a radiation fraction of about 60% and ITER compatible moderate W concentrations below $3 \cdot 10^{-5}$ using NBI and central wave heating. The divertor is now the largest W source, but this source plays only a minor role for the tungsten in the core plasma. The removal of all macroscopic carbon sources facing the plasma led to a reduction of the C content to about 4 per mille. Applying ICRH, results in large W influxes due to sputtering from light impurities accelerated by electrical fields at the ICRH antennas. ICRH operation could be optimized using large plasma-structure distances and gas puffing close to the antennas.

High performance improved H-modes over the full ITER relevant parameter regime in β^* , β_N and n_e/n_{GW} as well as ion-ITBs were extensively investigated in previous campaigns with nearly complete W coverage using boronization to transiently suppress W sources. Applying central ECRF of 2 MW in the all-W machine allowed us to keep the central peaking of the W concentration low, to produce electron-ITBs and to achieve high confinement phases of improved H-modes with $H_{98P} \approx 1.2-1.3$ even without boronization. In improved H-modes the plasma energy was limited to $\beta_N \approx 2$ at the presently reduced heating power.

To elucidate the influence of a high-Z wall on all ITER relevant scenarios, especially the advanced operation modes, and to extend the working space in plasma shaping, density and beta the presently available power supplies for PF coils and heating systems was enhanced by 30 MVA and a new installed 1 MW gyrotron will allow more than 3 MW ECRF. Additionally, after the repeated restart without boronization this tool will be used again to improve the discharge conditions at low collisionality, in particular improved H-mode studies.

Three Dimensional Transport Analysis for ELM Control Experiments in ITER Similar Shape Plasmas at Low Collisionality in DIII-D*

O. Schmitz for the TEXTOR and DIII-D Teams

Research Center Jülich GmbH, IEF-Plasma Physics, 52428 Jülich, Germany

The mitigation of large type-I edge localized modes (ELMs) is important to maintain long term integrity of the ITER first wall. At the DIII-D tokamak, application of resonant magnetic perturbation (RMP) was pioneered as a tool to control edge transport and thereby the ELM characteristics [T.E. Evans, *et al.*, Nucl. Fusion **48**, 024002 (2008)]. In this contribution we present recent results from experiments in ITER similar shape plasmas with high average triangularity ($\bar{\delta} = 0.56$) at low ITER similar collisionality ($\nu_e^* \leq 0.2$). Here complete ELM suppression was achieved robustly at an edge safety factor of $q_{95} \sim 3.5$. The resonant window width $\Delta q_{95} \sim 0.1-0.3$ was increased by a factor 2-4 by optimizing the RMP spectrum and increasing the RMP amplitude. In general suppression of ELMs is achieved via a reduction of the pedestal pressure gradient below the stability limit of the peeling ballooning modes, mainly by a decrease in pedestal density while pedestal temperatures slightly increase.

The transport characteristics in the perturbed, three dimensional magnetic field structure are analyzed in a collaborative approach by comparison of experimental and numerical results from TEXTOR-DED and DIII-D. For both devices, modelling of the magnetic topology and transport modelling with the E3D thermal transport code and with the plasma and neutral transport code EMC3-EIRENE were carried out. From this comparative analysis the magnetic topology suggests for DIII-D three radial transport domains for normalized flux Ψ_N : *resonant magnetic island chains* in $0.7 < \Psi_N < 0.85$ and a *highly stochastic volume* closer to the separatrix ($0.85 < \Psi_N < 0.99$) lead to enhanced radial transport. The last step towards the divertor target is governed by parallel transport along *open magnetic field lines* which end in a striated, non-axisymmetric pattern of the perturbed separatrix. They have a connection length $L_c \leq 500$ m of the same order as the thermal correlation length $L_t \simeq 400$ m and small compared to the electron mean free path $\lambda_e \sim 10^3-10^4$ m. From field line tracing it is shown that they penetrate as deep as $0.8 \leq \Psi_N \leq 1.0$ in the perturbed boundary. Therefore large parallel heat conduction and a clear imprint of the striated separatrix in the target heat flux were expected.

At TEXTOR-DED a striation of heat and particle fluxes caused by the helical ergodic divertor separatrix was observed for high $\nu_e^* > 0.9$ [M. Jakubowski, *et al.*, J. Nucl. Mater. **363-365**, 371 (2007)]. In DIII-D these fluxes also show striation during complete ELM suppression at high ν_e^* . However, at low ν_e^* a weak heat transport to the outer lobes of the separatrix and strong parallel particle flux along all lobes of the separatrix are measured. Here, the stochastic domain is not well-connected thermally to the separatrix structure at the target while parallel particle fluxes yield a strong particle loss from the pedestal region. In contrast, large heat and particle flux along the open field lines was detected for low ν_e^* also in strike point splitting of particle and heat flux for (a) interaction of the RMP with ELM filaments and (b) during pellet injection. Such an enhanced radial heat transport – which was originally anticipated to be dominant for transport in a stochastic magnetic boundary – is not apparent during ELM suppression. To explain these counter-intuitive experimental observations two mechanisms are discussed here: a limitation of the parallel heat conduction [M. Tokar, *et al.*, Phys. Rev. Lett. **98**, 095001 (2007)] and a screening of the external RMP field by plasma rotation [A. Cole, *et al.*, Phys. Plasmas **13**, 32503 (2006)].

*Work supported by DFG grant SFB591 and the U.S. Department of Energy under DE-FC02-04ER54698.

Beta Limit in JET

M P Gryaznevich¹, and JET-EFDA Contributors*

JET-EFDA, Culham Science Centre, OX14 3DB, Abingdon, UK

¹Euratom/UKAEA Fusion Association, Culham Science Centre, Abingdon, Oxon, OX14 3DB, UK

Advanced tokamak regimes are associated with increased normalised beta, $\beta_N = \beta_t B_t a / I_p$ ($\beta_t = 2\mu_0 \langle p \rangle / B_t^2$) and are often limited by MHD instabilities. Although the presence of a conducting wall increases this beta limit, it is important to know the no-wall ideal β -limit to be able to prevent/avoid the most dangerous pressure-driven disruptions in JET and ITER.

Systematic studies of the no-wall beta limit have been carried out on JET, for the first time in tokamaks, by measuring the plasma response to an externally applied helical magnetic perturbation. This Resonant Field Amplification (RFA) is strongly enhanced when a plasma exceeds the ideal no-wall stability limit or an ideal beta-limited determined by other modes, so it can be used as an indication of the beta limit. This method of the beta limit identification has been routinely used in scenario development of high-beta discharges on JET in several advanced regimes: the hybrid low-shear regime with $q(0)$ close to 1, the high-beta low shear regime with less than or $\sim 1 < q(0) < 2.0$ and in a reversed shear ITB regime.

It was shown that increase in $q(0)$ results in significant reduction in the measured beta limit going down to $\beta_{\text{lim}}^{\text{RFA}} \sim 1.5$ at $q(0)$, or q_{min} in a case of a slightly reversed shear, going down close to 2. Numerical stability simulations based on JET pulses have been performed and confirm this observed trend. It was observed that the measured β -limit has been routinely exceeded on JET by $\sim 10\%$.

Comparison of beta limits in different advanced regimes has been made and shows similar beta limit in hybrid and high-beta no-ITB scenarios for same $q(0)$. However, for the ITB scenario, the q_{min} has been found to be more relevant to characterise the beta limit.

The method developed for β -limit identification will be used to carry out β -limit dependence studies on q and pressure profile in AT scenarios on JET and to optimise plasma parameters in development of high performance regimes.

This work was funded by the UK Engineering and Physical Sciences Research Council and by the European Communities under the contract of Association between EURATOM and UKAEA. The views and opinions expressed herein do not necessarily reflect those of the European Commission.

* See annex to M. Watkins et al, Fusion Energy 2006 (Proc. 21st IAEA Conf., Chengdu, 2006) IAEA Vienna.

Physics issues in the new high current regimes on RFX-mod.

M. Valisa and the RFX team

*Consorzio RFX, Associazione Euratom-ENEA sulla fusione
35127 Padova- Italy*

Remarkable progress has been reported in the recent past by the Reversed Field Pinch community worldwide, with enhanced plasma performances and new contributions to the wider fusion environment in terms of both physics understanding and plasma control. Results of general interest regard themes like MHD active control, current profile control, density limit, fast particles confinement, spontaneous momentum generation, core transport barriers, electrostatic instabilities, edge turbulence, spontaneous transition from magnetic chaos to order, to name some of them. This paper describes in particular the physics issues emerging in RFX-mod where for the first time good quality RFP plasmas with a 1.5 MA current have been obtained. The progress towards higher currents has been permitted by the improvement of the model-based algorithm that drives as an artificial shell the large set of saddle coils tightly wrapping a conducting shell of 50 ms penetration time. Successful phase decoupling and amplitude reduction of the $m=1$ tearing modes resonating in the core has led to improved performance, reduced plasma-wall interaction and discharge duration well beyond the wall penetration time with full suppression of the Resistive Wall Modes. At high plasma current and with the improved magnetic boundary the MHD spectrum spontaneously evolves towards the Quasi Single Helicity regime, that is toward a better ordered magnetic topology, favored by the higher Lundquist number. The boundaries of the magnetic island with the dominant helicity are a transport barrier for the electron energy, with temperatures beyond 1 keV at densities of $2 \cdot 10^{19} \text{ m}^{-3}$. The island boundaries have been studied with the aid of a field line tracing code and investigated at the light of electrostatic turbulence theories. QSH islands generated in induced enhanced confinement events can become remarkably large and represent an interesting possibility for an advanced RFP scenario. The $m=0$ modes, resonating at the reversal surface, have been studied in particular for their relation with the Greenwald density limit. Where $m=0$ modes induce an inward excursion of the Last Closed Flux Surface, at high density, locally increased density, enhanced radiation and converging ExB flows are seen, similarly to the MARFE. The thermal instability that develops, expanding towards the plasma core ultimately quenches the discharge, in a non disruptive way. Control of the $m=0$ activity is speculated to allow the overcome of the density limit.

Integrated modelling of ITER steady-state scenarios

J. Garcia, G. Giruzzi, J.F. Artaud, V. Basiuk, J. Decker, F. Imbeaux, Y. Peysson,
M. Schneider

*Association EURATOM-CEA, CEA/DSM/DRFC, CEA-Cadarache,
F-13108 St. Paul lez Durance.*

Steady-state scenarios in ITER combine a high number of challenges, which are not only technical, but mainly conceptual. The simultaneous constraints of vanishing loop voltage and $Q \geq 5$ can only be satisfied for extremely high bootstrap current fractions (significantly higher than 50 %), which, in turn, are more likely to be obtained in the presence of an Internal Transport Barrier (ITB). In ITER, ITBs would be associated to negative magnetic shear rather than to rotation shear, owing to the lack of a powerful torque source. This implies that the control of the current density profile by non-inductive current drive (CD) is essential to sustain ITBs for a long time, but this is notoriously difficult when the bootstrap fraction is the dominant contribution (current alignment problem). Although various scenarios have been considered for steady-state operation on ITER, no steady sustainment of ITB for times of the order of 3000 s, with the amount of additional power expected on ITER, has been documented in simulations so far.

In this work, state-of-the-art integrated simulations with the CRONOS suite of codes [1] are used to study the physics involved in the ITB sustainment, and to identify the main obstacles to the establishment of a steady-state scenario in ITER. These simulations integrate, for the first time, advanced computational modules such as MonteCarlo calculations of the alpha particle distribution function and a 3D Fokker-Planck code for Lower Hybrid CD (LHCD), which proved essential for the correct simulation of this complex non-linear system. Since low rotation levels are expected in ITER, the empirical transport model used only takes into account the anomalous transport reduction due to negative magnetic shear. It is shown that any current driven inside the ITB leads to the progressive shrinking and disappearance of the barrier (current alignment current [2]). This physics property has strong implications on the choice of the current drive sources: for instance, Neutral Beam Current Drive, which is naturally localised in the central part of the plasma, proves to be of little use in these scenarios.

In contrast, a pure Radio Frequency (RF) scenario is proposed using 20 MW of Ion Cyclotron Resonant Heating (ICRH), 20 MW Electron Cyclotron Resonant Heating (ECRH) and 13 MW of LHCD. Within a framework of reasonable assumptions, it is shown that such a power combination provides a solution of principle to the current alignment problem. The main feature of this scenario is that there is a minimum negative magnetic shear, $s=-0.8$, to steadily sustain the ITB for 3000s, below which, low performance inductive scenarios are recovered. The actual design of the ECRH power system in ITER can provide such a negative magnetic shear at $\rho=0.45$ through Electron Cyclotron Current Drive (ECCD), which leads to a clear dependence of the temperature gradient (with a well defined threshold) on the $P_{ECH}/\langle n_e \rangle$ parameter. The threshold obtained for the ECRH power can be characterized as a second order phase transition as it has been done previously in the ITB formation of other completely different fusion devices as, e.g., the Large Helical Device (LHD) [3].

[1] V. Basiuk et al., Nucl. Fusion 43 822 (2003).

[2] W.A. Houlberg et al., Nucl. Fusion 45 1309 (2005).

[3] J. Garcia et al., Phys. Rev. Lett. 96 105007 (2006).

Radiation Pressure Acceleration by Ultraintense Laser Pulses

T. Liseykina

Institute of Computational Technologies SD RAS, Novosibirsk, Russia

The future applications of the short-duration, multi-MeV ion beams produced in the interaction of high-intensity laser pulses with solid targets will require improvements in the conversion efficiency, peak ion energy, beam monochromaticity, and collimation. Regimes based on Radiation Pressure Acceleration (RPA) might be the dominant at ultrahigh intensities [1] and be most suitable for specific applications. These regimes may be reached already with present-day intensities using circularly polarized pulses [2, 3] thanks to the suppression of fast electron generation, so that RPA dominates over sheath acceleration at any intensity.

We present the results of a comparison of 1D, 2D and 3D PIC simulations for circularly (CP) and linearly polarized (LP) pulses, which evidenciate the different features of ion acceleration and help in deeper understanding of RPA mechanisms. A detailed 1D study of the interaction of the CP laser pulse with thin, solid density targets is performed in order to find the optimal thickness of the target as well as scaling for ion energy and efficiency vs laser and plasma parameters. The 2D and 3D PIC simulations show that the onset of density rippling at the target surface is affected by the pulse polarization. Rippling of the front surface was observed in early simulations of high intensity laser pulse interaction with overdense plasmas [4]. Recently this topic has been revisited for thin plasma foils accelerated in the radiation-pressure-dominated regime [5]. Explanation of the surface rippling have been mostly based on Rayleigh-Taylor like instabilities due to the strong acceleration of the target driven by the radiation pressure. The case of CP is most adequate to test such theoretical description and its scaling with laser and plasma parameters since radiation pressure dominance holds at any intensity. On the other hand, the differences observed between CP and LP suggest that additional effects are at play for linear polarization. These effects might be due to fast electrons or to stimulated surface instabilities.

References

- [1] T. Esirkepov, M. Borghesi, S. V. Bulanov et al., PRL, **92**, 175003 (2004)
- [2] A. Macchi et al., arXiv:physics/0701139 (2007); T. V. Liseykina, A. Macchi, App. Phys. Lett., **91**, 171502 (2007); A. Macchi, F. Cattani et al., PRL, **95**, 195001 (2005)
- [3] X. Zhang et al., Phys.Plasmas, **14**, 073101 (2007); A. P. L. Robinson et al., New J.Phys., **10**, 013021 (2008)
- [4] S.C.Wilks et al., PRL, **69** (1992); S.C.Wilks, W.L.Kruer, IEEE J.Quant.Electr., **33** (1997)
- [5] F. Pegoraro, S. V. Bulanov, PRL, **99**, 065002 (2007)

One-to-one direct modelling of experiments and astrophysical scenarios: pushing the envelope on kinetic plasma simulations

R. A. Fonseca^{1,2}

¹*DCTI/Instituto Superior de Ciências do Trabalho e da Empresa, Lisboa, Portugal*

²*Instituto de Plasmas e Fusão Nuclear/Instituto Superior Técnico, Lisboa, Portugal*

There are many astrophysical and laboratory scenarios where kinetic effects play an important role. These range from astrophysical shocks and plasma shell collisions [1], to high intensity laser-plasma interactions, with applications to fast ignition [2] and particle acceleration [3,4]. Further understanding of these scenarios requires detailed numerical modelling, but fully relativist kinetic codes [5] are computationally intensity, and the goal of one-to-one direct modelling of such scenarios and direct comparison with experimental results is still difficult to achieve.

I will discuss the issues involved in performing such numerical experiments, focusing on what needs to be achieved for one-to-one direct modelling. I will also discuss the computational requirements involved, and present the recent developments in the efficiency and algorithms of the simulation tools, pointing out some future directions (e.g. dynamic load balancing, high-order interpolation and boosted frame simulations). Finally, I will present recent simulation work, illustrating these techniques and key results, in both laser wakefield acceleration, and astrophysical shock acceleration.

In collaboration with, M. Fiore, F. Fiuza, J. Martins, S. F. Martins, F. Peano, J. Vieira, L. O. Silva, J. Tonge, F. S. Tsung and W. B. Mori.

References

- [1] R. A. Fonseca *et al.*, POP 10, 1979 (2003); L. O. Silva *et al.*, ApJL 596, L121 (2003)
- [2] C. Ren *et al.*, PRL 93, 185004 (2004)
- [3] L. O. Silva *et al.*, PRL 94, 015002 (2004)
- [4] F. S. Tsung *et al.*, PRL 93, 185002 (2004); W. Lu *et al.*, PRSTAB 10, 061301 (2007)
- [5] R. A. Fonseca *et al.*, LNCS 2331, 342 (2002)

Quantum vacuum effects in strong laser beams

A. Di Piazza, K. Z. Hatsagortsyan, E. Lötstedt, U. D. Jentschura, and C. H. Keitel

Max-Planck-Institut für Kernphysik, Heidelberg, Germany

In view of the increasingly stronger available laser fields it is becoming feasible to use them to probe the nonlinear dielectric properties of vacuum as predicted by quantum electrodynamics (QED) and to test QED in the presence of intense laser beams. We first study the process of light-by-light diffraction mediated by the virtual electron-positron pairs present in vacuum [1]. The typical laser intensity at which these nonlinear vacuum effects are predicted to become apparent is of order of $I_{cr} \sim 10^{29}$ W/cm². We investigate a mechanism to enhance vacuum polarization effects (VPEs) at a given laser intensity by exploiting the dielectric properties of a cold plasma [2]. Our results show a large enhancement of VPEs in a plasma with respect to those predicted in pure vacuum when the frequency of the probe field (that in our case is also the field that polarizes the vacuum) approaches the plasma frequency. Moreover, we analyze the process of photon splitting in a laser field as a consequence of the vacuum-mediated interaction between the photon and the laser field. The possibility of the experimental observation of this process is also discussed [3].

The study of the properties of quantum vacuum is closely related to the possibility of testing QED in the presence of strong background fields. We investigate in detail two processes which soon could be in principle feasible experimentally: laser photon merging in laser-proton collisions [4] and laser-assisted bremsstrahlung [5]. In the first case, we show that laser photons merge due to VPEs when interacting with the electromagnetic field of a high-energy proton, manifesting an observable, non-perturbative dependence on the laser field parameters. In the second one, the dramatic influence of the presence of a strong laser beam on the bremsstrahlung process is pointed out.

References

- [1] A. Di Piazza, K. Z. Hatsagortsyan, and C. H. Keitel, Phys. Rev. Lett. **97**, 083603 (2006).
- [2] A. Di Piazza, K. Z. Hatsagortsyan, and C. H. Keitel, Phys. Plasmas **14**, 032102 (2007).
- [3] A. Di Piazza, A. I. Milstein, and C. H. Keitel, Phys. Rev. A **76**, 032103 (2007).
- [4] A. Di Piazza, K. Z. Hatsagortsyan, and C. H. Keitel, Phys. Rev. Lett. **100**, 010403 (2008).
- [5] E. Lötstedt, U. D. Jentschura, and C. H. Keitel, Phys. Rev. Lett. **98**, 043002 (2007).

CHARGING of AEROSOLS and NUCLEATION IN ATMOSPHERIC PRESSURE ELECTRICAL DISCHARGES

JP. Borra

*Laboratoire de Physique des Gaz et Plasmas UMR CNRS-Univ. Paris-Sud, Orsay, F-91405
Supélec, 3 Rue Joliot Curie, Gif-sur-Yvette/, F-91192, France*

The goal of this presentation is to highlight potential applications of plasmas produced in Atmospheric Pressure Electrical Discharges (dc corona, streamer and spark filamentary discharges, as well as for ac filamentary and homogeneous Dielectric Barrier Discharges).

At first, respective properties of electrical regimes that can be induced in such discharges are briefly depicted to introduce applications of these atmospheric pressure plasmas in aerosol processes for Materials and Environment (filtration, diagnostics).

Then, the charging mechanisms of submicron sized particles by collection of ions are presented in corona, post-corona and Dielectric Barrier Discharges. In such defined electric field and ion densities profiles, both field and diffusion charging laws are presented to account for the related potential applications of controlled kinematics of charged aerosol (electro-filtration, homogeneous/focussed deposition and coagulation to produce composites).

The last part addresses key parameters controlling both the formation by nucleation and the growth by coagulation of particles in plasmas. Two sources of vapour leading to nucleated nano-particles are depicted in Atmospheric Pressure Electrical Discharges: (i) when dc streamer and spark filamentary discharges as well as ac filamentary Dielectric Barrier Discharges interact with the surface of electrodes or dielectrics, and (ii) when both filamentary and homogeneous Dielectric Barrier Discharges induce reactions with gaseous precursors in volume. In both cases, condensable gaseous species are produced, leading to nano-sized particles by physical and chemical routes of nucleation. It will be shown how composition, size and structure of primary nano-particles as well as the final size of agglomerates are related to plasma parameters (Energy, number per unit surface and time and thermal gradients around each filament as well as the transit time). Once produced, so-formed nano-sized aerosol can either be deposited in the plasma for thin films coatings or kept in suspension to produce fine powders, depending on both charging and electro-thermal collection.

PLASMA SYNTHESIS OF SILICON QUANTUM DOTS FOR PRINTED ELECTRONICS AND PHOTOVOLTAICS

U. Kortshagen

University of Minnesota, Mechanical Engineering, Minneapolis, MN, USA

Plasmas are a unique source of semiconductor nanocrystals. Exothermic surface reactions combined with slow cooling at low pressures selectively heat nanoparticles immersed in plasmas to temperatures exceeding the gas temperature by hundreds of Kelvin. This enables the synthesis of nanocrystals even of high melting point materials. Moreover, the electrical charging of nanocrystals allows for the generation of non-agglomerated nanoparticles, conserving the size-dependent properties of quantum dots.

We have developed a plasma approach for the synthesis [1], electrical doping, and surface functionalization of silicon nanocrystals [2]. Silicon crystals are generated in a continuous flow-through RF-plasma process, and injected into a second capacitively coupled RF-plasma, in which organic molecules are grafted to the hydrogen-terminated nanocrystal surfaces. The so functionalized nanocrystals are readily soluble in organic solvents and form stable silicon nanocrystal colloids or “inks.”

This talk will equally focus on a description of the plasma process and a discussion of the materials properties. We will discuss issues of nanoparticle charging and heating in plasmas as well as aspect of dopant incorporation, activation, and location within the nanocrystals. Finally, we will review materials properties of functional semiconductor films prepared from plasma-synthesized and functionalized nanocrystals.

This work was supported by the National Science Foundation under award CMMI-0556163, IGERT grant DGE-0114372, and NIRT grant CBET-0506672. Partial support was provided by the MRSEC Program of the National Science Foundation under Award Number DMR-0212302 and by the Initiative for Renewable Energy and the Environment under grant LG-C5-2005.

References

- [1] L. Mangolini, E. Thimsen, and U. Kortshagen, *Nano Letters* 5, 655 (2005)
- [2] L. Mangolini and U. Kortshagen, *Adv. Materials* 19, 2513 (2007)

Low temperature plasma synthesis of silicon nanocrystals: the way for high deposition rate and efficient polymorphous and microcrystalline solar cells

Y. Djeridane, Th. Nguyen-Tran, E.V. Johnson, A. Abramov, Q. Zhang, and
P Roca i Cabarrocas

LPICM, Ecole Polytechnique, CNRS, 91128 Palaiseau, France

With the spectacular increase in photovoltaic solar energy (~40% annual growth over the last 10 years) and the anticipated increase in the market share of thin films (20% in 2010), new more stringent demands are being placed on thin film deposition technologies, and low temperature plasma processes need to be revisited. Indeed, the standard a-Si:H deposition process based on the production of SiH_x radicals by the dissociation of silane suffers from a low deposition rate. In previous studies we have addressed the synthesis of silicon clusters and nanocrystals which offer a new route for thin film deposition [1]. Here, we focus on plasma diagnostics which provide a clear signature for the presence of nanocrystal formation in the gas phase, as well as the application of this synthesis route to polymorphous and microcrystalline silicon solar cells. We show that superior electronic transport properties are achieved at higher deposition rates, and the device properties reflect this result.

Hydrogenated polymorphous silicon (pm-Si:H) has developed as an alternative to a-Si:H and its application to PIN solar cells has resulted in devices with improved stability [2]. In this presentation we summarize our progress in the understanding of this material, with particular emphasis on its application to PIN solar cells and mini modules deposited at high rates.

It is quite generally accepted that the growth of microcrystalline silicon films involves four phases: incubation, nucleation, growth, and steady state, and that atomic hydrogen is a key element at each stage. As a result, the film structure develops in a columnar fashion with an amorphous interface with the substrate. Moreover, the increase in deposition rate results in a decrease of the crystalline fraction as the competition between growth rate and crystallization rate is in favour of the growth. However, for practical applications one needs μ c-Si films with thicknesses in the range of 1-2 microns and thus a high deposition rate is mandatory. The synthesis of silicon nanocrystals in the plasma allows to circumvent this hurdle. Indeed the growth rate of nanocrystals in the plasma can be extremely large (up to 100 nm/s). Thus, the incubation and nucleation phases, difficult to achieve on the substrate, are easily obtained in the plasma and allow an increased deposition rate. We have applied this concept to the deposition of microcrystalline silicon solar cells and have achieved short circuit currents up to 25 mA/cm² for 1.5 μ m thick solar cells, resulting in efficiencies of 8-9%. Plasma diagnostics during these depositions show low frequency oscillations in the self-bias voltage, which provide a signature for nanocrystal nucleation and growth in the plasma [3].

In summary the increasing demands being placed on solar cell fabrication technology is driving an intensification in the development of low temperature plasma processes able to produce high quality silicon thin films at high rates. Processes employing plasma-synthesized nanocrystals and clusters address this demand in an elegant way, and demonstrate tremendous potential in both deposition rate as well as device quality.

1. P. Roca i Cabarrocas, A. Fontcuberta i Morral, S. Lebib, and Y. Poissant, *Pure Appl. Chem.* **74**, 359 (2002).

2 P. Roca i Cabarrocas, Th Nguyen-Tran, Y. Djeridane, A. Abramov, E. Johnson and G. Patriarche. *J. Phys. D: Appl. Phys.* **40** (2007) pp. 2258-2266

3 E. V. Johnson, Y. Djeridane, A. Abramov and P. Roca i Cabarrocas, *Plasma Sources Sci. Technol.*, *under submission*.

LABORATORY INVESTIGATIONS OF AURORAL CYCLOTRON EMISSION PROCESSES

K. Ronald¹, D.C. Speirs¹, S.L. McConville¹, K.M. Gillespie¹, A.D.R. Phelps¹, A.W. Cross¹,
R. Bingham^{1,3}, C.W. Robertson¹, C.G. Whyte¹, I. Vorgul², R.A. Cairns², B.J. Kellett³ and
W. He¹

¹*SUPA Department of Physics, University of Strathclyde, Glasgow, G4 0NG, Scotland*

²*School of Mathematics and Statistics, University of St. Andrews, St Andrews, KY16 9SS,
Scotland*

³*Space Physics Division, STFC Rutherford Appleton Laboratory, Didcot, OX11 0QX,
England*

Auroral **Kilometric Radiation, AKR**, occurs naturally in the polar regions of the Earth's magnetosphere where electrons are accelerated by electric fields into the increasing planetary magnetic dipole where conservation of the magnetic moment converts axial to rotational momentum forming a horseshoe distribution in velocity phase space. This distribution is unstable to cyclotron emissions and radiation is emitted in the X-mode. In the laboratory a 75-85kV electron beam of 5-40A was magnetically compressed by a system of solenoids. Results are presented for an electron beam gyrating at cyclotron frequencies of 4.42GHz and 11.7GHz resonating with near cut-off TE₀₁ and TE₀₃ modes respectively. Measurements of the electron transport demonstrated that the horseshoe distribution function was formed and were analysed to yield the 1D number density as a function of pitch angle. The total power emitted experimentally was ~19-35kW [1] with a maximum emission efficiency of ~2%. These results were compared to those obtained numerically using a 2D PiC code KARAT with a maximum efficiency of 2% predicted for the same mode and frequency, comparable with astrophysical and theoretical results. The experiment is currently being modified by introducing a background plasma to give a better representation of the natural environment.

References

- [1] K. Ronald, D.C. Speirs, S.L. McConville, A.D.R. Phelps, C.W. Robertson, C.G. Whyte, W. He, K.M. Gillespie, A.W. Cross and R. Bingham, 2008, Physics of Plasma, in press
- [2] D.C. Speirs, S.L. McConville, K.M. Gillespie, K. Ronald, A.D.R. Phelps, A.W. Cross, R. Bingham, C.W. Robertson, C.G. Whyte, I. Vorgul, R.A. Cairns and B.J. Kellett, 2008, Plasma Physics and Controlled Fusion, in press

13.054, Wednesday 11 June 2008

Astrophysical Jet Experiments

C. D. Gregory¹, B. Loupiaz¹, J. Howe², J. Waugh¹, S. Myers², M. M. Notley³, Y. Sakawa⁴, A. Oya⁵, R. Kodama⁵, S. Bouquet⁶, E. Falize^{6,7}, C. Michaut⁷, M. Koenig¹, N. C. Woolsey²

¹ *LULI laboratory, Ecole Polytechnique, France*

² *Department of Physics, University of York, England*

³ *Central Laser Facility, Rutherford Appleton Laboratory, England*

⁴ *Institute of Laser Engineering, Osaka University, Japan*

⁵ *Graduate School of Engineering, Osaka University, Japan*

⁶ *CEA, Bruyeres Le Chatel, France*

⁷ *Observatoire de Paris, University Paris Diderot, France*

Some of the most inspiring images in science are of astronomical objects, and the study of the phenomena responsible for such images has long been of interest. Traditionally, such understanding has come from theoretical models and computational simulations. The current capabilities of pulsed power devices, such as high-intensity lasers and z-pinch facilities, can deliver energy densities comparable to those found in astrophysical objects. This allows us to perform laboratory experiments that, if correctly designed and interpreted, can provide valuable insight into some of the outstanding problems in astrophysics.

An area of considerable progress in this field is the laboratory simulation of astrophysical jets, and in particular those associated with the accretion phase of young stellar objects. The relative proximity of these objects, and their ubiquity, has led to a large amount of high quality observational data. There remain a number of uncertainties about these systems, for example: how are these jets launched? Why are they so well collimated over such long length scales? To what extent do magnetic fields, radiative losses and the ambient medium affect their dynamics?

This talk will give a brief introduction to young stellar object jets, and outline some of the questions that may be addressed in the laboratory. The focus will be on laser-plasma experiments, in which jets have been created through the collision of two expanding plasmas. These experiments have succeeded in driving high-velocity outflows that are in a regime which suggests scaling to astrophysical systems is possible, and have begun to investigate the effects of an ambient gas on the jet propagation.

Experiments on interstellar cloud evolution following strong shock passage*

J. Freddy Hansen[†],

Lawrence Livermore National Laboratory, Livermore CA 94550, USA

The evolution of interstellar clouds following the passage of a supernova shock is an important astrophysical phenomenon; the shock passage may trigger star formation and the post-shock flow surrounding the clouds will strip them of material, effectively limiting cloud life times. Experiments conducted at the Omega laser attempt to (a) quantify the mass-stripping of a single cloud, and (b) simulate the effects of nearby clouds interacting with each other. A strong shock is driven (using 5 kJ of the 30 kJ Omega laser) into a cylinder filled with low-density foam with embedded 120 m Al spheres simulating interstellar clouds. The density ratio between Al and foam is ~9. Material is continuously being stripped from a cloud at a rate which is inconsistent with laminar models for mass-stripping; the cloud is fully stripped by 80ns-100ns, ten times faster than the laminar model. A new model for turbulent mass-stripping is developed [1,2,3] that agrees with the observed rate and which should scale to astrophysical conditions. Two interacting spherical clouds are observed to turn their upstream sections to face each other, a result that is completely opposite of earlier work [4] on two interacting cylinders. The difference between these two cases is explained by the relative strength of shocks reflected from the clouds.

*Prepared by LLNL under Contract DE-AC52-07NA27344. [†]In collaboration with H. F. Robey, R. I. Klein, A. R. Miles, Lawrence Livermore National Laboratory; C. F. McKee, University of California Berkeley.

1. J.F. Hansen et al, "Mass-Stripping Analysis of an Interstellar Cloud by a Supernova Shock," *Astrophys. Space Sci.*, , *Astrophys. Space Sci.* **307**, 147-152 (2007).
2. J.F. Hansen et al, "Experiment on the Mass-Stripping of an Interstellar Cloud Following Shock Passage," *Astrophys. J.* **662**, 379-388 (2007).
3. J.F. Hansen et al, "Experiment on the mass-stripping of an interstellar cloud in a high Mach number post-shock flow," *Phys. Plasmas* **14**, 056505 (2007).
4. C. Tomkins et al, "A quantitative study of the interaction of two Richtmyer-Meshkov-unstable gas cylinders," *Phys. Fluids.* **15**, 986 (2003).

LASER-DRIVEN PROTON ACCELERATION: SOURCE OPTIMIZATION AND PERSPECTIVES FOR APPLICATIONS

M.Borghesi

School of Mathematics and Physics, The Queen's University, Belfast, United Kingdom

Ion acceleration from solid targets irradiated by high-intensity pulses is a burgeoning area of research, and is currently the focus of intense research activity worldwide. Under presently achievable irradiation conditions, the acceleration is driven by relativistic electrons, which acquire energy directly from the laser pulse and set up extremely large (\sim TV/m) space charge fields at the target interfaces. The properties of laser-driven ion beams (high brightness and laminarity, high-energy cut-off, ultrashort burst duration) are, under several respects, markedly different from those of “conventional” accelerator beams. In view of these properties, laser-driven ion beams have the potential to be employed in a number of innovative applications in the scientific, technological and medical areas.

We will review here some of the most recent results of research in this area by our group and collaborators, and we will discuss prospects for further developments and applications.

Important results in some applicative areas have been obtained already with currently available beam characteristics (e.g. broadband spectrum and \sim 50 MeV cut-off energy). In particular the use of these beams as a particle probe for the detection of electric fields in plasmas has led in recent years to a wealth of novel information regarding the ultrafast plasma dynamics following high intensity laser-matter interactions. We will discuss some of the most recent results obtained with this technique, applied to the diagnosis of transient self-generated electric and magnetic field during high-power laser-plasma interactions.

Other applications (including the possible use of laser-driven protons for cancer radiotherapy) will require optimized performance compared to characteristics currently available, in terms of particle numbers, energy, spectral content or beam divergence. Some recent experimental studies aimed to characterize and optimize the beam properties and to better gauge perspectives in these areas will be reported. Laser facilities currently becoming available or being planned will open up over the next few years previously inaccessible interaction regimes. This, coupled to ongoing developments in targetry and laser beam control, will lead to the possible implementation of novel ion acceleration schemes, highly promising for the delivery of optimised beams for applications.

HALL EFFECT THRUSTERS FOR SATELLITE PROPULSION

J.P. Boeuf

LAPLACE, University of Toulouse, CNRS, France

Hall Effect Thrusters (HETs) are a class of gridless ion sources that can generate thrust from 10's to 100's of mN, with specific impulse in the 2000 s range (i.e. exhaust velocity of the propellant on the order of 20 km/s). They are well suited for tasks such as satellite station keeping and are also considered for interplanetary missions. For these missions, where a relatively small thrust is needed for a very long period of time, their large specific impulse makes them much more efficient than chemical thrusters and allows important cost reduction.

After a general introduction on space propulsion, the lecture will be centred on the principles and the physics of Hall Effects Thrusters. We will focus on basic physics questions related to electron and ion transport in a HET. HETs use an EXB configuration, where an external magnetic field perpendicular to the applied electric field and discharge current increases the residence time of electrons in the thruster and allows ionization of the xenon neutral flow. The gridless ion acceleration is provided by the electric field resulting from the drop of electron conductivity associated with this EXB configuration. Most of the neutral flow is ionized and the neutral gas density in the exhaust region of the thruster is not large enough to allow sufficient electron transport across the magnetic field and to explain experimental measurements.

The physics of electron transport in HETs is still an open question although important progress have been made in the last ten years. We will describe the recent efforts¹ toward the understanding of charged particle transport in HETs, and present a synthesis of the combined results of Particle-In-Cell models, hybrid models, Laser Induced Fluorescence measurements and Collective Scattering experiments. One possible explanation of the observed anomalous electron transport is the generation of an azimuthal drift instability that has been predicted by PIC models. Experimental efforts are aimed at confirming the anomalous turbulent transport predicted by the kinetic models.

References

- [1] TELIOPEH project (“Transport Electronique et Ionique dans les Propulseurs à Effet Hall”), ANR contract N° ANR-06-BLAN-0171

SPONTANEOUS ROTATION IN ALCATOR C-MOD PLASMAS

J.E. Rice, A.C. Ince-Cushman, Y. Podpaly

M.I.T. P.S.F.C., Cambridge, MA, USA

Spontaneous toroidal rotation, self-generated in the absence of external momentum input, exhibits a rich phenomenology. In L-mode plasmas, the rotation varies in a complicated fashion with electron density, magnetic configuration and plasma current, and is predominantly in the counter-current direction. The rotation depends very sensitively on the balance between upper and lower null, and plays a crucial role in the H-mode power threshold [1]. Rotation inversion between the counter- and co-current direction has been observed following small changes in the electron density and plasma current, with very distinct thresholds [2,1]. In stark contrast, the intrinsic rotation in H-mode plasmas has a relatively simple parameter dependence, with the rotation velocity proportional to the plasma stored energy [3], and is always directed co-current. A comparison of spontaneous rotation in H-mode plasmas from many devices leads to a relatively simple scaling, with the observed thermal Mach number proportion to the normalized pressure [4]. This scaling obtains over a wide range of operational parameter space, and for H-modes produced by many different techniques (ICRF heating, Ohmic heating, ECH, ECH with LHH), indicating a universality of the phenomenon. Extrapolation to ITER plasmas suggests RWMs may be suppressed without external momentum input. In plasmas with internal transport barriers, formed either with off-axis ICRF heating or LHCD, the rotation velocity inside of the ITB foot is found to be in the counter-current direction.

References

- [1] J.E. Rice et al., Nucl. Fusion **45**, 251 (2005)
- [2] B.P. Duval et al., Plasma Phys. Control. Fusion **49**, B195 (2007)
- [3] J.E. Rice et al., Nucl. Fusion **38**, 75 (1998)
- [4] J.E. Rice et al., Nucl. Fusion **47**, 1618 (2007)

14.059, Thursday 12 June 2008

Innovative Diagnostics for ITER Physics addressed in JET

A.Murari* and JET-EFDA Contributors¹

JET_EFDA, Culham Science Center, OX14 3DB, Abingdon, UK

*Consorzio RFX-Associazione EURATOM ENEA per la Fusione. I-35127 Padua, Italy

The JET scientific mid-term programme, whose main pillars are the installation of a completely new first wall (made of Beryllium and Tungsten) and a significant increase in the additional heating power, is aimed at controlling plasmas of performance closer to the next step device, ITER. Extending the operational space towards more reactor relevant parameters requires further understanding of various physical phenomena including a) the dynamics of low temperature plasmas close to the containment wall b) the effects of turbulence, at the macroscopic and meso-scale level, on the transport of energy, particles and momentum in the plasma internal region c) the burning plasma aspects linked to the interplay between collective instabilities and energetic particles generated by the fusion reactions. Obtaining the necessary experimental information on these issues poses significant challenges for the measurement systems. Therefore, during the last couple of years, about thirty new or improved diagnostics were installed and a similar number will be finalised during next campaigns, providing JET with state of the art instruments, covering all the main measuring techniques used in physics, from interferometry to scattering, from spectroscopy to tomography, from radar to thermography.

The boundary region of fusion plasmas is particularly difficult to study because of the often non-linear mutual influences between plasma physics effects, atomic processes and material properties. With regard to the interactions of the plasma with the surrounding material surfaces, significant improvements in JET infrared systems and magnetic diagnostics have allowed, for the first time, a careful evaluation of the power losses caused by the most harmful global instabilities, which can even cause the premature termination of the discharge and structural damage to the machine. Innovative detectors and techniques, from Quartz microbalances to visible and infrared spectroscopy, have provided new information on processes typical of low temperature plasmas, like erosion, re-deposition and material migration. They have also contributed to elucidate the main physical and chemical aspects of these phenomena.

Plasma properties at the edge have to be determined with high accuracy and resolution mainly in order to control the performance and the transient thermal loads on the wall. The gradients of the electron fluid have been resolved for the first time with spatial resolution of about 1.5 cm using the new High Resolution Thomson Scattering; the ion temperature can be measured with a spatial resolution of a few centimetres from upgraded active spectroscopy. The effects of the changes in the magnetic topology (toroidal field ripple, ergodization etc) on the plasma transport have been quantified. A high time resolution bolometric tomography has been systematically used to characterise the total radiation pattern during fast instabilities and the radiation peaking factor during disruptions. Advanced modelling, integrating atomic physics and impurity transport, is essential for stabilising low temperature plasmas at the limit of detachment, a particular plasma state close to the target tiles where the pressure is not longer constant along the magnetic field lines. A new fast visible camera has confirmed the presence in JET edge plasmas of various structures like filaments and blobs. This diagnostic is expected not only to shed light on the macroscopic instabilities at the edge but also to provide information about meso-scale phenomena and turbulence.

In the plasma core, the energy, particle and momentum confinement is crucially determined by the non-linear saturation level of the turbulence and its effects on transport. In order to understand the impact of these phenomena on the global machine performance, the main plasma parameters have been measured with higher spatial and time resolution using upgraded active spectroscopy, Thomson scattering and microwave diagnostics. Recently particular attention has been devoted to the transport of momentum, the accumulation of light impurities and their dependence from the current profile and the strength of the transport barriers. Advances in the atomic physics of high Z species, mainly tungsten, have been promoted to determine their behaviour in all the various regions of JET plasmas (from edge to core). Neutron diagnostics, with their spectrometric and imaging capability, are essential for burning plasma studies and to accommodate the future changes to the environment (mainly Be tiles).

A multi year upgrade programme has been devoted to the detection of energetic particles. For the first time energetic ions can be measured at JET during their whole life time. In particular their interplay with collective Magneto-Hydro-Dynamic instabilities, which can significantly increase their losses, has been investigated with a new scintillator probe and a set of Faraday cups. To understand their thermalisation process, several advances in detection techniques and atomic physics, of relevance also for various atmospheric physics studies, have proved to be necessary.

In addition to a discussion of the various measuring techniques prospects for ITER, the relevance of the implemented diagnostic upgrades for other scientific communities, from low temperature plasmas to astrophysics and inertial fusion, will also be addressed.

¹ See appendix of M Watkins et al., *Fusion Energy 2006 (Proc. 21st Int. Conf. Chengdu, 2006) IAEA Vienna (2006)*

Fast-Ignition Target Design and Experimental Concept Validation on OMEGA

C. Stoeckl,¹ K. S. Anderson,¹ R. Betti,^{1,2} J. A. Delettrez,¹ J. A. Frenje,³ V. N. Goncharov,¹
V. Yu. Glebov,¹ A. J. Mackinnon,⁴ R. L. McCrory,¹ D. D. Meyerhofer,^{1,2} J. Myatt,¹ P. A.
Norreys,⁵ P. M. Nilson,¹ R. D. Petrasso,³ T. C. Sangster,¹ A. A. Solodov,¹ R. B. Stephens,⁶
M. Storm,¹ W. Theobald,¹ B. Yaakobi,¹ and C. D. Zhou¹

¹*Laboratory for Laser Energetics, University of Rochester, NY, USA*

²*Depts. of Mechanical Engineering and Physics, University of Rochester, Rochester, NY, USA*

³*Massachusetts Institute of Technology, Cambridge, MA, USA*

⁴*Lawrence Livermore National Laboratory, Livermore, CA, USA*

⁵*Rutherford Appleton Laboratory, Didcot, UK*

⁶*General Atomics, San Diego, CA, USA*

The OMEGA EP Laser Facility [1] will be completed in Spring 2008, adjacent to the 60-beam, 30-kJ, OMEGA Laser Facility [2] at the University of Rochester's Laboratory for Laser Energetics. OMEGA EP consists of four beamlines with a NIF-like architecture [3]. Each of the beams will ultimately produce 6.5 kJ in 10-ns pulses directed into the OMEGA EP target chamber. Two of the beamlines can operate as high-energy petawatt (HEPW) lasers, with up to 2.6 kJ each at a 10-ps pulse duration. The HEPW beams can be injected into either the OMEGA EP chamber or combined collinearly into the existing OMEGA target chamber for integrated fast-ignitor experiments. A comprehensive scientific program is being pursued to explore the physics of fast ignition for both channeling and cone-in-shell approaches. Multidimensional hydrodynamic simulations integrated with a hybrid PIC code are used to optimize ignition designs and to prepare for integrated experiments using OMEGA/OMEGA EP. Fuel-assembly experiments on OMEGA explore the options to achieve high-fuel-areal densities and the effects of a cone on the fuel assembly. Experiments on short-pulse laser systems investigate the conversion efficiency from laser energy to fast electrons, the transport of the electrons, and the energy deposition in plasma.

This work was supported by the U.S. Department of Energy Office of Inertial Confinement Fusion under Cooperative Agreement No. DE-FC52-08NA28302.

References

- [1] C. Stoeckl *et al.*, Fusion Sci. Technol. **49**, 367 (2006).
- [2] T. R. Boehly *et al.*, Opt. Commun. **133**, 495 (1997).
- [3] G. H. Miller, E. I. Moses, and C. R. Wuest, Opt. Eng. **43**, 2841 (2004).

Overview of PETAL, the multi-Petawatt project on the LIL facility

N. Blanchot¹, G. Behar¹, T. Berthier¹, E. Bignon¹, F. Boubault¹, C. Chappuis¹, H. Coïc¹,
C. Damiens-Dupont¹, G. Deschaseaux¹, Y. Gautheron¹, P. Gibert¹, O. Hartmann¹,
E. Hugonnot¹, F. Laborde¹, D. Lebeaux¹, J. Luce¹, S. Montant², S. Noailles¹, J. Néauport¹,
A. Roques¹, C. Rullière¹, F. Sautarel¹, M. Sautet¹, C. Sauteret¹ et C. Rouyer¹

1) Commissariat à l'Énergie Atomique, Centre d'Études Scientifiques et Techniques
d'Aquitaine, BP 2, 33114 Le Barp Cedex, France

2) Centre Lasers Intenses et Applications, Unité mixte de Recherche 5107,
Université de Bordeaux I, 351 Cours de la Libération, 33405 Talence Cedex, France

E-mail : nathalie.blanchot@cea.fr, clauderouyer@cea.fr

PETAL (PETawatt Aquitaine Laser), this projected up-graded LIL⁽¹⁾ (LMJ prototype), will offer a unique combination of one of the highest intensity beams, synchronized nanosecond LIL beams. The primary system requirement is the addition of one short-pulse (500 fs to 10 ps) ultra-high-power, high-energy beam (3.5 kJ compressed energy) to the LIL facility motivated by specific needs, such as:

- as a first step for the HiPER⁽²⁾ project, to carry out fast ignition related experiments, providing fundamental information on fusion plasma physics and demonstration of the required laser and optics technology.
- to widen the field of research in High Energy Density Physics, particle production and acceleration and nuclear physics that can be done on this facility, among other possibilities providing a short pulse, high-energy backlighting capability that also allows the development of backlighting techniques.

We will present the conceptual design of PETAL, the experimental realization of the front-end with OPCPA⁽³⁾, the compression⁽⁴⁾ stage and the longitudinal chromatism corrector⁽⁵⁾.

This work is being performed under the auspices of the *Conseil Régional d'Aquitaine* and the technical supports of the *Institut Lasers et Plasmas*.

(1) J.M. Di-Nicola et al., "LIL Facility Quadruplet Commissioning", IFSA (2005).

(2) M. Dunne, "A European path to Fast Ignition Fusion Energy", ICUIL (2006).

(3) E. Hugonnot et al., "OPCPA for the PETAL front-end: design and results", ASSP (2007).

(4) N. Blanchot et al., "Synthetic aperture compression scheme for Multi-Petawatt High Energy laser", Appl. Opt. 45, (2006).

(5) J. Néauport et al., "Chromatism compensation of the PETAL multi-Petawatt high energy laser," Appl. Opt. 46, (2007).

Present Status of Pinch Plasmas for EUV and Soft X-ray Radiation

K. Bergmann

Fraunhofer Institute for Laser Technology, Steinbachstr. 15, D-52074 Aachen Germany

Discharge plasmas are well known as intense emitter of soft x-ray and extreme ultraviolet radiation with wavelengths ranging from 1 nm to 50 nm (XUV). The basic mechanism of generating the characteristic short wavelength radiation by heating and compressing a plasma to temperatures of several tens to several hundreds of electron volts and densities of 10^{18} - 10^{19} cm⁻³ has been intensively investigated for several decades. However, mainly driven by the activities in extreme ultraviolet lithography aiming at a compact and powerful source at a wavelength of 13.5 nm these sources have experienced a remarkable progress over the last ten years with respect to technological aspects. These are operating at several tens of kilowatts electrical input power with related challenges in cooling of the electrode system, repetition rates up to 10 kilohertz and more, debris and lifetime. These technological problems have in turn triggered basic studies in different areas, since the systems have to be pushed to their respective theoretical limits, which also have to be explored. The current status of source development for EUV lithography at different places will be presented with focus on the Philips's vacuum arc as the most advanced technology. Strategies and state of the art of the system lifetime, radiation and input power levels as well as integration into the optical system will be addressed. Taking into account that small source for power levels much lower than required for EUV lithography are already commercially available this technology envisions a new generation of small and cost effective XUV sources. So they might be the appropriate light source for many applications of analysis and patterning on the nanometer scale required in future disciplines of semiconductor industry, life- and material sciences. Scaling of the EUV source technology to ever smaller wavelengths will be presented using the example of a radiation source in the water window spectral range at 2.88 nm to be used in x-ray microscopy.

IN-SITU DUST DETECTION IN FUSION DEVICES

S. Ratynskaia¹, C. Castaldo², E. Giovannozzi², D. Rudakov³

¹*Royal Institute of Technology, Stockholm, Sweden*

²*Euratom ENEA Association, Frascati, Italy*

³*University of California, San Diego, USA*

It is expected that during the discharge most of the dust particles concentrate in the scrape-off layer (SOL) close to the chamber wall. Currently established diagnostics for monitoring the dust during the discharge are visible imaging and laser light scattering. The first can yield velocity of the dust particles provided particles are bigger than a few μm and their velocities are below 1 km/s. The scattering gives an insight on the amount of submicron dust though the interpretation of the scattered signals might be complicated as it depends on the optical properties of the dust grains and can require modelling of the laser-dust nonlinear interaction.

The dust-impact ionization phenomenon can be used for detection of particles with velocities above few km/s. Impact events can be registered by electrostatic probes, by analysis of the surfaces where the events took place and by light emission associated with the impact ionization. Particularly valuable for such diagnostic could be targets of aerogel – light porous material which allows capturing of fast particles without destroying them, hence providing information on their velocity distribution, size and composition. Preliminary outgasing tests demonstrated that pure silica aerogels are compatible with tokamak plasma conditions in SOL.

Other diagnostics include the microbalance technique which permits measurements of the cumulative weight of the collected dust and electrostatic dust detectors counting impinging dust particles.

Recently the possible use of changes in the collective scattering cross-section due to the presence of dust (provided that the dust number density is sufficiently high) was proposed for diagnostic purposes.

The Dynamic Similarity Between Polygonal Satellite Vortices and Electron Columns in a Malberg-Penning Trap

G. H. Vatistas^{*}, H. Ait Abderrahmane, and M. H. Kamran Siddiqui

*Department of Mechanical and Industrial Engineering University of Concordia Montreal
1455 de Maisonneuve Blvd. West, Montreal, Quebec, H3G 1M8, CANADA*

When employed judiciously, classical analogy is a sensible method of scientific inquiry. Two systems, that may not necessarily resemble physically each other, are considered to be analogous, if both are described by the same set of evolutionary equations. For instance, the stability of point vortices arranged in a ring has its foundation in the similarity among point vortices and the gravitating N -body problem, whereby the vortex strength is replaced by the mass. Furthermore, the Two-Dimensional (2-D) Drift-Poisson equations describing strongly magnetized electron columns and those of 2-D Eulerian fluid motion are dual. In this paper we revisit the dynamics of polygonal vortex core formations, generated under shallow water conditions inside a cylinder by a revolving disk. The observed fluid vortex patterning is isomorphic to pure electron plasma diocotron waves generated in Malmborg-Penning Traps. The present work adds on the description of the event via targeted experiments using the image processing technique. We show the interfacial axial symmetry not to break spontaneously but through spectral development, and the functional relationship amongst the polygon rotation and the disk speed to be surprisingly simple. The route to turbulence first begins by spectral development distinguished by an increase of the number of satellite vortices (up to six) orbiting the parent vortex. Due to resonance inside the bulk flow, the last stage is succeeded by an amplification of dynamical noise that destroys the sharp spectral peaks and eventually gives rise to fully blown turbulence. Power spectrum analysis reveals that harmonic waves modulate the fundamental patterns. At the end of the state, a solitary wave revolving at approximately the frequency of the next equilibrium appears. This system can also be viewed as vortices rotating with a solitary vortex (solitron) encircling the pattern. As the solitron gyrates, about the N pattern, makes each consecutive ridge to appear momentarily fatter. As the $N+1$ state is reached the wave locks-in at a frequency of $1/3$ thus producing the extra apex required to form the next equilibrium pattern. A large distortion of the pattern precedes the birth of the new one.

* vatistas@encs.concordia.ca

Studies of blob formation, propagation and transport mechanisms in basic experimental plasmas (TORPEX and CSDX)

S. H. Müller^{2,1}, A. Diallo¹, A. Fasoli¹, I. Furno¹, B. Labit¹, M. Podestà^{3,1}, C. Theiler¹
G. R. Tynan², M. Xu², Z. Yan², J. H. Yu²

¹*Centre de Recherches en Physique des Plasmas, Association EURATOM – Confédération Suisse, CRPP EPFL, Lausanne, Switzerland*

²*Center for Energy Research, University of California, San Diego, CA-92093, USA*

³*Department of Physics and Astronomy, University of California, Irvine, CA-92697, USA*

Plasma blobs are ubiquitous in the tokamak edge and responsible for the majority of transport across the Scrape-Off Layer (SOL). Their generation and propagation mechanisms have been widely studied theoretically, but limited experimental information is available to validate these models. Here, results from basic experiments are presented, in which plasma blobs are studied with much better access and control than possible in tokamaks, using both conditional-averaging and new pattern-recognition analysis techniques.

On the basic toroidal device TORPEX, the blob formation mechanism is found to be related to the breaking of an interchange-driven wave. Blobs form when wave crests extend into regions where they completely dominate the background plasma parameters. The self-generated electric shear is found responsible for the detachment of blobs. Theoretical models of blob propagation are tested by investigating the statistical relation between blob speeds and dimensions. Direct measurements of the blob-induced transport reveal that blobs constitute the dominant cross-field particle and heat transport mechanism across the TORPEX SOL region. Their effect on toroidal momentum transport is investigated using correlated Mach probe measurements.

On the linear device CSDX, radial bursts are observed to emerge from a coherent $m=1$ mode. The conditions under which these bursts form detached blobs are investigated using combined fast-camera and probe measurements. In the absence of an interchange driving force, blobs lose their initial radial momentum quickly and stagnate in the SOL region. During bursts, the azimuthal rotation of the plasma column is slowed down significantly, indicating the conservation of angular momentum when the plasma's moment of inertia increases.

The magnetopause is really a transport barrier like in tokamaks

R. Trines¹, R. Bingham¹, M.W. Dunlop¹, A. Vaivads²,
J.A. Davies¹, L.O. Silva³, J.T. Mendonça³, P.K. Shukla⁴

¹ STFC Rutherford Appleton Laboratory, HSIC, Didcot, United Kingdom

² Swedish Institute for Space Physics, Uppsala, Sweden

³ Instituto Superior Técnico, Lisbon, Portugal

⁴ Ruhr-Universität Bochum, Bochum, Germany

E-mail: R.M.G.Trines@rl.ac.uk

Internal transport barriers (ITB) are indispensable for reaching high-confinement modes in tokamaks. An ITB is set up by introducing a shear in the magnetic field or the $\mathbf{E} \times \mathbf{B}$ rotation velocity. This shear stabilises plasma turbulence and prevents particles and energy from escaping the plasma core, thus improving confinement. The most characteristic feature of an ITB is the appearance of strong gradients near the plasma edge. In this lecture, we will show that the magnetopause, the boundary between the shocked solar wind and the Earth's magnetospheric plasma, is a transport barrier in its own right. Strong density gradients, magnetic field and velocity shear, as well as stabilisation of turbulence, can all be observed at the magnetopause.

Recently, we investigated the interaction between broadband drift mode turbulence and zonal flows near the edge of a region of magnetised plasma [1, 2]. Our simulation results showed the development of a zonal flow through the modulational instability of the drift wave distribution, as well as the existence of solitary zonal flow structures about an ion gyro-radius wide, drifting towards steeper relative density gradients. Both the growth rate of the turbulence and the particle/energy transport across the plasma boundary can be stabilised by adjusting the plasma density gradient. This spontaneous formation of solitary wave structures has also been found in Cluster satellite observations [3], confirming our earlier theoretical predictions. We will discuss the consequences of our results for our understanding of the Earth's magnetopause, as well as for the study of Edge Localised Modes in tokamaks.

This work was supported by the STFC Centre for Fundamental Physics and the STFC Accelerator Science and Technology Centre (ASTEC).

References

- [1] R. Trines et al., Phys. Rev. Lett. **94**, 165002 (2005).
- [2] R. Trines et al., Physica Scripta **T116**, 75 (2005).
- [3] R. Trines et al., Phys. Rev. Lett. **99**, 205006 (2007).

Expansion of nanoplasmas in ultraintense laser-matter interactions

F. Peano

GoLP/Instituto de Plasmas e Fusão Nuclear, Instituto Superior Técnico, Lisboa, Portugal

The expansion dynamics of nanometer-sized plasmas is a relevant physical problem for applications such as the laser-induced production of nuclear particles in jets of clusters or nanodroplets [1,2], or the imaging of biological samples with ultraintense x-ray pulses [3]. These scenarios involve the prompt formation and expansion of dense nanoplasmas [1], with cold ions and hot electrons. Depending on the physical conditions, the electrons are heated by the laser, driving the hydrodynamic-like expansion of electron-ion plasmas, or swept off the single clusters, causing the Coulomb Explosion (CE) of pure ion plasmas.

The transition from the hydrodynamic-like regime to the CE regime is investigated with a novel ergodic model, which provides a self-consistent, kinetic description of the collisionless expansion of spherical plasmas driven by hot electrons: simple relationships are deduced for the key expansion features, valid for a wide range of initial conditions [4], and a threshold electron energy marking the transition to CE-like ion energy spectra is identified.

A technique to control the expansion regime by acting on the amount of energy delivered to the electrons is described, wherein suitable sequences of intense radiation pulses are used to tailor the phase-space dynamics of the ions [5], inducing the formation of large-scale shock-shell structures [6], capable of driving intracluster nuclear reactions. A new solution to the pure CE problem is also illustrated, which involves the simultaneous overtaking of all the ions initially contained in a given 3D volume (dimensional collapse), and the corresponding formation of a density singularity containing a finite amount of charge [7].

Work partially supported by FCT, and performed in collaboration with: J. L. Martins, R. A. Fonseca, and L. O. Silva (IST); F. Peinetti, R. Mulas, and G. Coppa (PoliTo).

- [1] T. Ditmire *et al.*, Nature **386**, 54 (1997); T. Ditmire *et al.*, Nature **398**, 489 (1999).
- [2] I. Last and J. Jortner, Phys. Rev. Lett. **97**, 173401 (2006)
- [3] R. Neutze *et al.*, Nature **406**, 752 (2000); H. Wabnitz *et al.*, Nature **420**, 482 (2002).
- [4] F. Peano *et al.*, Phys. Rev. Lett. **96**, 175002 (2006); Phys. Rev. E **75**, 066403 (2007)
- [5] F. Peano *et al.*, Phys. Rev. Lett. **94**, 033401 (2005); Phys. Rev. A, **73**, 053202 (2006).
- [6] A. E. Kaplan *et al.*, Phys. Rev. Lett. **91**, 143401 (2003)
- [7] F. Peano *et al.*, in preparation.

15.068, Friday 13 June 2008

Fast ignition: original concept and new developments*

Max Tabak

Lawrence Livermore National Laboratory, Livermore, CA, USA

Over the last decade many scientists around the world have studied Fast Ignition, an alternate form of inertial fusion. In this scheme, the fuel is first compressed by a long pulse driver and then ignited by the short pulse laser. Due to technological advances, external energy sources (such as short pulse lasers) can produce focused power density equivalent to that produced by the hydrodynamic stagnation of conventional inertial fusion capsules. This review will discuss the ignition requirements and gain curves starting from simple models and then describing how these are modified as more detailed physics understanding is included. The critical design issues revolve around two questions: How can the compressed fuel be efficiently assembled? And how can power from the driver be delivered to the ignition region? Schemes to shorten the distance between the critical surface and the ignition region will be discussed. The status of the project is compared with our requirements for success. Recent approaches to point designs that integrate all of the relevant physics will also be discussed.

*This work performed under the auspices of the U.S. Department of Energy by Lawrence Livermore National Laboratory under Contract DE-AC52-07NA27344.

Lightning-related transient luminous events at high altitude in the Earth's atmosphere

Victor P. Pasko

*Department of Electrical Engineering, Communications and Space Sciences Laboratory
Penn State University, University Park, Pennsylvania 16802, USA*

Transient luminous events (Fig. 1) are large-scale electrical discharges occurring at high altitude in the Earth's atmosphere, which are directly related to the electrical activity in underlying thunderstorms. Several different types of transient luminous events have been documented and classified. These include relatively slow-moving fountains of blue light, known as 'blue jets', that emanate from the top of thunderclouds up to an altitude of 40 km; 'sprites' that develop at the base of the ionosphere and move rapidly downwards at speeds up to 10,000 km/s; 'elves', which are lightning induced flashes that can spread over 300 km laterally, and upward moving 'gigantic jets', which establish a direct path of electrical contact between thundercloud tops and the lower ionosphere. The goal of this talk is to provide an overview of the history of discovery of different types of transient luminous events, and some of the recent modeling efforts directed on interpretation of observed features of these events. We will discuss a physical mechanism proposed for explanation of sprites, which is build on original ideas advanced many decades ago by the Nobel Prize winner C. T. R. Wilson. We will also discuss similarity properties of electrical discharges as a function of gas pressure in the context of a selected set of results from the recent laboratory and modeling studies of streamers, which are directly applicable for understanding of recent high spatial and temporal resolution imagery of sprites revealing many internal filamentary features with transverse spatial scales ranging from tens to a few hundreds of meters.

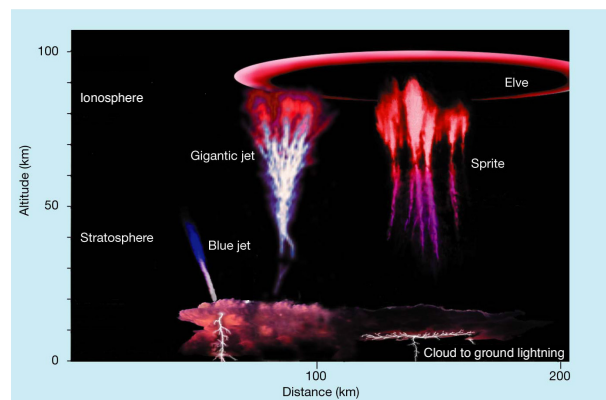


Figure 1: Lightning related transient luminous events. Reprinted from [1] by permission from Nature.

References

- [1] V. P. Pasko, *Nature* **423**, 927 (2003)

The response of tokamak plasmas to 3D magnetic field perturbations*

J.E. Menard¹, J.-K. Park¹, A.H. Boozer², T. Evans³, D.A. Gates¹, S.P. Gerhardt¹,

S.A. Sabbagh², M.J. Schaffer³, and the NSTX Research Team

¹*Princeton Plasma Physics Laboratory, Princeton, New Jersey, USA*

²*Columbia University, New York, New York, USA*

³*General Atomics, P.O. Box 85608, San Diego, California 92186, USA*

The loss of axisymmetry in tokamak plasma has wide-ranging implications for plasma performance in both present experiments and ITER burning plasmas. An important new tool for understanding 3D magnetic field effects in tokamaks is the Ideal Perturbed Equilibrium Code (IPEC) [1], which can treat ideal plasma response effects including poloidal mode coupling, plasma amplification, and flux-surface displacement. IPEC has been used for optimizing Resonant Magnetic Perturbation (RMP) coil designs for ELM suppression in ITER, and all the above plasma response effects are found to be important. IPEC RMP optimizations minimize resonant perturbations in the plasma core which could excite locked modes, and also minimize plasma flow-damping in the core and edge. IPEC results indicate that coils above, below, and possibly at, the midplane are required to achieve simultaneous minimization of core island excitation and flow damping. Another key question is how much rotation is required to shield low- n (in particular $n=1$) error fields (EF) that would otherwise excite magnetic islands potentially leading to disruption. IPEC calculations show that poloidal mode coupling effects are needed to explain EF correction results on DIII-D and NSTX [2], and recent NSTX results indicate that local magnetic shear at the $q=2$ surface is an important parameter determining the $n=1$ locked mode threshold scaling. The inclusion of plasma response effects can significantly reduce the predicted locking threshold for ITER, but the predicted threshold is estimated to be a factor of two above ITER's minimum correction capability. RMP coils in ITER might also provide additional EF correction capability. Finally, beyond IPEC results, NSTX has discovered that $n > 1$ EFs can be just as important as $n=1$ EFs at high β_N . Correction of $n > 1$ intrinsic EFs is not commonly considered in existing tokamaks or ITER, and without such correction in NSTX, some discharges are prone to rotation decay and $n=1$ Resistive Wall Mode (RWM) growth and plasma disruption. For these discharges, surfaces with $q > 2$ are apparently most important for providing RWM stabilization, a result that is providing new insight into the stabilization physics of the RWM.

[1] J.-K. Park, A.H. Boozer, and A.H. Glasser, *Phys. Plasmas* 14, 052110 (2007)

[2] J.K. Park, M.J. Schaffer, J.E. Menard, and A.H. Boozer, *Phys. Rev. Lett.* 99, 195003 (2007)

*This research was supported by U.S. DOE contract DE-AC02-76-CH03073.

15.071, Friday 13 June 2008

Plasma performance and confinement in the TJ-II stellarator with lithium-coated walls

F.L. Tabarés and the TJ-II Team.

Laboratorio Nacional de Fusión. CIEMAT. Avenida Complutense 22, 28040 Madrid, Spain

e-mail: tabares@ciemat.es

As it is well known, proper selection of the plasma facing components is one important tool for the control of plasma parameters and confinement. The effect is typically ascribed to the associated changes in recycling, radiated power and impurity penetration, all of them having direct impact in the plasma parameters critically governing particle and energy confinement. In the last experimental campaign, the TJ-II stellarator, which has been operated under boronized first wall condition until now, has been coated with lithium by vacuum evaporation. This has led to important changes in plasma performance. Particularly conspicuous has been the change in recycling associated to the new wall conditions, but also impurity content, with direct impact on radiative losses and total energy confinement is modified by the type of coating, as expected in a first-wall dominated plasma-wall interaction device. Changes in the shot by shot fuelling characteristics as well as in the total particle inventory compatible with good density control and plasma reproducibility under ECRH scenarios have been recorded after the Li deposition. Thus, a rise by a factor of 4 in the fuelling rate at constant density compared with the B-coated walls was recorded, and even a higher factor was estimated for the allowed H inventory at the walls. These changes were also mirrored in the radiation and edge radial profiles, with increased electron temperatures. The replacement of dominant impurity at the edge also led to the extension of the effective density limit in NBI heating scenarios. This limit, formerly ascribed to the development of a radiation instability at the edge, seems to be due to a global energy balance mismatch under the new wall conditions, opening the way to heating upgrading for high beta operation in TJ-II. Transport analysis with Proctr code to fit the different impurity profiles and the changes in the effective electron heat diffusivity is ongoing. The radiation radial profiles, which are basic for understanding the local power balance, are obtained considering four impurity species (Li, C, B, O) and using the local corona equilibrium. At densities above $3 \cdot 10^{13} \text{ cm}^{-3}$, higher plasma energy contents were measured under Li-coated wall conditions as compared with boronized conditions under the same heating scheme, and the effect of such scheme (ON-OFF axis ECRH launching, OH induction, etc) on absolute W_{dia} values has also been addressed. Of special relevance in the confinement properties of TJ-II plasmas is the spontaneous development of radial electric fields at the edge at a critical density, concomitant to the transition to the enhanced global particle confinement (EPC) mode. The apparent lack of such a transition under Li walls, easing the way to density control by external puffing, has been analyzed through the associated development of a velocity shear layer at the edge, as measured by Langmuir probes, and changes in plasma potential by the HIBP diagnostic, and results in this line will be also presented.

Global Plasma Oscillations in ITBs

V.S. Udintsev, E. Asp, T.P. Goodman, O. Sauter, G. Turri and TCV Team

*Ecole Polytechnique Fédérale de Lausanne (EPFL),
Centre de Recherches en Physique des Plasmas,
Association Euratom-Confédération Suisse,
CH-1015 Lausanne, Switzerland*

In the Tokamak à Configuration Variable (TCV; $R/a = 0.88$ m/ 0.25 m, $BT < 1.54$ T), global plasma oscillations have been discovered in fully non-inductively driven plasmas featuring Electron Internal Transport Barriers (eITBs) with strong Electron Cyclotron Resonance Heating and Current Drive (ECRH/ECCD). They are linked to the destabilisation and stabilisation of MHD modes near the foot of the internal transport barrier and can lead to large oscillations of the total plasma current and line-averaged density for example. These regimes are similar to the so-called O-regime first observed on Tore Supra [1], but are actually of much more general nature. Indeed they are intrinsically linked to the fact that ITBs have large pressure gradients in a region of low magnetic shear. Therefore the ideal MHD limit is relatively low and infernal modes can be unstable. When these ideal infernal modes are destabilised, minor or major disruptions can be observed. However depending on the proximity to the ideal limit, small crashes or resistive modes can appear which affect the time evolution of the discharge. They reduce the improved confinement, which lowers the pressure and thereby decreases the bootstrap current density. Since bootstrap fraction is large, the total plasma current is also affected. Being near marginal stability, the modes can self-stabilise due to their modification of the pressure gradient and local q profile. The plasma recovers good confinement, reverse shear and the build up of the internal transport barrier, until a new MHD mode is destabilized.

TCV has shown that this cycling behaviour can be controlled by modifying the current or the pressure profiles, either with Ohmic current density perturbation or by modifying the ECH/ECCD power. It has also been shown that either resistive type modes or ideal type crashes can lead to similar oscillations observed on the plasma current time evolution. These are consistent with the fact that near an ideal limit, resistive modes can also be unstable due to the pole in Δ' . Therefore we can see that many observations like $q = 2$ sawteeth, beta collapse and minor disruption in ITBs, oscillation regimes, periodic relaxation regimes can be assigned to the same physics origin: the proximity to the infernal mode stability limit [2].

This result is important since it is inherent to any steady-state type scenario. Indeed, the latter needs ITB, large bootstrap fraction and no inductive current contribution [2]. These lead to reverse shear q profiles and therefore large pressure gradient near q_{\min} . These scenarios are only weakly controlled by external actuators, since most of the current profile is sustained by the bootstrap current. It was also shown that a small perturbation to an existing electron internal transport barrier by power modulation triggered an oscillation regime, which continued after the power modulation was stopped. As steady-state burning plasmas might also incur small perturbations, it is very likely that such oscillations will occur; which may be very damaging. This detailed study will show the relation between oscillations and MHD modes and how the scenarios can be controlled and modified with current density tailoring or with a modification of the pressure profile.

[1] G. Giruzzi *et al.*, Phys. Rev. Lett. **91**, 135001 (2003).

[2] O. Sauter *et al.*, Phys. Rev. Lett. **94**, 105002 (2005)

Access to H-mode on JET and implications for ITER

Y Andrew¹, NC Hawkes¹, YR Martin², K Crombe³, E de la Luna⁴, A Murari⁵, I Nunes⁶, R Sartori⁷ and JET EFDA contributors*

JET-EFDA Culham Science Centre, Abingdon, UK, OX14 3DB

1. Euratom/UKAEA Fusion Association, Culham Science Centre, Abingdon, UK, OX14 3DB, 2. Ecole Polytechnique Federale de Lausanne (EPFL), Centre de Recherches en Physique des Plasmas, Association Euratom-Confederation Suisse, CH-1015 Lausanne, Switzerland. 3. Department of Applied Physics, Ghent University, Belgium, 4. Asociación EURATOM-CIEMAT, CIEMAT, Madrid, Spain, 5. Consorzio RFX, ENEA-Euratom Association, Padua, Italy, 6. Associacao EURATOM/IST, Centro de Fusao Nuclear, Lisbon, Portugal, 7. EFDA CSU, Boltzmannstrasse 2, 8674 8 Garching, Germany

One of the critical issues for ITER is access to an H-mode regime with good confinement, $H_{98} = 1$. Studies of the transition from L-mode to H-mode (the L-H transition) have been carried out for many years on a wide range of different sized devices such as, JET, JET-60U, DIII-D, ASDEX, Alcator C-MOD, MAST and NSTX. Experiments across the world have contributed data on H-mode access to an international threshold database (13 tokamaks) managed by the International Tokamak Physics Activity (ITPA) Confinement Database and Modeling (CDM) Topical Group, from which several scalings for the power threshold for the L-H transition, P_{th} , have been derived. The most basic scaling laws for P_{th} take in account the variation with plasma density, magnetic field and plasma size. However, the large variation in P_{th} data from the values estimated with such simple scaling laws indicate other underlying dependencies. Another important consideration is that P_{th} corresponds to the power required to enter the H-mode, but not necessarily the power needed to obtain an H-mode with good confinement. H-modes with higher values of energy confinement are often only achieved with input power values much greater than P_{th} .

This paper will present results from recent studies on JET to assess possible hidden variables for H-mode access over a wide range of plasma conditions. These experiments have also benefited from recent improvements to the spatial and temporal edge plasma diagnostics on JET, providing a unique opportunity to improve our understanding of the physics of H-mode transitions. A key result from this work is the significant variation in the plasma density dependence of P_{th} with divertor X-point and strike-point configuration, ranging from $n_e^{1.26}$ to $n_e^{0.12}$. Sensitivity to the divertor geometry could account for some of the scatter in the international threshold P_{th} database. Hysteresis in the L-H transition P_{th} has also been studied on JET by comparing values of P_{th} at the forward and back H-mode transitions over a range of densities. No evidence of hysteresis in the H-mode power threshold is observed for the two different magnetic configurations considered. The impact of edge plasma rotation on H-mode access has also been studied on JET with a Toroidal Field ripple scan of the L-H transition and ELM phase access. Despite a large change in edge toroidal rotation velocity no significant variation in P_{th} was measured, however the subsequent access to high confinement H-mode is clearly altered. Finally, results from experimental studies of the total input power, P_{in} , requirements relative to measured values of P_{th} will also be shown for a highly shaped magnetic configuration. The data show that $P_{in}=1.5P_{th}$ is necessary on JET for the Type-III to Type-I ELM transition. The implications of all these results for the attainment of H-mode with good confinement on ITER will be discussed in terms of present-day scaling laws and ongoing studies.

*See appendix of ML Watkins et al., 2006 Proc. 21st IAEA Fusion Energy Conference (Chengdu, China 2006).

This work was partly supported by the UK Engineering and Physical Sciences Research Council and by the European Communities under the contract of Association between EURATOM and UKAEA. The views and opinions expressed herein do not necessarily reflect those of the European Commission. This work was partly conducted under the European Fusion Development Agreement.

MAGNETIZED PLASMA ERUPTIONS IN THE SOLAR ATMOSPHERE

F Moreno-Insertis,
Instituto de Astrofísica de Canarias,
Tenerife, Spain.

Abstract:

Magnetized plasma is emerging continually from the solar interior into its atmosphere. Magnetic flux emergence events and their consequences at different levels in the solar atmosphere are being observed with high space, time and spectral resolution by a large number of space missions in operation at present (e.g. SOHO, Hinode, Stereo, Rhesi), sent by different international space agencies (ESA, NASA, ISAS). The collision of an emerging and a preexisting magnetic flux system in the solar atmosphere leads to the formation of current sheets and to field line reconnection. Reconnection under solar coronal conditions is an energetic event; the reconnecting outflows lead to launching of high-speed (hundreds of 1000 km/s), high-temperature (order 10 million K) plasma jets, which are conspicuous features in the observations with the X-Ray and EUV detectors currently in orbit. Further, the spectacular increase in computational power in recent years thanks to the new supercomputer installations permits to carry out three-dimensional numerical experiments of the time evolution of magnetic flux emerging systems that include magnetofluid and radiative transfer aspects in large computational grids.

In this lecture, the state-of-the-art in this field of research will be reviewed. Observations of X-Ray jets in the solar corona by the satellite missions Hinode and Stereo will be presented. The focus of the lecture will be on the theoretical understanding of these processes. An important computational effort is being done by teams in different countries to model and understand the physics of flux emergence events and its related phenomena. Recent advances obtained through the interplay of theory, numerical simulation and direct observation will be presented.

Recent progress in understanding the behavior of dust in fusion devices

S. I. Krasheninnikov

University of California at San Diego, 9500 Gilman Dr., La Jolla, California 92093, USA

It is known that micro-particles (dust) exist in fusion devices. Some of them, seen with cameras and for a long time known as “UFOs” (e.g. see Ref. 1), travel through hot fusion plasma on rather large distance and may contribute to the contamination of core plasma with impurities. Amount of such UFOs significantly increases during abnormal events (e.g. large ELM, disruption). Yet, an impact of dust on plasma contamination, material migration, and performance of fusion devices is still under debate (e.g. see Ref. 2-4 and the references therein). Meanwhile, ITER-scale plasma experiments bring another dimension to the dust’s story: dust can pose safety problems related to its chemical activity, toxicity, tritium retention, and radioactive content [5]. In order to address these safety and performance issues we need to understand the physics of dust generation, dynamics, and transport. However, the physics of dust is very complex and multifaceted. Here, the results of recent theoretical and experimental studies of dust in fusion plasmas are reviewed. We consider the latest experimental observations of dust dynamics in fusion plasmas with fast cameras, dust statistics obtained with Thomson scattering systems, the results of analysis of dust collected from the walls of fusion devices, and dust generation mechanisms. We also discuss different aspects of the physics of dust motion in fusion plasmas including dust-plasma, and dust-surface interactions. We consider the physics of dust charging, heating, destruction, spinning, forces acting on dust, dust collision with material walls, etc. The numerical models of these processes have been incorporated into the dust transport code DUSTT, which is capable of tracking of dust particles in 3D geometry (needed plasma parameters can be taken either from edge plasma codes or from experiments). The results of the simulations of dust particle dynamics, transport, and the impact on edge plasma performance will be discussed.

[1] D. H. J. Goodall, *J. Nuclear Materials* **111** & **112** (1982) 11

[2] J. Winter, *PPCF* **46** (2004) B583; **40** (1998) 1201

[3] G. Federici, et al., *Nuclear Fusion* **41** (2001) 1967

[4] S. I. Krasheninnikov, et al., *PoP* **11** (2004) 3141; *PPCF* **47** (2005) A339

[5] J.-Ph. Girard, et. al., *Fusion Engineering and Design*, **82** (2007) 506

[6] A. Yu. Pigarov et al., *PoP* **12** (2005) 122508; R. D. Smirnov et al., *PPCF* **49** (2007) 347

Technology and science of steady state operation in magnetically confined plasmas

A. Bécoulet

Association EURATOM-CEA sur la fusion, DSM/IRFM, Cadarache, France.

The steady-state operation of magnetically confined fusion plasmas is considered as one of the “grand challenges” of the future decades, if not the ultimate goal of the research and development activities towards a new source of energy. Reaching such a goal requires the high-level integration of both the science and technology aspects of magnetic fusion into self-consistent plasma regime(s) in the relevant devices.

On the physics side, the first constraint addresses the magnetic confinement itself which must be made persistent. This means either rely on intrinsically steady-state configurations, like stellarator one, or turn the inductively driven tokamak configuration into a fully non inductive one, through a mix of additional current sources. The low efficiency of the external current drive methods and the necessity to minimize the re-circulating power claim for a current mix strongly weighted by the internal “pressure driven” bootstrap current, itself strongly sensitive to the heat and particle transport properties of the plasma. A virtuous circle then forms as the heat and particle transport properties are themselves sensitive to the current profile conditions. Note that several other players, e.g. plasma rotation profile, magneto-hydro-dynamics activity, ..., also influence the equilibrium state. In the present tokamak devices, several examples of such “advanced tokamak” physics research demonstrate the feasibility of such steady-state regimes, though with a number of open questions still under investigation. The modelling activity also develops very fast in this domain and supports understanding and extrapolation.

This high-level of physics sophistication of the plasma scenario then needs to be combined with steady-state technological constraints. The technology constraints for steady-state operation are basically twofold: the specific technologies required to achieve the steady-state plasma conditions and the generic technologies linked to the long pulse operation of a fusion device. The first ones include specific additional heating and current drive methods (through externally launched waves or fast particles), fuelling and pumping methods, dedicated plasma diagnostics as well as software and middleware technologies used to create the mandatory real time control loops, involving such actuators and sensors. The second class of technologies, generic to any magnetic fusion device, include the superconducting magnet technologies, in order to provide stationary confinement magnetic field, the actively cooled plasma facing components handling either radiated or convected power fluxes (often in excess of several tens of MW/m²), dedicated diagnostics monitoring the interfaces (like infrared survey of plasma facing components), ... The detailed specifications of such elements must comply with reactor relevant parameters, in terms of operational parameters as well as life time.

The paper presents an overall picture of the present status and understanding of the technology and science of the steady state operation in magnetically confined plasmas, as well as the forthcoming work programme dedicated to the vast R&D programme undertaken in this domain, in particular within the European fusion framework.

Magnetic Collimation of Fast Electrons using Structured Targets

A.P.L. Robinson¹, M.Sherlock¹, M.Zepf², S.Kar², P.A.Norreys¹

¹ *Central Laser Facility, STFC Rutherford-Appleton Laboratory, Chilton, United Kingdom*

² *Dept. of Physics and Astronomy, Queen's University Belfast, Belfast, United Kingdom*

The propagation of beams of multi-MeV fast electrons with current densities of the order of 10^{16} Am^{-2} through solid targets irradiated by ultra-intense ($> 10^{18} \text{ Wcm}^{-2}$) lasers is a subject of great interest to many in the ultra-intense laser-plasma community. The collimation or divergence of the fast electron beam, and how this might be controlled, is particularly important for Fast Ignition Inertial Confinement Fusion, x-ray production from solid targets, heating solid targets, and ion acceleration from the rear surface of the target.

Our recent work has focussed on a target engineering approach to controlling collimation (the “structured collimator”) [1]. The basic idea is to use a fibre which surrounded by less resistive material. Since one expects that the electric field required to draw a return current is determined by $\mathbf{E} = -\mathbf{h}\mathbf{j}_{\text{fast}}$, there is a gradient in the electric field at the interface between the two materials. The curl of the electric field is in the correct sense to generate a collimating B-field. Furthermore, simple estimates (using a ‘rigid beam’ model) indicate that the magnetic field should grow fast enough to be able to bend divergent fast electrons back towards the target axis. When this concept is investigated using 2D hybrid Vlasov-Fokker-Planck codes, it is indeed found that strong collimation occurs.

The theory and simulation studies on this concept will be discussed, and different geometries will be considered and compared to initial experimental studies validating the concept.

References

- [1] A.P.L.Robinson and M.Sherlock, *Phys.Plasmas*, **14**, 083105 (2007)

ELECTRON TRANSPORT IN IMPLoded FAST IGNITION TARGETS

J.J. Honrubia¹ and J. Meyer-ter-Vehn²

¹ *GIFI, Universidad Politécnica, Madrid, Spain*

² *Max-Planck-Institut für Quantenoptik, Garching, Germany*

Fast ignition involves transport of GA currents of laser-driven electrons through dense coronal plasma of imploded fusion targets [1, 2]. Recently, we have reported integrated simulations of target ignition by fast electrons by means of a hybrid approach that allowed us to investigate important transport features such as current filamentation and magnetic beam collimation simultaneously with ignition physics [3, 4]. In those simulations, we assumed that the electron kinetic energies are given by the ponderomotive scaling and considered an initial divergence half-angle of 22.5°, consistent with the experiments reported in Ref. [1]. We found minimum ignition energies from 25 to 30 kJ, depending on the distance from the cone tip to the compressed core. Assuming a laser-to-fast electron conversion efficiency of 40%, those energies correspond to laser beam energies from 60 to 75 kJ, of the same order than those envisioned for HiPER [5].

Recent experiments carried out at RAL [6] at laser intensities relevant to fast ignition have evidenced an enhancement of the beam divergence with the laser intensity and electron kinetic energies lower than those predicted by the ponderomotive scaling [7]. We have re-computed the ignition energies of fast electron beams taking into account those experimental results. We have taken divergence angles consistent with the experiments of Ref. [6] and mean energies of fast electrons from 1 to 2 MeV. In addition, we have accounted for the scattering of electrons with the cone tip, typically a gold layer of tens of microns, which may induce a beam divergence comparable with those measured in the experiments. In this talk, we will present a parametric study on fast electron energy deposition and actual ignition of an imploded target configuration for different mean kinetic energies and divergences of the relativistic electrons.

References

- [1] R. Kodama et al., *Nature* **412**, 798 (2001) and *Nature* **418**, 933 (2002).
- [2] R.B. Stephens et al., *Phys. Rev. Lett.* **91**, 185001 (2003).
- [3] J.J. Honrubia and J. Meyer-ter-Vehn, *Nucl. Fusion* **46**, L25 (2006).
- [4] J.J. Honrubia and J. Meyer-ter-Vehn, *IFSA 2007 Proceedings* (2007).
- [5] M. Dunne, *Nature Physics* **2**, 2 (2006).
- [6] J.S. Green et al., *Phys. Rev. Lett.* **100**, 015003 (2008).
- [7] Y. Sentoku et al., *IFSA 2007 Proceedings* (2007).

New Phenomena in Liquid Complex Plasmas

A. Ivlev¹, V. Steinberg², R. Kompaneets¹, H. Thomas¹, G. Morfill¹

¹ *Max-Planck-Institut für extraterrestrische Physik, Garching, Germany*

² *Weizmann Institute of Science, Rehovot, Israel*

Rheology of strongly coupled complex (dusty) plasmas is remarkably diversified and often reveal essential features peculiar to regular complex fluids. We will present a few highlights from recent dedicated experiments where rheology of complex plasmas was investigated under different conditions.

In ground-based experiments with the PK 4 dc discharge setup the flow curves (shear stress vs. shear rate) were measured [1]. Shear flow of microparticles was induced either by inhomogeneous flow of neutral gas, or by using the laser forces. Combination of the two methods allowed us to investigate the entire range of shear rates up to the limit where discreteness enters and complex plasmas cannot be formally considered as a continuous medium. Analysis of experiments suggests that liquid complex plasmas exhibit strong non-Newtonian behavior, which can be accompanied by significant shear thinning (more than an order of magnitude).

Another series of experiments was performed with PK 3 Plus rf discharge setup under microgravity conditions onboard ISS, where “electrorheological plasmas” were discovered [2]. In contrast to conventional electrorheological fluids where the dipoles (induced by external electric fields) are due to polarization of microparticles themselves, in complex plasmas the primary role is played by clouds of compensating plasma charges (mostly, excessive ions) surrounding negatively charged grains. This discovery adds a new dimension to the research of strongly coupled particle systems – in terms of time/space scales and for studying new phenomena.

Also, we briefly discuss a novel and quite general type of the shear flow instability [3] that can occur in complex fluids with density-dependent viscosity. We show that this instability can be easily triggered in shear flow experiments with complex plasmas, and also can explain shear-induced cavitation observed in numerous experiments with regular complex fluids.

References

- [1] A. V. Ivlev *et al.*, *Phys. Rev. Lett.* **98**, 145003 (2007).
- [2] A. V. Ivlev *et al.*, “First Observation of Electrorheological Plasmas”, to be published in *Phys. Rev. Lett.*.
- [3] V. Steinberg *et al.*, “Shear instability in fluids with density dependent viscosity” submitted to *Phys. Rev. Lett.* (2008).

Monolayer complex plasma experiments

V. Nosenko, S. Zhdanov, and G. Morfill

Max-Planck-Institut für extraterrestrische Physik, D-85741 Garching, Germany

A complex (dusty) plasma is a suspension of charged solid particles in a plasma. Typical particle size ranges from tens of nanometers to tens of microns. The particles are either grown *in-situ* or introduced into a plasma of a radio-frequency (rf) or direct current (dc) gas discharge. Usually particles acquire a large negative charge, because they collect more electrons than ions from plasma. Due to the mutual interaction of particles and their confinement by electric fields present in plasma they self-organize in an ordered structure that is called a plasma crystal. In the presence of gravity, a monolayer plasma crystal can be formed. In this two-dimensional (2D) crystal, particles interact through a screened Coulomb (Yukawa) potential and self-organize in a triangular lattice with hexagonal symmetry. A typical interparticle separation is of the order of 0.1-1 mm, characteristic frequencies are of the order of 10-100 s⁻¹, and the speed of sound is of the order of 10 mm/s. In addition, the particle motion is not overdamped. Therefore, the fully resolved dynamics of a 2D plasma crystal can be studied using direct video imaging. This makes 2D plasma crystals an excellent model system to study phase transitions, transport phenomena, and linear and nonlinear waves, all at the kinetic level.

Recently, dislocation nucleation and dynamics were observed in a 2D plasma crystal [1]. Edge dislocations were created in pairs in the lattice locations where the shear stress exceeded a threshold. The shear stress was presumably introduced due to the differential rotation of the lattice with two “rigid” domain walls imbedded in it. After nucleation, dislocations moved apart in the glide plane at a speed of approximately twice the sound speed of shear waves and created shear-wave Mach cones.

Observing dislocation nucleation and dynamics at the level of individual “atoms” and in real time allows us to reveal new details of these complex multi-stage processes. We also discuss laser manipulation as an alternative method of creating dislocations in a plasma crystal in a controllable way.

[1] V. Nosenko, S. Zhdanov, and G. Morfill, Phys. Rev. Lett. **99**, 025002 (2007).

LABORATORY MODELING OF SUPERSONIC RADIATIVE JETS PROPAGATION IN PLASMAS AND THEIR SCALING TO ASTROPHYSICAL CONDITIONS

V.T. Tikhonchuk¹, Ph. Nicolai¹, X. Ribeyre¹, C. Stenz¹, G. Schurtz¹, A. Kasperczuk²,
T. Pisarczyk², L. Juha³, E. Krousky³, K. Masek³, M. Pfeifer³, K. Rohlena³, J. Skala³,
J. Ullschmied⁴, M. Kalal⁵, D. Klir⁵, J. Kravarik⁵, P. Kubes⁵

¹*Centre Lasers Intenses et Applications, Université Bordeaux I-CNRS-CEA, Talence, France*

²*Institute of Plasma Physics and Laser Microfusion, Warsaw, Poland*

³*Institute of Physics AS CR, Prague, Czech Republic*

⁴*Institute of Plasma Physics AS CR, Prague, Czech Republic*

⁵*Czech Technical University in Prague, Prague, Czech Republic*

Laboratory studies can address issues relevant to astrophysics [1] and in some cases improve our understanding of the physical processes that occur in astrophysical objects. The issues related to the jet propagation and collimation over considerable distance and their interactions with surrounding media have begun to be addressed these last years. Laboratory plasmas and astrophysical objects have different length, time and density scales. However, the typical velocities are the same, of a few hundred km/s and the similarity criteria [2] can be applied to scale the laboratory jets to astrophysical conditions. Moreover, by choosing appropriate pairs of colliding plasmas, one can fulfil the scaling conditions for the radiation emission rates.

In this presentation, we use a method of jet formation [3], which allows launching a very fast jet having a velocity ~ 400 km/s and the Mach number ~ 10 by using a relatively small laser energy ~ 100 J. The interaction of these jets with a gas puff has been recently studied in an experiment carried out at the PALS laser facility. Varying gas pressure and composition, we show that the nature of interaction zone changes from a quasi adiabatic outflow to a strongly radiatively cooling jet. The fine scale structures of the interaction zone are studied by means of optical and x-ray diagnostics, and they are interpreted with a semi-analytical model and 2D radiation hydrodynamic simulations.

The conclusions from the laboratory experiment are rescaled to the astrophysical conditions.

References

- [1] B. Remington et al, Rev. Mod. Phys. 78, 755 (2007)
- [2] D. Ryutov et al, Phys. Plasmas 8, 1804 (2001)
- [3] Ph. Nicolai et al, Phys. Plasmas 13, 062701 (2007)

High-Mach Number Collisionless Shock and Photo-ionized Non-LTE Plasmas for Laboratory Astrophysics with Intense Lasers

H. Takabe¹, Y. Sakawa¹, T. Kato¹, Y. Kuramitsu¹, H. Nishimura¹, S. Fujioka¹, M. Koenig²,
N. C. Woolsey³, F. L. Wang⁴, G. Zhao⁴, Y. T. Li⁵ and J. Zhang⁶ and K. Mima¹

¹*Institute of Laser Engineering, Osaka University, Osaka 565-0871, Japan*

²*LULI, Ecole Polytechnique, Palaiseau cedex, 91128, France*

³*Department of Physics, University of York, Heslington, YO10 5DD, UK*

⁴*National Astronomical Observatories, CAS, Beijing 100012, China*

⁵*Institute of Physics, CAS, Beijing 100080, China*

⁶*Shanghai Jiao Tong University, Shanghai 200030, China*

Large scale laser facilities mainly constructed for fusion research can be used to produce high-energy-density plasmas like the interior of stars and planets. They can be also used to reproduce the extreme phenomena of explosion and high Mach number flow in mimic scale in laboratory. With advanced diagnostic technique, we can study the physics of plasma phenomena expected to appear in Universe. The subjects studied so far are reviewed, for example, in [1], [2].

The project to promote the laboratory astrophysics with Gekko XII laser facility at Osaka was initiated from April 1, 2007 as a project of ILE institute. It consists of four sub-projects:

1. Physics of collisionless shock and particle acceleration,
2. Physics of Non LTE (local thermodynamic equilibrium) photo-ionized plasma,
3. Physics of planets and meteor impact,
4. Development of superconducting Terahertz device.

Regarding the first sub-project, we have carried out hydrodynamic and PIC simulation to design the experiments with intense laser. We clarified the physical mechanism of generation of the magnetic field in non-magnetized plasma and the collisionless shock formation caused by the ion orbit modifications by the magnetic fields generated as the result of plasma instability, Weibel instability. Detail simulations have been carried out to see the physics of the generation of magnetic fields.

The Weibel instability which is founded in 1959 in plasma physics region is found to be the main reason for the field generation. It has been studied in laser plasma society in 1970-now in relation to ablation instability to fast ignition. It was common in Astrophysics that in order to explain the collisionless shock, for example, of supernova remnants an external weak magnetic fields are essential, because of the resemblance with the bow shock on the earth driven by the solar wind. The detail of this physics is reported by Dr. T. Kato in case of electron-positron plasma[3] and such usual plasma[4]. In the first sub-project, we aim at the experimental measurement of the generation of the Weibel instability and related plasma dynamics. The experiment of this subject has been carried out as joint experiment with UK and France.

The second topics is researched as joint experiment with China. By use of the X-ray radiation generated inside the gold cavity in irradiating intense laser, we can generate the photo-ionization dominant plasma. Two experiments have been done at Osaka and Shanghai. The experimental data has been analyzed with non-LTE atomic code newly developed. We found that the nitrogen plasma spectrum heated by 80 eV Planckian radiation is highly ionized, while the free electron temperature reached only to 20 eV[5]. We will report the physical mechanism and give notice that this spectrum can also reproduced with assumption of LTE with 60 eV.

[1] H. Takabe, Prog. Theo. Phys. Suppl. No. 143, pp.202-265 (2001).

[2] S. V. Lebedev ed, *High Energy Density Laboratory Astrophysics*, (Springer, 2007).

[3] T. N. Kato, *Astrophysical J.* **668**, 974 (2007)

[4] T. N. Kato and H. Takabe, to be submitted to *Astrophysical J.* (2008)

[5] F. L. Wang et al., to be published in *Physics of Plasmas* (2008)

AUTHOR INDEX

- Abanades A.*, P2.135
Abdulaev S., P1.079
Abgrall R., P2.065
Abramov A., I3.052
Abreu E., P1.138, P1.139
Acedo P., P5.072
Adachi M., P1.148
Adam J.-C., O4.042, P4.139, P5.151
Adamovich X.G., P4.158, P5.137
Adams D., P1.131, P1.134
Adams M., P5.023
Afarideh H., P4.140
Afeyan B., P5.128
Agostini M., I1.017, O4.049, P4.074
Agren O., P2.114, P4.184
Agullo O., O4.028, P1.066, P2.072
Ahn J.W., P2.109
Aiba N., P2.071
Airaj M., P2.112
Airoidi A., P1.113
Aissi A., P5.090
Ait Abderrahmane H., I4.064
Aizawa M., P4.023
Ajendouz A., P1.046, P4.046
Akers A.J., P5.084
Akers R., P1.057, P1.073, P2.018
Akiyama T., P1.056, P2.107
Akli K., O5.061
Albanese R., P2.080, P4.078
Albert F., I1.011
Alberti S., P2.036
Albright B., P4.130
Alcator C-Mod Team, P5.085
Aleksandrov S.E., P2.108
Alekseyev A.G., P4.004
Alexeev N.N., O2.012
Alfier A., O4.034, O4.049, P2.054, P4.005, P5.097
Ali H., P1.012, P2.008
Aliev Yu.M., P5.096
Aliverdiev A., P5.119
Alladio F., I2.029
Allegra L., P1.174
Allen J.E., P2.158, P5.152
Allmaier K., P4.017
Almagri A.F., P2.017, P2.110
Alo E., O2.013
Alonso J.A., P2.028
Alozy E., I2.027
Alper B., O4.034, P1.101
Altukhov A.B., O4.046, P2.087
Ambrosino G., P2.080
Amendt P., D5.001
Amin M., P5.113
Anabitarte E., P2.033
Anan'ev S., P2.137
Anania M.P., P1.148
Anda V., P5.076
Anderson J., P1.033
Anderson J.K., P1.075, P2.110
Anderson K.S., I4.060
André F., P5.090
Andrè M., O4.057
Andreev A.A., P4.128
Andreev N.E., P4.134
Andreev V.F., P4.095
Andrei A., P1.166
Andrejev A.A., P1.126
Andrenucci M., I1.017
Andrew P., O4.033
Andrew Y., I5.073, P4.018, P4.094
Androulakis G.C., P1.122, P2.148, P2.154
Angelino P., I2.023, P1.019, P4.033
Anghel A., P1.168, P1.171
Angioni C., O4.047
Aniel T., P1.022, P1.044
Anikeev A.V., P1.098
Annaratone B.M., P5.136
Annenkov V.I., P2.149
Annou K., P5.161
Ansar Mahmood M., P4.024
Anthony R., I3.051
Antici P., I2.024, O4.042, O4.043, P2.118, P5.113, D5.006
Antipov S.N., P1.160, P1.161, D1.001
Antoni V., I1.017, P1.026
Antonucci A., O5.061
Antonov V.M., P1.142, P1.192
Antonova T., P5.136
Apfelbaum E.M., P1.159
Apicella M.L., P4.004
Apostolaki D., P2.057
Appel L., P2.055, P2.112, P4.064
Applegate D.A., P4.051
Apruzzese G., P4.004
Arad R., O4.055
Aranyi A., P2.070
Arevalo C., P2.135
Argouarch A., P5.088
Arhipenko V.I., P4.188
Arosio M., P2.027
Artaud J.F., I3.046, O2.004, P5.027, P5.068
Arzhannikov A.V., P4.103, P5.098
Ascasibar E., P2.030, P2.113
ASDEX Upgrade Team, I1.004, O4.032, P1.034, P1.101, P2.037, P2.071, P4.011, P4.039

Ashikawa N., P4.101
Asinovskii E.I., D1.001
Askarova A.S., P5.148
Askinazi L.G., P1.080, P2.093, P2.103
Asp E., I5.072, P2.036
Assas S.C., P4.041
Astrelin V.T., P4.103, P5.098
Asunta O., O4.036, P5.001, P5.069
Atanasiu C.V., P4.069
Atherton B., P4.127
Atzeni S., P5.106
Audebert P., I2.024, O4.042, P1.135, P2.118, D5.006
Auriemma F., P4.019
Aushin B.B., P2.108
Austin M.E., P5.099
Avdoshin V.V., P2.136
Avramides K.A., P4.105
Axon K.B., O4.054
Ayushin B.B., P1.109, P2.046, P2.097, P2.104
Azechi H., O4.038
Azizov E., P1.008
Baba M., O3.020
Babi D., P1.164
Babich L.P., O3.027, P1.115, P1.151, P4.181, P5.153
Babichev V.N., P5.171
Bacharis M., P2.158, P5.152
Baciero A., P1.094, P2.090, P2.094
Back C.A., P2.127
Badziak J., O4.043, P1.127, P5.125
Bagryansky P.A., P1.098
Bahamida S., P5.157
Bahloul D., P4.117
Bailescu V., P4.113
Bailly I., I2.027
Baity F.W., P4.097
Bak J.G., P2.084, P4.087, P4.089, P4.096
Bakarezos M., P1.122, P2.148, P2.154
Bakharev P.V., P4.192
Bakhareva O.A., P4.106
Bakshaev Yu., P2.137
Balan N., P4.113
Balan P., P2.025, P2.037
Balat – Pichelin M., P1.014, P1.164
Bamford R., I2.036
Baranov Yu., O2.006
Barengolts S.A., P4.012
Barni R., P2.027
Baronova E.O., P2.148, P2.154
Barrera L., P1.095
Barsukov A.G., P1.109
Bartos P., P2.155
Bartov A., P2.137
Baruzzo M., P2.066
Barz J., I1.012
Basiuk V., I3.046, O2.004, P2.112, P5.027, P5.068
Basko M.M., P2.130
Basner R., P2.165
Bastiani-Ceccotti S., I2.024, P1.135
Batani D., O5.061, P4.129, P5.109, P5.119, P5.123, P5.126
Bateman G., P1.001
Batkin V.I., P4.103
Baton S.D., O5.061, P5.109, P5.112
Bauer D., P5.127
Baylor L.R., O4.054, P2.101, P4.098
Bazylev B., P1.015, P5.011
Becker S., P4.127
Becoulet A., I5.076, O4.035
Beg F.N., P5.114
Behar G., I4.061
Behler K., P4.082
Behn R., P1.072
Beidler C.D., P2.113
Beiersdorfer P., P1.084
Beketov I.M., P1.151
Burenkov I.M., P1.151
Bekhouche M., P4.117
Beklemishev A.D., P1.047, P4.052
Beleites B., P4.137
Bell A., D5.002
Bell M.G., P1.009, P2.109, P4.076
Bell R.E., P1.009, P1.059, P1.108, P2.109, P5.022, P5.060
Bellecci C., P1.170, P1.175
Bellei C., O3.021, O4.040, P4.144, P5.108, P5.116
Belo P., P1.106
Belonohy E., P2.034
Belyaev V.S., P1.120
Belykh V.V., P5.098
Ben Ayed N., I2.020, P1.007, P5.052
Benavides S., P4.136
Bencheriet F., P5.160
Bendoyro R.A., P4.153
Benismail A., P4.132
Benisti D., P2.138, P5.105, P5.112
Benkadda S., O4.028, P1.027, P1.066, P2.045, P2.072, P4.042, P5.059
Benova E., P2.163, P4.081
Benuzzi A., P1.140
Benuzzi-Mounaix A., P5.119
Berardo J., P1.149, P2.150
Berbri A., P1.153
Berger M., P1.103, P2.102
Bergmann K., I4.062
Berk H.L., P5.099
Berkery J.W., P1.059, P4.187
Berry L.A., P1.108
Bertalot L., O2.001, P4.084
Berthelier J.-J., P4.191
Berthier T., I4.061
Bertrand P., P1.040, P1.041, P4.038
Bertschinger G., P4.092
Bessarab A.V., P2.149
Besse N., P1.040, P1.041, P4.038

Betti R., I4.060, P1.059, P2.126, P2.127, P5.102
Beurskens M., O2.006, O4.034
Beurskens M.N.A., P4.005
Beyer P., O4.028, P1.027, P2.045, P2.072
Bhattacharyay R., P5.003
Bialek J.M., P1.059
Biancalani A., P1.051, P1.180, P2.176
Biel W., P4.092, P5.078
Bienkowska B., P2.120
Bierwage A., P5.028
Biewer T.M., P4.018, P4.094
Bignon E., I4.061
Bilato R., P2.099, P4.114, P5.094, P5.095
Bilyková O., P2.098
Bindslev H., P1.034, P2.086, P5.070, P5.077
Bingham R., I2.036, I3.053, I4.066, P1.128, P1.130, P2.141,
P2.186, P4.179, P4.180, P4.185, P5.155
Bint-e-Munir F., P2.005
Birkenmeier B., P4.110
Bitter M.L., P1.084
Bizarro J.P.S., P4.063, P4.065
Blackwell B.D., P2.113
Blancard C., I2.024
Blanchard P., P1.067
Blanchot N., I4.061
Blanco E., P4.050, P5.013
Blazec J., P2.165
Blaževi A., P4.122, P4.127
Blinov P., P2.137
Bobashev S.V., P1.152
Bobkov V., P4.041, P5.005
Bochkarev S.G., P4.121
Bochkov E.I., P4.181
Bódizs D., P5.079
Boedo J., P1.009, P2.003, P2.109
Boerner P., P4.009
Boeuf, J.-P., I4.057, P5.151
Bogatu I.N., P4.056
Bogdanenko A.O., P2.087
Bogdanov T., P2.163
Bogomolov A.V., P2.046
Bohlen H.G., P4.122
Bohley T., P1.140
Bolzonella T., P2.066, P2.067, P5.097
Bombarda F., P1.113, P2.101, P4.073
Bondarenko I., P1.088
Bonfiglio D., O4.029
Bongers W.A., P1.081
Bonheure G., P4.084
Bonhomme G., P1.006, P2.189, P4.049
Bonitz M., P4.156
Bonnin X., P2.007
Bonoli P.T., P1.108, P2.099, P4.111, P4.114, P5.085
Bonomo F., I1.017, P1.075, P2.054, P4.019
Bonville O., P2.117
Boozer A.H., I1.006, I5.070, P4.187, P5.058
Borghesi M., I4.056, P5.113
Borisenko N.G., I2.027, O2.013
Borra J.P., I3.050
Borrielli A., P2.144
Bortolon A., P2.020, P2.036
Boscheron A., P2.117, P5.126
Boswell R., P1.191
Bottino A., I2.023, P1.019, P4.033
Boubault F., I4.061
Boufendi L., I1.014, O2.016, O3.023, P5.135
Bougdira J., P5.138
Bouquet S., I3.054
Bouquey F., P1.058, D4.004
Bourdelle C., O4.050, P1.017, P1.022, P1.044
Bourdon A., P4.161
Bourgade A., P5.150
Bourgeade A., P2.151, P5.150
Bourgeois N., O3.021, P2.118
Boutin J.Y., I2.027
Bowden M., I2.039
Boyarintsev E.L., P1.142, P1.192
Bozhenkov S.A., P1.079, P1.089
Brabrel B., P1.140
Bradford J., I2.036
Brakel R., P2.113
Brambilla M., P2.099, P4.114, P5.094, P5.095
Brambrink E., P1.135, P1.140, P2.187, P5.109
Brandão B., P1.130, P2.141
Braun F., P5.005
Breil J., I2.027, P4.118
Brémond S., P5.088
Brennan D.P., P2.059, P2.060
Brenner P.W., P4.187
Bret A., P5.105
Breyiannis G., P2.038, P5.033
Brezinsek S., I1.005, O4.033
Briguglio S., P5.028, P5.055
Brix M., O2.006, P4.085
Brochard F., P2.189, P4.049, P5.138
Broennimann Ch., P1.084
Brok W., I2.039
Brooks A., P5.058
Brooks N.H., P4.003
Brower D.L., P2.017
Brown C.R.D., P4.131
Browning P.K., P4.007
Bruedgam M., O4.030
Brunetti E., P1.150
Brunsell P., P1.071, P2.056, P4.075
Brygoo S., I2.027
Brzozowski J., P4.115
Budaev V.P., P4.166, P5.019
Budny R.V., P5.022, P5.099
Buechner J., P5.168
Bugrov S., O3.026
Bulanin V.V., P2.093

Bulir J., P5.142
Buratti P., O2.006, P1.069, P4.062
Burcea G., P4.113
Burchenko P.Ya., P1.061
Burdakov A.V., P1.112, P4.103, P5.098
Burenkov O.M., P2.136
Bürger A., P1.081
Burhenn R., P2.113
Burke D.R., P2.110
Burmasov V.S., P4.103, P5.098
Burrell K.H., P5.022
Burza M., P4.134
Bush C., P1.009
Bustos A., P5.135
Butikova J., P2.010
Buyko A.M., P1.115, P1.116
Buzhinskij O., P1.008
Bychenkov V.Yu., P4.121, P4.135
Bychkov V., P2.123
Byhring H.S., P1.191
Cairns R.A., I3.053, P1.128, P2.186, P4.179, P4.185
Calabrò G., O2.006, P2.106, P5.055
Caldas I.L., P1.024
Califano F., P1.176, P2.184
Calvo I., P1.031, P2.043, P4.020
Campbell D., P1.109, P5.087
Camplani M., P4.070
Canal P., P2.117
Canaud B., P2.122
Candy J., P1.017, P1.044
Cang Y., P2.132
Canik J., P2.013
Cannas B., P4.070
Cantarini J., P5.078
Canton A., O4.029, P4.019, P4.074, D1.002
Cao J.Y., P5.086, D2.005
Cao Z., P5.086, D2.003, D2.005
Cappa A., P1.094, P1.107, P5.018
Cappello S., P4.074, P5.035
Carati D., P2.044
Caravelli G., P2.081
Carbone V., O4.057, P1.026
Cardinali A., P2.106, P5.055
Caridi F., P2.144
Carpeggiani P., P5.109, P5.123
Carralero D., O4.048, P2.028
Carraro L., O4.029, P2.026, P4.019, P5.097
Carreras B.A., O4.048, P1.031, P1.042, P2.029, P2.043, P2.053, P4.020
Carrere M., P1.002
Carroll D.C., P5.103, P5.108, P1.134
Cartry G., P1.002
Carvalho P.J., P1.065
Casanova M., I2.027, O2.013, P2.153
Casati A., P1.017, P1.044
Casner A., I2.027, P2.117, P5.126
Caspary K., P1.075
Casper T.A., P2.073, P2.079
Cassart B., P2.044
Casse F., I2.030
Cassou K., P1.132, P1.141, P4.134
Castaldo C., I4.063, P2.106
Castaldo R., O2.006
Castejón F., P1.025, P1.035, P1.095, P1.107, P2.030, P2.113, P5.018, P5.135
Castellanos O.F., P2.033
Castro E., P4.059, P4.167, P5.042
Catto P.J., P4.034
Caturla M.J., P2.135
Caughman J.B.O., P2.101
Caumes J.P., P1.132
Cavallaro S., P4.154
Cavazzana R., I1.017, O4.029, O4.049, D1.002
Ceccherini F., P2.176
Cecconello M., P1.071, P2.056
Ceccotti T., I1.008
Cédric T., I1.010
Celestin S., P4.161
Celona L., P1.174
Cenacchi G., P1.113
Cercek M., P2.166, P2.181
Cerfon A.J., P4.053
Cesario R., O2.006, P2.106
Chakraborty-Thakur S., P1.166
Challis C.D., I2.021, O2.006, P1.069, P1.073
Chambers D.M., P2.129
Chance M.S., P4.055
Chandra D., P1.066
Chang C.S., P1.001, P5.029
Chapman B.E., P1.075
Chapman I., P5.062
Chappuis C., I4.061
Charboneau-Lefort M., P5.128
Charles C., P1.191
Charrier J.F., P2.117
Chaschin M.S., P4.052
Chatzakis J., P1.122, P2.148, P2.154
Chatziantonaki I., P5.093
Chebotarev V.V., P2.170
Chen Guanglong, P1.121
Chen J.B., D2.003
Chen L., I1.001, P1.051, P5.028, P5.056
Chen M., P5.124, D2.003
Chen M.X., P4.112
Chen Z., P4.139
Chenais-Popovics C., I2.027
Cheng J., P2.014
Cheng L.Y., P5.086, D2.005
Cheon J.K., P2.084, P4.087, P4.089
Cherigier-Kovacic L., P1.186
Chernenko A., P2.137

Chernyshev F.V., P1.080, P1.109, P2.046, P2.097, P2.103, P5.081
Chernyshev V.K., P1.115, P1.116, P1.151, P2.136
Chernyshova M., P2.120
Chiavassa G., P5.008
Chmyga A., P1.088
Cho M.H., P4.175
Choi S.W., O3.024
Chowdhuri M.B., P2.082
Chrisman B., P5.117
Christ-Koch S., P2.102
Chu M.S., P4.055, P4.056, P4.083, P5.028
Chudin N.V., P1.045
Chudnovskiy A.N., P1.068
Chung H., I2.025
Chung K.-S., P4.090, P4.091
Chuyanov V.A., P1.109
Ciavola G., P1.174
Ciobanu S.S., P5.144
Cipiccia S., P1.144
Cirant S., P2.026, P4.082
Ciraolo G., P1.020, P5.008
Citrin J., O4.055
Claire N., P4.046, P5.169
Clairat F., P1.017, P1.022, P1.044, P1.106, P5.088
Clark D., D5.001
Clark E.L., P1.122, P2.148, P2.154, P4.131
Clark R.J., P5.108
Clarke R.J., O4.040, P5.113, P5.116
Classen I., P1.090
Clayton C., P2.150, P4.153
Clever M., P4.016
Coad P., O4.033, P4.113
Coda S., P1.099, P5.062
Coddet C., P5.146
Coelho R., P1.065
Coenen J.W., P4.016
Coïc H., I4.061
Colas L., P5.088
Cole A., O4.035
Combis P., I2.024, P4.141
Combs S.K., P2.101, P4.098
Conde L., P5.165
Connor J.W., P4.051
Conway G., I3.040, O4.032, P4.041
Conway N.J., P2.018, P2.088
Cooper W.A., P4.061
Coppa G., P4.147
Coppi B., P1.113, P1.177, P2.023, P2.101, P4.027, P4.073, P5.154
Coppins M., P2.158, P5.152
Corde S., I1.011
Corrigan G., P1.106, P5.053, D1.003
Cossé P., I2.024
Coster D., P2.007, P2.112, P4.003, P5.027
Costin C., P4.093
Costley A., O2.001
Couëdel L., O2.016, O3.023, P5.135
Counsell G., I2.020, P1.007, P2.048, P4.035, P5.152
Courtois C., I2.027, O2.010, P2.129
Cowan J.S., P4.142
Cowan T.E., P4.119, P4.142
Cox W.A., P2.110
Crabtree C., P2.023
Craig D., P1.075
Cramer N.F., P2.160
Criado A.R., P5.072
Crisanti F., P5.055
Crocker N.A., P5.060
Crombe K., I5.073, P4.018, P4.094
Cros B., P4.134
Cross A.W., I3.053, P2.186, P4.179
Cui Z., P5.026
Cunningham G., P1.073, P4.066, P5.084
Cupido L., O4.032, P4.050, P5.013
Curchod L., P1.099
Czarnecka A., P1.127, P4.123
Czifrus Sz., P5.079
D'Humières E., P4.119
D'Oliveira P., I1.008
D'yachkov L.G., P1.160, P1.161
Da Graca S., O4.030, O4.032
Dal Bello S., D1.002
Damiens-Dupont C., I4.061
Dangor A.E., O3.021, O4.040, P4.144, P5.108, P5.116
Danko S., P2.137
Dannert T., I2.023
Darbon S., I2.027
Darbos C., P1.058, D4.004
Darrow D., P5.060
Dasgupta B., O4.059
Daughton W., P4.130
Davidson R.C., P2.139
Davies J.A., I4.066
Davies J.R., P5.106, P5.120
Davoine X., P5.130
D'Azevedo E.A., P2.058
De Andrea González A., D2.002
De Angelis R., O2.006
De Baar M., P1.081
De Blank H.J., P4.009
De Gevigney B.D., P4.187
De la Cal E., P2.028
De la Fe J.M.G., P2.183
De la Luna E., I5.073, P1.095, P2.030, P5.074
De Loos M.J., P1.148
De Pablos J.L., P2.028
De Vries P., I2.021, P4.018
Debbache D., P4.117
DeBoo J.C., I2.021, P2.073
Decker J., I3.046, P1.097, P1.099, P2.098, P4.062
Decyk V., P1.042

DeGrassie J.S., P5.022
DeGrassie V., O2.005
Dejarnac R., P4.081
Delabie E., P4.092, P5.063
Delahaye F., O3.025
Del-Castillo-Negrete D., P4.042
Delettrez J.A., I4.060, P2.127
Delgado J.M., P2.047
DelRio E., P2.135
Demidov V.S., P2.145
Demidova E.V., P2.145
Den Hartog D.J., P1.075
Dendy R., I2.020, P2.048
Deng W., P5.101
Denner P.J., P4.064
Depierreux S., I2.027, O2.013
Desai S.S., P4.089
Desai T., P4.129
Deschaseaux G., I4.061
Desgranges C., P5.088
Deshko G., P1.088
Detragiache P., P1.113
Devoy P., P4.007
DeVries P.C., O2.006, P4.022
Dewhurst J.M., P2.048
Dezairi A., P1.046
Dezulian R., P5.119
Di Piazza A., I3.049
Di Troia C., P5.055
Diaconu C., P1.166
Diallo A., I4.065, P1.184
Diamond P., I2.028, P5.016, P5.158
Dias F.M., P4.081
Dias J.M., P1.149, P2.150
Diaz D., P2.135
Dieckmann M.E., O5.067, .174, P4.182
Dif-Pradalier G., P1.017, P4.033
DIII-D Team, P2.071
Dinescu G., P1.167, P2.167
Ding B.J., P4.102
Ding W.X., P2.017
Ding X., P5.026
Ding X.T., D5.003
Di-Nicola P., I2.027, O2.013
Dinklage A., P2.113
Dinuta G., P4.113
Djebli M., P5.160
Djeridane Y., I3.052
Doerner R. P., P2.004
Dokouka V., O2.004
Dokuka V., P4.066
Dolgachev G.I., P2.134
Dolin V., P1.151
Dolin Yu.N., P2.136
Domier C.W., P1.090
Dong J.Q., P2.014, D5.003

Donin A.S., P1.098
Donné A.J.H., P1.090
Donoso J.M., O2.017, P5.165
Donsko Á.N., O3.027
Donskoi Á.N., P5.153
Dorchies F., P1.135, P5.109
Doron R., O4.055
Douglas J., P1.023
Doveil F., P1.186, P5.090, P5.169
Dowling J., O4.054
Doyle E.J., P2.073
Drake J.R., P2.056
Dréan V., O5.060, P2.124, P2.126
Drenik A., P1.014, P1.166
Dromey B., P1.131, P1.134, P5.108
Drouin M., P4.141, P5.112
Drozdovskii A.A., P2.130
Drury L.O.C., O5.067
Duan X., P5.026
Duan X.R., D5.003
Duarte P., P1.021, P5.075
Dubrouil A., P5.109
Dubuit N., P5.151
Duday P.V., P1.151, P2.136
Dudin S.V., P2.145
Dudin V.I., P1.151, P2.136, P5.006
Dudson B., I2.020, P1.007, P2.048
Dumbrajs O., P1.062, P4.047, P4.105
Dumont R., P1.058, P2.042, P2.100
Dumortier P., P1.104, P4.107
Dunai D., O4.031, P5.076
Dunlop M.W., I4.066
Dupuis C., I1.014
Durut F., I2.027
Duval A., I2.027
Duval B.P., P2.020, P2.036
Dux R., P2.083, P4.011, P4.039
Dyachenko V.V., P2.087, P2.097
Easter J., P5.107
Ebrahimi F., P1.075, P2.017
Edlund E.M., P5.100
EFDA-JET contributors, P4.084
Egorychev B.T., P2.131
Ehsan Z., P5.167
Eich T., P2.012
Eikenberry E.F., P1.084
Ekedahl A., P5.088
Elbaz D., P2.122
Elbeze D., P4.062
Elkin B., I1.012
Elkina N., P5.168
El-Taibany W.F., P4.164
Endler M., P1.043, P5.078
Endo T., P1.140
Endstrasser N., P5.007
Ennis D.A., P1.075

Eremin D.Yu., P5.051
Erents S.K., O4.034
Eriksson A., P1.048
Eriksson L.E., P2.123
Eriksson L.-G., P1.022, P1.058, P1.087, P2.042, P2.100, P2.112, P4.041, P4.115, P5.027, P5.054, P5.062
Ersfeld B., P1.137, P1.150, P4.151
Escande D., I2.034
Escarguel A., P4.046
Esipov L.A., O4.046, P2.087, P4.043
Es-sebbar Et., P2.169
Estrada T., P1.025, P2.030, P2.113, P4.050, P5.013
Ethier S., P5.023
Evans R.G., O5.061, P5.118
Evans T.E., I5.070P2.003, P2.009, P4.097, P4.098
Faganello M., P1.176
Fahrbach H.-U., P1.055
Faivre G., P1.132
Fajardo M., I2.025, P1.132, P1.138, P1.141
Fajardo R.M., P2.125
Falchetto G., I2.023, P1.017, P1.022, P1.044
Falize E., I3.054
Falter H.-D., P1.103
Fang F., P4.153
Fanni A., P4.070
Fantz U., P1.103, P2.102
Farengo R., P2.115, P5.049
Farina D., P5.074
Farokhi B., P4.165
Fasoli A., I4.065, P1.067, P1.184, P2.182, P5.083
Fassina A., O4.049, P4.019
Faure J., P4.132, P5.130
Faussurier G., I2.024
FBX team, P4.100, P5.082
Fedotkin A.S., P2.134
Fehér T., P4.077
Fehske H., P4.156
Fendrych F., P1.162
Feng B.B., P5.101, P5.026, D5.003
Feng J.Q., P4.102
Feng K., P5.086, D2.005
Feng Y., P2.009, P2.013, P2.085, P2.113
Fenstermacher M.E., P2.009, P4.098
Fenzi C., P1.006, P1.022
Fenzi-Bonizec C., P1.044
Fernandes H., P1.021, P1.065, P2.040, P5.075
Fernández A., P1.094, P5.018
Fernandez J.C., P4.130, P4.119, P4.142
Fernández L.A., P5.135
Ferrari H., P2.115
Ferron J.R., O2.006, P2.073, P2.079
Fertman A.D., P2.145
Fesenyuk O.P., P4.072
Fessey J., P5.074
Feugeas J.L., I2.027, P2.126
Fichtner H., P5.156
Field A.R., O4.031, P2.018
Figini L., P1.095, P5.074
Figueira G., P1.149
Figueiredo H., P1.021, P2.025
Fiksel G., P1.075, P2.017
Filinov A.V., P4.156
Filinov V.S., P4.156
Filippov A.V., P5.171
Filler A., O4.055
Finken K.H., O4.052, P1.079, P1.089, P4.016
Finkenthal M., P2.081
Finnegan S.M., P1.190
Fischer R., O2.002, P4.010
Fisher R., O4.032
Fitour R., I1.011, P4.132
Fiuza F., P1.149, P4.150, P5.120
Flacco A., P4.129, P4.141
Fletcher L., P4.037
Flippo K.A., P4.119, P4.130, P4.127, P4.142
Florido R., O2.011, P2.147
Foerster E., O5.061, P2.129
Foest R., P4.173
Fogaccia G., P5.055
Földes I.B., O2.014
Fonseca R.A., I2.036, I3.048, P4.143, P4.148, P4.150, P4.155, P4.180, P5.120
Fontanesi M., P2.027
Foord M.E., I2.025
Forest C.B., P2.110
Fortov V.E., I2.033, O2.007, P1.160, P1.161, P1.187, P2.145, P2.162, P4.156, P4.158, P5.137, P5.139, P5.162, P5.166, P5.171, D1.001
Foster A., D1.003
Foster P.S., P1.131, P1.134
Fourment C., I2.027, P5.109, P5.126
Foust C., P2.101
Frank A., O3.026, P2.188, P4.122
Frantzeskakis D., P4.162
Franz P., I1.017, P1.075
Franzen P., P1.103, P2.102
Frassinetti L., P1.071, P2.056
Frattolillo A., P2.101
Fredrickson E.D., P4.058, P5.060
Fredriksen A., P1.191
Freidberg J.P., P4.053
Frenje J.A., I4.060, P2.127
Frerichs H.G., P2.009, P4.016
Frigione D., P1.101, P4.099, P4.104
Fröschle M., P1.103, P2.102
Fruchtman A., O5.065
FTU team, P2.026
Fu G., P5.050, P5.099
Fu S., D5.004
Fuchs J., I2.024, O4.033, O4.042, O4.043, P2.012, P2.118, P5.113, D5.006
Fuchs M., P4.143, P4.146

Fuchs V., P2.015, P2.096, P2.098
Fuentes C., P1.094
Fuhr G., P1.027, P2.045
Fujieda H., P2.075
Fujimoto Y., O4.038
Fujioka S., I5.082, O4.038, P5.126
Fujisawa A., P2.113, P4.044, P5.158
Fukao M., P5.158
Fukumasa O., P5.147
Fukuyama A., P1.049
Fülöp T., P1.032, P2.042, P4.077
Fulop T., P2.078
Funaba H., I2.022, P1.054, P2.113
Fundamenski W., O4.033, P4.005, P5.053
Furno I., I4.065, P1.184, P2.182
Furtula V., P2.086, P5.070
Fussmann G., P5.002
Futatani S., P4.042
Gabellieri L., P2.026
Gaillard S.A., P4.119, P4.142
Gaio E., P4.075
Gál K., P1.101, P1.109, P4.077
Galca A.C., P1.166
Galeotti L., P2.184
Gallacher J.G., P1.149
Gambino N., P1.174, P2.142
Gamez B., P2.135
Gámez L., P2.135
Gammino S., P1.174, P2.142, P2.144
Ganeev R.A., O3.020
Gans T., I2.038
Gao W., P5.146
Gao X., P4.102
Gao Y., D2.001, D5.003
Garanin S.F., P1.115, P1.116
Garanin S.G., P2.149
Garavaglia S., P5.074
Garbet X., O4.028, O4.050, P1.017, P1.020, P1.022,
P1.027, P1.066, P2.045, P4.033, P4.062, P5.008
García C., O5.062
García G., P1.094
García J., I3.046, P5.018
García L., P2.043, P4.020
García-Fernández C., P1.141, P2.133
García-Martínez P.L., P5.049
García-Muñoz M., O4.030, P1.055, P1.094
García-Regaña J.M., P1.107
Gargate L., I2.036, P4.180
Garkusha I.E., P2.170
Garofalo A.M., O4.035, P4.055, P4.056, P5.022
Garrigues L., P5.151
Gary S., I2.027
Garzotti L., O4.054, P1.048, P4.099, P4.104
Gates D.A., I5.070, P1.009, P1.059, P2.109
Gaudio P., P1.170, P1.175
Gautheron Y., I4.061
Gauthier E., P1.006
Gauthier J.C., I2.027, P1.132
Gautier C., P4.130
Gautier D.C., P4.119, P4.142
Gavrikov A.V., P1.187, P5.162, P5.171
Geiger J., P2.051, P2.062, P2.113
Geindre J.-P., I1.010, I2.024
Geissel M., P1.134, P1.135, P1.145, P4.127
Geissler M., O3.019, O4.039, P1.131, P4.136, P4.143
Gemisic-Adamov M., P2.001, P4.002
Genoud G., P4.134
Gerbaud T., P1.006, P1.017, P1.044
Gerhardt S.P., I5.070
Gericke D., I1.016, P2.152
Ghendrih Ph., P1.020, P4.033, P5.008
Gherardi N., P2.169
Ghezal A., P4.117
Ghoranneviss M., P1.069
Giannone L., P2.012, P4.082
Gibert P., I4.061
Gibson K.J., I2.036
Gil J.M., O2.011, P2.147
Gillespie K.M., I3.053, P2.186, P4.179, P4.185
Gimblett C.G., P4.007
Giovannozzi E., I4.063, O2.006, O4.034, P4.005
Girling M.T., P4.131
Giroud C., O2.006, P4.018, P4.022
Giruzzi G., I3.046, P1.058, P5.068, D4.004
Giulietti A., O5.061
Giulietti D., O5.061
Gizzi L.A., O5.061
Glebov V.Yu., I4.060
Globus-M Team, P2.046
Glowacz S., P5.027
Glushkov A.V., P1.128, P2.175
Glybin A.M., P2.136
Gobbin M., P2.054, P5.035
Godyak V., P1.183
Goedheer W., I2.032, P4.009
Goetz J.A., P2.110
Gohil P., O2.005
Golant V.E., P1.080, P2.103
Goldman M.V., O4.058
Golikov A.A., P4.108
Golish V.I., P1.010
Goloborod'ko V., P1.087
Golubev A.A., P2.130, P2.145
Golyatina R.I., P4.159
Goncharov A., P2.172
Goncharov V.N., I4.060
Gondhalekar A., P1.093
Goniche M., P1.106, P4.062
Gonzalez C., P1.117
González M., O5.062, P1.117, P2.133
Goodman J., O5.066
Goodman T.P., I5.072

Gopal A., O3.021, P1.122, P2.148, P2.154
Goranskaya D.N., P5.162
Gorbachev Yu.N., P1.116
Gorbunov Ya.V., P5.004
Gorelenkov N.N., P5.060, P5.099
Gori S., P1.065
Goshu S., P1.085
Goto M., P2.082, P2.095
Graffagnino V., P2.186
Grandgirard V., I2.023, P1.017, P4.033, P5.008
Granja C., P1.126
Granstedt E.M., P4.058
Granucci G., P2.026
Grasso D., P2.116, P2.179, P5.054
Graswinckel M.F., P1.081
Grauer R., P5.156
Graves J.P., P4.061, P5.062
Gravier E., P1.040, P1.041, P4.038
Gray T., P1.009
Grebenshchikov S.E., P5.071
Grech M., I2.027, O2.013, P2.118, P2.140
Green J.S., O5.061, P5.108
Greenwald M., P1.074
Gregory C., I3.054, P1.140, P2.129, P2.187
Gremillet L., P2.138, P4.141, P5.105, P5.112
Grésillon D.M., P4.086, P4.189
Gribov Y.V., P2.074
Grinenko A., P2.152
Grinevich B.E., P1.116
Grismayer T., P2.118, P4.139
Groebner R.J., P2.024, P2.073
Grossetti G., P5.074
Groth M., P4.003
Gruber O., I3.042, O2.003
Grüner F., P4.127, P4.143, P4.146
Gryaznevich M., I3.044, O2.006, P1.069, P2.040, P4.064
Gu M.-F., P1.084
Gu Y., D5.004
Guasp J., P1.094, P2.049
Gubarev S.P., P1.061
Gubskii K.L., P2.130
Guenter S., I1.004, O4.030, P2.071
Guillbaud O., P1.132
Guillerminet B., P2.112
Guimaraes-Filho Z.O., P1.024
Guimaraes L., P4.050
Guirlet R., O4.050
Gumbrell E.T., P4.131
Gunn A.G., P2.186
Gunn J.P., P2.015, P1.006, P5.088
Günter S., P1.055, P1.077, P1.078, P2.064
Günther M., P4.122
Guo S.C., P5.035
Gupta A., P1.011
Gurcan O.D., P5.016
Gurchenko A.D., O4.046
Gurl C., O4.054
Gurnitskaya E.P., P2.175
Gusakov E.Z., O4.046, P1.082, P1.096, P2.089, P4.086, P4.188
Gusein-zade N.G., P2.161
Gusev V.K., P1.109, P2.046, P2.097, P2.104, P2.108
Gushenets V., P2.171
Gutierrez-Tapia C., P1.021
Gutser R., P2.102
Gyergyek T., P2.166, P2.181
Haass M., P2.165
Habara H., P5.111
Habs D., O4.039, P4.127, P4.130, P4.136, P4.143, P4.146
Hagelaar G.J.M., P5.151
Hagl T., O2.007
Hagnestål A., P4.184
Hahn T.S., P5.016, P5.023
Hahn M.S., P4.187
Haines M.G., P5.107, P5.114
Hajakbari F., P1.069
Hajdu J., P1.139
Hall I.M., P2.129
Hallatschek K., P1.036
Hallo L., O5.060, P2.151, P5.150
Halpern F., P1.001
Handley R., P4.113
Hansen A., P1.166
Hansen F., I3.055
Hapgood M., I2.036
Happel T., P4.050, P5.013
Hardin R.A., P1.166, P5.143
Harhausen J., P4.003
Harmand M., P1.135
Harres K., P4.119, P4.122, P4.127, P4.142
Harris J.H., P2.113
Hartfuß H.-J., P5.078
Harting D., P2.009
Hartmann O., I4.061
Harvey R.W., P1.108, P4.111
Harvey Z., P1.166
Hassan S.M., P1.122, P2.148, P2.154
Hassanein A., P2.170
Hastie R.J., P2.116
Hatsagortsyan K.Z., I3.049
Haupt M., I1.012
Havlicek J., P4.080
Havlickova E., P2.155
Hawkes N.C., I5.073, P4.018, P4.085, P4.094
He J., D5.004
He W., I3.053
Heathcote R., O3.021, O4.040, P5.116
Hébert D., P5.150
Hegelich B.M., P4.119, P4.130, P4.142
Hegelich M., P4.127
Heidbrink W.W., P5.028, P5.060, P5.099
Heidinger R., P1.081
Heikkinen J.A., P4.045, P4.047, P5.015, P5.036

Heinemann B., P1.103, P2.102
Helander P., P1.032, P2.078, P2.116, P4.077
Hellsten T., P4.115, P5.014
Hender T.C., O2.006, P1.069, P4.066
Henderson M.A., P5.087
Henig A., O4.039, P4.130, P5.108, P5.116
Hennen B.A., P1.081
Hennequin P., P1.017, P1.020, P1.022, P1.044, P4.021
Henry O., I2.027, P2.117
Herman Z., P5.007
Héron A., O4.042, P4.139, P5.151
Herranz J., P5.018
Herreras Y., P2.135
Herrmann A., P2.010, P2.012, P2.037, P4.075
Herrmann D., P4.136
Hervé A., I2.027
Hervé G., I1.010
Heßling T., P4.122
Heuraux S., P1.044, P1.082, P1.096, P2.089, P4.021
Heyn M.F., P5.009
Hicks N.K., O4.030, P4.082
Hidalgo C., O4.048, P1.021, P2.021, P2.028, P2.113, P5.013
Hidding B., P4.136
Hildebrandt D., P5.078
Hill K.W., P1.084
Hillis D.L., P4.094
Himura H., P4.067, P4.068
Hirsch M., P2.034, P5.078
Hirshman S.P., P2.058, P4.061
Hizanidis K., O4.051, P2.045, P2.185
HL-2A team, D5.003
Hnat B., I2.020, P2.048
Ho D., D5.001
Hoarty D.J., P4.131
Hobirk J., I2.021
Hobrik J., O2.003
Hoekzema J.A., P1.081
Hoffmann D.H.H., P4.122
Hogeweyj G.M.D., O2.003, P5.034
Höhnle H., P4.110
Hojabri A., P1.069
Hojo H., P1.085
HoKim G., P4.174
Holcomb C.T., P2.073
Hollmann E.M., P2.004, P2.003
Holmström K., P4.115
Holzhauer E., P4.110
Hölzl M., P2.064
Homer P., I2.025
Homma H., O4.038
Hong M.P., O3.024
Hong W., P5.026
Hong W.Y., P2.014
Honrubia J., I5.078, P5.125
Hooker S.M., P4.143, P4.146
Horacek J., P4.080
Hörlein R., O4.039, P1.131, P1.134, P1.145, P4.143, P4.146
Horton L.D., O2.003, P2.024, P2.071, P2.083
Hosea J.C., P1.108, P4.097
Hou B., P5.107
Houlberg W., P1.109
Howe J., I3.054, P2.129
Howell D., O2.006
Hrach R., P2.155
Hrachova V., P2.155
Hristov V., P1.028
Hu B., P1.059
Hua M-D., P2.018, P4.022
Huang X., D5.004
Huang Y., P5.026
Huart R., P2.065
Hubbard A., P1.074
Hubbard A.E., O4.034, P1.005, P4.111
Huber A., O4.033
Huber P., P2.162
Hueller S., O4.042
Hughes D., I2.031
Hughes J.W., O4.034, P1.005, P1.074
Hugon R., P5.138
Hugonnot E., I4.061
Hulin S., I2.027, P5.109
Hüller S., O2.013
Humphreys D.A., P2.073, P2.079, P2.003
Huser G., I2.027, O2.010, P2.117
Huysmans G.T.A., O4.035, P2.052, P2.065, P2.112, P5.027
Hyatt A.W., P2.073
Hynönen V., O4.036, P5.001
HyunCho J., P4.174
Ibañez L.F., P5.122
Ichiguchi K., P2.053
Ida K., I2.022, P1.054, P1.056, P2.113
Ide S., I1.007
Ido T., P1.054
Igami H., P4.101
Igitkhanov Y., P1.015, P5.011
Ignatov A.M., P1.157
Igochine V., O4.030, P1.055, P1.062, P2.066, P2.070
Ikeda R., P2.107
Ikezoe R., P4.067, P4.068
Il'kaev R.I., P5.153
Ilgisonis V.I., P1.053
Imai N., P1.085
Imai T., P1.085
Imbeaux F., I3.046, O2.003, O4.050, P1.017, P1.022, P1.044, P2.112, P5.027, P5.034
In Y., P4.055, P4.056
Inagaki S., P1.054, P4.044, P5.017, P5.158
Ince-Cushman A.C., I4.058, P1.084, P4.111
Innocente P., P4.019, P4.074, P5.097, P5.126, D1.002
Ionita C., P2.025, P2.037, P2.177, P4.093
Ionita E.R., P2.167

Ionita M.D., P2.167
Iosseliani D.D., P2.130
Iraji D., P1.184
Irie M., P4.100, P5.082
Irzak M.A., P1.080
Isaev N.V., P5.145
Isayama A., P2.067, P2.092
Ishida A., P5.048
Islam M.R., P4.151
Isliker H., P1.027, P1.029, P2.041, P2.045
Isobe M., O4.038, P1.054, P1.056, P2.107
Issac R.C., P1.149
Itakura A., P1.085
Itoh K., P5.059, P5.158
Itoh S.-I., P4.044, P5.059, P5.158
Itoh V., P4.044
Ivanov A.A., P1.072, P1.098, P1.112, P2.069
Ivanov A.I., O2.007
Ivanov A.S., P5.162
Ivanov I.A., P4.103, P5.098
Ivanov I.B., P5.009
Ivanov N.V., P1.068
Ivanov V.À., P1.151, P2.136
Ivanova D.M., P4.106
Ivanova P., P4.081
Ivanova-Stanik I.M., P2.120
Ivanovskiy A.V., P1.115, P1.116, P1.151, P2.131, P2.136
Ivantsivsky M.V., P4.103, P5.098
Ivlev A.V., I5.079, O2.007, P1.154, P2.162, P5.139
Iwamoto A., O4.038
Izgorodin V.M., P2.149
Jablonski S., O4.043, P5.125
Jachmich S., O4.033, O4.052, P4.013
Jäckel O., P4.137
Jackson G.L., P2.073, P2.079, P4.055, P4.056, P5.022
Jadaud J.P., I2.027
Jaeger E.F., P1.108
Jaeger S., P4.046
Jafer R., P5.103
Jakubowski L., P5.075
Jakubowski M.W., O4.052, P1.079, P1.089, P2.016, P4.013, P4.016
James A., P2.003
James B.W., O2.016
James M., P4.051
Janeschitz G., P1.015, P4.079, P5.011, P5.057
Janhunnen S., I2.023, P4.045, P4.047, P5.015, P5.036
Janvier M., P4.022
Jarboe T.R., P4.076
Jaroszynski D.A., I1.009, P1.137, P1.144, P1.147, P1.149, P1.150, P4.151
Jaspers R., P1.079, P1.090, P4.092
Jenko F., I2.023, P1.038
Jentschura U.D., I3.049
Jequier F., I2.027
Jernigan T.C., P2.003, P4.098
JET EFDA contributors, I1.005, I2.018, I2.021, I3.044, I4.059, I5.073, P1.067, P1.069, P1.093, P1.101, P4.094, P5.029, P5.083
Ji X.Q., P5.101
Jiang S.E., P2.121, D2.003
Jiang S.F., D2.005, P5.086
Jiang T., P5.086, D2.005
Jie Y.X., P4.102
Jiménez-Gómez R., P1.094
Jimenez-Rey D., P1.094, P2.090, P2.094
Jitsuno T., O4.038
Joffrin E., I2.021, O2.006, P1.069
Johnson E.V., I3.052
Johnson M.F., P4.022
Johnson R., P4.130
Johnson R.P., P4.119
Johnson T., O4.036, P1.093, P4.115, P5.001, P5.014, P5.029, P5.062
Johzaki T., O4.038, O4.045, P4.120, P5.117, P5.121
Jolliet S., I2.023, P1.019, P4.033
Joseph I., P2.009
Joshi C., O4.040
JT-60 team, I1.007
Jucker M., P5.041
Juha L., I5.081, P1.126, P2.120
Jung M., P4.175
Jungwirth K., P4.133
Juul Rasmussen J., P2.025
Ka E.M., P4.096
Kadomtsev M.B., P1.003, P1.004
Kaempfer T., O5.061
Kagan G., P4.034
Kaganovich I.D., O4.044, P2.139, P5.149
Kai T., P5.126
Kaita R., P1.009, P2.081, P2.109
Kakurin A.M., P1.068
Kalal M., I5.081, P1.117, P1.118
Kalhoff T., P2.021
Kaliakatsos J., P1.122
Kalinin Yu., P2.137
Kalinina D., P4.106
Kalinowska Z., P2.120
Kallenbach A., P4.003, P4.010, P4.011, P4.039
Kallman J., P1.009
Kalupin D., P2.112, P4.048, P5.027
Kaluza M., O4.040, P4.137, P5.108, P5.116
Kalvin S., P2.070, P2.111
Kamada Y., P2.068
Kamataki K., P4.044, P5.158
Kamberov G., P1.028
Kamelander G., P4.099, P4.104
Kamneva S.A., P4.166
Kamperides C., O4.040, P4.144
Kamran Siddiqui M.H., I4.064
Kang Z.H., P5.086, D2.005
Kantor M., P1.079

Kantsyrev A.V., P2.130
Kar S., I5.077, P1.131, P1.134, P5.103, P5.108, P5.116
Karabourniotis D., I1.015
Karpenko E.I., P1.010, P5.148
Karpov G.V., P1.151
Karpov M.A., P2.130
Karpushov A., P2.020
Karsch S., O4.039, P4.143P4.146
Kasahara H., P4.101
Kasilov S.V., P4.017, P5.009, P5.021
Kasotakis G., O4.056
Kasperek W., P4.110
Kasperczuk A., I5.081, P1.117, P1.118
Kasuya N., P4.044, P5.158
Kato T., I5.082
Kato V., P1.148
Katsuro-Hopkins O.N., P1.059
Katz M.M., P2.145
Kaufman M.C., P2.110
Kaveeva E., P5.020
Kavin A.A., P2.074
Kawaguchi M., P5.158
Kawahata K., P5.017
Kawai Y., P4.044, P5.158
Kawamura T., P5.126
Kawanaka J., O4.038
Kaye S., P1.009, P5.022, P5.023
Kazakov E., P2.137
Kedziora D.J., P1.157
Keeling D., P1.073
Keitel C.H., I3.049
Kellett B.J., I3.053, P2.186, P4.179, P4.185, P5.155
Kemp A., P5.117
Kempenaars M.A.H., O4.034, P4.005
Kendl A., I2.023, P1.018, P2.037, P5.007
Kern S., P4.105
Kernbichler W., P4.017, P5.009, P5.021
Kersten H., P2.164, P2.165, P4.168
Kevrekidis P., P4.162
Khalzov I.V., P1.053
Khan M.W.M., P1.071, P2.056
Kharchenko N., P4.176
Khayrutdinov R.R., O2.004, P2.074, P4.066
Khetselius O.Yu., P1.129, P2.175
Khimchenko L.N., P4.166
Khishchenko K.V., P1.181
Khitrov S.A., P2.097
Khodeev I.A., P2.134
Khomkin A.L., P1.185
Khorshid P., P1.086
Khrapak S.A., O2.007, O2.008
Khrebtov S., P1.088
Khromov N.A., P2.108
Khrustalev Yu.V., P5.137
Kick M., P5.081
Kiefer D., O4.039, P4.130
Kilkenny J.D., P2.127
Killian T., I2.019
Kim C.-B., P2.022
Kim C.C., P2.060
Kim D.C., O3.024, P4.175
Kim E., O5.068, P1.033
Kim Eun-jin, P1.023
Kim G.H., O3.024
Kim J.Y., P5.025, P5.091
Kim S.H., O2.004
Kim S.S., P5.091
Kimura K., P1.085
Kimura T., P1.140
Kingsep A., P2.137
Kinjo K., P4.109
Kinsey J., P4.036
Kiptily V., P1.087, P1.093
Kireenko A.V., P1.098
Kirillin A.V., D1.001
Kirillov G.A., P2.149
Kirillov K.Yu., P1.098
Kirk A., I2.020, P2.048, O4.031, P1.007, P4.035
Kislov D.A., P2.069
Kisslinger J., P2.085
Kissmann R., P5.156
Kiviniemi T.P., P4.045, P4.047, P5.015, P5.036
Kleimann J., P5.156
Klein A., P1.067, P5.083
Klein R., P1.040, P1.041, P4.038
Klimo O., P2.143, P4.138
Kline J., P4.119
Klir D., I5.081, P2.143
Klumov B., P1.155, P2.162
Kmetik V., P2.143
Knauer J.P., P2.127
Kneip S., O3.021, O4.040, P4.144, P5.108, P5.116
Knobloch-Maas R., P4.122
Knudsen D.J., P1.190
Ko J.-S., P4.111
Ko M.K., P4.171
Kobayashi M., P1.076, P2.113
Kocan M., P1.006
Koch R., P2.105
Kochergin M.M., P2.104, P2.108
Köchl F., O2.003, O4.054, P4.099, P4.104, P5.034, P4.028
Kocsis G., P5.079, P1.101, P2.070, P2.111, P5.078
Kodama R., I3.054, O4.038, P2.118, P2.187, P5.111, P5.113
Koenig M., I3.054, I5.082, O5.061, P1.135, P1.140, P2.187, P5.109, P5.119, P5.126
Koepke M.E., P1.190
Koester P., O5.061
Koga M., O4.038
Köhn A., P4.110
Kolerov S.B., P2.145
Kolesnichenko Ya.I., P4.072
Kolesnikov S.A., P2.145

Kolosov M.V., P5.098
Komarov A., P1.088
Komarov V., P1.013
Kominis Y., O4.051, P2.185
Komori A., I2.022, P1.076, P2.048, P4.101, P5.003
Kompaneets R., I5.079, P1.154
Kondo K., O4.038, P4.042, P5.111
König R., P2.113, P5.078
Konopka U., P1.154
Konz C., P2.024, P2.071, P2.112
Korchagin V.P., P1.151, P2.136, P5.006
Kornejew P., P5.078
Kornev V.A., P1.080, P2.093, P2.103
Korolev V.A., P2.137, P2.145
Korotkov A., O4.033, P1.093
Korsholm S.B., P1.034, P1.081, P2.086, P5.070, P5.077
Kortshagen U., I3.051
Koryagin S.A., P1.178
Korzhavina M.S., P1.098
Kos M., P1.132
Koshkarev D.G., O2.012
Koskela T., O4.036, P5.001
Kosłowski H.R., P5.063
Kosolapova N.V., P1.082
Kostomarov D.P., P1.091
Kotov V., P1.013, P4.009
Koukoulouyannis V., P4.162, P4.165
Kouprienko D.V., O4.046
Kourakis I., P4.162, P4.164, P4.165
Kovalenko V.P., P2.149
Kovalev V.F., P4.135
Koyama K., P1.148
Kozachok A., P1.088
Kozlová M., I2.025
Kraemer M., P5.096
Kraev A.I., P1.151, P2.131
Králik M., P2.120
Kramer G.J., P1.090, P5.099, P5.100
Krämer-Flecken A., P2.016, P4.016
Krasa J., P1.126, P2.120, P4.123
Krasa V., P4.133
Krashennikov S.I., I5.075, P1.050, P4.058, P5.012
Krasilnikov A., O2.001
Kraus W., P1.103, P2.102
Krausz F., O4.039, P4.136, P4.143, P4.146
Kravarik J., I5.081, J., P2.120
Kravtsov D.E., P4.095
Krayev A.I., P2.136
Krikalev S.K., O2.007
Krikunov S.V., P1.080, P2.097, P2.103
Kritz A.H., P1.001
Kroesen G., I2.039
Krotov V.A., P2.149
Krousky E., I5.081, P1.117, P1.118, P1.126, P2.143
Krousky V., P4.133
Krstic P.S., P2.004
Kruger S.E., P2.059
Kruglyakov E.P., P1.112
Kruijt O.G., P1.081
Krupnik L., P1.088
Krushelnick K., O3.021, O4.040, P5.107, P5.108
Krygina A.S., P5.098
Ku S., P1.001, P5.029
Kubeš P., I5.081, P2.120
Kubo S., P4.101
Kubo-Irie M., P4.100, P5.082
Kubota S., P5.060
Kudel'kin V.B., P1.151, P2.136
Kudrin A.V., P4.192
Kudryavtsev A.Y., O3.027
Kudryavtseva M.L., O3.027
Kudryakov T., P1.089
Kugel H.W., P1.009, P2.109
Kuhn S., P2.005
Kühner G., P2.113
Kuklin K.N., P4.103, P5.098
Kukushkin A.B., P1.016, P5.134
Kukushkin A.S., P1.013, P1.109, P4.079
Kulpin J.G., P2.110
Kumazawa R., P4.101
Kunin A.V., P2.149
Kuramitsu Y., I5.082, P2.187
Kuritsyn A., P2.017
Kurki-Suonio T., O4.036, P5.001, P5.069
Kurnaev V.A., P5.145
Kuroda H., O3.020
Kurskiev G.S., P1.109, P2.046, P2.097, P2.104, P2.108
Kurzan B., P2.001, P2.010, P4.002, P4.039
Kus A., P2.113
Kusama Y., P2.075
Kushev S.A., P4.172
Kushner M., I1.013
Kuteev B.V., P2.069, P4.106, P4.166
Kutsyk I.M., O3.027, P4.181, P5.153
Kuznetsov A.P., P2.130
Kuznetsov P.G., P2.149
Kuznetsova I.V., P1.152
Kuz'yayev A.I., P1.115, P1.116
Kwak J.G., P4.101
Kwon Jr.M., P1.090
Kyrie N.P., P2.188
Kyun Na H., P4.088
L'huillier A., P1.132
La Haye R.J., P2.059, P4.055, P4.056
Labate L., O5.061
Labaune C., O2.013, P1.119
Labaune Ch., I2.027
Labit B., I4.065, P1.184, P2.182
LaBombard B., O4.034, P1.005, P1.074
Laborde F., I4.061
Laborde L., I2.021, P1.038
Lackner K., I1.004, P1.101

Lackner L., P2.070
Lacroix D., P5.138
Ladygina M.S., P2.170
Lafortune K.N., P5.102
Lafuente A., P2.135
Lalescu C., P1.188
Lalousis P., P4.116
Lambert R., P1.058
Lamela H., P5.072
Lamers B., P1.081
Lancaster K.L., O5.061
Lancia L., I2.024, O4.042, P2.118, P5.113
Lancok A., P1.162
Lancok J., P5.142
Lancot M.J., P4.055
Liu Y.Q., P4.055
Lancot M.J., P4.056
Land V., I2.032
Landen O.L., P2.127
Landman I., P4.014, P5.011, P5.057
Landreman M., P4.027
Lang P.T., P1.101, P1.109, P2.070
Langer B., O2.002, P2.083
Lashkul S.I., O4.046, P2.087, P4.043
Laska L., P4.123, P4.133
Lasnier C.J., P4.003
Latkowski J., D5.001
Lauber Ph., I1.004, O4.030
Lauro Taroni L., P2.026, D1.003
Laux M., P5.078
Lavender D., P4.131
Lavrishshev O.A., O2.018
Layden B., O3.023
Layet J.M., P1.002
Lazarev V.B., P4.004, P5.004
Lazurenko A., P2.189
Lazzaro E., P4.025, P4.026, P5.046
Lebeaux D., I4.061
Lebedev S.V., P1.080, P2.093, P2.103
LeBlanc B.P., P1.009, P1.059, P1.108, P2.109, P5.022
Leboeuf J.N., P1.042
Lecherbourg L., I2.024
Leclert G., P4.021
Lee B.J., O3.024, P4.175
Lee H.J., P4.171
Lee K.W., P5.168
Lee M.J., P4.090, P4.091
Lee P., P2.148
Lee R.W., I2.025
Lee S.G., P1.084, P2.084, P4.087, P4.089, P4.096
Lee W.W., P5.023
Leekhaphan P., P4.015
Leemans W.P., P4.142
Leerink S., P4.045, P4.047, P5.015, P5.036
Lefebvre E., P4.141, P5.105, P5.112, P5.130
Lefrancois R.G., P4.187
Lehnen M., O4.052, P1.079, P1.089, P4.013, P4.016
Lei A., P5.111
Lei G.J., P5.086, D2.005
Leipold F., P1.034, P1.081, P2.086, P5.070, P5.077
Leitold G.O., P4.017, P5.021
Lejeune A., P1.186
Lemoine N., P2.189, P4.049, P4.189
Lemos N., P1.149, P2.150
Lennholm M., P1.058, D4.004
Leonard A.W., P2.024, P4.003
Leonov V.M., P2.077
Lepage C., P2.117
Lepreti F., P1.026
Leprovost N., O5.068
Lesnyakov G.G., P1.061
Letzring S., P4.130
Leuer J.A., P2.079
Leuterer F., P1.034
Levashov P.R., P4.156
Levashova M.G., P1.003, P1.004
Levato T., O5.061
Levinton F.M., P5.022, P5.060
Lévy A., I1.008
LHD Experimental Group, I2.022, P1.076, P4.101
Lho T., P4.091, P4.175
Li B., P5.086, D2.005
Li C.K., P2.127
Li J.G., P4.102, P5.024
Li Jinghong, D2.004
Li L., P5.086, D2.005
Li Ruxin, P1.121
Li S.W., P2.121
Li W., P5.026
Li Y., P5.024
Li Y.T., I5.082, P5.123, P5.124
Li Yunsheng, D2.001
Liang Y., P5.063
Liao H.L., P5.146
Lifschitz A., P5.130
Lilley M.K., P1.056, P2.055, P4.064
Lim J., P4.132
Limpouch J., I2.027, O2.013, P2.143, P4.128, P4.138, P4.149
Lin C.Y., P2.076
Lin L., P5.100
Lin S.Y., P5.024
Lin T., P2.118
Lin X.X., P5.123
Lin Y., P5.085
Lin Z., P5.028
Lindl J., D5.001
Ling J.H., P4.102
Linhart V., P1.126
Liniers M., P1.094
Lipaev A.M., O2.007, P2.162, P5.139
Lipschultz B., P1.005
Lisak M., P2.078

Liseykina T., I3.047
Lisitsa V.S., P1.003, P1.004
Liska R., P2.143
Lisovskiy V., P4.176
Lister J.B., O2.004, P2.112, P4.060, P4.066
Litaudon X., O2.003, P5.034, P5.068
Litovko I., P2.156, P2.171, P2.172
Liu Adi, P2.014
Liu C.Y., P4.112
Liu D., P5.060
Liu F., P5.123
Liu F.K., P4.102
Liu H., P5.086, D2.005
Liu Jiansheng, P1.121
Liu N., P4.161
Liu Y., P1.048, P5.026, P5.101
Liu Y.Q., P2.067, P2.080, P4.056
Liu Yi, D5.003
Liu Zh.J., D2.003
Lizunov A.A., P1.098
Lloyd B., I2.020
Loarer T., P1.101
Loarte A., O4.033, P1.109
LoDestro L.L., P2.079
Loiseau P., I2.027, O2.013
Lomas P., O2.003, O2.006, P5.045
Lombard G., P5.088
Lönnroth J., O4.036, P5.001, P5.053
Lontano M., P4.025, P4.026
Lopes N., O4.040, P1.149, P4.153
Lopes-Cardozo N.J., P4.093
Lopez Bruna D., P2.113, P1.025, P2.030, P2.049, P5.018
Lorenzini R., O4.049, P2.054, P4.019, P4.074
Lotov K.V., P5.104
Lötstedt E., I3.049
Louche F., P4.107
Loupasakis I., P4.116
Loupias B., I3.054, P2.187
Loureiro N.F., P4.029
Lozin A.V., P1.061
Lu D.L., P5.086, D2.005
Lu Haiyang, P1.121
Lu W., P4.155
Lubashevsky I.A., P2.161
Luce J., I4.061
Luce T.C., I2.021, O2.006, P1.069, P2.073, P2.079, P4.055, P4.083
Luebcke A., O5.061
Luhmann N.C., P1.090
Lukash V.E., O2.004, P2.074, P4.066
Lukiachshenko V.G., P1.010
Lukianitsa A.A., P1.092
Lundberg D.P., P2.109
Lungu A.M., P1.168, P1.173, P4.113
Lungu C.M., P1.166, P1.168, P1.171, P1.172, P1.173
Lungu C.P., P2.002, P4.113

Lunt T., P5.002
Luo G.L., P4.102
Lupelli I., P1.175
Lütjens H., P2.052
Lutz O., I2.027
Lyachev A., P1.150
Lynch V.E., P2.058
Lyssovan A., P1.104
Maaßberg H., P2.113
Mackinnon A.J., I4.060
Macor A., P4.062
Maddison G.P., O4.034, O4.054, P4.005
Magee R.M., P1.075
Maget P., P2.052, P4.062
Maggi C.F., P2.024, P2.071, P2.083, P4.011, P4.039, P4.041
Maggiora R., P2.105
Magne R., P1.058, D4.004
Mahdizadeh N., P4.028
Mailloux J., I2.021, O2.006
Maimone F., P1.174
Maingi R., P1.009, P2.013, P2.109
Maiorov S.A., P1.158, P2.161, P4.159, P4.160, P4.163, D1.001
Maire P.H., I2.027
Majeski R., P1.009
Major Zs., O4.039, P4.143, P4.146
Makowski M.A., P4.085, P5.099
Maksimchuk A., O3.021
Malaquias A., P2.040
Malara F., P1.039
Malinovskaya S.V., P2.175
Malinovski K., P5.075
Malizia A., P1.175
Malka G., P5.126
Malka V., P4.129, P4.132, P4.141, P5.119, P5.130
Mamyshev V.I., P1.115, P1.116
Mancic A., I2.024, O4.042, O4.043, D5.006
Mancuso A., I2.029
Manduchi G., P2.112
Mangeant M., I2.027
Mangeney A., P2.184
Mangles S.P.D., O3.021, O4.040, P4.144, P5.108, P5.116
Manickam J., P1.059, P5.044
Mansfield D., P1.009
Manso M.E., O4.032, P4.050
Mansur R.M., P4.171
Mantsinen M.-J., P1.055
Manuel M., P2.127
Maraschek M., O4.032, O4.030, P1.055, P1.101, P2.037, P2.070, P4.041, P4.082
Marchand R., P4.191
Marchenko A.K., P2.170
Marchetto C., P5.046
Marchiori G., P2.066, P2.067, P5.047, P5.065
Marchuk O., P4.092
Marcinkevicius A., P4.136
Marcus F.A., P1.024

Margarone D., P2.142, P2.144, P4.154, P4.170
Marian J., P2.135
Marinov P., P1.028
Marinucci M., P2.026, P2.106, P5.055
Märk T.D., P5.007
Markevisev I.M., P1.151
Markey K., P1.131, P1.134, P5.103, P5.108, P5.116
Marklund M., I2.037, P2.123
Markov V., O3.026, P2.188
Markovets V.V., D1.001
Marksteiner Q.R., P4.187
Marmande L., P2.117
Maron Y., O4.055
Marquès J.R., O3.021, O4.042, P2.118
Marr K., P1.005
Marrelli L., I1.017, O4.029, P2.054, P5.035, P5.047, P5.065, P5.097
Marsen S., P1.043
Marsh K., O4.040
Marshall F., P2.127
Martel P., O2.011, P2.147
Martellucci S., P1.170
Martens C., P2.102
Martens Ch., P1.103
Martin J.D., P5.152
Martin P., I1.010, I1.017, P1.055, P4.059, P4.167, P5.042
Martin Ph., I1.008
Martin R., P4.064
Martin Y.R., I5.073, P1.072, P2.036, P4.060
Martinell J.J., P2.125
Martines E., I1.017, O4.029, O4.049, P2.135
Martín-Mayor V., P5.135
Martins J.L., P4.148
Martins S.F., P4.155
Martynenko S.P., P2.149
Martynov A.A., P1.072, P2.063, P2.069
Marusov N.L., P5.134
Maruta T., P4.044, P5.158
Maruyama S., P1.109
Marx B., P4.143, P4.146
Masamune S., P4.067, P4.068
Mascali D., P1.174, P2.142
Masek K., I5.081, P1.117, P1.118, P2.143
Mašek M., P5.129
Maslennikov D.D., P2.134
Massines F., P2.169
Masson-Laborde P.E., P5.107
MAST team, P1.007
Masuzaki S., P1.076, P2.048, P4.101, P5.003
Matafonov A.P., P1.120
Matsumoto T., P1.085
Matsuoka K., P1.056, P2.107
Mattei M., O2.003, P4.078
Matthews G.F., O4.033
Mattioli M., P2.026
Mavrin A.A., P5.037
Maximov V.V., P1.098
Mayer M., P4.011
Mazataud E., P2.117
Maznichenko S.M., P1.061
Mazouffre S., P2.189
Mazzitelli G., P4.004
Mazzotta C., P2.026
McCarthy P.J., P2.071
McCarthy K., P2.113
McClements K.G., P4.037, P5.043, P5.052
McCone J.F.G., P2.088
McConville S.L., I3.053, P2.186, P4.179, P4.185
McCormick K., O4.033, P2.034
McCrorry R.L., I4.060
McCune D., P1.001
McDermott R., P1.005
McDevitt C.J., P5.016
McDonald D., I2.021, O2.006, P4.022
McKay R.J., P4.037
McKee G.R., O2.005, P5.099
McKenna P., P1.134, P5.103, P5.108, P5.109
McMillan B.F., P4.033, P1.019
McNeely P., P1.103, P2.102
Medina F., P2.030
Medley S.S., P5.060
Medvedev S.Yu., P2.063, P1.072, P2.069
Mehdipoor M., P1.182
Méheut H., P4.190
Mehlmann F., P2.037
Meigs A., P4.018
Mekler K.I., P4.103, P5.098
Melekhov A.V., P1.142, P1.192
Melnik A.D., P1.080, P2.103
Melnikov A., P1.021, P1.088, P5.037
Menard J., I5.070, O2.006, P1.009, P1.059, P2.109, P5.022
Mendes A., P5.088
Mendonça J.T., I4.066, P5.141
Mendoza M.A., O2.011, P2.147
Meneghini O., P4.111
Meng L.G., P4.102
Meng L.M., P5.123
Menmuir S., P2.056
Meo F., P1.034, P2.086, P5.070, P5.077
Merdji H., P1.132
Merkel P., I1.004, P1.077, P4.061
Merola M., P1.013
Mertens Ph., O4.033
Mertens V., P2.070
Meshcheryakov A.I., P4.108, P5.071
Messerle V.E., O2.018, P1.010, P5.148
Messiaen A., P1.104, P4.107
Mesyats G.A., P4.012
Meyer C., I2.027, O2.013, P2.117
Meyer H., P1.073
Meyer O., P1.006
Meyer W.H., P2.079

Meyerhofer D.D., I4.060, P2.127
Meyer-ter-Vehn J., I5.078, O3.019, P1.133, P1.145, P1.146, P2.132, P4.136
Mezel C., P2.151, P5.150
Miao W.Y., D2.003
Michaut C., I3.054
Michel D.T., I2.027, O2.013
Michelsen P.K., P1.034, P2.086, P5.070
Micozzi P., I2.029
Mier J.A., P4.020
Migliori S., P2.101
Mihaila I., P4.093
Mikhailov O.D., P1.151, P2.136
Miki M., P1.049
Mikic Z., O5.066
Mikikian M., I1.014, O3.023, P5.135
Mikkelsen D., P2.113
Milanesio D., P2.105, P5.088
Miles A.R., P5.102
Miller M., P2.017
Millon L., P5.088
Miloch W.J., P5.132
Mima K., I5.082, O4.038, O4.045, P4.120, P5.111, P5.121
Minaev V.B., P1.109, P2.046, P2.097, P2.104, P2.108
Minami T., P1.056, P2.113
Minardi S., P1.122, P2.148, P2.154
Minashin P.V., P1.016, P5.134
Mineev A.B., P2.074, P2.108, P5.067
Mingaleev A.R., P4.186
Mínguez E., O2.011, P2.147
Mintzev V.B., P2.145
Miquel J.L., I2.027
Miracoli R., P1.174, P2.142
Mirnov S.V., P5.004, P4.004
Mirnov V.V., P2.017
Mironov M.I., P1.109, P2.097
Miroshnikov I., P4.106
Mirza A., P5.064
Mishra L.N., P1.191
Misina M., P5.142
Mito T., O4.038
Mitri M., O4.052, P4.013, P4.016
Miura E., P1.148
Miyamoto S., P2.075
Miyanaga N., O4.038
Miyata Y., P1.085
Miyazawa J., P1.076
Mizhiritsky V., P2.137
Mizuguchi M., P1.085
Mizuno N., P4.157
Mizuuchi T., P2.113
Mlynar J., P4.084
Mocek T., I2.025, P1.132
Modestov M., P2.123
Moiseenko A.N., P1.151,
Moiseenko V.E., P1.061, P2.114, P4.184
Mok Y.S., P4.171
Mokhov V.N., P1.115, P1.116
Molaii M., P1.086
Molchanov P., P4.035
Molina D., P1.058
Mollard P., P5.088
Moller A., P4.167
Molodtsov N.A., P1.083
Molotkov V.I., O2.007, P2.162, P5.139
Mondio G., P4.170
Monot P., I1.008, I1.010
Montagna C., P2.178
Montant S., I4.061
Monteil M.C., I2.027, O2.010
Monticello D., P2.013
Moon M.K., P2.084, P4.087, P4.089
Moon S.J., I2.025
Moore A., P4.131
Mora P., P4.139
Morace A., O5.061, P5.123, P5.126
Moradi S., P4.048, P5.027
Moraru A., P4.069
Mordovanakis A.G., P5.107
Moreau P., P1.058
Moreau Ph., P2.052
Morel P., P1.040, P1.041, P4.038
Moreno-Insertis F., I5.074
Morfill G.E., I5.079, I5.080, O2.007, O2.009, P1.154, P1.155, P2.159, P2.162, P5.136, P5.139, P5.140
Mori W.B., O3.021, P4.155
Morice O., P2.153
Morikawa J., P4.109
Morisaki T., P1.076, P2.048, P2.061, P5.003
Morita S., P1.054, P1.105, P2.061, P2.082
Morize C., P1.020
Morlens A.S., P1.132
Morozov A.E., P4.108
Morozov D.Kh., P5.067
Morozov I.V., P1.151, P2.131, P2.136, P5.006
Moskalenko I.V., P1.083
Moslem W.M., P5.160
Mota F., P2.135
Motojima O., I2.022, O4.038, P1.076, P4.101, P5.003
Moudden M.El., P1.046
Mourou G., P1.119, P5.107
Moustaizis S.D., O4.041, P1.123, P4.116
Moyer R.A., P2.003, P2.009, P4.098
Mozeti M., P1.166
Mozetic M., P1.014
Mueller D., P1.009, P4.076
Mueller M., I1.012
Muir D., P2.088
Mukhin E.E., P2.104, P2.108
Mulas R., P4.147
Mulec M., P5.009
Müller H.W., P2.010, P2.019, P2.037, P4.003

Müller S., I4.065, P1.184,
Mulser P., P5.127
Muraglia M., O4.028
Murakami M., O2.006, O4.038, P2.073
Murakami S., P2.113
Murakhtin S.V., P1.098
Murari A., I4.059, I5.073, P4.084
Murata K., P4.067, P4.068
Murmann H., P4.002
Murtaza G., P5.167
Murugov V.M., P2.149
Musil J., P5.142
Mustata I., P1.168, P1.169, P1.171
Mutoh T., P4.101
Muxlow T.W.B., P2.186
Myatt J., I4.060
Myers S., I3.054
Myra J.R., P4.001
Na Y.-S., P5.025
Nagai K., O4.038, P5.111
Nagaoka K., P1.054, P1.056
Nagashima Y., P4.044, P5.158
Nagatomo H., O4.038, O4.045, P4.120, P5.121
Nagatomo K., P5.111
Nagel S.R., O3.021, O4.040, P4.144, P5.108, P5.116
Nagy K., P5.079
Najmu Z., O3.021
Najmudin Z., O4.040, P4.144, P5.108, P5.116
Nakada M., P1.085
Nakai M., O4.038
Nakajima N., P2.113
Nakamura T., O4.038, P4.120, P5.121, P5.126
Nakamura Y., P2.075, P4.042, P4.101
Nakao Y., O4.038, O4.045
Nakatsutsumi M., P2.118
Nakonechny G.V., P4.172
Nam U.W., P2.084, P4.087, P4.089
Nanobashvili S., P2.096
Nardon E., O4.035
Narihara K., P1.054, P2.061
Narushima Y., I2.022, P1.054, P2.061
Naudé N., P2.169
Naudy M., I2.027
Naulin V., I2.023, P2.025, P2.037
Naumova N., P1.119
Nave F., P4.115
Navratil G.A., P4.055, P4.056
Nazarov W., I2.027, O2.013, O4.040, P2.143
Nazikian R., P5.099
Néauport J., I4.061
Nedzelskij I., P1.021
Neely D., P1.131, P1.134, P5.103, P5.108
Nees J., P5.107
Negishi S., P1.085
Negutu C., P5.144
Nehme H., O4.054, P1.109, P4.099, P4.104
Nejoh Y., P4.157
Nekhaevsky Yu.Yu., P5.137
Nelson B.A., P4.076
Nemov V.V., P5.021
Neu R., P4.011, P4.039
Neubauer O., P4.075
Neudatchin S.V., P5.038
Neumann H., P2.164
Neverov V.S., P1.016, P5.134
Newman D.L., O4.058
Newman D.E., P1.042, P2.029, P4.020
Newton A.P., P1.023
Newton S.L., P4.054
Nguyen C., P4.062
Nguyen-Tran Th., I3.052
Ni Guoquan, P1.121
Nickles P.V., P4.145
Nicolai P., I2.027, O2.013
Nicolai Ph.X., I5.081
Nielsen A.H., I2.023, P2.037
Nielsen S.K., P1.034, P5.070, P5.077
Nilson P.M., I4.060, O3.021, O4.040
Nish K., O4.038
Nishijima D., P2.004
Nishijima T., P5.158
Nishimura H., I5.082, P5.126
Nishimura S., P1.056, P2.107, P5.059
Nishimura Y., P5.028
Nkonga B., P2.065
Noack K., P2.114
Noailles S., I4.061
Nold B., P2.019
Nomura G., P4.101
Nomura Y., P1.131, P1.134, P1.145
Nonn P.D., P2.110
Nora M., P4.045, P4.047, P5.015, P5.036
Norberg C., I2.036
Nordman H., P2.042, P4.036, P4.048
Norreys P.A., I4.060, I5.077, O5.061, P1.128, P5.103, P5.108
Nosenko V., I5.080
Nosov S.V., P1.092
Noterdaeme J.-M., P4.041, P5.005
Notimasu T., P5.111
Notley M.M., I3.054, P5.113
Noto M., P1.085
Novello L., P5.065
Novikov V.G., P1.125
Novotny M., P5.142
Novozhilov Yu.B., P2.130
Nowak S., P2.026, P5.046, P5.074
NSTX Research Team, I5.070, P2.109
Nuernberg F., P4.127
Nunes I., I5.073, O2.003, O4.034
Nürnberg F., P4.119, P4.122, P4.142
Nuter R., P4.141
O'Connell R., P1.075

O' Mullane M., D1.003
Ockenga T., P2.165
Oehr C., I1.012
Ogando F., P4.045, P4.047, P5.015, P5.036
Ogawa Y., P4.109
Oh K.S., O3.024
Ohdachi S., I2.022, P1.054, P2.061
Ohl A., P4.173
Ohno N., P2.048, P2.095
Ohyabu N., P1.076
Oikawa T., P5.087
Okabayashi M., P4.055, P4.056
Okamoto M., P2.095
Okamura S., P1.056, P2.107, P2.113
Okano Y., P5.126
Oki K., P4.067, P4.068
Olazabal-Loumé M., O5.060, P2.124, P2.126
Oldenbürger S., P2.189, P4.049
Oliva E., O5.062, P1.117, P1.132, P1.141
Oliva S.P., P2.110
Olofsson K.E.J., P1.071, P2.056
Onchi T., P4.067, P4.068
Oncioiu G., P1.166
Ongena J., P1.106, P4.115
Onjun O., P4.015, P4.030
Onjun T., P4.015, P4.030
Ono M., P1.009
Onofrei R., P1.149
Onofri M., P1.039
Oohara W., P5.147
Oono Y., P1.085
Oosterbeek J.W., P1.081, P5.077
Opaleva G.P., P1.061
Oreshko A.G., D5.005
Orlovskiy I.I., P1.068
Orozco R.O., O4.048
Orsitto F., O2.006
Ortiz C., P2.135
Osadchaya E.F., O2.018
Osakabe M., P1.054
Osborne T.H., P4.003
Osmanov Z., P1.179
Osterhoff J., O4.039, P4.143, P4.146
Otroschenko V., P1.008
Ottaviani M., I2.023
Otte M., P1.043, P1.088, P2.051, P5.078
Oya A., I3.054
Ozaki T., O3.020
Ozhereliev F.I., P1.061
Paccagnella R., P2.067, P4.074, P5.065, P5.095
Pacella D., O4.050
Pacher G.W., P1.013, P4.079
Pacher H.D., P1.013, P4.079
Paganucci F., I1.017
Pagonakis I.Gr., P4.105
Pais V., P1.124, P5.144
Pak S.V., P1.151, P2.136
Pakzad Hamid Reza, D2.006, D4.002
Pal' A.F., P5.171
Pálfalvi J., P5.079
Palmer C., P5.108, P5.116
Pamela S., P2.065
Pan C.H., D5.003
Pan Y.D., P2.076
Panasenkov A.A., P1.109
Pancheshnyi S., P2.169
Pandey B.P., P1.156, P1.163
Pánek R., P2.098
Panis T., P1.067
Pankin A.Y., O5.066, P1.001
Papadogiannis N.A., P1.122, P2.148, P2.154
Papp G., P2.034
Parail V., O2.003, O4.036, P5.001, P5.029, P5.034, P5.053
Parisot T., O4.050
Park B.H., P5.091
Park G.Y., P1.001, P5.029
Park H.K., P1.090
Park J.-K., I5.070
Park Y.C., O3.024
Parker R.R., P4.111
Parks P.B., P2.003, P4.098
Parra F., P4.034
Parys P., O4.043, P1.127, P4.123
Pascal J.-Y., P1.006
Pasch E., P5.078
Pashnev V.K., P1.061
Pasko V., I5.069, P4.161
Pasley J., P5.110
Pasqualotto R., O4.034, P2.054, P4.005, P4.019, P5.073, P5.097
Passarelli M., P1.014
Passas M., P2.033
Pastukhov V.P., P1.044
Patrov M.I., P1.109, P2.046, P2.108
Paul S., P1.009
Paulicelli E., P4.073
Pautasso G., P2.007
Pavlenko V.P., P5.041
Pavlov A.V., P4.172
Pavlovskiy E.S., P1.115
Pázmándi T., P5.079
Peano F., I4.067, P4.147, P4.148
Pearlstien L.D., P2.079
Pécseli H.L., P5.132
Pedreira P., P5.072
Pedrick L., P4.113
Pedrosa M.A., O4.048, P1.021, P2.021, P2.028
Peeters A.G., O4.047, P2.032
Peeters Ph., P2.038
Pegoraro F., P1.051, P1.176, P1.180, P2.176, P2.178, P2.179, P2.184
Pégourié B., O4.054, P1.109, P4.099, P4.104
Peksa L., P1.162

Peláez R.J., P2.094
Pelka A., P4.122
Peng Y., P5.138
Peng Y.K.M., P5.048
Pereverzev G., P2.112, P5.027, P5.032
Perez F., O5.061, P5.109, P5.112
Perez-Luna J., P5.151
Perfilov S., P1.088
Pericoli V., P2.026
Pericoli-Ridolfini V., I2.021, O2.006, P2.106
Perkins L.J., P5.102
Perlado J.M., P2.135
Perona A., P5.054
Perri S., O4.057, P5.170
Persson A., P4.134
Persson M., P4.024
Peskov V.V., P5.145
Pesme D., O2.013, P2.140
Pestchanyi S., P4.014
Petrasso R.D., I4.060, P2.127
Petravich G., P5.076
Petrenko M.V., P1.152
Petridis C., P1.122, P2.148, P2.154
Petrie T.W., P2.073
Petrov A.V., P2.093
Petrov O.F., I2.033, P1.160, P1.161, P1.187, P2.162, P4.158, P5.137, P5.162, P5.171, D1.001
Petrov S.I., P2.149
Petrov Yu.V., P1.109, P2.046, P2.097, P2.104, P2.108, P2.170
Petrukhin A.A., P1.115, P1.116, P2.131
Petrzilka V., P1.106
Petty C.C., O2.005, P2.024, P2.073, P4.083, P5.022
Peyrusse O., I2.027, P1.135
Peysson Y., I3.046, P1.099, P2.098, P2.112, P5.027
Pfeifer M., I5.081, P1.117, P1.118, P4.133
Pfotenhauer S., P4.137
Phelps A.D.R., I3.053, P2.186, P4.179, P4.185
Philippe F., I2.027, P2.122
Philipps V., O4.033
Phillips C.K., P1.108, P2.099, P4.114
Piccolo F., P5.045
Picha R., P4.015, P4.030, P4.040
Piel A., I1.003
Pierre Th., P1.046, P4.046, P5.169
Pigarov A.Yu., P2.004
Pikuz S.A., P2.137, P4.186
Pinches S.D., I2.018, O4.034, P1.055, P2.018, P2.055, P4.064
Pinegin A.V., P2.149
Pinsker R.I., P4.097
Pinzhenin E.I., P1.098
Piovesan P., O4.029, P1.055, P5.047, P5.065
Pipahl C.A., P5.113
Piron R., P2.122
Pironti A., P2.080
Pisarczyk P., P1.117, P1.118
Pisarczyk T., I5.081, P1.117, P1.118
Pisarev V.A., P4.086, P4.189
Pisokas Th., P2.041
Pitts R.A., O4.033, P4.005
Pizzicaroli G., P4.073
Platania P., P5.074
Platonov K.Yu., P4.128
Ploumistakis I., O4.041, P1.1 23
Plyushchev G., P1.184
Plyusnin V.V., P5.075
Poberaj I., P1.014
Pochelon A., P1.072, P1.099, P2.020
Podestà M., I4.065, P1.184, P2.182, P5.060
Podoba Y., P1.088
Podpaly Y., I4.058
Poedts S., P4.178, P5.040, P5.061
Pokol G., P2.034, P2.078
Pokorny P., P5.142
Polan J., I2.025
Polevoi A.R., P1.109
Poli E., P5.095
Poli F.M., P1.052, P1.184, P4.071
Politzer P.A., P2.073
Polomarov O.V., O4.044
Polosatkin S.V., P4.103, P5.098
Polster R., P4.145
Poltierova J., P1.162
Polyushko S.M., P2.136
Polz J., P4.137
Pomaro N., P5.073
Pomphrey N., P5.050, P5.058
Ponomarenko A.G., P1.142, P1.192
Poolyarat N., P4.015, P4.030
Popa G., P4.093
Popov A.M., P1.063, P1.096, P2.069P2.089
Popov A.Yu., P4.043
Popov K. I., P4.121, P4.135
Popov S.D., P4.172
Popov S.S., P4.103, P5.098
Popov Tsv.K., P4.081
Popova E.V., P5.080
Popova L., P1.028
Popovichev S., P4.084
Popp A., P4.143, P4.146
Por G., P5.079
Porfiri M.T., P1.175
Porkolab M., P4.111, P5.085, P5.100
Porosnicu C., P1.168, P1.171
Porte L., P2.036
Porter G.D., P4.003
Portone A., O2.003, P2.080, P4.078
Poshekhonov Yu.Yu., P1.072
Pospieszczyk A., P5.078
Postupaev V.V., P4.103, P5.098
Posukh V.G., P1.142, P1.192

Potapenko I.F., P5.012
Prager S.C., P1.075, P2.017, P2.110
Preinhaelter J., P2.096
Pretty D., P2.113
Preuss R., P2.113
Price M., O4.054
Prikhodko V.V., P1.098
Primavera L., P1.039
Prompting J., P4.030
Pronin O.V., P2.130
Przybysz W.S., P1.165
Pshenov A.A., P5.067
Psikal J., P4.138, P4.149
Psimopoulos M., O4.056, P1.122
Puerta J., P4.059, P4.167
Pueschel M.J., I2.023, P1.038
Puetterich T., P4.011
Pugno R., P2.010, P4.011, P4.039
Puiatti M.E., P2.026, P4.019, P4.074
Pukhov A., I1.011
Punjabi A., P1.012, P2.008
Puscas N.N., P5.144
Pustovitov V.D., P1.060, P2.069
Pusztai I., P1.032
Pütterich T., P2.083, P4.039
Qian J., P2.014
Qin Y.L., P4.102
Qotb K., P1.046
Quade A., P4.173
Quéré F., I1.010
Quinn K., P5.113
Quinn M., P5.109
Quotb K., P4.046
Rabec le Gloahec M., P1.140, P2.128, P5.109
Rabinski M., P5.075
Raffestin D., I2.027, P2.117
Rafiq T., P1.001, P4.024
Raitses Y., P5.149
Ram A.K., O4.051, O4.059, P1.097, P1.099, P2.185
Ramahkrishna B., P5.113
Raman R., P1.009, P2.109, P4.076
Rambo P., P4.127
Ramet P., P2.065
Ramis R., O2.015
Ramisch M., P2.019, P4.028, P4.110
Ramogida G., P4.073
Rantamaki K., P2.035
Rao J., P5.086, D2.005
Rapp J., O4.033, P4.093
Rasmussen J.J., P2.037
Rassuchine J., P4.119
Rasul B., P5.007
Ratynskaia S., I4.063
Raupp G., P4.082
Razavi M., P1.086
Razumenko D.V., P1.080, P2.103
Réau F., I1.008
Rebont C., P4.046, P5.169
Rebusco P., P5.154
Rechatin C., P4.132, P5.130
Recsei S., P5.078
Redaelli R., P5.123, P5.126
Reed S., O3.021
Reich M., P4.082
Reimerdes H., P4.055, P4.056, P5.022
Reinke M., P1.005, P1.084
Reiser D., I2.023, O4.052, P2.016, P2.031
Reiter D., O4.052, P1.013, P1.079, P2.009, P2.085, P4.009, P4.092
Reitsma A., P1.144, P4.151
Reitsma A.J.W., P1.148
Remacle V., P1.188
Renaudin P., I2.024, P1.135
Renner O., P1.126, P2.129, P2.143
Repa P., P1.162
Reshko M., P4.029
Reusch J.A., P1.075
Reverdin C., I2.027
Rewoldt G., P5.016, P5.023
Reynolds J.M., P2.049
Rezaei-Nasirabad R., P4.140
RFX team, I3.045
Riazuelo G., O2.013, P2.140
Ribeiro T., I2.023, P5.039
Ribeyre X., I5.081, O5.060, P2.124, P2.126, P4.118
Riccardi C., P2.027
Ricci P., P1.184, P2.182
Rice J.E., I4.058, P1.074, P1.084, P4.111
Richert T., P5.081
Richetta M., P1.170, P1.175
Riconda C., O2.013, O4.042
Riedl R., P1.103, P2.102
Rimini F., O2.006, P1.058
Roach C.M., P4.029
Robertson C.W., I3.053, P2.186
Robiche J., I2.024, D5.006
Robinson A., I5.077
Robinson A.P.L., P5.103
Roca P., I3.052
Roccella M., O4.036, P5.001
Rodionov N., P1.008
Rodionova V., P1.008
Rodrigues P., P4.063, P4.065
Rodriguez J., P4.190
Rodríguez R., O2.011, P2.147
Rodríguez-Barquero L., P1.094
Rohde V., P2.010, P2.019, P2.037, P4.011
Rohlens K., I5.081, P1.117, P1.118, P4.133, P5.129
Romagnani L., P2.118, P5.113
Romanelli M., I2.023, P2.026, P2.112, P5.027
Romano A., P2.026
Romanova V., P2.137, P4.186

Romary Ph., I2.027
Ronald K., I3.053, P2.186, P4.179, P4.185
Ronneberger F., P4.137
Roquemore A.L., P1.009, P2.109
Roques A., I4.061
Ros D., P1.132
Rosato J., P1.004
Rosch R., I2.027
Rose S., P4.124, P5.118
Rosinski M., O4.043, P1.127, P4.123
Rosmej F.B., P1.004
Ross P.W., P1.009
Rossetti P., I1.017
Roth M., P4.119, P4.122, P4.127, P4.142
Rothermel H., O2.007
Rott M., P4.075
Rouak A., P1.046
Rousse A., I1.011, O3.021
Rousseaux C., I2.027, P5.109
Rouyer C., I4.061
Rovenskih A.F., P4.103, P5.098
Roveta G., P2.101
Rowlands G., P4.182
Rowlands Rees T.P., P4.143, P4.146
Rozhansky V., P4.035, P5.020
Rozhansky V.A., P1.109, P2.046, P2.108
Rozhdestvensky V.V., P1.080, P2.103
Rozmus W., P4.121, P4.135, P5.107
Rubel M., P4.113
Rubiano J.G., O2.011, P2.147
Rubinacci G., P2.067, P2.080
Rubinacci R., P4.073
Rubinstein B., O4.055
Rubin-Zuzic M., O2.007, P2.159, P5.139
Rudakov D., I4.063, P2.003
Ruhl H., P5.127
Rullier J.L., P2.117
Rullière C., I4.061
Rus B., I2.025, P1.132
Rushkevich A.A., P1.080
Russo C., P4.153
Rutberg Ph.G., P4.172
Ryan P.M., P1.108, P4.097
Ryc L., P4.123
Rygg J.R., P2.127
Rykovanov S.G., O3.019, O4.039, P1.131, P1.134, P4.143, P1.145
Ryokai T., P5.003
Rypdal K., P1.037
Ryter F., I2.021, P4.039
RyulHuh S., P4.174
Ryzhkov S., P1.114
Saarelma S., I2.020, P4.005
Sabbagh S.A., I5.070, P1.009, P1.059, P5.022
Sabot R., P1.017, P1.022, P4.062
Sadovski A., P2.173
Sadowski M.J., P5.075
Saevert A., P5.108
Saibene G., O2.003, O2.006, O4.036, P1.101, P4.078, P5.001
Saïfaoui D., P1.046
Saito K., P4.101
Saito N., P1.148
Saitou Y., P5.133
Sakagami H., O4.045, P4.120, P5.121
Sakakibara S., I2.022, P1.054, P2.061, P2.113
Sakamoto R., I2.022, P1.076, P5.017
Sakata D., P4.109
Sakawa Y., I3.054, I5.082, P2.187
Sakharov N.V., P1.109, P2.046, P2.097, P2.104, P2.108
Saleem H., P5.061
Salem M.K., P1.070
Salewski M., P1.034, P2.086, P5.070, P5.077
Salmi A., O4.036, P5.001, P5.029
Salomaa R., P5.069
Samaddar D., P2.029
Samaras T., P5.089
Samaritan A.A., O3.023, O2.016, P1.156, P1.157, P1.163, P2.157, P5.135
Samm U., O4.052, P4.016
Sánchez Burillo G., P2.039
Sánchez J., P5.072
Sánchez M., P5.072
Sanchez R.A., P1.031, P1.042, P2.029, P2.043, P2.058, P4.020
Sandberg I., P1.027, P2.045
Sandner W., P4.145
Sangster T.C., I4.060
Sano F., P2.113
Sanpei A., P4.067, P4.068
Santos J.E., P1.130, P5.126
Santos J.J., P5.109
Sanz J., P2.124, P2.126, P5.122
Sarakovskis A., P2.011
Sarazin Y., P1.017, P1.020, P4.033, P5.008
Sardei F., P2.013, P2.085, P2.113
Sarff J.S., P1.075, P2.017
Sarichev D.V., P5.080
Sárközi J., P5.076
Sarris I.E., P2.044
Sartori F., P5.045
Sartori R., I5.073, O2.003
Sasao M., O2.001
Sasorov P.V., P2.130
Sassenberg K., P1.055
Sataline C., P1.183
Sato K., P4.106
Sato M., P2.092
Sattin F., I2.034, P5.035
Saut O., P2.151
Sautarel F., I4.061
Sauter O., I5.072, P1.072, P2.020, P2.036
Sauteret C., I4.061
Sautet M., I4.061

Sautivet A.M., P2.128
Saveliev A.N., P5.092
Sävert A., P5.116
Savin S.M., P2.130
Savkin V.Ya., P1.098
Savrukhin P.V., P5.080
Scannel R., O4.054
Scarabosio A., P2.001
Scarin P., I1.017, O4.049, P4.074
Schäfer J., P4.173
Schaffer M.J., I5.070, O4.035
Schaumann G., P4.122
Scheffel J., P5.064
Scheier P., P5.007
Schekochihin A., I2.035
Schiavi A., P4.126, P5.106
Schiesko L., P1.002
Schlegel T., P1.119
Schlickeiser R., P2.174
Schlossberg D.J., O2.005
Schmid K., P4.136, P4.146
Schmidt A.E., P4.111
Schmidt H., P2.120
Schmitt S., I2.027
Schmitz O., I3.043, O4.052, P1.104, P2.009, P4.013, P4.016
Schnack D.D., O5.066
Schneider H., P1.009
Schneider M., I3.046
Schneider V., P2.164
Schneider W., P5.078, P5.081
Schnürer M., P4.145
Schoepf K., P1.087
Schökel A., P4.122
Schollmeier M., P4.119, P4.122, P4.127, P4.142
Scholz M., P2.120
Scholze F., P2.164
Schram P.P.J.M., P1.158
Schramm U., P4.136, P4.143, P4.146
Schreiber J., O3.019, O4.039, P1.145, P4.127, P4.130, P5.108, P5.116
Schrittwiesser R., P2.025, P2.037, P2.177, P4.093
Schubert G., P4.156
Schubert M., P1.088, P1.096
Schuhmacher D., P4.122
Schurtz G., I2.027, I5.081, P4.118
Schüttertrumpf J., P4.122, P4.127
Schwabe M., P5.139
Schwander F., P5.008, P5.043
Schwarz J., P4.127
Schweer B., P4.016, P5.076, P5.078
Scime E.E., P1.166, P5.143
Scott B.D., I2.023, P1.018, P5.030, P5.031, P5.039
Scott S.D., P1.084, P4.111
Sebban S., P1.132
Sedighi-Bonabi R., P4.140
Seemann K., P1.162
Sefkow A.B., P2.139
Ségui J.L., P1.006, P1.058, P2.052, P4.062, D4.004
Séguin F.H., P2.127
Séгур P., P2.169
Seidel U., P4.075
Seki T., P4.101
Sekine K., P4.157
Selemir D., P2.158
Semenov V.V., P2.108
Sempf M., P1.077
Sen A., P1.066
Sengupta A., P2.051
Senichenkov I.Yu., P1.109, P2.046, P2.108
Senik A.V., P2.149
Senties J.M., P2.033
Sentoku Y., O4.045, P4.119, P5.117
Seol JaeChun, P1.100
Sepehri Javan N., P1.136, P5.163, P5.164
Serafino T., P4.170
Serban G., P4.113
Sergeev V.Yu., P4.106
Sergeev Yu.F., P1.061
Sergienko G., O4.033
Serianni G., I1.017, O4.049, P5.073
Serra F., O4.032
Serre E., P5.008
Shah H.A., P5.167
Shah R., I1.011, P4.130
Shaidulin V.Sh., P1.115
Shaikhislamov I.F., P1.142, P1.192, P4.177
Shakhalkin A.T., P2.136
Shan J.F., P4.102
Shapoval A.N., P1.061
Sharapov S.E., O2.006, P1.052, P1.056, P1.087, P1.093, P2.055, P4.054, P4.064, P4.071
Sharkov B.Yu., O2.012, P2.130, P2.145
Sharov I. A., P4.106
Shatalin S.V., P2.087, P4.043
Shcheglov D.A., P1.083
Shcherbakov A.A., P4.160, P4.163
Shcherbinin O.N., P2.097
Shelkovenko T.A., P2.137, P4.186
Shen B., P4.102
Sheng Z.M., P5.123, P5.124
Shepherd R., I2.024
Sherlock M., I5.077, P4.124
Shibata Y., P2.095
Shima Y., P1.085
Shimada T., P4.119, P4.130
Shimazu H., P4.067, P4.068
Shimizu A., P1.054, P1.056
Shimozuma T., P2.113, P4.101
Shimpo F., P4.101
Shinohara S., P4.044, P5.158
Shipuk I., P1.008
Shiraiwa S., P4.111

Shoji T., P2.107
Shoshin A.A., P4.103, P5.098
Shoucri M., P4.006, P4.152, P5.128
Shu H., D5.004
Shukla P.K., I4.066, O5.067, P4.165, P4.182
Shumikhin S., P1.185
Shurygin R.V., P5.037
Shustin E.G., P5.145
Shuvaev D.A., P1.083
Shvarts D., P2.127
Shvedov A.A., P2.134
Shvets G., O4.044
Shvets O.M., P1.061
Shyshkin O.A., P4.031
Sid A., P4.117
Signori M., I1.017
Silva A., O4.032
Silva C., O4.048, P1.021, P2.025, P2.040, P5.075
Silva L.O., I2.036, I4.066, P1.128, P1.130, P1.149, P2.141,
P4.143, P4.147, P4.148, P4.150, P4.155, P4.180,
P5.120
Simakov A.N., P4.034
Simonchik L.V., P4.188
Simonetto A., P5.074
Simpson P., P5.108, P5.116
Singh R., P2.042, P4.048
Singleton R., I2.026
Sinitsky S.L., P4.103, P5.098
Sinor M., P2.143
Sipilä S., O4.036, P5.001, P5.069
Sips A.A., P4.078
Sips A.C.C., O2.003, P2.024, P4.082, P5.034
Skala J., I5.081, P1.117, P1.118
Skalny J.D., P5.007
Skinner C.H., P1.009
Skobelev A.N., P2.136
Skoulakis A., P1.122, P2.154
Smadi M., P4.117
Smalyuk V.A., P2.127
Smeulders P., O2.006, P1.069
Smirnov A.I., P1.080
Smirnov G.N., P2.145
Smirnov V., P2.137
Smith H., P2.078, P4.077
Smith H.M., P1.030, P1.057, P2.055
Smolyakov A.I., P1.053, P1.050, P5.149
Snipes J.A., O4.034, P1.067, P1.074, P5.083
Snyder P.B., P2.071
Soboleva T.K., P5.012
Sobur D.A., P2.130
Sokolov I.V., P1.119
Solano E.R., P2.035, P4.070
Soldatkina E.I., P1.098
Soldatov S., P2.016
Solodov A.A., I4.060
Solomakhin A.L., P1.098
Solomon M.L., P4.093
Solomon W.M., P4.056, P5.022, P5.099
Solomyannaya A.D., P1.125
Solyakov D.G., P2.170
Sonato P., P4.070, D1.002
Song S., P1.058
Song S.D., D4.004
Song X.M., D5.003
Sonnino G., P2.038
Soppelsa A., P2.066, P2.067, P5.047, P5.065
Sordo F., P2.135
Sorokin A.E., O3.022
Sorokina N.V., P4.103, P5.098
Sorriso-Valvo L., O4.057
Sotnikov S., P1.008
Soukhanovskii V.A., P1.009, P2.109
Soullié G., I2.027
Sozzi C., P5.074
Spatschek K.H., I3.041
Speirs D.C., I3.053, P2.186, P4.179, P4.185
Speth E., P1.103, P2.102
Spizzo G., I1.017, O4.049, P4.074
Spolaore M., O4.029, O4.049, P1.026, P5.073
Spong D., P5.028
Stäbler A., P1.103
Staebler G.M., O4.053
Stafe M., P5.144
Stahl M., P4.168
Stamm R., P1.004
Stamp M., O4.033
Stamper R., I2.036
Stancalie V., P1.124, P5.144
Stancu C., P1.166, P2.167
Stanglmaier S., O4.039
Stankiewicz R., P5.027
Starostin A.N., P5.171
Startsev E.A., P2.139
Starz R., P4.093
Steinberg V., I5.079
Steinhauer L.C., P5.048
Stenz C., I5.081, O2.013
Stenz Ch., I2.027
Stenzel R., P2.177
Stepanov A.Yu., O4.046
Stepanova Z.A., P1.152
Stephens H.D., P1.075
Stephens R.B., I4.060, P5.114
Sternberg N., P1.183
Stevenson T., P1.009
Stober J., P1.034, P4.082
Stöckel J., P2.098, P4.081
Stockem A., P2.174
Stoeckl C., I4.060, P2.127
Stoican O.S., P4.169
Stokes J.D.E., P2.157
Storm E., D4.001, D5.001

Storm M., I4.060
Stotler D.P., P2.109
Strachan J., D1.003
Strait E.J., P2.003, P4.055, P4.056, P5.022, P5.099
Strand P., P2.042, P2.112, P4.036, P5.027
Stránský M., P2.098
Strege C., P4.094
Streibl B., P4.075
Strintzi D., O4.047, P2.032
Stroth U., P2.019, P2.113, P4.028, P4.110
Strozzi D.J., P2.138
Strumberger E., I1.004, P1.077
Stupka M., I2.025
Stutman D., P2.081
Suárez D., O2.011, P2.147
Suchkov E.P., P1.091
Sudo S., P4.106
Suetterlin R.K., O2.007
Sugihara M., P1.109
Sukboon D., P4.015
Sulyaev Yu.S., P4.103, P5.098
Summers H.P., D1.003
Sun H.J., D5.003
Sun P., P5.026
Sun Y.W., P4.102
Sunn Pedersen T., P4.187
Surdubob C.C., P1.172
Surdu-Bob C., P1.171
Surov A.V., P4.172
Sushkov A.V., P4.095
Suslov N.A., P2.149
Suttrop W., P4.002, P4.010, P4.075, P4.082
Suwanna S., P4.015, P4.030
Suzuki C., P1.056, P2.061, P2.107
Suzuki M., O3.020
Suzuki Y., I2.022, P2.113
Svensson J., P5.078
Sydora R.D., P4.121, P4.135
Sydorenko D., P5.149
Sylla F., P4.129
Szabó V., P5.078
Szappanos A., P5.079
Szatmári S., O2.014
Szepesi T., P1.101, P2.070
Szerypo J., O4.039
Szydlowski A., O4.043
Ta Phuoc K., I1.011, O3.021, P4.132
Tabak M., I5.068, D5.001
Tabares F., I5.071
Tachaev G.V., P2.149
TaekLim S., P4.174
Tagger M., P4.190
Taguchi M., P4.183
Takabe H., I5.082, P2.187
Takahashi C., P4.101
Takahashi H., P4.055, P4.058, P4.101
Takahashi R., P2.060
Takei N., P2.075
Takeiri Y., P2.113
Takeuchi M., P2.107
Tala T., P2.035, P4.018, P4.022, P5.069
Tale I., P2.011
Tallents S., I2.020, P4.035
Talmadge J., P2.113
Tamain P., P1.020, P4.107
Tamas M., P1.143
Tampo M., P5.113
Tamura N., P4.106, P5.017
Tanaka K., I2.022, P1.054, P2.061, P5.017, P5.111
Tanaka S., P4.109
Tang W.M., P5.023
Tanimoto M., P1.148
Tanimoto T., P5.111
Tanriverdi S., O4.056
Taran V.S., P1.061
Tarancón A., P1.035, P2.049, P5.135
Tardini G., O2.003, P4.039
Tartz M., P2.164
Tassi E., P2.179
Tassin V., I2.027
Tasso H., P2.057, P2.180
Tatarakis M., O4.056, P1.122, P2.148, P2.154
Tautz R., P4.136
Tavella F., P4.136
Taylor G., P1.108
TCV Team, I5.072, P2.036
Teaca B., P1.188
Teliban I., P2.164
Temporal M., P5.125
Tendler M., P5.020
Teodorescu M., P2.167
Terasa C., P4.168
Terasaka K., P4.044, P5.158
Ter-Avetisyan S., P4.145
Terças H., P5.141
Terekhov A.V., P5.104
Tereshchenko M., P1.107
Tereshin V.I., P1.061, P2.170
Ter-Oganesyan A.E., P4.186
Terranova D., P2.054, P4.019, P4.074,
Terry J.L., P1.005
Terzolo L., P5.025
Tessier Y., I1.014
Testa D., P1.067, P5.083
TEXTOR Team, O4.052, P1.081, P1.104, P4.016, P5.063
Thanasutives P., P4.015
Theiler C., I4.065, P1.184, P2.182
Theobald M., I2.027
Theobald W., I4.060, P2.127
Thessieux C., I2.027
Thiell G., I2.027
Thoen D.J., P1.081

Thomas A.G.R., O4.040, P4.144, P5.118
Thomas H.M., I5.079, O2.007, P2.159, P2.162, P5.136, P5.139, P5.140
Thomsen H., P1.065, P2.034, P2.113, P5.078
Thornton A.T., I2.036
Thornton L., P4.131
Throumoulopoulos G.N., P2.057, P2.180
Thyagaraja A., P1.023, P2.039, P4.037, P5.043, P5.052
Ticos C.M., O5.064, P1.169, P1.171
Tikhonchuk V.T., I2.027, I5.081, O2.013, O4.042, P1.119, P2.124, P2.140, P4.138, P4.149
Tilinin G.N., P1.110
Timberl J., P1.009
Timirkhanov R.A., P5.162
Timneanu N., P1.139
Timofeev I.V., P5.104
Timokhin V.M., P4.106
Titov S., O5.066
TJ-II Team, I5.071
Tkachenko S.I., P2.137, P4.186
Todd T., I2.036
Todo Y., P1.056
Toi K., I2.022, P1.054, P1.056, P2.061, P2.107
Toigo V., P4.075
Tokar M., P1.011, P2.042, P4.048, P5.027
Tokarev V.I., O2.007
Tokuzawa T., I2.022, P1.054, P2.061, P5.017
Tolstyakov S.Yu., P1.110, P2.046, P2.097, P2.104, P2.108
Toncian T., P5.113
Toniolo C., P1.188, D4.003
Torrise L., P2.142, P2.144, P4.154, P4.170
Toscano D., P1.170
Totsuji H., O5.063
Toussaint U.v., P1.065
Town R.P.J., P2.127, D5.001
Traisnel E., P1.058, D4.004
Tran T.M., P1.019, P4.033
Trapeznikov A., P1.008
Treutterer W., P4.082
Tribaldos V., P2.090, P2.113
Tribeche M., P1.153
Trier E., P1.022
Trigger S.A., P1.158
Trines R., I4.066
Trines R.M.G.M., P1.128
Tritz K., P1.059
Tronnier A., P2.132
Trottenberg T., P2.164
Trubchaninov S.A., P2.170
Truhachev F.M., P4.188
Trulsen J., P5.132
Trunev Yu.A., P4.103, P5.098
Tsakiris G., I1.002, O3.019, P1.131, P1.134, P1.145
Tsalas M., P2.010
Tsikata S., P4.189
Tsintsadze N.L., P5.167
Tsironis C., P5.089, P5.093
Tskhakaya sr. D.D., P2.005
Tsohantjis I., O4.041, P1.123
Tsuchiya H., P5.003
Tsujii N., P5.100
Tsung F.S., O3.021
Tsushima A., P5.133
Tsvetoukh M.M., P4.012, P4.057
Tsybenko S.A., P1.061
Tsyganov D., P2.169
Tsytovich V.N., O2.009, P1.154, P5.131
Tudisco O., P2.026, P4.032
Tugarinov S., P1.008
Tukachinsky A.S., P1.080, P2.093, P2.103
Tumakaev G.K., P1.152
Turan R., P1.127
Turco F., P1.058
Turkin Yu. A., P2.113
Turnyanskiy M.R., P5.081, P5.084
Turri G., I5.072, P2.020
Turtikov V.I., P2.145
Tynan G.R., I4.065, P5.158
Tzianaki E., P1.122, P2.148, P2.154
Tzoufras M., O3.021
Udintsev V., I5.072
Ullschmied J., I5.081, P1.117, P1.118, P4.133
Ulmer J.L., I2.027
Umansky M.V., P4.001
Unterberg B., O4.052, P1.104, P2.009, P4.016, P4.075
Unterberg E.A., P2.013
Urban J., P2.096, P2.098
Urso L., P2.067
Uschmann I., O5.061, P2.129
Ushakov A.G., P2.134
Ushanov V.Zh., P1.010
Ustimenko A.B., O2.018, P1.010, P5.148
Utkin A.V., P2.145
Uzdensky D.A., O5.066
Vaessen B.C.E., P1.081
Vafin I.Yu., P5.071
Vaivads A., I4.066
Vajnov P.V., P4.043
Valdettaro L., P4.026
Valeo E.J., P1.090, P1.108, P2.099, P4.114
Valisa M., I3.045, O4.029, P4.074, P5.073
Valougeorgis D., P5.033
Valovic M., O4.054, P2.098
Van Compernelle B., P2.105
Van de Pol M.J., P1.090
Van den Berg M.A., P1.081
Van der Geer S.B., P1.148
Van der Meiden H.J., P4.093
Van der Mullen J., I2.039
Van Dijk J., I2.039
Van Milligen B.Ph., P1.031, P2.021, P2.039, P2.043
Van Oost G., P1.021, P2.040

Van Rooij G.J., P4.093
Van Schoor M., O4.052, P4.013
Van Wassenhove G., P1.079, P1.104, P5.077
Van Zeeland M.A., P2.003, P4.083, P5.099
Vanhaelen Q., D4.003
Vann R.G.L., P1.007, P4.064
Varfolomeev V.I., P1.110, P2.108
Vargas V.I., P2.030, P5.018
Varischetti M.C., P4.025, P4.026
Varnière P., P4.190
Vasiliev M.M., P1.160, P1.161
Vasiliev M.N., P1.187
Vatistas G., I4.064
Vatulin V.V., P2.146, P2.149
Vaulina O.S., I2.033, P4.158, P5.137
Vchivkov K.V., P1.192
Vdovin V., P1.102
Vecchi G., P2.105
Vega J., P2.113
Veisz L., P4.136, P4.146
Vejpravova Poltierova J., P1.162
Vekshina E.O., P2.087, P4.043
Velarde M., P2.135
Velarde P., O5.062, P1.117, P1.132, P1.141, P2.133
Velasco J.L., P1.035, P2.049, P5.135
Veltcheva M., P4.129, P5.109
Veltri P., P1.039
Velyhan A., P2.120, P4.133
Venkatakrishnan N., P4.129
Veres G., P2.111
Vergote M., O4.052
Vermare L., P1.017, P1.044, P4.021
Vervier M., P1.104, P5.077
Verwichte E., P1.030, P2.055
Vesel A., P1.014, P1.166
Vianello N., O4.029, O4.049
Vichev I.Yu., P1.125
Victoria M., P2.135
Vid'junas M.I., P1.080
Videau L., I2.027
Vieira J., P4.143, P4.147, P4.150
Vierle T., P4.075
Vieux G., P1.150
Vikherv V.V., P2.148, P2.154
Vildjunas M.I., P2.093, P2.103
Villar T., P2.135
Villard L., P1.019, P1.072, P2.063, P4.033
Villegas D., O4.050
Villette B., I2.027
Villone F., P2.067, P2.080, P4.073, P5.047
Vincena S., P1.190
Vinci T., P5.119
Vinogradov P.V., O2.007
Vinogradov V.I., P1.120
Vlachos N.S., P2.044
Vlad G., P5.028, P5.055
Vladimirov S.V., O3.023, P1.154, P1.155, P1.156, P1.157, P1.163, P2.157, P5.132
Vlahos L., P2.041, P5.089, P5.093
Vohrer U., I1.012
Voitsekhovitch I., O2.006, P2.098
Volkov E.D., P1.061
Volkov G.I., P2.131, P2.136
Volkov G.S., P1.125
Volpe D., P5.088
Volpe F., P5.095
Vomvoridis J.L., P4.105
Von Hellermann M.G., P4.092
Von Oertzen W., P4.122
Vorberger J., P2.152
Vorgul I., I3.053, P2.186, P4.179, P4.185
Vorona N.A., P1.187
Voronin A.V., P2.104, P2.108
Voronov G.S., P2.188
Voskoboynikov S., P4.035
Voslion T., P2.072
Vranjes J., P4.178, P5.040, P5.061
Vrba P., P1.143
Vrbova M., P1.143
Vulkay I., P1.170
Vulliez K., P5.088
Vyacheslavov L.N., P4.103, P5.098
Wadati M., P4.164
Wade M.R., P2.073
Waelbroeck F.L., P2.006
Wagenaars E., I2.039
Wagner D., P1.034, P2.111
Wagner F., P1.043, P1.088
Wahlström C.-G., P4.134
Waldmann O., P5.002
Walker C., O2.001
Wallace G.M., P4.111
Walsh M., O4.054
Waltz R.E., O4.053, P1.017, P1.044, P5.028
Wan B.N., P4.102
Wang Cheng, P1.121
Wang D.X., P4.102
Wang F.L., I5.082
Wang M., P4.102
Wang M.W., P5.086, D2.005
Wang S.J., P5.123, P5.124
Wang W.M., P5.124
Wang W.X., P5.016, P5.023
Wang X.M., P4.102
Wang X.Y., P5.086, D2.005
Wang Z., O5.064
Wang Z.H., P5.123, P5.124
Watanabe F., P1.054, P2.061
Watanabe K.Y., I2.022, P1.054, P2.061, P2.095, P2.113
Watkins J.G., P4.003
Wattieux G., I1.014
Waugh J., I3.054, O5.061

Waugh J.N., P2.187
 Weber J.W., P4.005
 Weber S., O2.013, O4.042, P2.118, P2.140
 Wei H.G., P1.140
 Wei M., P5.114
 Wei Z.Y., P5.123, P5.124
 Weiland J., P1.048, P2.032, P2.036, P2.042, P4.024, P4.036
 Weingartner R., P4.143, P4.146
 Welander A.S., P2.079, P4.055
 Weller A., P1.065, P2.113, P4.072, P5.078
 Weltmann K.-D., P4.173
 Wenninger R., P1.101
 Werner A., P2.034, P2.051, P2.113, P4.072, P5.078
 Wesley J.C., P2.003
 West W.P., P2.003, P2.073
 Westerhof E., P1.081, P5.077
 Weynants R.R., O4.052, P4.013
 Weyssow B., P1.188, P4.031, P4.048, D4.003
 White A.E., P5.099
 White R.B., P5.099
 Whiteford A., D1.003
 Whittaker D.S., P1.132
 Whyte C.G., I3.053
 Whyte C.G., P2.186
 Whyte D., P2.081
 Wieggers R.C., P4.009
 Wiesen S., P5.053, D1.003
 Wilgen J.B., P1.108
 Willi O., P1.089, P5.113
 Willingale L., O3.021, O4.040, P4.144, P5.108, P5.116
 Wilson H.R., I2.020, P1.007, P4.029, P4.051
 Wilson J.R., P1.108, P2.099, P4.111
 Wilson L.A., P2.187
 Wilson P.A., P5.113
 Windridge M.J., P4.066
 Wischmeier M., P2.010, P4.003
 Wisse M., P2.018, P2.088
 Wojda F., P4.134
 Wolf R.C., P1.079, P2.113, P5.078
 Wolfe S., P1.005
 Wolfrum E., O2.002, O4.032, P2.010, P2.083, P4.010
 Wolowski J., O4.043, P1.127, P4.123
 Wolter M., P2.165, P4.168
 Woo H.-J., P4.090, P4.091
 Woolsey N.C., I3.054, I5.082, O5.061, P2.129, P2.187
 Wortman P.M., P1.081
 Woskov P., P1.034, P5.077
 Wright G., P2.081
 Wright J.C., P1.108, P2.099, P4.111, P4.114, P5.085
 Wrobel R., I2.027, O2.013
 Wu B., P2.076, P4.112
 Wu H.-C., P1.133, P1.146
 Wu J., D5.004
 Wu W., P2.003
 Wukitch S.J., P5.085, P5.100
 Wunderlich D., P2.102
 Wurden G.A., O5.064
 Wyman M.D., P1.075
 Xiao W.W., D5.003
 Xiaoa W.W., D4.004
 Xie W.M., P5.101
 Xu M., I4.065
 Xu M.H., P5.123, P5.124
 Xu Y., O4.052, P1.089, P4.013
 Xu Zhizhan, P1.121
 Xuan W.M., P5.086, D2.005
 Yaakobi B., I4.060
 Yabu-uchi T., P5.111
 Yadikin D., P2.066, P4.075
 Yagi M., P4.044, P5.059, P5.158
 Yakovenko Yu.V., P4.072
 Yakubov V.B., P1.115, P1.116
 Yamada H., I2.022, P1.076, P2.113, P5.003
 Yamada I., I2.022, P2.061, P5.017
 Yamada T., P4.044, P5.158
 Yamaguchi N., P2.082
 Yamamoto S., P1.054
 Yamashita T., P4.067, P4.068
 Yan L.W., P2.014, D5.003
 Yan Z., I4.065
 Yanenko V.V., P2.130
 Yang J.F., P5.086, D2.005
 Yang J.X., P5.086, D2.005
 Yang Q., P5.026
 Yang Q.W., P5.101, D5.003
 Yang X., P1.150
 Yao L.H., D5.003
 Yao L.Y., P5.086, D2.005
 Yaroshenko V.V., P5.140
 Yashin A.Yu., P2.093
 Yatsuka E., P4.109
 Yavorskij V., P1.087
 Ye J., D5.004
 Ye M.Y., P5.078
 Yegorenkov V., P4.176
 Yerci S., P1.127
 Yin L., P4.130
 Yokota M., P4.101
 Yokoyama M., P2.113
 Yoneda Y., P1.085
 Yong Liu, D5.003
 Yoo S.J., O3.024, P4.175
 Yoon S.W., P5.091
 Yordanova E., O4.057
 Yoshikawa M., P1.085
 Yoshimura Y., P1.056, P4.101
 Yoshino R., P2.075
 Yu J.H., I4.065, P2.003, P4.083, P4.098
 Yu L.M., P5.086, D2.005
 Yu Q., P1.078, P2.064
 Yu Q.Z., P5.124
 Yuan B.S., P5.101

Yuan X.H., P5.124
 Yuh H., P1.108, P5.022, P5.060
 Yun E. Y., P4.171
 Zabiralov A.A., P2.136
 Zaboronkova T.M., P4.192
 Žáček F., P2.098
 Zaitsev F.S., P1.091, P1.092, P1.093
 Zaitsev V.I., P1.125
 Zajac J., P2.096
 Zakharov L.E., P4.058, P4.069
 Zakharov Yu.P., P1.142, P1.192
 Zamponi F., O5.061
 Zanca P., O4.029, P5.065
 Zappa F., P5.007
 Zarnstorff M., P5.058
 Zarnstorff M.C., P2.013, P5.050
 Zaroschi V., P1.171
 Zastrow K.D., P4.022, P4.094, P4.115
 Zebrowski J., P5.075
 Zedda M.K., P4.070, P5.045
 Zeitoun Ph., P1.132, P1.141
 Zelenin A., P2.137
 Zenkevich P.R., O2.012
 Zepf M., I5.077, O3.019, P1.131, P1.134, P5.103, P5.108,
 P5.116
 Zerbini M., P5.074
 Zhang G.Q., P5.086, D2.005
 Zhang J., I5.082, P5.123, P5.124
 Zhang L.Z., P4.102
 Zhang Q., I3.052
 Zhang T., P5.024
 Zhang W.L., P5.028
 Zhang X.D., P4.102, P5.024
 Zhang X.M., P5.086, D2.005
 Zhang Y., P5.123
 Zhang Z., P5.123
 Zhao G., I5.082
 Zhao H.L., P2.014
 Zhao K.J., P2.014
 Zhao Y.P., P4.101, P4.102
 Zhdanov S.K., I5.080, P2.159, P5.139
 Zheng Z.Y., P5.124
 Zhezhera A., P1.088
 Zhidkov N.V., P2.149
 Zhilin E.G., P1.110
 Zhogolev V.E., P2.077
 Zhong G.W., P5.086, D2.005
 Zhou C.D., I4.060
 Zhou H.Y., P2.082
 Zhou J., P5.101
 Zhou W.M., D2.003
 Zhou Y., P5.026, D5.003
 Zhu P.F., P5.123
 Zhubr N.A., P1.080, P2.103
 Zimbardo G., P5.170
 Zimmermann O., O2.006
 Zivkovic T., P1.037
 Zobdeh P., P4.140
 Zohm H., P1.055, P1.062, P1.101, P2.066, P2.067
 Zoletnik S., O4.031, P2.034, P5.076, P5.078, P5.079
 Zolototrubova M.I., P1.061
 Zonca F., P1.051, P2.038, P4.054, P4.062, P5.028, P5.055,
 P5.056
 Zou G.Q., P5.086, D2.005
 Zou X.L., D4.004
 Zoua X.L., D5.003
 Zubairov Ed.R., P4.103, P5.098
 Zuin M., I1.017, O4.029, O4.049
 Zurro B., P1.094, P2.090, P2.094
 Zushi H., P5.003
 Zwingmann W., P1.064, P2.112

